

GUIDEBOOK TO PERMAFROST AND QUATERNARY GEOLOGY OF THE FAIRBANKS AREA, ALASKA

Edited by D.S.P. Stevens

Guidebook 11 (Preliminary Draft)



Published by

STATE OF ALASKA
DEPARTMENT OF NATURAL RESOURCES
DIVISION OF GEOLOGICAL & GEOPHYSICAL SURVEYS



2008

DRAFT

GUIDEBOOK TO PERMAFROST AND QUATERNARY GEOLOGY OF THE FAIRBANKS AREA, ALASKA

Edited by D.S.P. Stevens

This preliminary guidebook is available in draft form to field trip participants only. Due to time constraints of the NICOP schedule, the guide has yet to undergo formal technical and editorial review to meet the publication standards of DGGS.

The editors anticipate finalizing this publication by early 2009, and a final version will then be made available. Please do not make copies of this manuscript. Rather, check our website (www.dggs.dnr.state.ak.us) or contact our publication desk (907-451-5020) to check availability of the updated version.

Division of Geological & Geophysical Surveys

Guidebook 11 (Preliminary Draft)

Prepared for
Ninth International Conference on Permafrost
June 29 – July 3, 2008
University of Alaska Fairbanks

Cover photo: *Massive ice in permafrost exposed in cut near Fox, Alaska. Photo taken September 2, 2006, by Vladimir Romanovsky.*



STATE OF ALASKA
Sarah Palin, *Governor*

DEPARTMENT OF NATURAL RESOURCES
Tom Irwin, *Commissioner*

DIVISION OF GEOLOGICAL & GEOPHYSICAL SURVEYS
Robert F. Swenson, *State Geologist and Acting Director*

Publications produced by the Division of Geological & Geophysical Surveys can be examined at the following locations. To order publications, contact the Fairbanks office.

Alaska Division of Geological &
& Geophysical Surveys
3354 College Road
Fairbanks, Alaska 99709-3707

Elmer E. Rasmuson Library
University of Alaska Fairbanks
Fairbanks, Alaska 99775-1005

Alaska Resource Library & Information Services (ARLIS)
3150 C Street, Suite 100
Anchorage, Alaska 99503

University of Alaska Anchorage Library
3211 Providence Drive
Anchorage, Alaska 99508

Alaska State Library
State Office Building, 8th Floor
333 Willoughby Avenue
Juneau, Alaska 99811-0571

This report has not been reviewed for technical content or for conformity to the editorial standards of DGGS.

INTRODUCTION

General Statement

by

Larry Hinzman

Director, International Arctic Research Center - University of Alaska Fairbanks

Program Chair, NICOP U.S. National Committee

This field guide was prepared to accompany the Ninth International Conference on Permafrost (NICOP) convened in Fairbanks, Alaska, 29 June – 3 July 2008. We anticipate this report will be useful for many years to come for those who have more than a casual interest in permafrost. Field site visits have always been a major component of the International Conferences on Permafrost and present the opportunity for scientists, engineers and land managers from around the world to observe the processes and challenges inherent in living with permafrost. We attempted to design these field trips to appeal to a broad range of interests, with individual trips focused on engineering applications, ecological interactions, hydrology and periglacial processes. Fairbanks is an ideal setting to view many permafrost features first-hand. Many aspects of our landscape, our ecology and our culture are dominated by the presence or absence of permafrost. Living in the zone of warm, discontinuous and ice-rich permafrost, local residents had to adapt or develop innovative building techniques to protect permafrost from thawing. This guide includes discussions of construction techniques that minimize thermal and mechanical disturbance to the underlying permafrost as well as an examination of the role played by permafrost in the boreal forest ecosystem. As a small city with a less than century-long history, it is still quite easy to find undisturbed permafrost features, including relict ice wedges and polygonal ground. We hope the reader finds this guide useful in developing a better appreciation for the challenges of living with permafrost in a warming climate.

ORGANIZATION

This guidebook includes updated information relating to some of the sites originally described in the 1965 “Central and South-central Alaska Guidebook F” (Péwé; reprinted 1977) for the Seventh International Quaternary Association (INQUA) Conference and the 1983 “Guidebook to Permafrost and Quaternary Geology along the Richardson and Glenn Highways between Fairbanks and Anchorage, Alaska” (Péwé and Reger) for the Fourth International Conference on Permafrost. It also includes descriptions of many new sites in the Fairbanks area. Authors are drawn from a wide spectrum of disciplines, including engineering, geology, hydrology and ecology, making this guidebook a truly interdisciplinary overview of the landscape of the Fairbanks area.

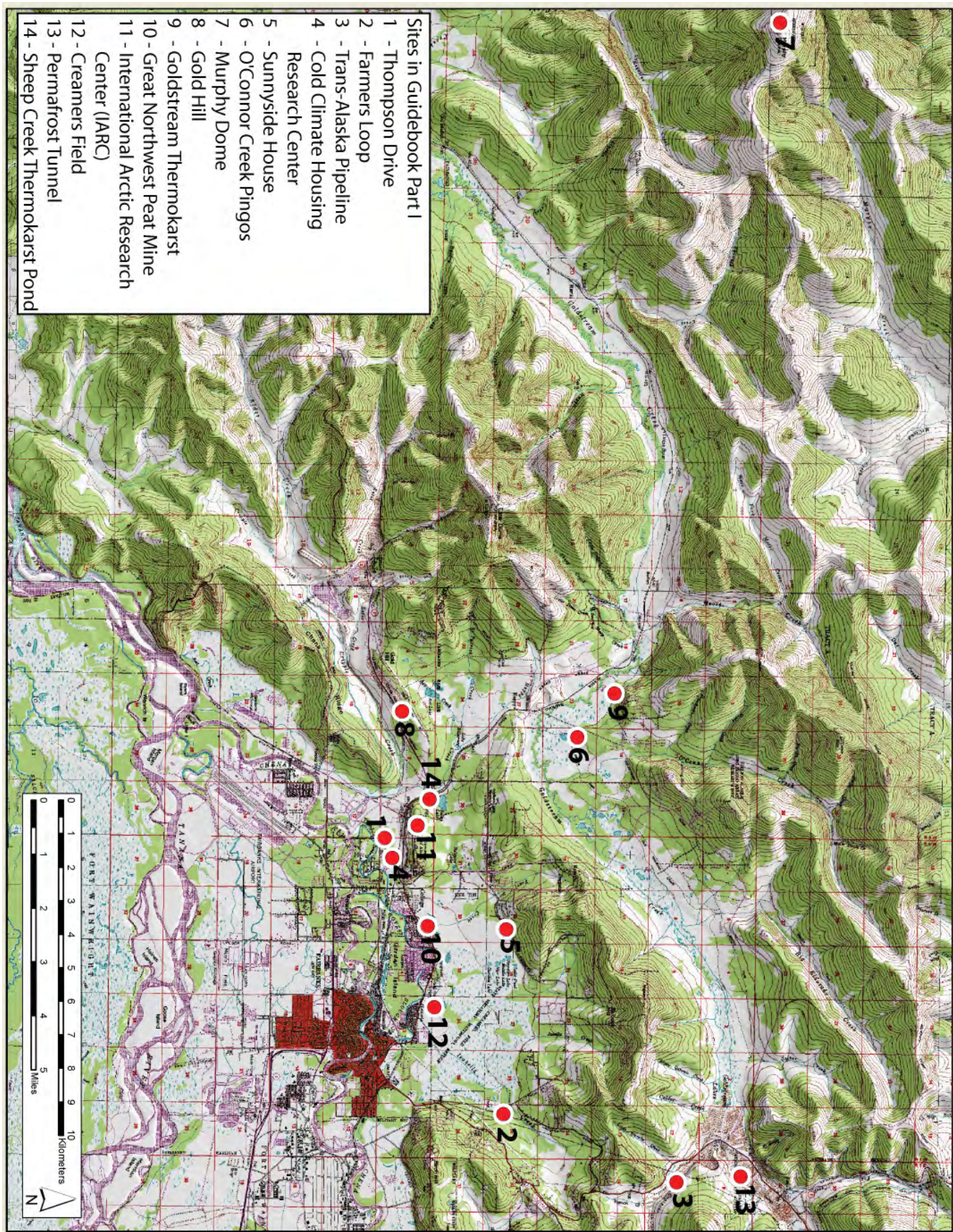
The guidebook is organized into two sections. The first section, “Part I: Field Guide to Permafrost, Periglacial, and Quaternary History Sites near Fairbanks, Alaska,” describes individual sites that were designed to be visited in various combinations and sequences by multiple groups attending the NICOP local field trips. These site descriptions are thus discrete entities and can be used as stand-alone field trip destinations. The site numbers for Part I are essentially random and do not imply any particular order. The second section of the guidebook, “Part II: Field Guide for Permafrost Features in Caribou-Poker Creeks Research Watershed (CPCRW) and Environs of Fairbanks, Alaska,” is a fully-realized field trip, and the site numbers are presented in the sequence visited during the official field trip.

ACKNOWLEDGEMENTS

The authors and editors appreciate the efficient publication support provided by Joni Robinson (DGGS). Without her assistance, this preliminary guidebook would not have been possible. Field trip logistics and scheduling were ably provided by Deb Bennett (Water and Environmental Research Center) and Elizabeth Lilly (Geo-Watersheds Scientific), whose tireless efforts in support of all the NICOP field trips are greatly appreciated.

REFERENCES CITED

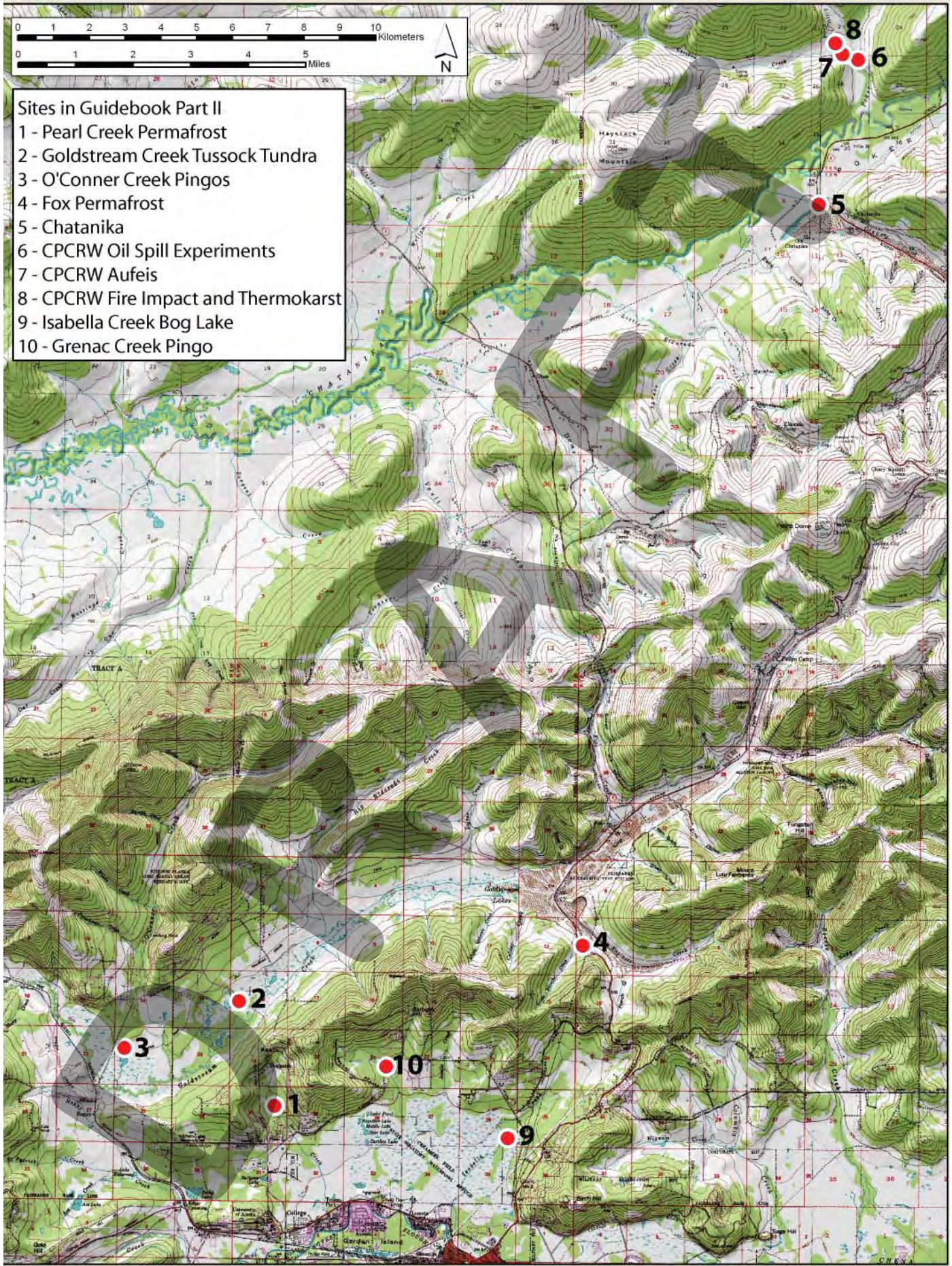
- Péwé, T.L. (ed.), 1977, 1965 INQUA Conference guidebook to central Alaska: Alaska Division of Geological & Geophysical Surveys Miscellaneous Publication 4, 141 p.
- Péwé, T.L., and Reger, R.D. (eds.), 1983, Guidebook to Permafrost and Quaternary Geology along the Richardson and Glenn Highways between Fairbanks and Anchorage, Alaska: Alaska Division of Geological & Geophysical Surveys Guidebook 1, 263 p., 1 sheet, scale 1:250,000.



CONTENTS

Part I Field Guide to Permafrost, Periglacial, and Quaternary History Sites near Fairbanks Alaska

Site	Page
1 Thompson Drive	1
<i>Doug Goering</i>	
2 The Fairbanks Permafrost Experiment Station, Alaska-Historical Highlights.....	5
<i>Karen S. Henry, Kevin Bjella and Thomas A. Douglas</i>	
3 Trans Alaska Pipeline and Permafrost.....	9
<i>Elden Johnson</i>	
4 Studying the Effectiveness of an Underground Adjustable Foundation on Alleviating the Problems Associated with Building on Permafrost	11
<i>Danielle L. Jamieson and Michael R. Lilly</i>	
5 Sunnyside House - Building on Permafrost: Failures and Solutions	15
<i>Michael R. Lilly and Dennis Filler</i>	
6 O'Connor Creek Pingos	17
<i>Kenji Yoshikawa</i>	
7 Murphy Dome	21
<i>De Anne S.P. Stevens</i>	
8 Gold Hill.....	27
<i>James E. Beget, David Stone, Paul Layer, Jeffrey Benowitz, and Jason Addison</i>	
9 Thermokarst Pits and Fens in Goldstream Valley	33
<i>Torre Jorgenson</i>	
10 Great Northwest Peat Mine	35
<i>Kenji Yoshikawa and Vladimir Romanovsky</i>	
11 GeoData Center - Map Office - Alaska Satellite Facility User Services Office	39
<i>Patricia Burns</i>	
12 Thermokarst and Drunken Forest.....	43
<i>Katey Walters</i>	
13 Late-Pleistocene Syngenetic Permafrost in the CRREL Permafrost Tunnel, Fox, Alaska.....	45
<i>M.Z. Kanevskiy, H.M. French, and Y.L. Shur (eds.)</i>	
14 Thermokarst Lakes and Methane Emissions	67
<i>Katey Walter</i>	



Part II
Permafrost Features in Caribou-Poker Creeks Research Watershed (CPCRW)
and Environs of Fairbanks Alaska

Kenji Yoshikawa, , Vladimir Romanovsky, Les Viereck, and Larry Hinzman

Stop		Page
1	Pearl Creek Elementary School Permafrost/Active Layer Monitoring Site (active layer, permafrost temperature).....	71
2	Goldstream Creek tussock tundra (permafrost condition and Holocene ice wedge).....	72
3	O'Connor Creek pingo site open system pingo	72
4	Fox gold mining site permafrost outcrop (Pleistocene ice wedge)	73
5	Chatanika (gold mine and convection heat transfer)	73
6	Caribou Poker Creeks Research Watershed oil spill experiments; Oil Spill and Frost Fire Experiments.....	74
7	Aufeis (Icing) and permafrost hydrology	78
8	Caribou Poker Creeks Research Watershed fire impact/ thermokarst developments	81
9	Isabella Creek bog lake.....	82
10	Grenac Creek (Farmer's loop) pingo.....	82

DRAFT

PART I

**FIELD GUIDE TO PERMAFROST, PERIGLACIAL,
AND QUATERNARY HISTORY SITES NEAR
FAIRBANKS ALASKA**

DRAFT

SITE #1 THOMPSON DRIVE

*Doug Goering
College of Engineering and Mines, University of Alaska Fairbanks*

Construction of Thompson Drive began in 2003 and was completed during the summer of 2005. It provides a new entrance to the University of Alaska Fairbanks campus by linking Geist Road with Tanana Loop. The project crosses two areas of previously undisturbed permafrost. In an effort to avoid the type of thaw settlement problems typically associated with roadway projects located in regions of warm thaw-unstable permafrost, the Alaska Department of Transportation worked with the University of Alaska to incorporate two different types of passive cooling technologies into the project. Three separate test sections were designed and instrumented so that performance could be monitored. The passive cooling systems being utilized include air convection embankments, ventilated shoulders, and hairpin thermosyphons. Figure 1 shows the layout of Thompson Drive with the three test sections identified. Test section #1 combines the use of hairpin thermosyphons with a ventilated shoulder on the right-hand side of the embankment, as shown in figure 1. Test section #2 incorporates both ventilated shoulders and a horizontal air convection layer. Finally, due to the low embankment height in the area of test section #3, which limits the usefulness of air convection layers, this test section utilizes only hairpin thermosyphons. Figure 2 shows the installation of the ventilated shoulder near test section #2, figure 3 shows the installation of the hairpin thermosyphons, and figure 4 shows the insulation layer being installed.

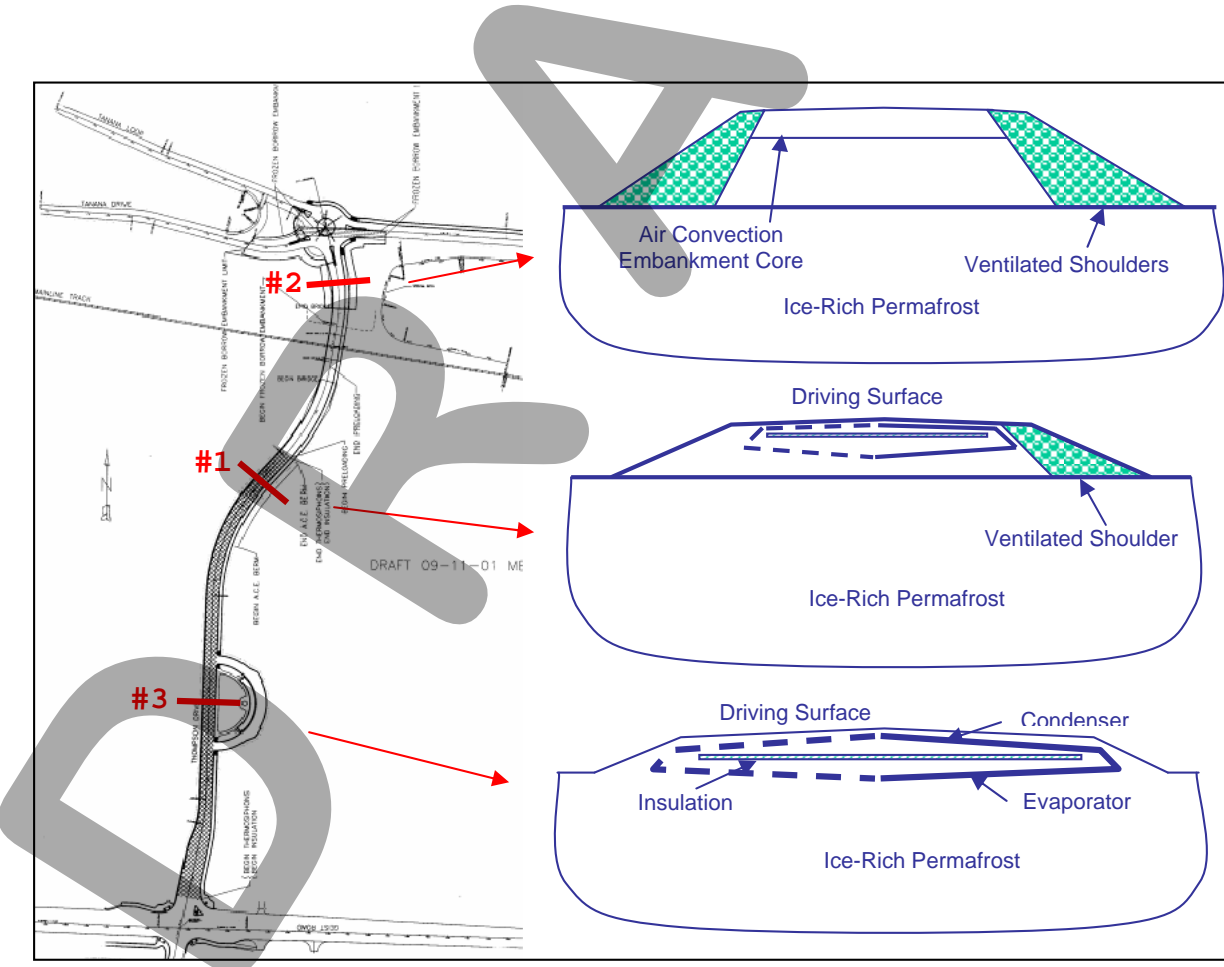


Figure 1. Thompson Drive test sections.



Figure 2. Shoulder installation.



Figure 3. Thermosyphon installation.



Figure 4. Insulation installation.

Air convection embankments were proposed approximately 15 years ago and have been the subject of previous experimental and theoretical studies. This technology employs a highly porous rock aggregate with a large particle size in order to achieve very high material permeability. When a road or rail embankment is constructed of such material, the high permeability allows air to circulate within the embankment, providing a cooling effect during winter. This cooling effect arises because of the instability of an air layer that is warmer on the bottom and cooler on top (such is the case for the air trapped within the embankment structure during winter). The winter-time instability causes the air to circulate, thus providing enhanced cooling of the permafrost foundation soil below.

Test section #2 is shown in figure 5 with the temperature measurement points shown by black dots. This test section is located on the northern approach to the railroad bridge. As the road approaches the bridge it gains height and, thus, the embankment in this area is approximately 10 m thick. Ventilated shoulders are used on both sides of the embankment and a horizontal air convection layer extends across the upper portion of the embankment.

Test section #1 combines a ventilated shoulder on the right side of the embankment with hairpin thermosyphons. Thermosyphons have been in use for many years for passive cooling of building foundations, and other structures in permafrost zones. Perhaps the best-known application of these devices was for chilling of the vertical support members used on the Trans Alaska Pipeline. In the past, thermosyphons have nearly always used an air-cooled condenser and thus always had a finned section projecting up into the ambient air. For use in highway structures, however, there are disadvantages to this design due to safety and vandalism concerns. In addition, the finned sections required for air cooling are expensive to manufacture and increase thermosyphon costs significantly. In an effort to avoid some of these problems, a new type of thermosyphon configuration is being utilized in Thompson Drive. The new devices are referred to as hairpin thermosyphons due to their shape, and do not require an above-ground air cooled condenser. Instead, the condenser pipe is buried underground and insulation sheeting is used to thermally separate the evaporator and condenser. Figure 6 shows a cross sectional view of test section #1 with the thermosyphon evaporator and condenser indicated by heavy lines and the temperature measurement points indicated by black dots. In this design, the thermosyphon condenser and evaporator are connected by soft copper tubing (visible in fig. 2) and charged in the field.

During operation the thermosyphons remove heat from the lower evaporator section and deposit it in the upper condenser section. The net effect is a removal of

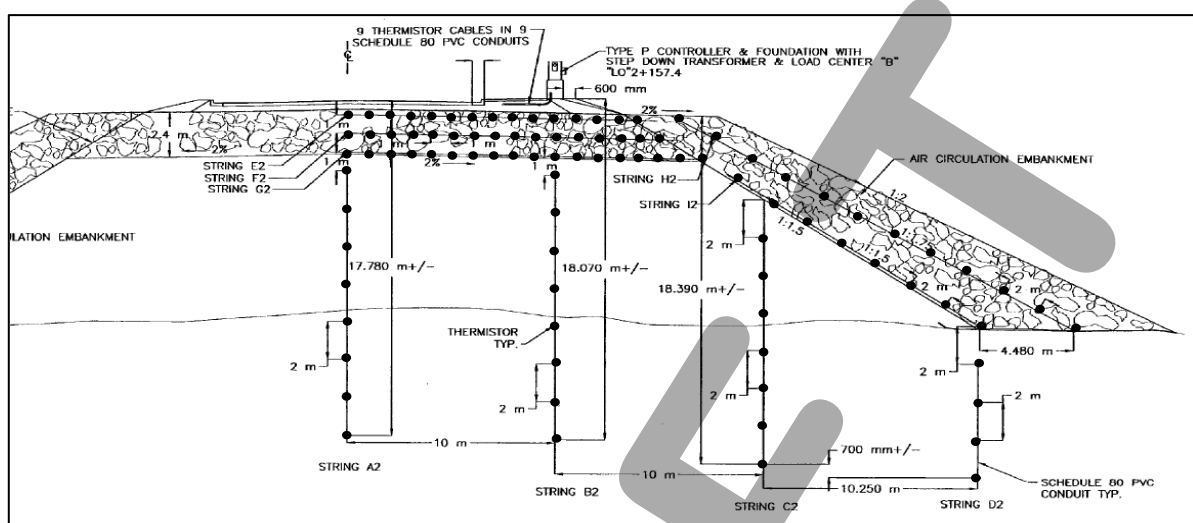


Figure 5. Cross sectional view of test section #2 showing temperature measurement points (black dots).

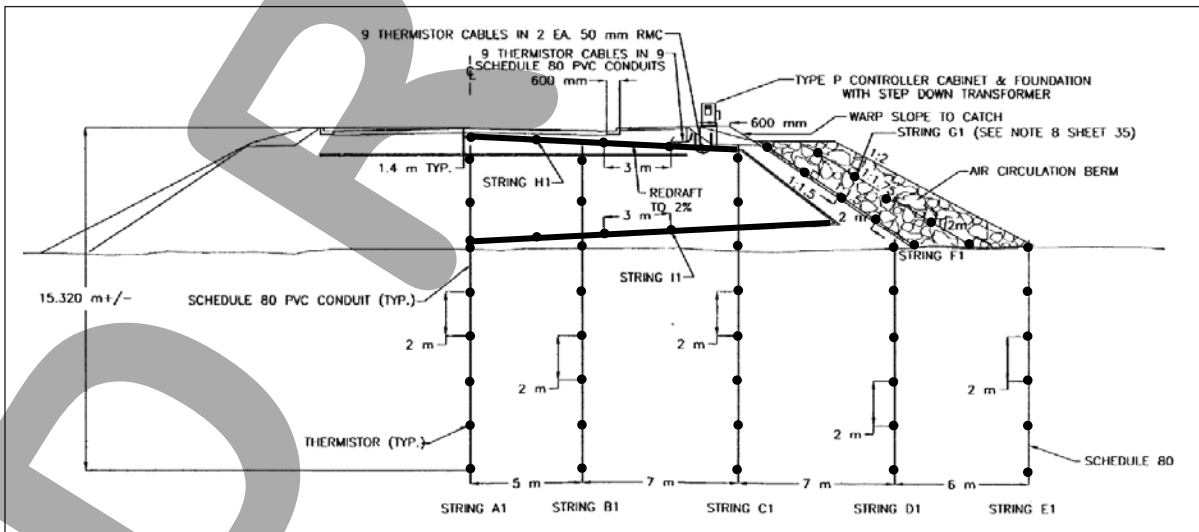


Figure 6. Cross sectional view of test section #1 showing temperature measurement points (black dots).

heat from the base of the embankment beneath the insulation sheet (the insulation is indicated by the horizontal line just beneath the condenser as shown in fig. 6) and rejection of heat through the asphalt surface at the top of the embankment. In this way the base of the embankment and underlying permafrost is cooled and the permafrost is preserved. The test section shown in figure 6 also contains a ventilated shoulder, which in this case is designed specifically to avoid problems with shoulder rotation and resultant destruction of the sidewalk on the right side of the roadway.

Figure 7 shows mean annual temperature contours for the December 2005 to December 2006 time frame. The shaded zones in the figure show the areas where the mean annual temperatures are -0.5°C or colder. The shading clearly demonstrates the cooling influence of both the ventilated shoulder and the thermosyphon with the low-temperature regions being located adjacent to the shoulder and thermosyphon evaporator. Comparison with data collected a year earlier indicates that these zones of the embankment foundation are currently cooling at the rate of about 1°C per year. Over time it is expected that the low temperature regions will expand downward helping to cool the warm permafrost below.

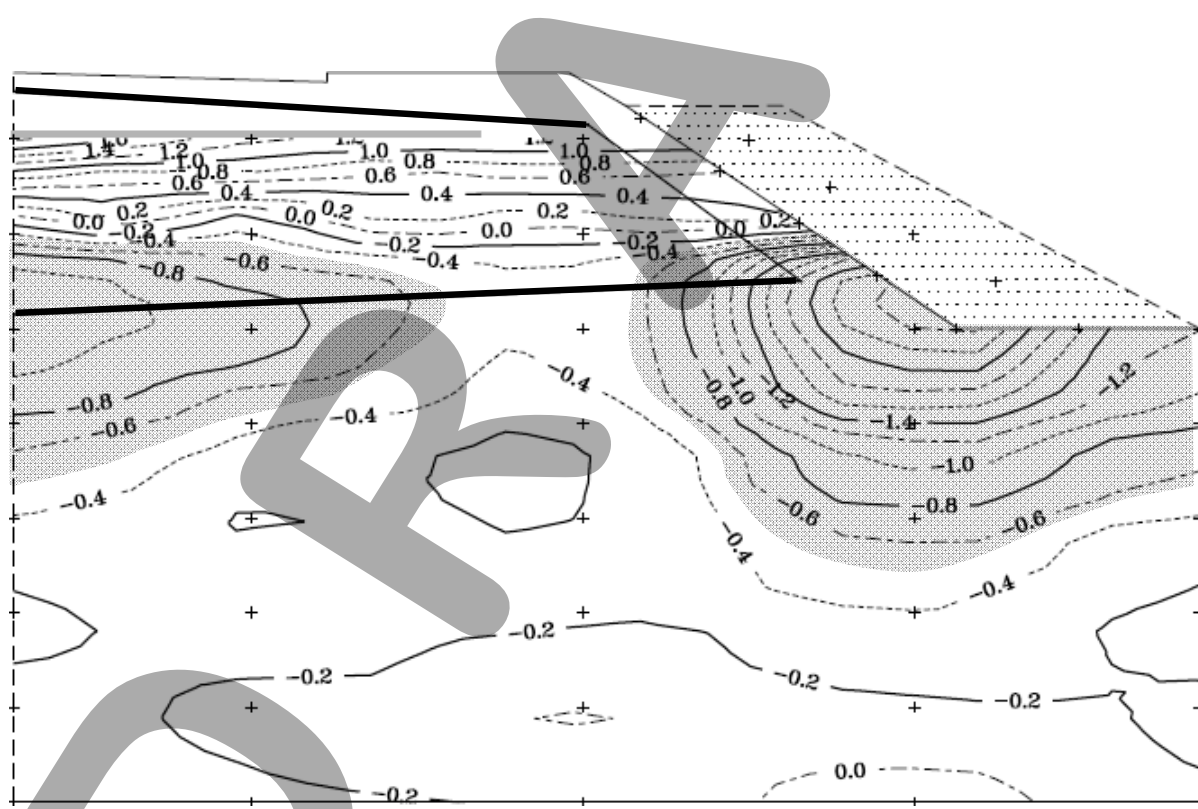


Figure 7. Mean annual temperature contours for test section #1 for the period December 16, 2005 to December 15, 2006.

SITE #2

THE FAIRBANKS PERMAFROST EXPERIMENT STATION, ALASKA-HISTORICAL HIGHLIGHTS

Karen S. Henry

Department of Civil and Environmental Engineering, USAF Academy, Colorado

Kevin Bjella and Thomas A. Douglas

U.S. Army Cold Regions Research and Engineering Laboratory Fairbanks, Alaska

INTRODUCTION

The Fairbanks Permafrost Experiment Station (FPES; 64.877N, 147.670W) is a 135-acre site established by the U.S. Army in 1945 to conduct geotechnical engineering and geophysical investigations on permafrost (fig. 1). The establishment of the site was related to the construction of the Alaska-Canadian (ALCAN) Highway in 1942 that linked the lower 48 states to Alaska via a route through Canada. The ALCAN Highway, considered a military necessity after the bombing of Pearl Harbor (1941), due to the possible invasion of Alaska by Japan, was constructed in just eight months from March through October 1942. The ALCAN immediately suffered considerable damage due to the response of the underlying permafrost to disturbance. It was the difficulties of construction and maintenance of the ALCAN Highway on permafrost that led to the establishment of the Fairbanks Permafrost Experiment Station.

Construction of research projects and support infrastructure began in 1946 by the Alaska Department of the U.S. Army Corps of Engineers for the Permafrost Field Office of the Saint Paul District. In 1953, this ‘Permafrost Field Office’ joined the Arctic Construction Frost Effects Laboratory, or ACFEL (Boston, Massachusetts), which then operated the site under the name of the ‘Alaska Field Station.’ Responsibility for the ‘Fairbanks Permafrost Experiment Station’ (FPES) was taken over in 1961 by the Cold Regions Research and Engineering Laboratory (CRREL), where it has remained since. The Fairbanks Permafrost Experiment Station was designated as a National Geotechnical Experimentation Site in 2003.

The ice-rich permafrost soil of FPES and its location in a discontinuous permafrost zone make it an ideal ‘worse-case-scenario’ for testing construction techniques, road and airfield designs, piling and other foundations. Projects have included the long-term influence of vegetation removal on permafrost stability, experimental road surfaces, insulation of roads, experimental foundations, the measurement of frost heave forces on piles, thawing of permafrost by passive solar means, the detection of permafrost by geophysical techniques and bioremediation.

In light of recent Arctic climate warming, all historical records of ground temperatures and/or depths and thickness of permafrost in Arctic regions are of potential interest since they can be compared to the present temperatures and state of permafrost. Ground temperatures and state of the ground (i.e., frozen or thawed) were often documented in detail for studies conducted at FPES from the 1940s through the 1970s. For example, one study included a ‘control’ plot of land that has been left undisturbed, yet ground temperatures and depth to permafrost were monitored over a period of 26 years- from 1946 through 1972 (Linell, 1973).

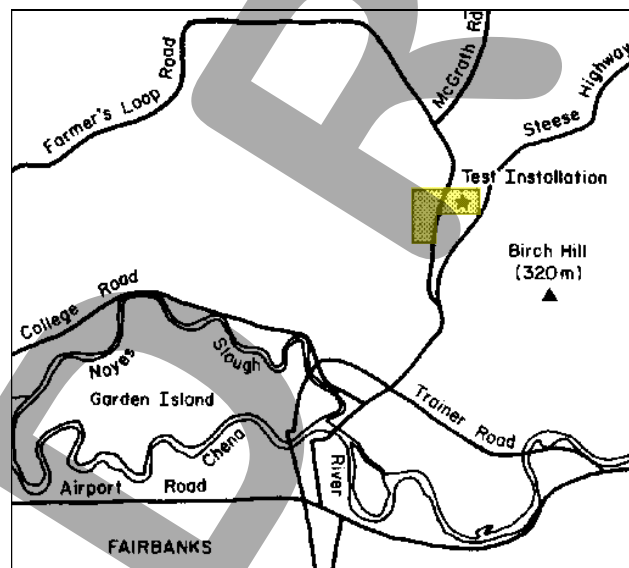


Figure 1. Map showing the location of the Fairbanks Permafrost Experiment Station site.

SITE DESCRIPTION

The Fairbanks Permafrost Experiment Station slopes to the west at a grade of about 3%, and has good drainage except for the lowest elevations (fig. 2). It is located on the lower colluvial slopes of Birch Hill (to the southeast) and partly on valley fill. The natural soils are primarily silts to depths of 15 to 45 m, with many peat and ice-lens inclusions (Linell, 1973). A thick layer of silts, silty sand and sand-gravel mixtures underlies the top layer of silt to bedrock at an approximate depth of 75 m. Because of the site's warm, discontinuous permafrost with frost-susceptible soil, there is considerable frost heave each winter, thaw settlement in the spring and sensitivity to permafrost degradation. In 1946, the top of permafrost was roughly 1 m and the lower boundary exceeded 49 m, while the water table fluctuated between 0 and 2 m during thaw season (Lobacz and Quinn, 1963). Yearly thaw depths measured at the site for the past three years have ranged from 35 to 80 cm each year.



Figure 2. An aerial view of the FPES taken in July, 1958. The buildings in the photograph are no longer at the site because ground thawing caused settlement and distortion of the buildings. The cleared 'Linell plots' can be seen in the upper right center of the photograph, and an experimental runway can be seen behind the building in the upper left portion of the photo.

PAST PERMAFROST RESEARCH CONDUCTED AT FPES

Past permafrost research at FPES falls into three categories: 1) Impact of vegetation removal and other construction on the thermal state of the ground, 2) Frost heave research (including frost-jacking of piles) and 3) Exploring means of maintaining frozen ground beneath roads and airfields. The earliest studies examined the influence of ground cover and its removal, building foundations, types of pavement bases, insulated pavements and various pavement surfaces on the thermal state of the ground below (e.g., U.S. Army Corps of Engineers. 1950). Henry and Bjella (2006) listed some of the projects conducted at FPES that generated ground thermal regime and other historical data related to the state of the permafrost.

PAST AND PRESENT RESEARCH EVIDENT AT THE SITE

The following descriptions of work are related to projects for which evidence of work can be observed on a site visit. Refer to figure 3 for the locations.

Circumpolar Active Layer Monitoring Site on historical 'Linell Plots'

In 1946 three square plots 61 meters on a side ($3,721 \text{ m}^2$) were identified to investigate the influence of vegetation removal on permafrost (Linell, 1983, now referred to as the 'Linell Plots'). One of the plots was left undisturbed to preserve the subarctic taiga forest of white and black spruce. Vegetation was removed from two study plots--one plot was stripped of trees by hand but the roots and organic mat were left intact while all surface vegetation and the organic mat were stripped from the other plot. Linell (1973) described permafrost degradation at the two disturbed sites after 35 years.

In 2005 a Circumpolar Active Layer Monitoring Network (CALM) site was established in the undisturbed Linell plot. Thaw depths are measured in early October at 121 locations on a 10 by 10 m-grid with 3-m spacing. The moss thickness and total thaw depth are measured and recorded at each probe location (table 1). Additionally, a 3-m-deep borehole with a thermistor string measuring ground temperatures at 10 depths was installed in the summer of 2007 and measurements are ongoing.

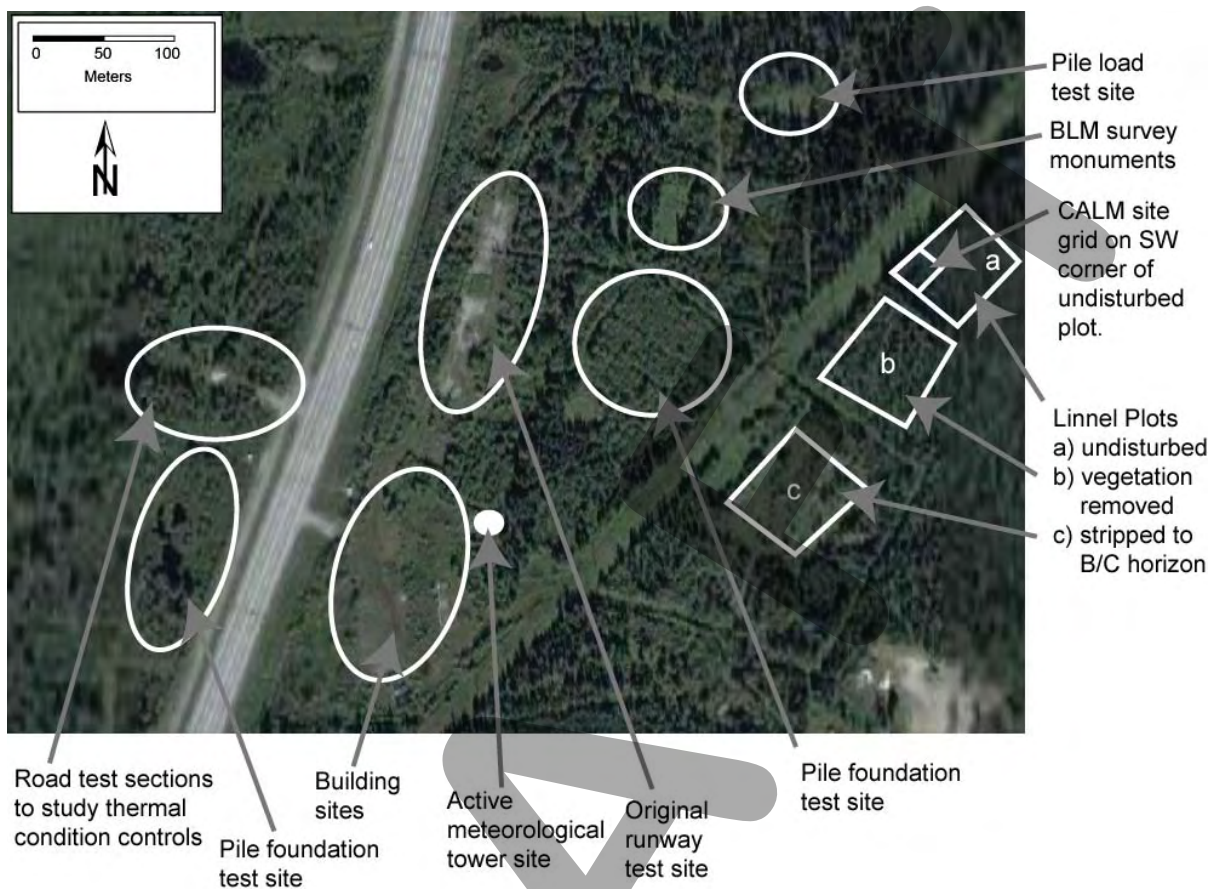


Figure 3. A recent aerial photograph of the FPES showing the main research site locations.

Table 1. A summary of the summer average temperatures, active layer depth and moss thickness from 121 points at the undisturbed Linell plot (CALM site) for 2005-2007.

Year	May-October mean air temperature (°C) ¹	Mean thaw depth with moss (cm)	Mean moss thickness (cm)
2005	13.7	57.5	13.0
2006	12.6	53.5	13.5
2007	12.9	57.3	13.6

¹Meteorological information from the Alaska Climate Research Center.

Direct current resistivity measurements were obtained across the three Linell plots, the summer of 2007 to delineate the current state of permafrost. The results indicate that permafrost degradation following vegetation disturbance is ongoing 61 years later.

Bureau of Land Management Survey Monuments

In 1987, the Bureau of Land Management initiated a study of various types of survey monuments, installed in this frost-prone area and a site on the Kenai Peninsula. Forty-three monuments were installed in August 1987, and monitored (via survey) for frost jacking through 1991. The monuments varied considerably in overall design from shallow rods, e.g., 0.76 m-deep, to rods over 6.4-m-long. Some were installed flush with the surface and others had between 100 mm and 0.9 m of ‘stick up,’ or portion of the monument above the ground surface. Different diameter rods were used and the rods are made of a variety of metals. Some short rod monuments were anchored with 100- or 127-mm-diameter anchor plates. The installation techniques included driven to refusal, driven to refusal with finned rod at the top, driven to refusal with finned rod at the bottom, driven to refusal with 0.9 of ‘stick up,’ driven short of refusal, driven short of refusal with a 76-, 100-, or 127-mm-diameter anchor plate. An August 1991 survey indicated that the maximum uplift experienced was 0.15 m, by a copper-weld rod. Some galvanized iron pipe monuments were experiencing corrosion, and pipe monuments where the vegetation had been carefully replaced around the base of the monument heaved less than other pipe monuments. A few monuments had actually sunk into the ground.

Painted pavement test sections

Berg and Aitken (1973) described the construction of a road test section in 1965 at FPES to investigate several means of controlling thermal conditions beneath the road. The entire road section was 100-m-long, and comprised five test sections—from East to West they were 1) gravel base with white-painted asphalt concrete surface, 2) gravel base with asphalt concrete surface, 3) compressed peat beneath asphalt concrete surface, 4) dark gravel surface and 5) gravel surface. The remnants of these test sections indicate the outstanding performance of the Eastern-most test section—that of the gravel base with white-painted asphalt concrete surface.

Pile load test site for pile foundations in permafrost

According to Crory (1966), pile load testing was initiated by the U.S. Army Corps of Engineers at the FPES in 1957 (pile installation techniques were studied earlier). The load tests were designed to study the factors that affect load capacity of the piles, including installation method, soil type, pile type, length, shape, whether point bearing, permafrost temperature and rate of loading (Crory, 1966).

REFERENCES

- Berg, R.L. and G. Aitken. 1973. Some passive methods of controlling geocryological conditions in roadway construction. in Proceedings, Second International Conference on Permafrost: North American contribution: Washington, D.C., National Academy of Sciences, pp. 581-596.
- Crory, F.E. 1966. Pile Foundations in Permafrost. in Proceedings, International Conference on Permafrost, Purdue University, Indiana, National Academy of Sciences, Washington, DC, National Research Council, Publication 1287, Washington, DC, pp. 467-476.
- Henry, K.S., and K. Bjella. 2006. History of the Fairbanks Permafrost Experiment Station, Alaska. In Proceedings, 13th International Symposium on Cold Regions Engineering, Cold Regions Engineering 2006: Current Practices in Cold Regions Engineering, July 23-26, Orono, ME. Reston, VA: American Society of Civil Engineers, 11 pp.
- Linell, K.A. 1983. Long-term effects of vegetative cover on permafrost stability in an area of discontinuous permafrost, in Proceedings of Permafrost: North American contribution to the Second International Conference, National Academy of Sciences, National Research Council, Washington, DC, pp. 688-693.
- Lobacz, E.F. and W.F. Quinn, 1966. in Proceedings, International Conference on Permafrost, Purdue University, Indiana, National Academy of Sciences, Washington, DC, National Research Council, Publication 1287, Washington, DC, pp. 247-252.
- Permafrost Division, U.S. Army Corps of Engineers. 1950. Investigation of military construction in arctic and subarctic regions, comprehensive report 1945-48; Main Report and Appendix III- Design and construction studies at Fairbanks research area. ACFEL Technical Report 28.

SITE #3 TRANS ALASKA PIPELINE AND PERMAFROST

*Elden Johnson
Alyeska Pipeline Service Company, Fairbanks, Alaska*

TRANS ALASKA PIPELINE

The 800-mile Trans Alaska Pipeline is operated by Alyeska Pipeline Service Co. (Alyeska) on behalf of the pipeline owners. It has its origin at the Prudhoe Bay oil fields on the North Slope of Alaska and its terminus at the ice-free port of Valdez. The pipeline route is underlain with continuous permafrost in the north where the climate is the coldest. South of the Brooks Range, across interior Alaska, the permafrost is discontinuous, transitioning to sporadic permafrost along the southern portion of the Copper River Basin. Climate records indicate a gradual warming trend along the entire pipeline route. Permafrost temperature monitoring shows similar trends but with slower warming. Alyeska has focused much of its attention where the permafrost is discontinuous and sporadic because it is closer to its melting temperature. Climate and ground temperature monitoring is ongoing in order to track and appropriately respond to these changes.

MONITORING THE AFFECTS OF CLIMATE CHANGE

Alyeska monitors climate change in several ways. Alyeska constructed and operates 43 instrumented thermal monitoring sites along the pipeline corridor from the Brooks Range to Thompson Pass. At these sites, air, surface, subsurface ground and permafrost temperatures are recorded three or four times a day, 365 days a year. Alyeska also analyzes local weather station data available from the Western Regional Climate Center along the pipeline corridor. In addition, there are over 80 thermistor strings installed in the ground along the pipeline route that measure soil temperatures. These strings are monitored every year or two with the temperature data available through Alyeska's Engineering Data Management system for trend monitoring. Alyeska records subsurface ground temperatures at the base of select VSMs following heat pipe maintenance as part of its trending program.

TAPS PIPELINE SUPPORT SYSTEM

Vertical Support Members (VSMs) are pipe piling embedded in the ground to support the aboveground pipe in areas of thaw-unstable permafrost. Most VSMs south of the Brooks Range have heat pipes installed to keep the ground surrounding the embedded portion of the VSMs frozen. These heat pipes are sealed thermo-siphons that begin to remove heat from the ground when air temperatures fall below ground temperatures. There are a total of 78,000 VSMs throughout the pipeline that are embedded in the ground 15 to 70 feet deep. 61,000 VSMs are configured with 122,000 individual heat pipes, two per VSM.

Alyeska heat pipe monitoring and other thermal studies indicate that the ground around VSM piling is effectively being maintained in a frozen state. The vast majority of VSMs are not moving which means climate changes are not presently affecting VSM stability. Any VSM settlement or movement can be caused by a variety of reasons. When discovered, engineering studies determine the appropriate action necessary to reestablish stability.

trans alaska pipeline system

Climate Monitoring

Recorded climate data are used by Alyeska as an input to computer models to determine the amount of thermal energy that must be removed from the ground to maintain frozen conditions of the permafrost surrounding the Vertical Support members (VSMs).

HEAT PIPE INFRARED EVALUATIONS

Infrared survey of all the heat pipes on the Trans Alaska Pipeline occurs on a three-year cycle. These data are used to predict the performance of the heat pipes installed at every thermal VSM. Heat pipes not meeting the required performance criteria are then listed for repair.

The repair procedure requires recharging the listed heat pipe with refrigerant and subsequent infrared surveys to check performance. After recharging, infrared evaluations are performed to ensure the heat pipes are working properly after maintenance.

The temperature of the permafrost at the base of the VSM is determined after the heat pipe has been recharged through pressure measurements that are converted to temperatures. If the permafrost temperature is approaching 32 degrees Fahrenheit, additional temperature monitoring is conducted. Other spot checks measure permafrost temperatures both where heat pipes have been recharged and where heat pipe recharging is not required to verify the methods used to maintain frozen conditions are working.

HEAT PIPE AND VSM SETTLEMENT MONITORING

The regions of the pipeline corridor where the majority of the heat pipe recharging has occurred lies at the southern fringe of permafrost within the Copper River Basin. This is an area of discontinuous permafrost transitioning to sporadic permafrost. The temperature of the permafrost is relatively warm often approaching the freezing point. At this region's southern boundary, north of Thompson Pass, some permafrost has thermally degraded.

Alyeska has replaced or modified a few thermal VSMs (VSMs with heat pipes) with standard non-thermal friction VSMs at several locations. However, permafrost in the majority of this region remains stable. Heat pipe recharge monitoring and other thermal studies, in addition to settlement surveys, indicate that the ground around VSM piling is effectively being maintained in a frozen state where needed, and that the VSMs are stable.

SITE #4

STUDYING THE EFFECTIVENESS OF AN UNDERGROUND ADJUSTABLE FOUNDATION ON ALLEVIATING THE PROBLEMS ASSOCIATED WITH BUILDING ON PERMAFROST

Danielle L. Jamieson¹ and Michael R. Lilly²

¹Cold Climate Housing Research Center, Fairbanks, Alaska; ²G.W. Scientific, Fairbanks, Alaska

The Cold Climate Housing Research Center (CCHRC) is a non-profit corporation performing research and education on energy efficient, affordable, and sustainable building techniques, designs, and materials. A business and education approach helps turn ideas into solutions. CCHRC carries out its research in its research and testing facility (RTF) figure 1. In the RTF, not only can research be performed, but the entire building is an ongoing experiment in cold climate building technology. The RTF has over 1,000 sensors installed to monitor moisture and temperature throughout the building and surrounding environment. The monitoring systems include monitoring of foundation and background soil and geotechnical conditions. One of the major research projects at CCHRC is gathering data on the permafrost below the building to see how it is affected by the building and, also, how the uniquely designed, underground adjustable foundation performs if permafrost does degrade.

The site on which the RTF is constructed is composed of alluvial silt (loess) which has been cleared of trees for approximately 40-50 years. The site is adjacent to wetlands which are covered by a black spruce forest. Due to the clearing of trees the underlying permafrost has receded over time to a depth between 12 and 30 feet. To study the changes in the permafrost over time, and the direct affects of the building on the permafrost degradation, thermistors were installed to monitor temperature changes in the foundation systems, the underlying soils, and in background sites from land surface to the top of permafrost figure 2. Ground temperatures are monitored by thermistor strings that measure soil temperature profiles. Data is recorded by Campbell Scientific data loggers. Additionally, ground water wells where installed so manual measurements could be made of the water table.

The ground-water observation wells are located at the four corners of the property and range in depth from 18 to 25 feet. The underlying permafrost in each of these four points ranges in depth from 15 to 25 feet. The wells were installed using a solid-stem auger to drill boring holes in which a galvanized pipe was driven to a set depth below the water table. The wells were screened to account for vertical seasonal variation in the water table. Initial drilling provided information on preliminary ground-water levels and direction of flow, which is generally west to east. The wells placed in shallow permafrost areas were driven into the permafrost so that they could also provide data on changes in the top of permafrost elevation over time.

Temperature profiles are gathered at two areas around the building. The first is the located near the southwest corner of the facility. It provides data that has minor disturbance by the building. The second profile section is located on the on the east side of the facility and monitors changes closer to the building. To install the thermistor strings boring holes were drilled and the strings were placed using a custom driving rod. The boreholes were then filled with the same soil that was removed during the drilling process. The soil was compacted with a tamping rod as it was replaced to diminish the air spaces left in the drilled area. Each data gathering string has 12 thermistors spaced to gather relevant data at different depths in the ground. Each hole may have a number of different thermistor profile strings installed. The thermistor strings are attached to a Campbell Scientific data acquisition system. Hourly recordings are taken by each thermistor set. The spacing of the sensors was designed to provide information on the active soil layer, ground water, and permafrost. This information will help with understanding both standard changes in permafrost over time and the affects the building has on degradation of the permafrost.

The building foundation was engineered to be able to adjust to changes in the underlying permafrost figure 3. It is constructed using individually adjustable spread footers placed under a continuous, reinforced grade beam. These two systems can move independently of each other and can be adjusted to accommodate movement of the underlying permafrost. This adjustability is accomplished by the way the two support systems are designed to work together.

To install the foundation, native soils were removed and gravel back fill was placed and compacted to form the base of the spread footers. The spread footers of reinforced concrete with integrated jacking pads were then poured on the compacted fill and non-frost susceptible gravel backfill was compacted around each footer up to the

bottom of the jacking pad. Next, the frame for the reinforced grade beam was constructed on top of the spread footers. It was placed so that the grade beam surrounded each jacking pad. The reinforced grade beam was then poured as a separate unit on top of the spread footers and around each jacking pad. Attached to, and resting on the grade beam is an insulated concrete form wall with built in jacking columns, which protrude inside the basement. The jacking columns align with each jacking pad. Insulation was added to the exterior of all basement surfaces which come into contact with the ground. Following the construction of the foundation and basement walls non-frost susceptible gravel fill was compacted around the exterior of the basement level. If changes in the permafrost below occur the building can be leveled from the interior of the basement.

If the frozen ground starts to recede, hydraulic jacks can be placed on the jacking pads below the jacking columns in the basement. The jacks can be used to push individual spread footers down until the soils reach a stable compaction state, while the reinforced grade beam supports the weight of the building. Then structural foam can be injected through pre-installed tubes to fill the space between the grade beam and the spread footers. The building can be adjusted at 52 interior access points around the basement of the building allowing for leveling of the structure.

Data on the surrounding soil is currently being gathered and the building level is checked every 6 months to monitor relative changes in the height of control points around the basement and first floor levels of the building.

Monitoring of the surrounding soils and the building foundation enables researchers to assess changes in the building's relative level over time and adjust the foundation accordingly. Research on adjustable underground foundations is important because if they prove to be effective they will create another long term option for building on permafrost. This is especially important in areas of discontinuous permafrost where melting and subsidence is more likely to occur.

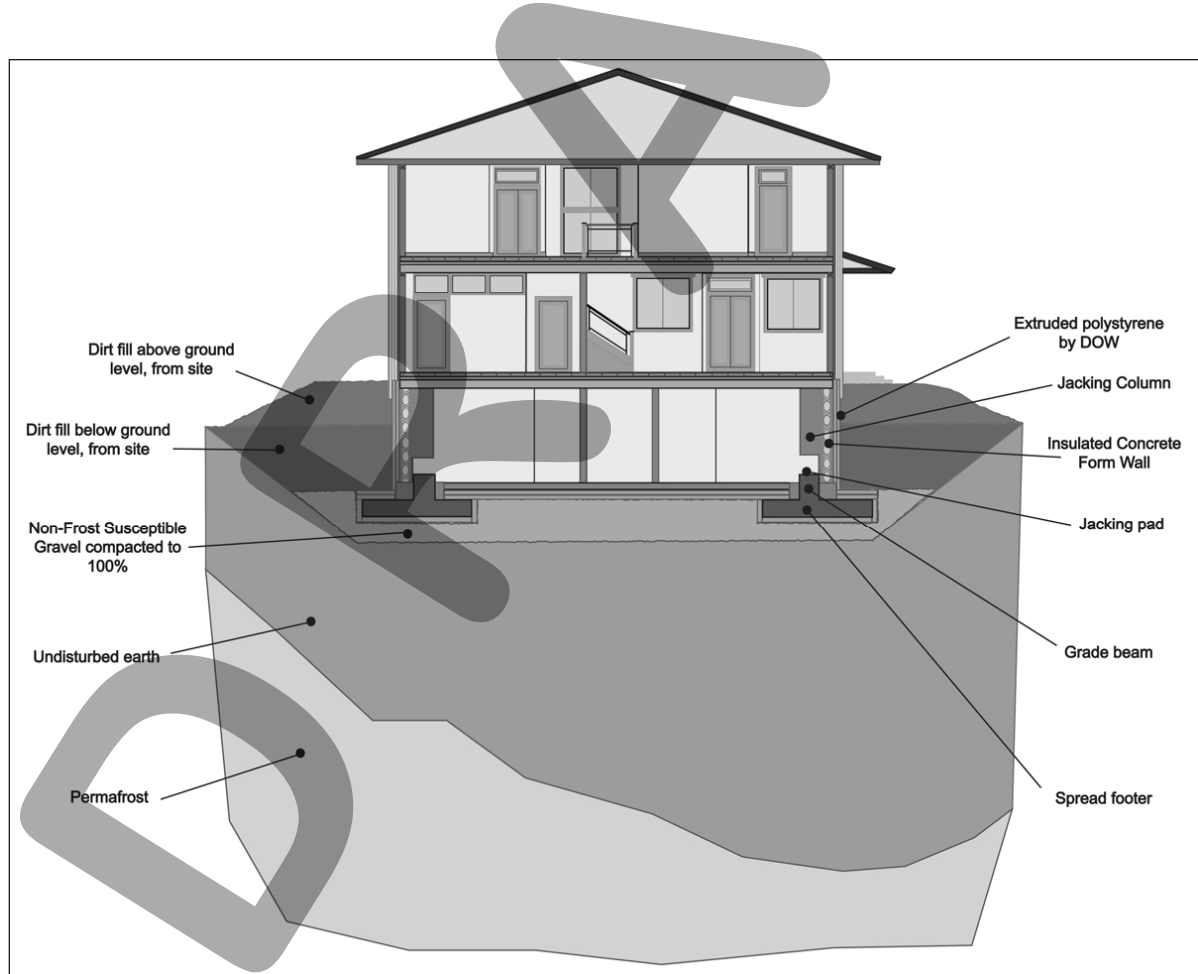


Figure 1. CCHRC Research and Testing Facility cross section

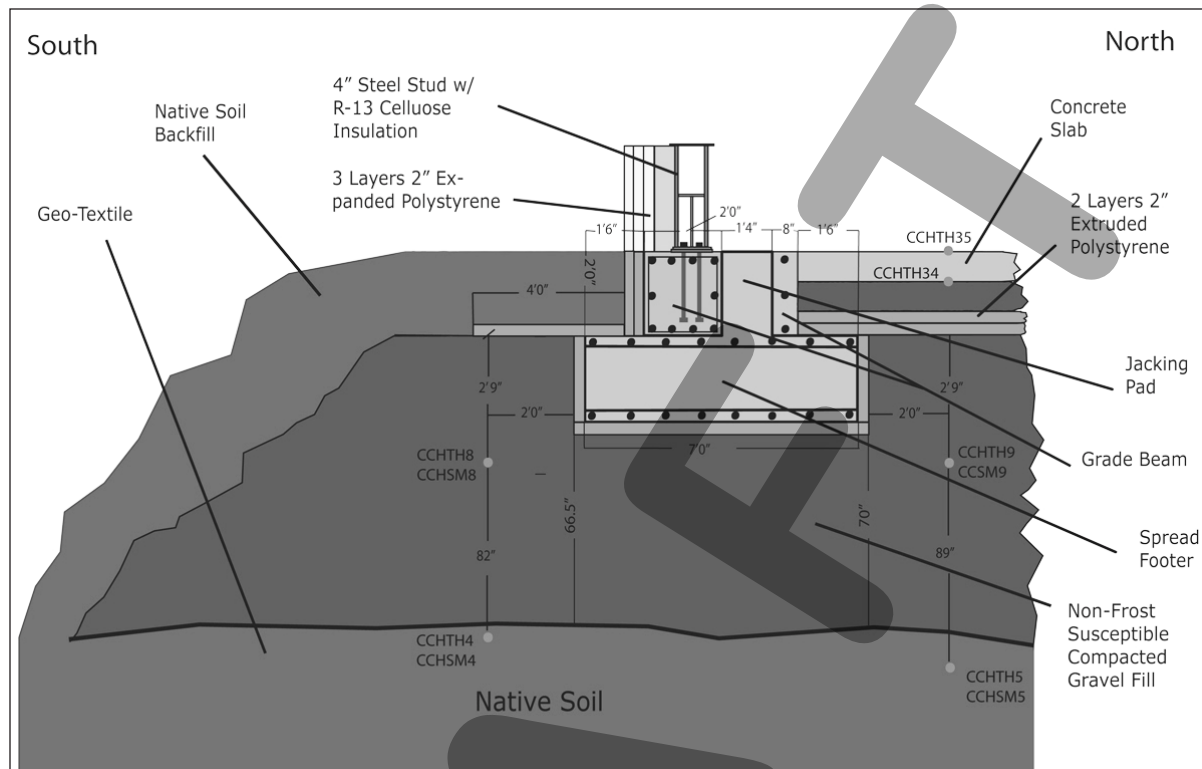


Figure 2. Selected test area of the Research and Testing Facility Foundation

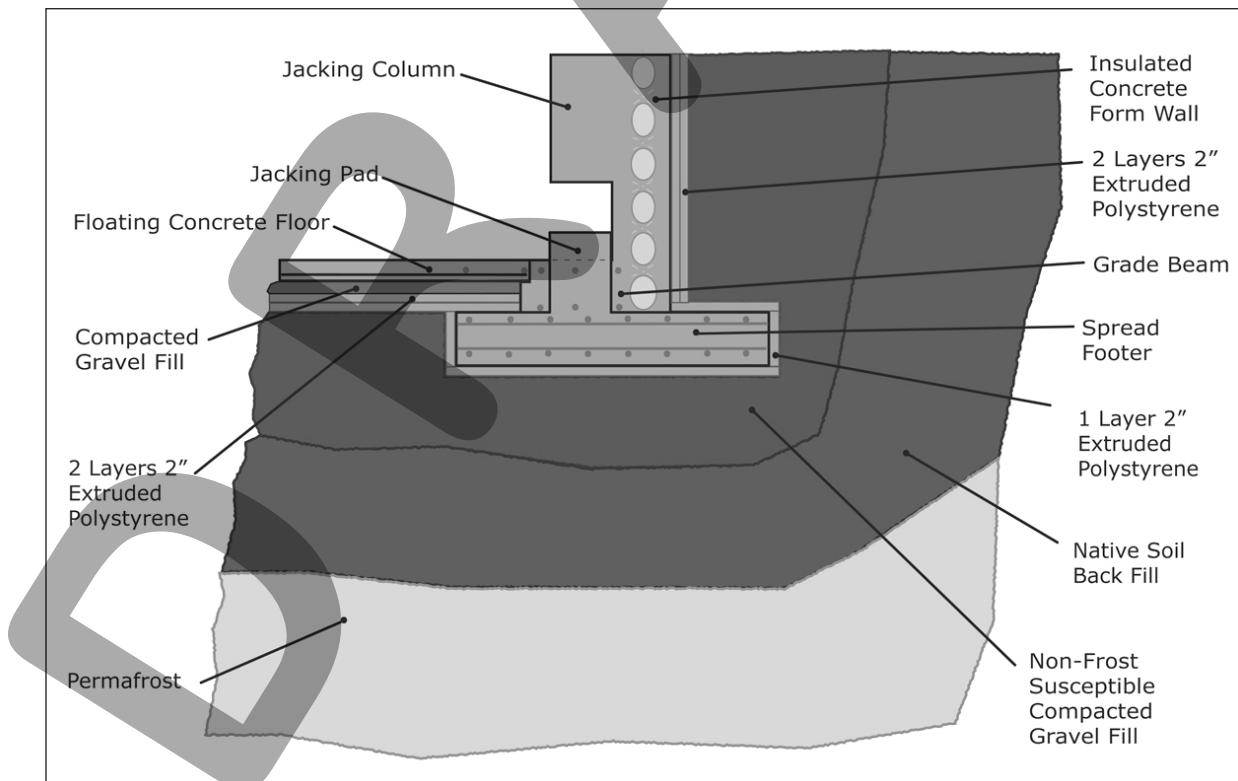


Figure 3. Adjustable foundation detail.

DRAFT

SITE #5

SUNNYSIDE HOUSE

BUILDING ON PERMAFROST: FAILURES AND SOLUTIONS

Michael Lilly¹ and Dennis Filler²

¹Geo-Watersheds Scientific, mlilly@gwscientific.com; ²University of Alaska Fairbanks, ffdmf@uaf.edu

This stop helps illustrate some common problems and solutions for building on permafrost and problems associated with water supply wells located in permafrost. Please do not walk to either house, as one is currently being lived in, and the other has some hazard conditions associated with it. The abandoned house on the west was built in several stages. The well was located in garage, and was drilled before the garage was in place. The well went through permafrost, primarily made of up colluvial deposits from the adjacent hillside. It is likely massive ice lenses are also found in the local permafrost for this area. Water supply wells tend to be completed in underlying bedrock, where adequate flow rates can be obtained from the fracture and foliation planes in the weathered bedrock. The permafrost acts as a local confining zone for the regional ground-water system. Ground-water flow is generally coming down from the bedrock aquifer in the hills directly to the north, and enters into the alluvial aquifer south of the property. The boundary between the hills and alluvial floodplain typically has colluvial silt deposits, rich in permafrost. In areas that have not been cleared in the past, the top of permafrost is relatively shallow, while areas cleared for farming, roads, and residential development will frequently have significant depths of thaw into the top of permafrost. The ground-water system below permafrost may be called a subpermafrost aquifer. Ground-water on top of permafrost is commonly called a suprapermafrost aquifer. In this area, the silts would provide relatively poor aquifer conditions and are not frequently used for water supply.

So, you have a well through permafrost. How do you keep it from freezing? If the well is artesian (flowing), you may let it run continuously so that it does not freeze up. This wastes a lot of water and can create problems with excess water in summer and ice in winter on the land surface. It may also result in thawing the soils outside of the well, enabling water to flow up outside of the well casing, where it can be harder to control. Another method of keeping wells in permafrost from freezing is through the use of heat tapes, which are installed down the well. The application of heat tapes needs to be carefully managed so the heat is turned on only enough to keep the inside of the well casing from freezing, and not cause excessive thawing on the outside of the well. When heat tapes are left on, they can cause the permafrost to melt on the outside of the well. This can often lead to well failure. Where massive ice, or ice-rich permafrost exists, thawing can lead to large voids, which can cause surface settlement around the well casing. These types of problems can be very costly to fix, and pose a problem in areas with warming permafrost in Alaska.

The house in question had a well through permafrost, in a heated garage, covered so conditions around the well could not be easily seen. This area had been developed as a farm many years ago for growing potatoes. The associated land clearing had likely resulted in melting the top of permafrost down from its stable condition. The well had a heat tape installed, which was reported to be left on for an extended period of time. This caused melting of permafrost so water flowed up and into the house during periods when it was not occupied, causing serious structural and environmental problems in the house. The increased settlement around the well and under the house is creating an escalating series of structural failures.

In comparison, the house built to the east was designed for permafrost conditions. Before the house was built, there was a homesteaded log cabin, with adjacent artesian well, which was allowed to freely flow year-round. During periodic freeze-ups, an installed electric tape was used to thaw the well until it flowed on its own again. The house was built on pilings into permafrost to help keep the house and permafrost both stable. The house is typical of structures found on the North Slope. The area under the house remains relatively snow free, which helps cool permafrost during the winter months. The well's own artesian pressure originally supplied the house with water to the first floor, until the recent problem with the house to the east with the failed well and foundation area. The free-flowing well likely dropped the artesian pressure enough that the water to the properly built house needs to be pumped in now.

These two properties help illustrate one of the common ways to build on permafrost, and one that frequently leads to problems. It also helps show the results of not maintaining an adequate ground-water well though permafrost, and the resulting problems that can occur.

DRAFT

SITE #6

O'CONNOR CREEK PINGOS

Kenji Yoshikawa

Institute of Northern Engineering, University of Alaska, Fairbanks

Five small open system pingos are located near O'Connor Creek. They occur near the toe of an alluvial fan. These pingos are among the oldest research pingos in Alaska. In the 1950s, T. Pewe named these pingos, biggest to smallest, as alpha, beta, and gamma. Alpha pingo is an elliptical mound about 100m long, 60m wide, and 10.4m high. The pingo has a breached crater ~6m deep in the center. Most of the pingo's overburden is composed of dry silt. The active layer thickness is 1-3m. Pingo ice was found from 6m to 10 m below surface, including organic layers. The area surrounding the pingos was originally black spruce, muskeg, and bog that had been cleared for farming.

Beta pingo lies about 120m to the northeast of Alpha pingo and is about one-half the size. It has no depression in the center. On the south side, which is steep and slumping, growing trees are deformed and several have split trunks. It seems the mounds have been relatively stable over 40 years. Some of the old bench marks, which Pewe and his student installed in September 1964, still exist without deformation.

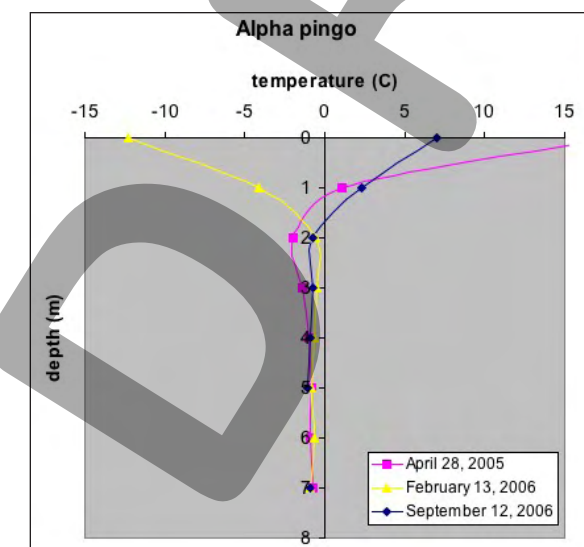
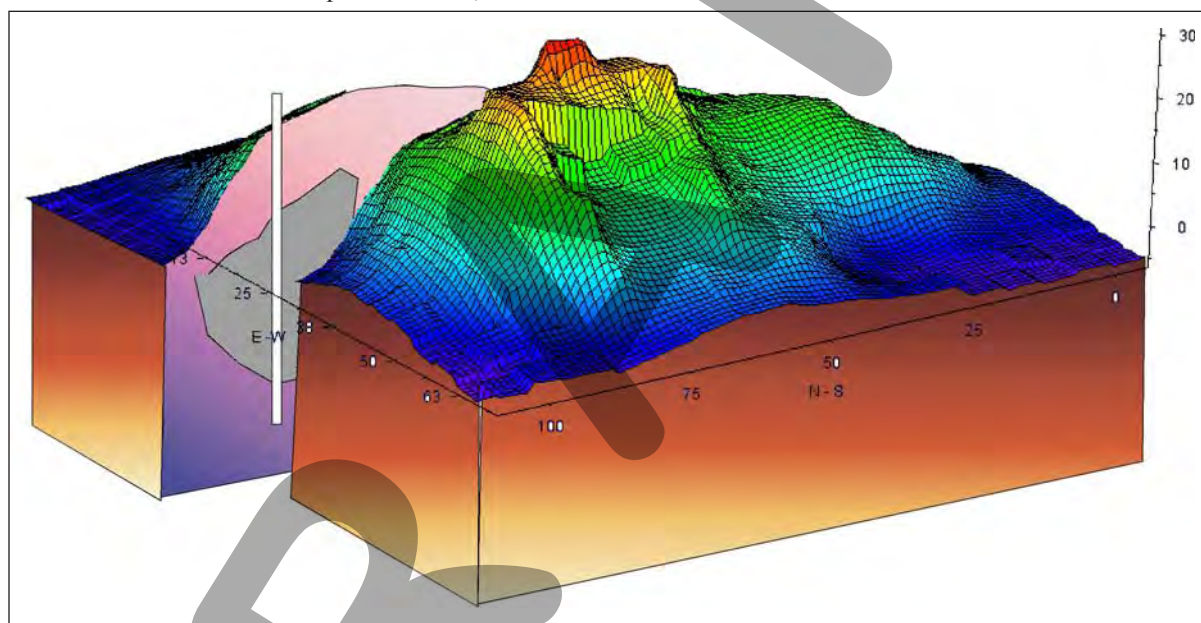


Figure 1 (above). The alpha pingo sketch viewed from north west side. A massive ice core was found 6-10m deep at the north side of the shoulder of pingo (drilled by Yoshikawa 2005).

Figure 2 (left). The temperature profile at Alpha Pingo displays stable cold temperatures below 2 m. A massive ice core was found between 6-10m.

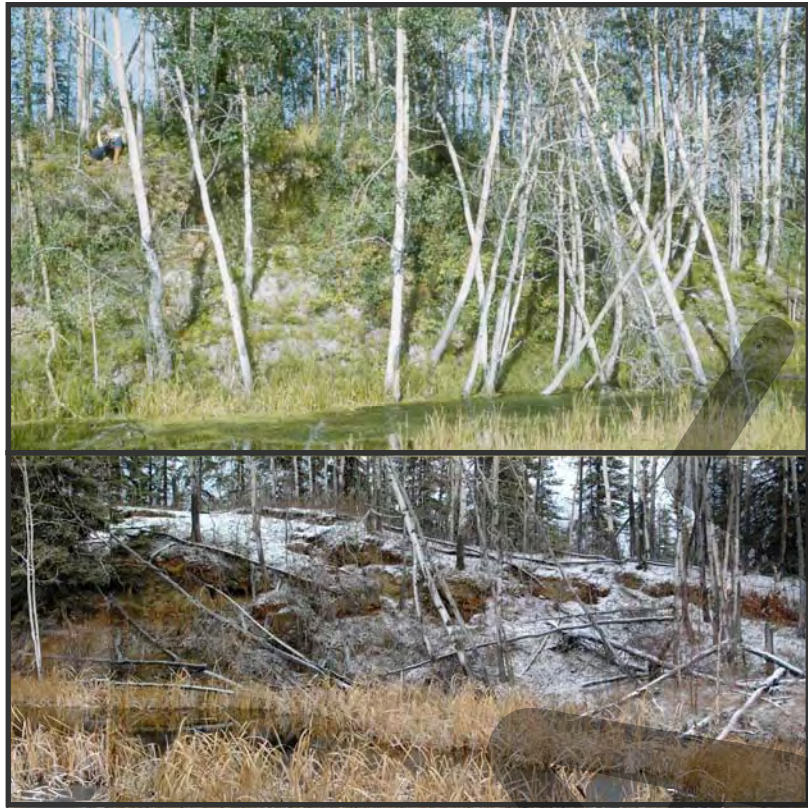


Figure 3. South facing slope of beta pingo (palsa) photo taken in 1965 (above) by D. Hopkins and 1998 (below) by K. Yoshikawa.

	Caribou Cr. A	Caribou Cr. B	O'Connor Cr. α & β	Alder Cr.	Cripple Cr.	Grenac Cr.
Max. active layer	5.60m	2.8m	2.55m	ND	ND	2.2m
Permafrost temp.	-0.70°C @10m	-0.63°C @13m	-0.63°C @6m	ND	ND	-0.72°C @4.5m
groundwater level	+>4 m	ND	+12.3m	ND	ND	+1m
depth to the ice	<5.35m	7.35m	4m	ND	10m	6.5m
activity	No (but icing blister) since 1987 survey	No since 1987 survey	No since Sep.1963 by T. Pewe	No since 1949 aerial photo	No since 1949 aerial photo	No since 1965 by T. Pewe
method						
permafrost thickness (m)	60m est.	60m est.	48.8m	ND	ND	33m
discharge water	1.25 L/sec	No flow	0.06 L/sec	1.25 L/sec	ca. 3 L/sec	0.13 L/sec
water temp.	-0.02 °C	ND	0.02 °C	0.03 °C	ND	ND

Figure 4. Characteristics of the pingos around Fairbanks area.

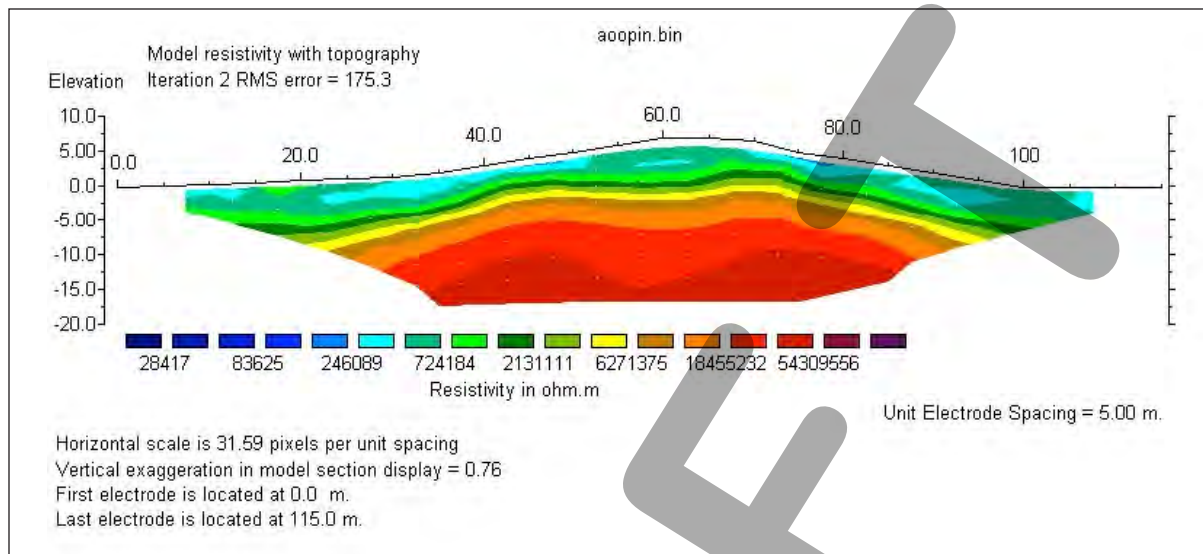


Figure 5. Resistivity tomography result at the Alpha pingo.

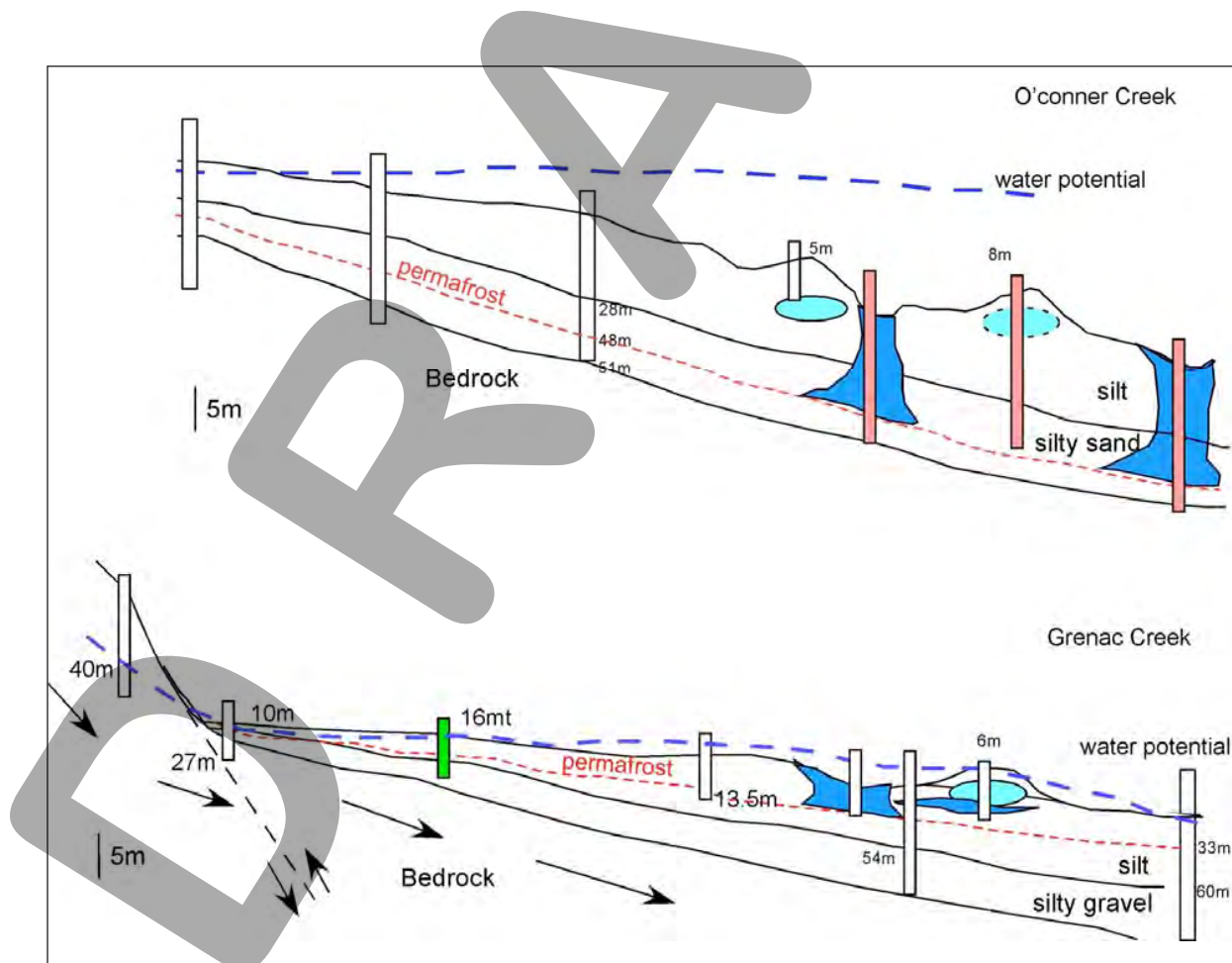


Figure 6. Groundwater potential and open taliks around Fairbanks.

In a nearby drill hole, the silt is 27m thick and overlies 15m of creek gravel. The permafrost is 43m thick. The hydraulic potential of the pingos and the nearby alluvium deposits are high (>68kPa), creating artesian conditions. Most of the homeowners have installed groundwater wells for domestic usage. Heating the well to prevent freezing by the permafrost is critically important and risky work. The permafrost temperature is very warm (>-1°C) and sub-permafrost groundwater is close to the freezing point. Groundwater leaking around the outside of the well casing is a typical problem in artesian wells. In some cases the ensuing discharge from the wells continued to flow through the winter that creating large masses of aufeis (icings), some of which have destroyed houses and covered roads. In November 2005, serious well leakage occurred near the pingo site. Liquid nitrogen was injected to freeze the seepage around the well on February 24, 2006. The well was completely frozen stopping the groundwater discharge. We had the opportunity to monitor sub-permafrost groundwater potentials during and after this event. After the well leakage was stopped, the groundwater hydraulic potential immediately began rising and within a few weeks, har returned to the original pressure.

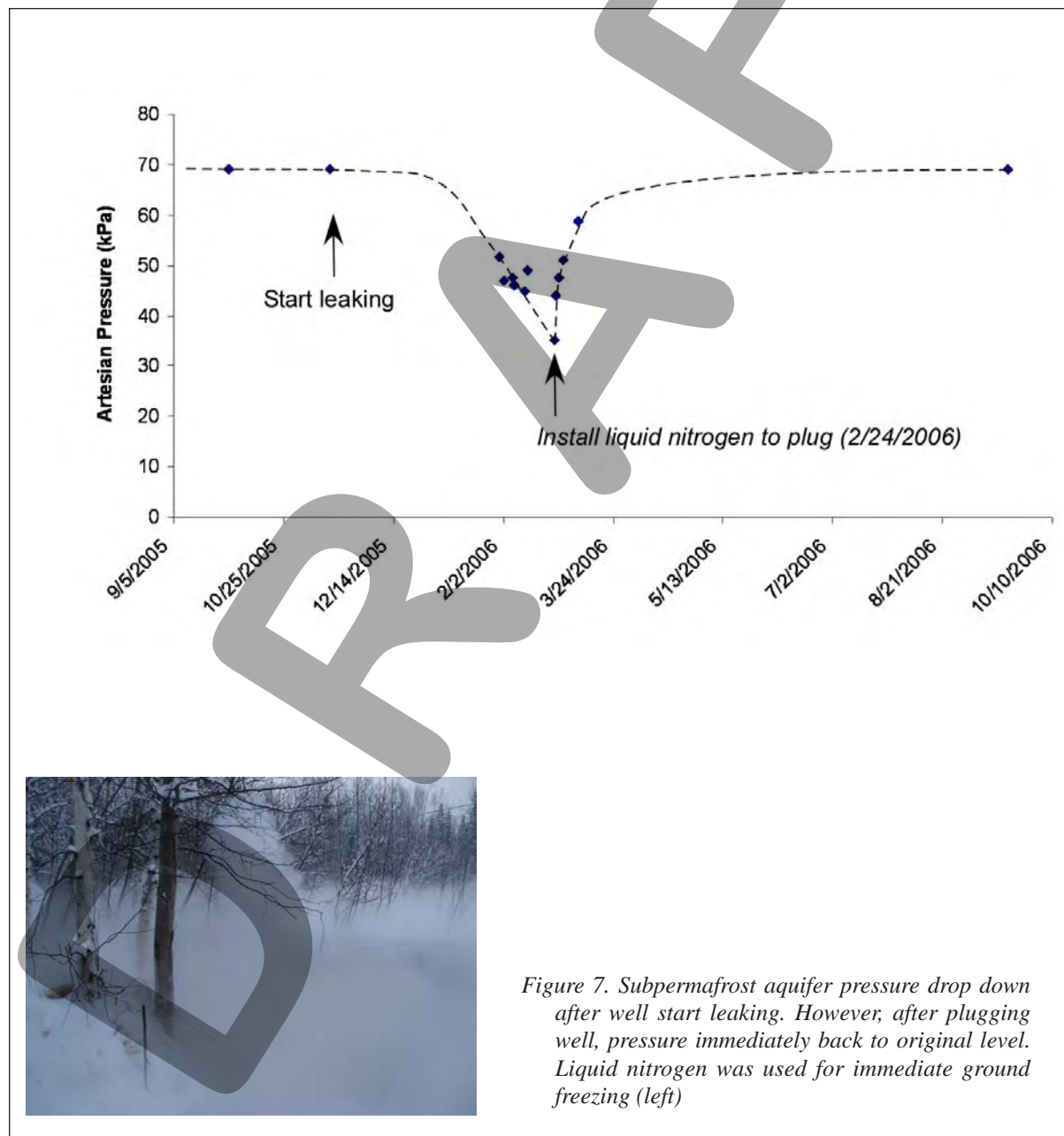


Figure 7. Subpermafrost aquifer pressure drop down after well start leaking. However, after plugging well, pressure immediately back to original level. Liquid nitrogen was used for immediate ground freezing (left)

SITE #7 MURPHY DOME

De Anne S.P. Stevens

Alaska Division of Geological & Geophysical Surveys, 3354 College Rd., Fairbanks, Alaska 99709-3707
deanne.stevens@alaska.gov

Murphy Dome is a scenic upland located approximately 30 km northwest of Fairbanks (fig. 1). It is accessed via Murphy Dome Road, which starts at Goldstream Road and follows the Alaska Railroad along Goldstream Creek valley for 12 km before heading north onto higher ground after crossing Spinach Creek. Murphy Dome is a popular recreation area for Fairbanks residents, with abundant opportunities for hiking, hunting, biking, camping, berry picking, snowshoeing, snowmobiling, and all-terrain vehicle (ATV) riding. It is also a key access point for overland travel to the lower Chathanika River and to Minto Flats and beyond, via ATV in summer and snowmobile in winter.

The accordant rounded ridges north of Fairbanks, including Murphy Dome, have never been glaciated (Pewé, 1953, 1975; Pewé and Rivard, 1961). During past glacial periods eolian loess derived from braidplains originating in the Alaska Range to the south and sediment sources along the Yukon River to the north was transported by winds and blanketed the area. This loess was reworked into thick slopewash and alluvial aprons that are visible in road cuts along Murphy Dome Road. Gullying is prevalent on the lower slopes of these reworked silt deposits. The broad valleys surrounding Murphy Dome are filled with thick alluvial deposits and overlying silt and peat. These valley deposits grade smoothly into the slopewash and alluvial aprons of the slopes.

Fairbanks is in the zone of discontinuous permafrost (Pewé, 1975), leading to many problems during road, railroad and building construction projects. Frost heave and thermokarst settling continue to be serious problems for roads and improperly built structures. Murphy Dome Road itself is in a constant state of disrepair due to these processes, as are most paved roads in Interior Alaska.

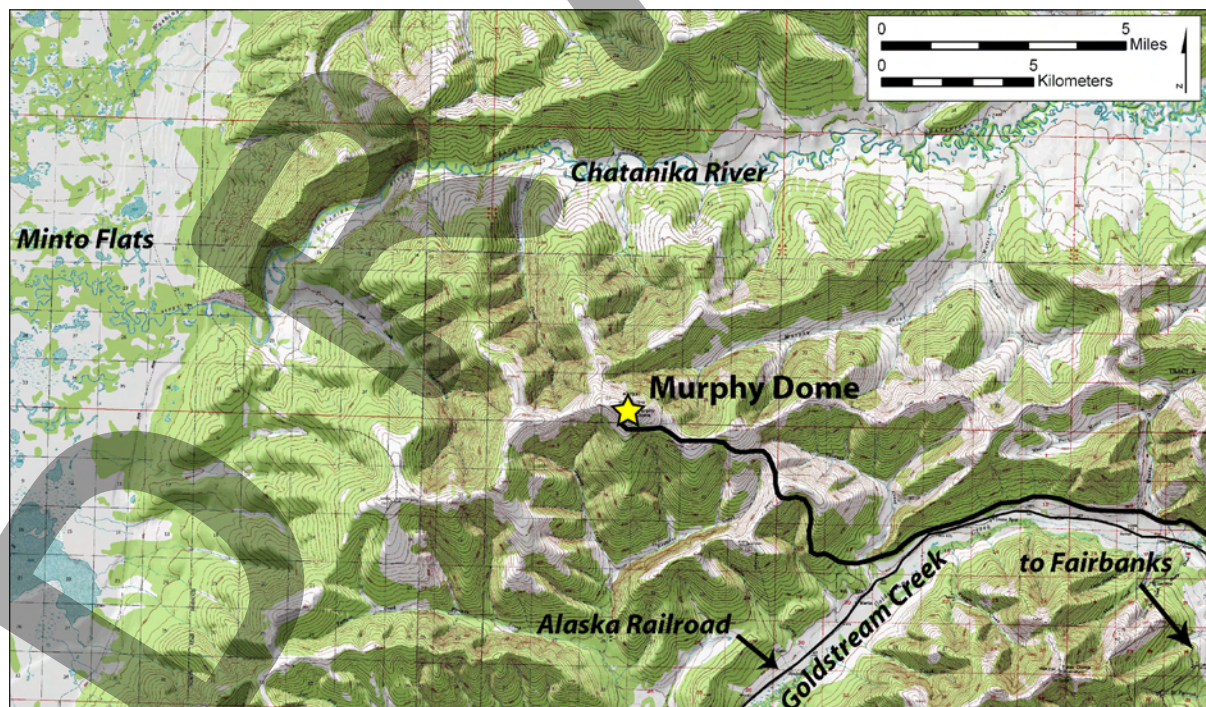


Figure 1. Murphy Dome, a scenic upland located approximately 30 km northwest of Fairbanks, is a popular recreation area for local residents.

The greater Fairbanks area, including Murphy Dome, is part of the Fairbanks mining district. It is located in the western portion of the Yukon-Tanana Terrane, a displaced portion of the North American continental margin. The Yukon-Tanana Terrane consists of Upper Paleozoic and older metasedimentary, metavolcanic, and metaplutonic rocks that crop out for more than 2,000 kilometers, reaching from western Canada and southeastern Alaska to western Alaska (Newberry et al, 1996). The bedrock of Murphy Dome is a very resistant, tor-forming metasandstone (fig. 2). This light to medium gray, quartz-rich, muscovite-biotite grit was probably originally a quartz-rich sedimentary rock that was deposited in a continental margin environment (Newberry et al, 1996).

Vegetation in this area is predominantly taiga, although the top of Murphy Dome is above treeline and is characterized by tundra vegetation (fig. 3). The taiga forest of Interior Alaska is part of the circumpolar boreal forest and consists of a mosaic of forest, grassland, shrubs, bogs, and alpine tundra that have formed primarily as a result of slope, aspect, elevation, parent material, and succession following disturbance. On Murphy Dome, the transition from taiga on the lower slopes to tundra at the top is primarily a function of elevation.

Environmental conditions at the top of Murphy Dome have resulted in a variety of phenomena that are typical of alpine-periglacial settings in Interior Alaska. Characteristic landforms include tors, felsenmeers, stone stripes and polygons, nivation hollows, frost-jacked stones, and solifluction lobes (fig. 4). Many of the scattered small spruce trees that have managed to take root in the upper slopes of Murphy Dome exhibit flagging due to persistent



Figure 2. Tors formed out of the resistant metasandstone bedrock of Murphy Dome.

high winds, especially in winter, or an absence of intermediate branches due to winter wind scour and small animal activity at a level just above typical snow-drift height (fig. 5). Disruption of the surface and subsequent modification of the local hydrology by the major ATV trail leading northwest from the top of Murphy Dome has resulted in thick stands of water-loving alder shrubs growing along the trail's margins. Off-road traffic across the fragile tundra to the lower group of tors has led to the development of areas of bog and mud that continue to expand as trail riders seek to circumvent the difficult trail conditions of prior disturbed areas.

The single radar tower and associated generator backup outbuilding located at the summit of Murphy Dome are all that remain of a former Air Force NORAD control center (fig. 6). This long range radar site is currently remotely operated and maintained, with technicians dispatched from Fairbanks as needed. Murphy Dome Air Force Station became operational in 1951 and included extensive facilities, including personnel living quarters and multiple radar towers. Operations were scaled back as remote control and maintenance became possible, and all military personnel were phased out by September 1983. The aircraft control and warning (AC&W) site was redesignated a long range radar site and a small number of contract civilian personnel remained to provide maintenance. The final phase of radar modernization was completed in the late 1980's with the change out of the older radar for the current AN/FPS-117 minimally attended radar (MAR).

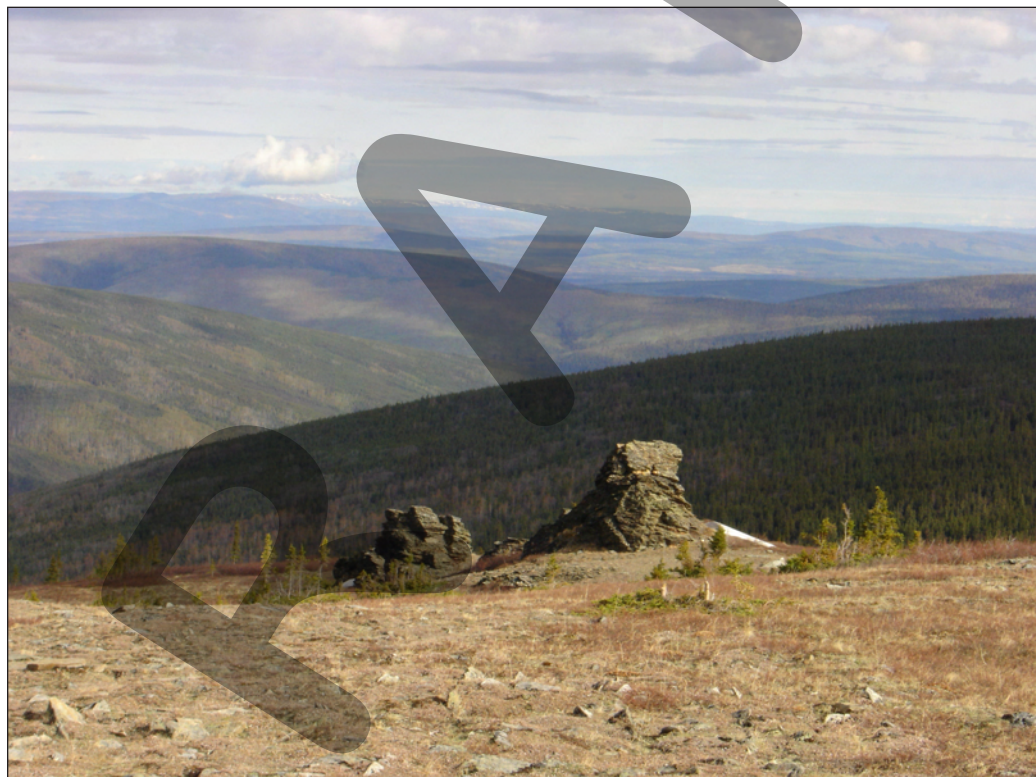


Figure 3. View northwest from Murphy Dome, with the lower group of tors visible in the middle-ground. The upper elevations of Murphy Dome are characterized by tundra vegetation, transitioning into taiga on the lower slopes and surrounding hills. Note frost-jacked stones and stone polygons.

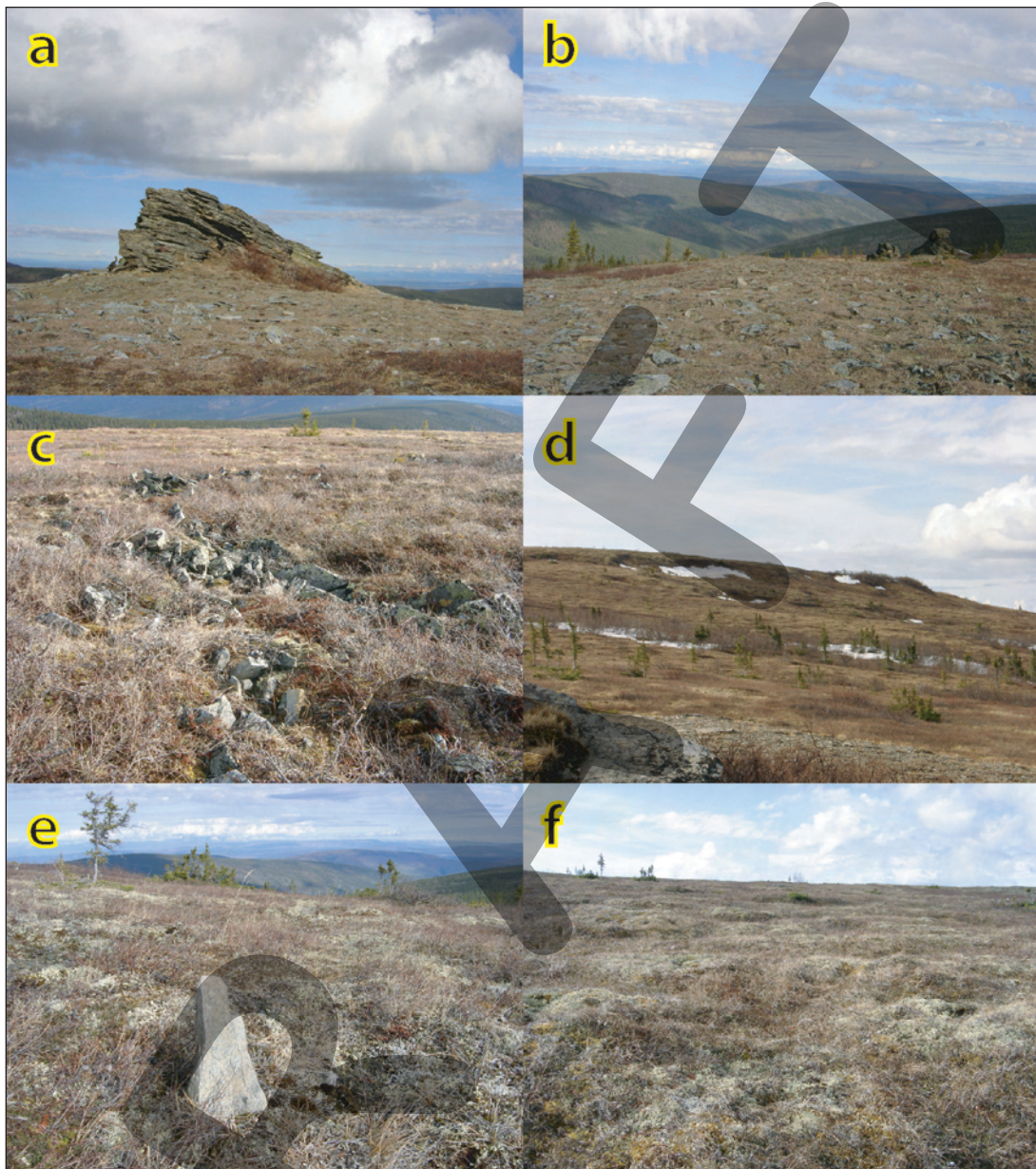


Figure 4. Some characteristic periglacial landforms of Murphy Dome include: a) tors; b) felsenmeers (block fields); c) stone stripes and polygons; d) nivation hollows; e) frost-jacked stones; and f) solifluction lobes.



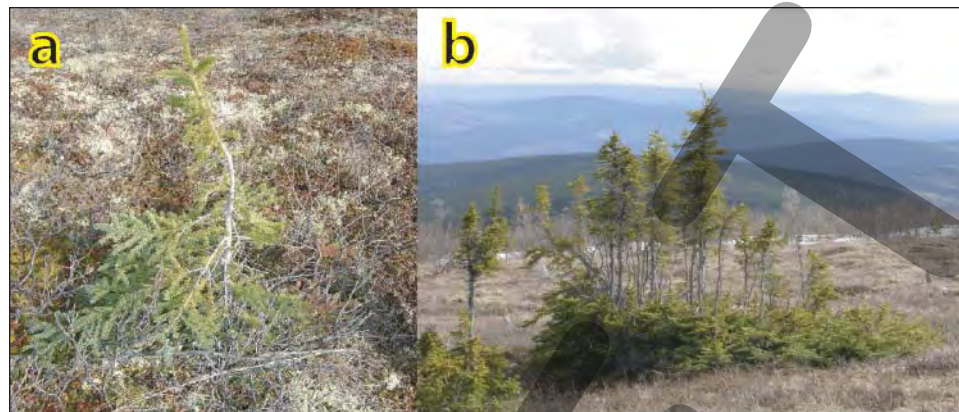


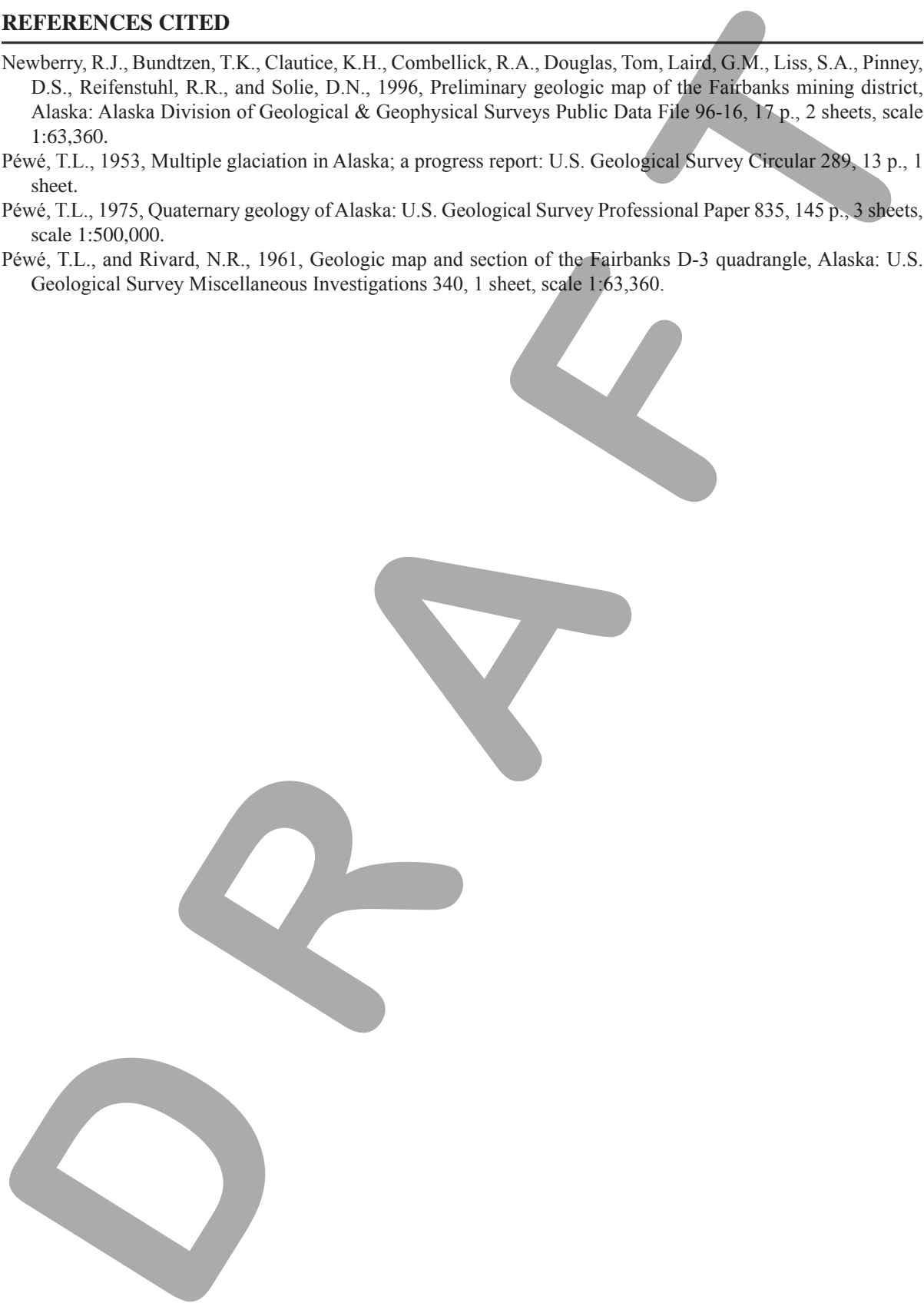
Figure 5. Spruce that have managed to take root in the alpine tundra of Murphy Dome are subjected to high winds and drifting snow. Evidence of the extreme conditions include: a) flagging; and b) absence of intermediate branches.



Figure 6. Radar tower at summit of Murphy Dome.

REFERENCES CITED

- Newberry, R.J., Bundtzen, T.K., Clautice, K.H., Combellick, R.A., Douglas, Tom, Laird, G.M., Liss, S.A., Pinney, D.S., Reifenstuhl, R.R., and Solie, D.N., 1996, Preliminary geologic map of the Fairbanks mining district, Alaska: Alaska Division of Geological & Geophysical Surveys Public Data File 96-16, 17 p., 2 sheets, scale 1:63,360.
- Péwé, T.L., 1953, Multiple glaciation in Alaska; a progress report: U.S. Geological Survey Circular 289, 13 p., 1 sheet.
- Péwé, T.L., 1975, Quaternary geology of Alaska: U.S. Geological Survey Professional Paper 835, 145 p., 3 sheets, scale 1:500,000.
- Péwé, T.L., and Rivard, N.R., 1961, Geologic map and section of the Fairbanks D-3 quadrangle, Alaska: U.S. Geological Survey Miscellaneous Investigations 340, 1 sheet, scale 1:63,360.



SITE #8 GOLD HILL

*James E. Begét, David Stone, Paul Layer, Jeffrey Benowitz, and Jason Addison
Department of Geology and Geophysics, University of Alaska-Fairbanks, Fairbanks, Alaska 997750-5780*

Abstract

Gold Hill has one of the longest records of permafrost history and climate change found anywhere on earth. Tephrochronology and paleomagnetic dating indicates loess began accumulating here ca. 4 million years ago. Sets of ice wedge casts and thermokarst features more than two million years old occur near the base of the 35 m high loess cliffs. Fluvial sediments and organic rich silts deposited before 3 million years ago record warmer and wetter conditions in interior Alaska. Geochemical studies show the loess is primarily derived from glacial silt transported downstream from the Alaska Range along the Tanana River, with a minor component being transported to this site from the Yukon River and the Brooks Range.

Keywords: Climate change; permafrost; loess, geochronology, Quaternary; Alaska.

TIME NEEDED FOR THIS SITE

Allow anywhere from 5 minutes to 2 hours for this stop. The bus will let people out near the Troy Péwé memorial stone. You can see and photograph much of the 35-m-high loess cliffs from the bus stop area. Alternatively, if you want to spend more time at this locality, then follow the signs and the trail 0.5 km to the east, where exposures of loess, volcanic ash and ancient ice wedges casts occur.

THE TROY L. PÉWÉ CLIMATIC CHANGE PERMAFROST RESERVE

In 1999 the University of Alaska became the owner of 25 acres of Gold Hill. The area you see before you was set aside as the “Troy L. Péwé Climatic Change Permafrost Reserve” Troy Péwé first studied the site while working for the U.S. Geological Survey in 1949. During the 1950s and 1960s Dr. Péwé was a professor at the University of Alaska in Fairbanks and continued his work on loess. Dr. Péwé then moved to the University of Arizona, but continued working with new colleagues in Alaska until the end of his career. Péwé received an honorary degree from UAF in 1991 for his contributions to the understanding of Alaska geology and his pioneering permafrost research.

The 35-m-high cliffs of wind-blown silt preserved at Gold Hill within Troy L. Péwé Climatic Change Permafrost Reserve contain the oldest loess deposits recognized in this area or anywhere in Alaska. The loess here is rich with clues to the last several million years of Alaska’s geological history.

From the stone you can see a dark horizon running across the loess cliff just below the top. This dark horizon is the last interglacial (Marine Isotope Stage 5) paleosol. The loess nearest and just north of the stone is more than a million years old at the base, and overlies gold-bearing gravel. The trail to the east leads to the fieldtrip stop where the loess is thickest and the base of the loess is about 4 million years old. If you want to spend more time at this stop, then hike the trail to the exposure.

Figure 1. Location of the field trip stop at Gold Hill.

You can see the 35-m-high loess cliffs from the bus stop at the Pewe Memorial Stone, or you can walk the trail to the exposure.



GRAVEL DEPOSITS LEFT BY HYDRAULIC GOLD MINING

As you walk along the trail, notice the coarse gravel around you. These are mine tailings. Gold was discovered in creeks around Fairbanks in 1902, causing a gold rush the next spring. By November 1903, Fairbanks had a population of several thousand and was an incorporated city.

In 1905, gold production had risen to \$6,000,000 a year, and gold was already being produced from underground tunnels dug to reach the gravels found under the loess deposits. By 1908 there were 18,500 people in the Fairbanks mining district, but by 1920 the town's population had shrunk to 1,100 as the miners had mined most of the easy surface gold but were unable to dig through thick loess like that exposed here at Gold Hill.



Figure 2. Example of gold-mining dredges used at Gold Hill. The gravel was taken into the dredge using the excavator buckets on the right. The gold was separated from the gravel within the dredge using mechanical and chemical processes, and the processed gravel was dumped behind the dredge by the large boom on the left.

Mining revived in the 1920s when a large corporation bought up the claims of individual miners and began industrial scale dredge mining that continued until the 1950s. The Gold Hill loess cliffs were excavated during this period. Miners used hydraulic giants (giant hoses) to direct streams of water at the loess cliffs to thaw the frozen silt and wash it away. Then they injected steam into the frozen gravel beneath the loess, and used dredges to mine the gold. The gold dredges were floating factories that slowly chewed their way through the gravel beds. The dredges excavated the gravel with huge buckets, creating a small pond in which the dredge floated. The waste gravel was left behind the dredge, and refilled the pond. Dredges operated in several of the valleys around Fairbanks up until 1959.

LOESS DEPOSITS AT GOLD HILL

Loess deposits are common across central Alaska and the northwestern Yukon Territory, especially in low-lying areas near the Tanana and Yukon and other glacier-fed rivers. Large areas of frozen ground in valley bottoms in central Alaska occur in loess and reworked eolian silts. River erosion or human disturbance of loess due to building or highway construction or sometimes reveal spectacular views of ice wedges, ice lenses, and other varieties of permafrost.

Péwé (1951) first recognized that the silts that blanket hillslopes and form thick deposits in valley bottoms near Fairbanks and other areas were eolian in origin, and suggested that the ice wedges and other periglacial features found in the loess were produced during the last ice age.

Large areas of valley filling loess deposits were washed away and destroyed by hydraulic excavation and dredging during 20th century industrial scale gold mining operations near Fairbanks, Ester, Chicken, and other mining areas in central Alaska. When the mining operations stopped, cliffs of loess and other sediments 10-40 m thick were left in some areas. As a result of the gold mining, numerous bones and occasional frozen carcasses of bison, mammoths and other extinct Pleistocene megafauna were collected from the loess and the alluvial gravels beneath the loess (Guthrie, 1990).

The Gold Hill site, located along the north side of the Parks Highway beginning about 3 km southwest of the University of Alaska Fairbanks campus, preserves a vertical bluff of loess almost 5 km long produced by hydraulic mining in the Fairbanks area. The highest cliffs of loess occur at the eastern end of the Gold Hill exposure and are as much as 35 m high. The original surface of the loess originally sloped gently downwards to the south, and small "islands" of the original loess valley fill left by the mining operations are preserved on the south of the Parks Highway.

Péwé (1975a, b) divided the loess at Gold Hill into four main stratigraphic units. An upper loess section locally overlies a zone of buried logs and named the Eva Creek Forest Bed, formed during the last interglaciation (Péwé et al., 1997), which in turn overlies thick deposits of loess the Gold Hill silt. A basal forest bed occurred in a few sites was named the Bonanza Creek Forest Bed (Péwé, 1975b). The base of the Gold Hill loess section was assumed to be “Illinoian” in age, i.e. less than 200,000 years old (Péwé, 1975a; Péwé and Reger, 1983).

The first indication that Alaskan loess deposits might be much older came from the discovery that the loess contained numerous paleosols, and the inference that the paleosols recorded many more warm periods in addition to those recorded by the Eva Creek and Bonanza Creek Forest Beds (Beget, 1988; 1991). The sequences of multiple paleosols and interstratified loess deposits found at Gold Hill and other sites were interpreted as glacial-interglacial cycles, requiring an age for the loess much older than originally inferred by Péwé. Subsequently Beget and Hawkins (1989) showed that the loess deposited in glacial and interglacial periods had different geophysical properties, and that changes in environmental magnetic signals recorded in the loess could be used to produce proxy climate records through loess sections in Alaska that correlated with Milankovitch models of insolation changes and marine isotope records (Beget et al., 1990). The environmental magnetic properties of loess and interglacial soils were reversed from those found in loess-paleosol sequences in China because of local differences in source material and high latitude pedogenic processes, including gleaming associated with permafrost (Beget, 1996; 2001).

Westgate et al. (1990; 2003) used tephrochronology and paleomagnetic stratigraphy to determine that the PA tephra found at ca. 21 m depth at Gold Hill was deposited ca. 2.02 ± 0.14 million years ago, and loess at the base of the Gold Hill section was as much as 3.1 million years old (fig. 3). Westgate and his co-workers took samples at 10 cm intervals, and found the upper loess was normally magnetized and correlative with the Brunhes paleomagnetic epoch. The lower part of the loess recorded mainly reversed magnetic fields, but in the overall reversely polarized section there were magnetic reversals back to normal polarity at about 2.5 meters, 3.5 meters, 5.5 meters, and 8.2 meters below the PA tephra layer. The initial transition from normal to the reversely magnetized loess was correlated with the Brunhes-Matuyama boundary, and the two normal epochs below the PA tephra were assigned to the Huckleberry Ridge and Reunion subchrons.

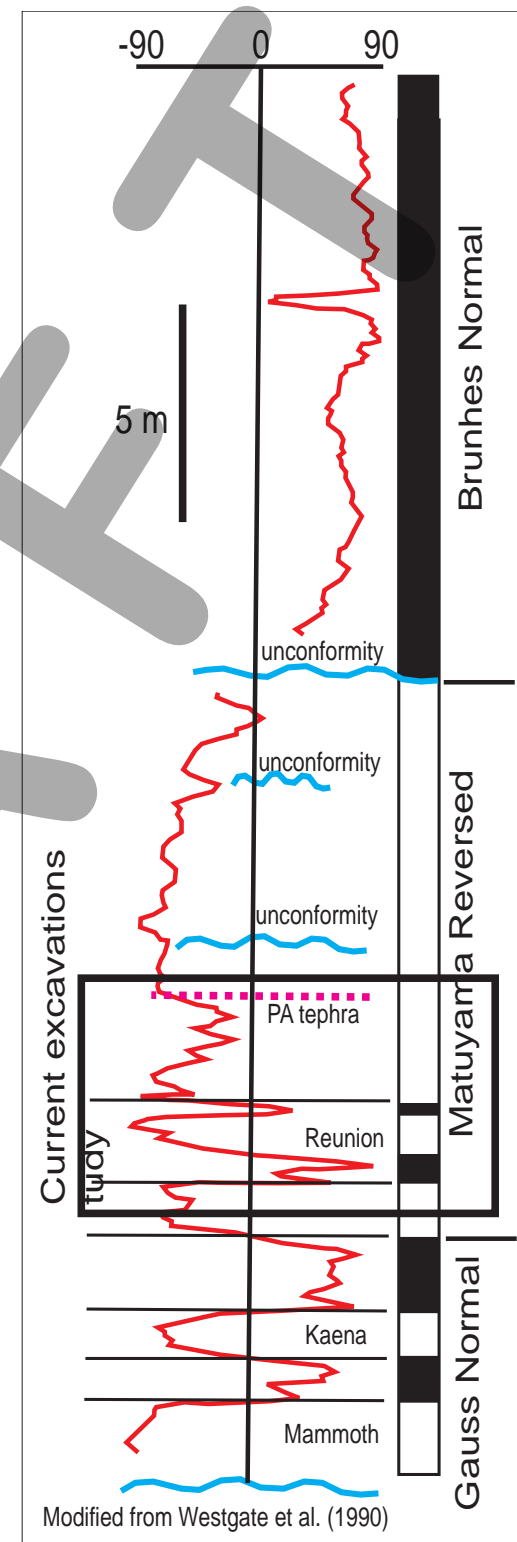


Figure 3. Preliminary geochronology for the Gold Hill Loess. Black vertical bars indicate zones of normal magnetization and white bars are reversed zones. Current excavations expose ice wedge casts and thermokarst collapse features formed during glacial to interglacial climate cycles 2.2-2.0 million years ago.

Recent work at Gold Hill has resulted in the discovery of ice wedge casts, thermokarst features, and interstratified loess and paleosol sequences found below the PA tephra at the base of the Gold Hill section (Beget et al., 2008). The paleosols and ice wedge casts were dated using a new paleomagnetic reversal stratigraphy developed for the Gold Hill loess. Our data suggests that Alaskan loess deposits are surprisingly good recorders of short-lived geologic events, including transient shifts in climate and fluctuations in the earth's magnetic field. Loess deposits can provide long paleoclimatic records of events in terrestrial areas during the last several million years.

FIELD STRATIGRAPHY AT GOLD HILL

The PA tephra layer is located 11 m from the bottom of the loess section, and forms a distinctive and marker bed that can be traced for more than 30 m across the lower part of the Gold Hill loess. In places the tephra is as much as 5 cm thick, although in most places it is broken into pods or several thinner layers. The PA tephra records the position of the ground surface ca. 2 million years ago. Because the PA tephra can be traced for more 25 m across the exposure, it was used as the datum from which local stratigraphic measurements were taken. It is also used as the tie point to correlate the magnetic work of Westgate et al (1990) with our current work.

Trenching and sampling was done at two new sites, one about 5 m east of the long section studied by Westgate et al. (1990) and second about 20 m east (fig. 4). These sites will be open for viewing and discussion during the field trip. The three trenches expose what we have interpreted as ice wedge casts and thermokarst collapse features extending as much as several meters deep below the PA tephra. Thermokarst collapse features of similar size are forming today in Fairbanks where permafrost is thawing.

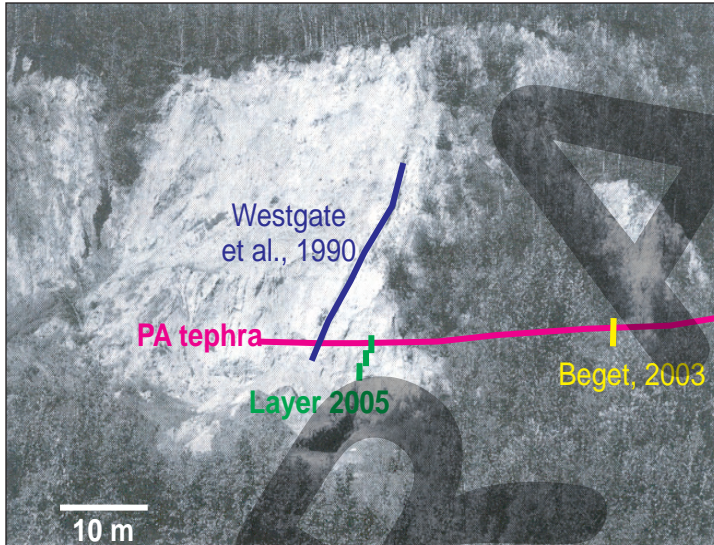


Figure 4 . Location of the PA tephra and trenches exposing ancient periglacial features at Gold Hill, Alaska.

FEATURES AT THE FIELD SITE

During our trenching and logging it became apparent that loess just below the PA tephra had been locally involved in a series of post-depositional collapses. The PA tephra was deposited on the ground surface ca. 2 million years ago, and thus sediments at Gold Hill that are overlain by the tephra can be precisely dated. Our trenching sites were chosen specifically at sites where we can demonstrate the trench sediments are overlain by the PA tephra (Naibert et al., 2005).

Our excavations reveal the PA tephra was incorporated in local depressions in 4 distinct areas along the 30-m-long exposure. At the eastern pit the tephra and the intercalated loess, which elsewhere are preserved in sub-horizontal beds, abruptly began to drop in elevation on each side of a 2-m-wide "V" shaped depression. Further excavations found pellets of the tephra and blocks of loess in a compact silt matrix within the depression. The "V" shaped depression was excavated to a depth of 2 m where it became narrow and terminated. This feature is interpreted as an ice-wedge cast (Beget et al., 2008).

At the western pit, a well-developed organic-rich paleosol about 20-60 m thick above the PA tephra appears to be involved in a high angle slump with the tephra. This paleosol can be traced along much of the exposure above

the PA tephra. The excavations in the western trench found crudely bedded organic-rich sediment and loess and pods of PA tephra had apparently collapsed into a broad depression. This feature is interpreted as a thermokarst collapse.

At the far eastern of the PA exposure, a loess cliff exposed a 3-m-thick diamictite that could be traced 5 m across the section. The diamictite contained rounded to elongate silt and multi-colored paleosol clasts ranging from 0.5-10 cm in diameter disseminated in a dense, fine-grained matrix. The eastern margin of this deposit cuts across undisturbed loess below the PA tephra and itself locally underlies the PA tephra and incorporates pods of the tephra. We interpret the diamictite as having formed by progressive collapse of wet, thawed pellets and blocks of sediment into a large thermokarst pit. Similar large pits can be seen today where frozen loess is thawing at several sites around Fairbanks, and bits of the thawed ground can frequently be heard falling into the pit. We believe this large thermokarst collapse feature formed in a similar fashion two million years ago.

The presence of ice wedge casts and thermokarst features below the PA tephra indicates climate in the Fairbanks had cooled sufficiently by two million years ago to allow the formation of permafrost. The climate subsequently warmed and caused the permafrost to degrade. A well-developed paleosol found above the PA tephra records an interglacial that occurred soon after the PA tephra fall. These features record a glacial-to-interglacial climate cycle similar in duration and intensity to those that occurred during late Pleistocene time.

REFERENCES

- Beget, J.E., 1988. Tephras and sedimentology of frozen loess: In: Senneset, I.K. (Ed.), Proceedings of the Fifth International Permafrost Conference, Tapir, Trondheim, p. 672-677.
- Beget, J.E., 1991. Paleoclimatic significance of high latitude loess deposits. In: Weller, G. (Ed.), Proceedings of the International Conference of the Role of the Polar Regions in Global Change, Geophysical Institute, Fairbanks, pp. 594-598.
- Beget, J.E., 1996. Tephrochronology and paleoclimatology of the last interglacial-glacial cycle recorded in Alaskan loess deposits. Quaternary International 34-36, pp. 121-126.
- Beget, J.E., 2001. Continuous late Quaternary proxy climate records from loess in Beringia. Quaternary Science Reviews 20, pp. 499-507.
- Beget, J.E., and Hawkins, D., 1989. Influence of Orbital Parameters on Pleistocene loess deposition in central Alaska. Nature 337, p. 151-153.
- Beget, J.E., Layer, P., Stone, D., Benowitz, J., and Addison, J., 2008. Evidence of Permafrost Formation Two Million Years Ago in Central Alaska. Proceedings of the Ninth International Permafrost Conference, Fairbanks, Alaska. In press.
- Beget, J.E., Stone, D.E., and Hawkins, D. 1990. Paleoclimatic forcing of magnetic susceptibility variations in Alaskan loess. Geology 18, 40-43.
- Guthrie, D.R., 1990. Frozen Fauna of the Mammoth Steppe: The Story of Blue Babe. Univ. Chicago Press, 338 p.
- Naibert, T.J., Domeier, M.M., Robertson, K.L., Fallon, J.F., Stone, D.B., Beget, J.E., and Layer, P.W., 2005. Re-evaluation of the magnetostratigraphy of the Gold Hill loess, Interior Alaska. American Geophysical Union. AGU Fall Meeting Abstracts, p. A96.
- Péwé, T.L., 1951. An observation on wind-blown silt. Journal of Geology 59, p. 399-401.
- Péwé, T.L., 1975a. Quaternary Geology of Alaska. U.S. Geological Survey Professional Paper 835, 145 p.
- Péwé, T.L., 1975b. Quaternary stratigraphic nomenclature in central Alaska. U.S. Geological Survey Professional Paper 862, 32 p.
- Péwé, T.L., Berger, G.W., Westgate, J.A., Brown, P.M., and Leavitt, S.W., 1997, Eva Interglaciation Forest Bed, Unglaciated East-Central Alaska: Global Warming 125,000 Years Ago: The Geological Society of America Special Paper 319, 54p.
- Péwé, T.L., and Reger, R.D., 1983, Richardson and Glenn Highway, Alaska, Guidebook to Permafrost and Quaternary Geology: Alaska Division of Geological & Geophysical Surveys Guidebook 1, 263 p., 1 sheet, scale 1:250,000.
- Westgate, J.A., Stemper, B.A., and Péwé, T.L., 1990, A 3 m.y. record of Pliocene-Pleistocene loess in interior Alaska: Geology, v. 18, p. 858-861.
- Westgate, J.A., Preece, S.J., Péwé, T.L., 2003, The Dawson cut forest bed in the Fairbanks area, Alaska, is about 2 million years old, Quat. Res., V. 60, p. 2-8.

DRAFT

SITE #9

THERMOKARST PITS AND FENS IN GOLDSTREAM VALLEY

Torre Jorgenson
ABR

Thermokarst pits and fens surrounded by collapsing forests can be found just south of the peat mine near the intersection of Murphy Dome and Goldstream Road (fig. X). Parking is available at the peat mine, which is filling with water and recovering naturally with abundant wetland vegetation. A 300-m long trail goes around the east side of the mine and leads to a deep thermokarst pit, a thermokarst fen, and a site with actively collapsing trees. The peat mine, which provided organic matter for landscaping for several years during the early 2000s, took advantage of thick peat deposits that had been long locked in permafrost.



Figure 1. Southeast of the peat mine are thermokarst pits, fens, and actively collapsing forests. A “moat” surrounds the margins of areas with rapidly collapsing permafrost. After collapse the groundwater-fed water body quickly becomes colonized by sedges and cattails to become a fen.

Thermokarst is abundant in ice-rich lowland areas around Fairbanks on fine-grained soils associated with lowland loess, retransported deposits, and abandoned floodplains. Typical thermokarst landforms include shallow thermokarst lakes, bogs, fens, and pits. Recent analysis indicates that permafrost covers ~62% of the discontinuous permafrost zone in central Alaska, thermokarst covers 5% of the landscape, 21% is unfrozen, and on 12% permafrost status remains undetermined. Thermokarst landforms are dominated by thermokarst fens (1.8% of area), bogs (1.0%), lakes (1.0%), and pits (0.3%). Fens and bogs predominate because the shallow water formed after collapse quickly fills in with either herbaceous fen or Sphagnum bog dominated vegetation.



Figure 2. The ice-rich lowlands in Goldstream Valley are susceptible to permafrost degradation that takes the form of thermokarst lakes, pits, bogs, and fens. The deep thermokarst pit (left) has relatively warm, nutrient-rich water, and abundant methane emissions. At an area of rapid collapse (right), the trees fall into the pit so quickly over a summer that they don't have a chance to adjust their growth, as evident by the curving trees along the edge of the pit shown on the left.

At this site, both thermokarst pits and fens are evident. The pit in Figure X has collapsed 2.5 m causing the trees to lean inward and fall into the water. The pit remains isolated from groundwater movement. Due to nutrients released from the previously frozen peat and silt, the water is quickly colonized by duckweed and algae. Stirring of the bottom sediments can cause vigorous bubbling of methane gas. Adjacent to the pit is a thermokarst fen that has become connected to groundwater moving down slope from the nearby hillside. In this minerotrophic environment, the collapsed area quickly becomes colonized by aquatic sedges and cattails. Immediately next to the steep collapsing bank an open-water “moat” forms, where vegetation has not yet colonized. The soil has become well-drained next to the fens and vegetation has converted from black spruce to birch trees. Beavers and waterbirds have colonized the open water within the fen and the beavers have felled many of the birch trees along the margins. Thus, the thermokarst has created a radical conversion in habitat and wildlife use.

Thawing of ice-rich soil also severely damages roads and creates costly maintenance problems. Nearby Goldstream Road develops long, shallow longitudinal cracks (0.5 m wide by 0.1-0.2 m deep) in the roadbed every year due to thawing and slumping of permafrost at the margins of the roadbed. Thawing along the margins is accelerated by insulating snow that is plowed off the road during winter and shallow ponds are developing in the ditches. Nearly every year road-maintenance crews fill in the long cracks with additional asphalt and substantial amounts of gravel has been added to the slumping shoulders of the road.

SITE #10

GREAT NORTHWEST PEAT MINE

Kenji Yoshikawa¹ and Vladimir Romanovsky²

¹*Institute of Northern Engineering, University of Alaska, Fairbanks*

²*Geophysical Institute, University of Alaska Fairbanks*

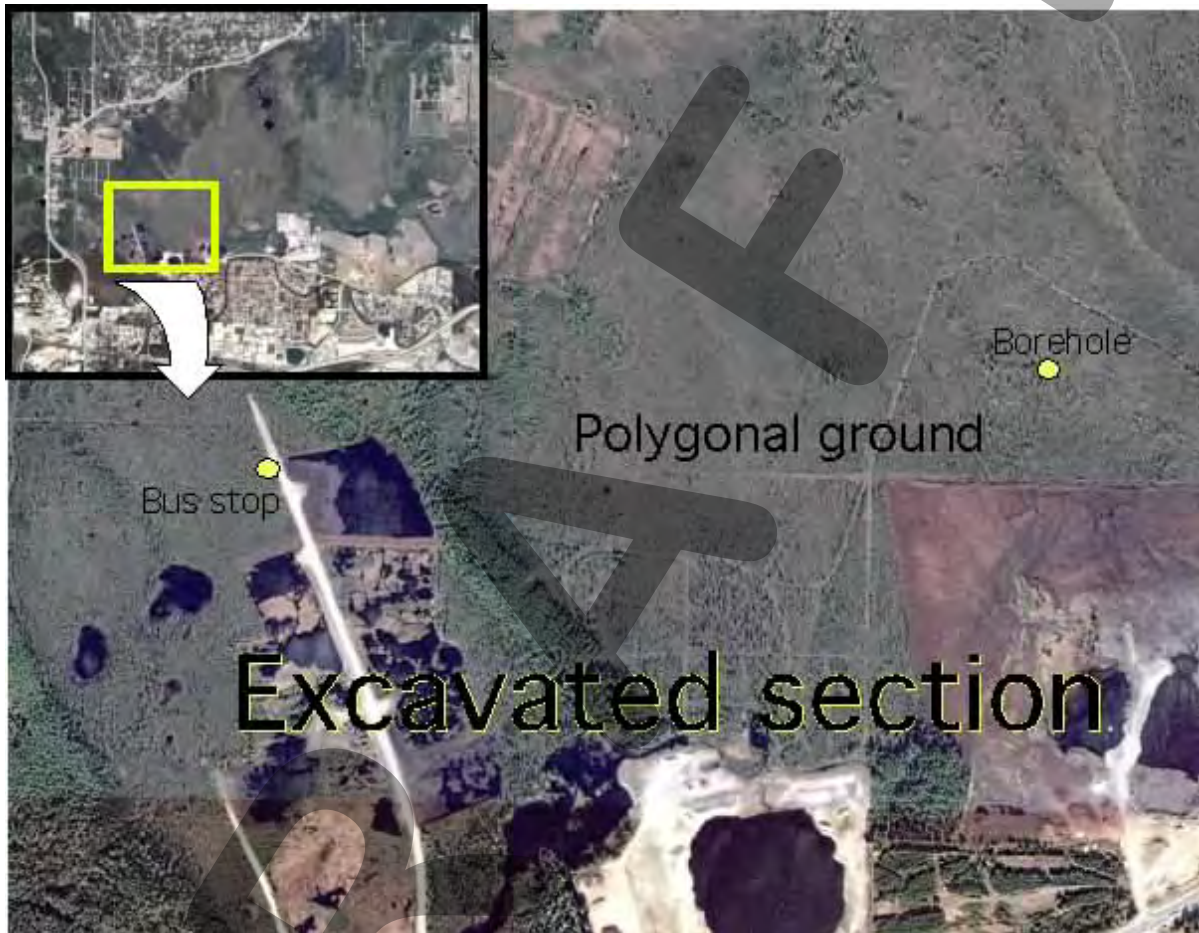


Figure 1. Satellite image for study site

A landscaping company that sells highly organic topsoil excavated into muskeg near Fairbanks and exposed a polygonal network of possibly still active ice wedges. The ice wedges occur in peat that have accumulated since about 3500 yr BP and have grown episodically as the permafrost table fluctuated in response to fires, other local site conditions and perhaps regional climatic changes (Hamilton et al 1983). Radiocarbon dates suggest one or two episodes of ice-wedge growth between about 3500 and 2000 yr BP as woody peat accumulated at the site (Hamilton et al 1983). In the current climatic condition, we observed at one of our research site with similar landscape characteristics (Smith Lake # 4) low ($<-4^{\circ}\text{C}$) annual mean permafrost surface temperatures event every 5-10 years, usually in concert with low snow years. The College Peat site is one of the coldest permafrost temperature places in Fairbanks (-3.1°C at 10m). Convective heat transfer is a major process of the ground cooling at this site. Thicker organic (moss) layer also developed strong thermal resistance during the summer and much less during the winter promoting a large thermal offset (up to -3.8°C). Thermal conductivity of the organic layer depends on water content (fig. 3). The thermal conductivities of live feathermoss, fibric, and humic layers are strongly affected by moisture content (Yoshikawa et al. 2003). Recent human activities (excavation) lowered the near surface ground-water level in some areas of these polygonal terrains, which could change the thermal offset in the near future.

Frost contraction cracking could still be observed during winter periods and ice wedge ice probably continues to form, although not every year. Secondary generation of the syngenetic ice wedges can be seen within the past few hundred years, more like during the Little Ice Age.

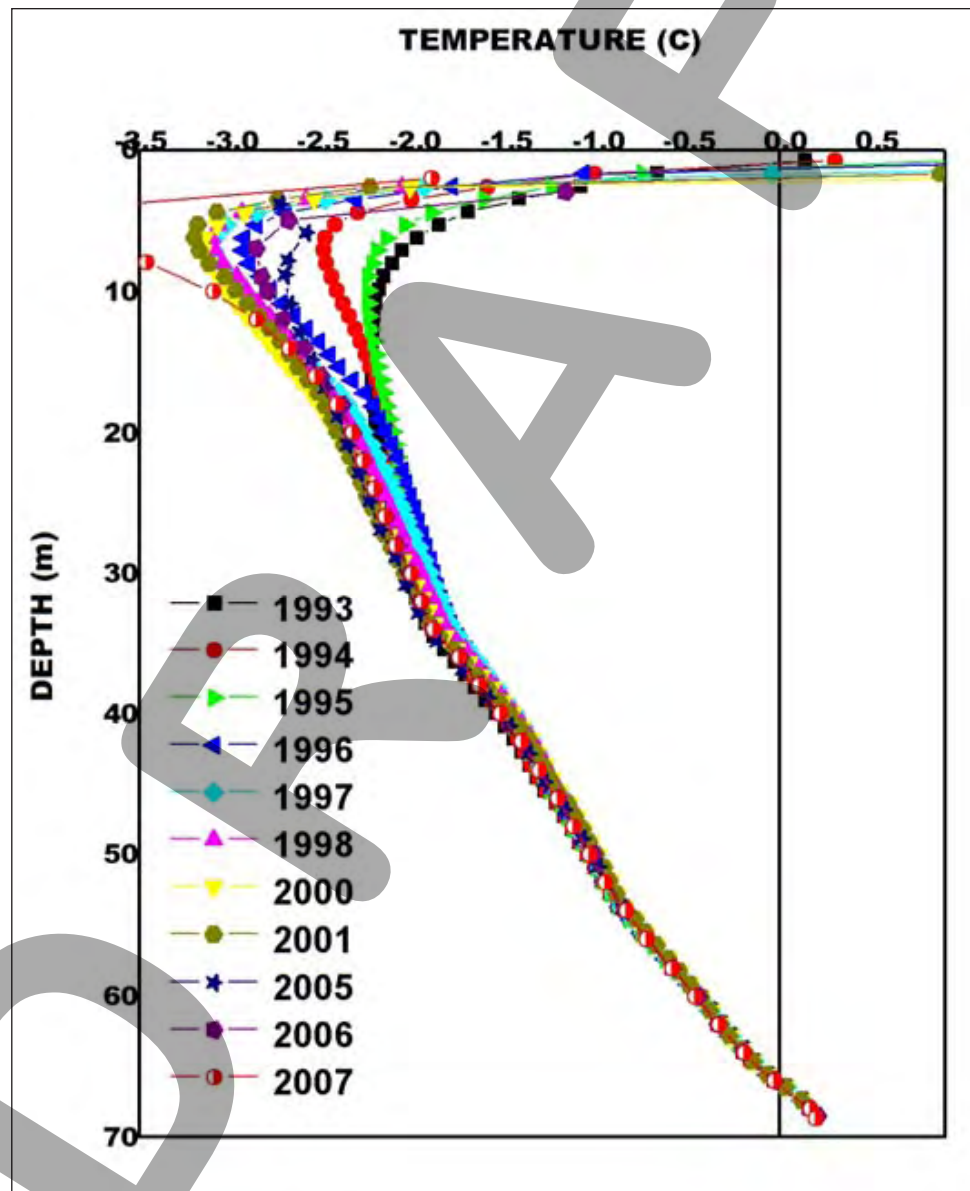


Figure 2. Permafrost temperatures near the peat mine since 1993. Permafrost temperature was -3.09°C at 10m depth on July 13, 2007.

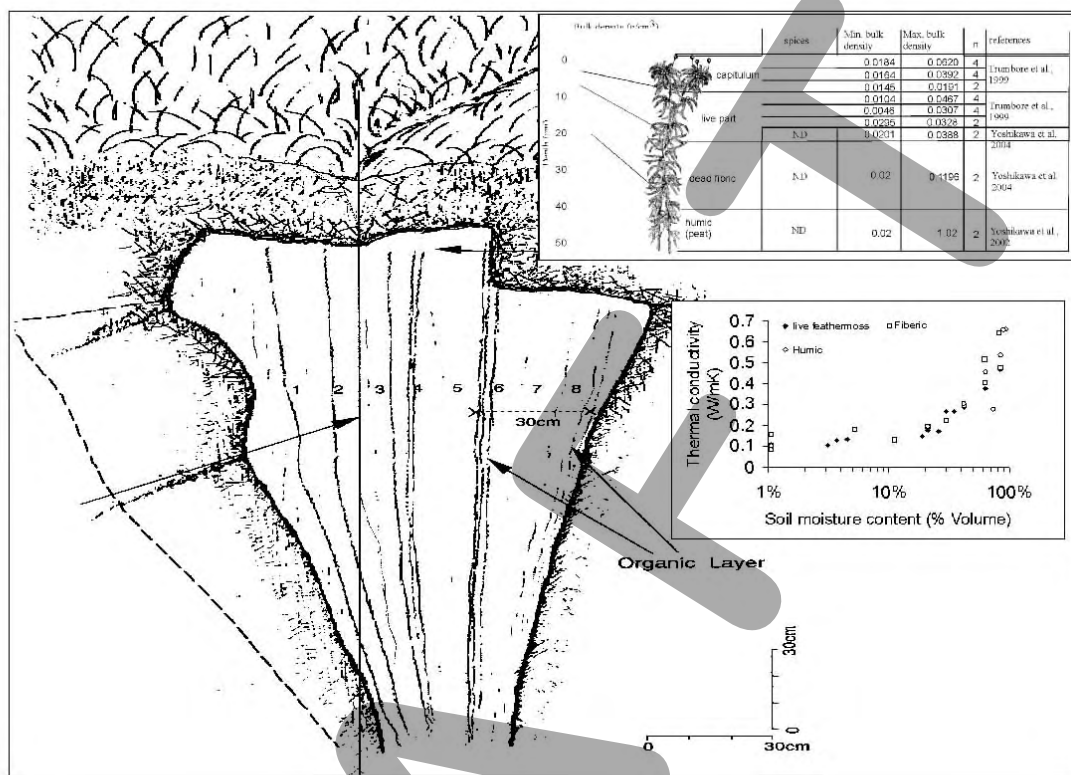


Figure 3. Sketch of the ice wedge and thermal/hydrologic properties of organic/peat layer (Yoshikawa et al. 2003).

REFERENCES

- Hamilton, T. D., T. A. Ager, S. W. Robinson, 1983, Late Holocene Ice Wedges near Fairbanks, Alaska, U.S.A.: Environmental Setting and History of Growth Arctic and Alpine research, Vol. 15, No. 2, pp. 157-168.
- Yoshikawa, K., Overduin, P.P. and Harden J.W. 2004. Moisture Content Measurements of Moss (*Sphagnum* spp.) Using Recently Developed Commercial Sensors. Permafrost Periglac. Process. 15: 1–11.
- Yoshikawa, K., W. R. Bolton, V. E. Romanovsky, M. Fukuda, and L. D. Hinzman, 2002 Impacts of wildfire on the permafrost in the boreal forests of Interior Alaska, J. Geophys. Res., 107, 8148, doi:10.1029/2001JD000438, 2002. [printed 108(D1), 2003]

DRAFT

SITE #11
GEODATA CENTER – MAP OFFICE – ALASKA SATELLITE
FACILITY USER SERVICES OFFICE
Room 204 Syun-Ichi Akasofu (IARC) Building

Patricia Burns
Geophysical Institute GeoData Center, University of Alaska Fairbanks

Many products and services relevant to permafrost researchers are currently available in Room 204 Syun-Ichi Akasofu Building.

The GeoData Center (GDC) provides data management and archive services for the Geophysical Institute and maintains a variety of geophysical data collections in support of scientific research. GDC collections include, but are not limited to, historic aerial photography and early satellite image acquisitions valuable for landscape change studies.

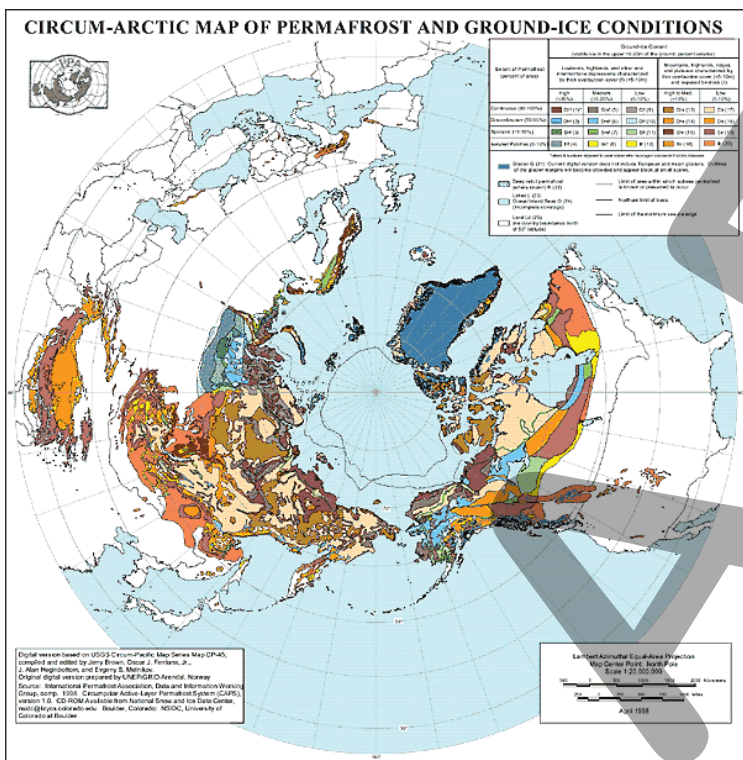


BAR aerial photography, Barrow, Alaska, 1945. Available from GDC.



National Ocean Service aerial photography, Barrow, Alaska, 1977. Available from GDC.

The Map Office sells statewide USGS topographic of Alaska in 1:250,000, 1:63,360 and 1:25,000-scales (limited to certain areas). In addition thematic maps are available that describe permafrost, ecology, and geology. Various trail maps and selected maps of the Yukon and British Columbia are available for purchase. Selected nautical charts published by National Ocean Service (NOAA) are available which include charts for Prince William Sound, Resurrection Bay, and Kachemak Bay.



*Circum-Arctic Map of Permafrost and
Ground-Ice Conditions. Available
from the Map Office.*



*Circumpolar Arctic Vegetation Map.
Available from the Map Office.*

The Alaska Satellite Facility (ASF) is involved in a wide range of activities – from downlinking satellite data to developing data-analysis tools, value-added products, and training for Synthetic Aperture Radar (SAR) users. SAR is the only satellite imagery that can be acquired at any time of the day or night and during adverse weather conditions. ASF's User Services Office provides a wide range of products, services and information to ASF data users.



AVNIR-2 satellite image of Barrow, Alaska, 2007. Available from ASF.



PRISM satellite image of Barrow, Alaska, 2007. Available from ASF.

DRAFT

SITE #12

THERMOKARST AND DRUNKEN FOREST

Katey Walter

Creamer's Field Waterfowl Refuge

Creamer's Field Waterfowl Refuge is managed for wildlife and the public by the Alaska Department of Fish and Game.

This area is perennially frozen, late Pleistocene-aged retransported organic-rich silt with well-developed thermokarst terrain. In the severe cold of winter, permafrost soils contract, crack and split into polygonal shapes. In spring, melt water seeps into the cracks, re-freezes and expands, enlarging the cracks. Over many years, these events create a pattern of deep troughs and raised hills which blend to create polygons. In many places, degradation of permafrost leads to deep troughs where surrounding trees slump into the growing trenches. These tilted trees are often referred to as 'drunken forest.' Thawing ground ice also results in formation of thermokarst pits, mounds and lakes. Lakes enlarge as permafrost along margins thaws and banks retreat.

Winter: temperatures: vary from an average of 27 °F (-3 °C) in October to -11 °F (-24 °C) in January. Extremes of -61 to +38 °F (-52 to 3°C) have been recorded in January. Extreme temperature fluctuations over short time periods (as much as 50 °F (28°C) in 24 hours) can occur in any month.

Vegetation: black spruce, white spruce, aspen, balsam poplar. Forest cover is less than 50 years old in this area.

Wildlife: Over 20 species of mammals, 30 species of birds, and hundreds of plants, fungi insects and smaller organisms remain in the boreal forest through winter. Many organisms endure the winter in a state of dormancy, a state where life is temporarily suspended. Many animals produce anti-freezes, special chemicals that lower the temperature at which their cells and body fluids will freeze, allowing the animals to survive severe cold. Many other animals remain active throughout winter including voles, red squirrels, snowshoe hares, porcupines, martens, red fox, moose and weasels.



DRAFT

SITE #13

LATE-PLEISTOCENE SYNGENETIC PERMAFROST IN THE CRREL PERMAFROST TUNNEL, FOX, ALASKA

M. Z. Kanevskiy, H. M. French, and Y. L. Shur (eds.)

CONTRIBUTING AUTHORS:

*Bjella, K.L.¹, Bray, M.T.², Collins, C.M.¹, Douglas, T.A.¹, Fortier, D.², French, H.M.³,
Kanevskiy, M.Z.², Shur, Y.L.²*

¹CRREL, ²University of Alaska Fairbanks, ³University of Ottawa, Canada

ABSTRACT

Late-Pleistocene syngenetic permafrost exposed in the walls and ceiling of the CRREL permafrost tunnel consists of ice- and organic-rich silty sediments penetrated by ice wedges. Evidence of long-continued syngenetic freezing under cold-climate conditions includes the dominance of lenticular and micro-lenticular cryostructures throughout the walls, ice veins and wedges at many levels, the presence of undecomposed rootlets, and organic-rich layers that reflect the former positions of the ground surface. Fluvio-thermal modifications are indicated by bodies of thermokarst-cave ('pool') ice, by soil and ice pseudomorphs, and by reticulate-chaotic cryostructures associated with freezing of saturated sediments trapped in underground channels.

INTRODUCTION

The CRREL permafrost tunnel is located at Fox, approximately 16 km north of Fairbanks, Alaska. Constructed 40 years ago, it is one of the few underground exposures of syngenetic Pleistocene-age permafrost. Naturally-occurring exposures of ice-rich permafrost quickly degrade and provide only opportunistic study. The permafrost tunnel allows hundreds of visitors the unhurried opportunity to become acquainted with ice-rich permafrost, and for professionals to study the peculiarities of syngenetic permafrost and its history.

This guide summarizes recent cryostratigraphic observations made from within the tunnel and re-evaluates earlier interpretations. Some observations have been described in previous publications (e.g. Shur et al. 2004, Bray et al. 2006) while others are presented in the NICOP proceedings volume (e.g. Bray 2008, Fortier et al. 2008, Kanevskiy et al. 2008).

THE CRREL TUNNEL

The CRREL permafrost tunnel was constructed in the early 1960's by the U.S. Army Cold Regions Research and Engineering Laboratory (CRREL) in order to test mining, tunneling, and construction techniques in permafrost. It continues to be maintained by CRREL for research opportunity. The plan of the tunnel is shown in figure 1. The tunnel entrance is located on the eastern margin of Goldstream Creek Valley where a steep 10 m high escarpment had been created by placer gold mining activities in the first part of the previous century. The surface of the valley that lies immediately above the long axis of the tunnel rises gently from the top of the escarpment in which the entrance is located towards the east side of Goldstream Creek Valley. The active layer of the terrain that overlies the tunnel is between 0.7 and 1.0 m thick. This is typical of the Fairbanks area.

The tunnel is composed of two portions (see fig. 1). The adit (a nearly horizontal passage from the surface into the hillside) was driven by the U.S. Army Corps of Engineers using continuous mining methods in the winters of 1963-64, 1964-65, and 1965-66 (Sellmann 1967). The winze (an inclined adit) was driven by the U.S. Bureau of Mines (USBM) from 1968 to 1969 using drill and blast, thermal relaxation, and hydraulic relaxation methods (Chester & Frank 1969). The adit extends approximately 110 m in length and is predominantly located in the frozen silt unit. The winze begins approximately 30 m into the adit and drops obliquely at an incline of 14% for 45 m, passing into the frozen gravel unit and ultimately into the weathered bedrock, where a Gravel Room was excavated (Pettibone & Waddell 1973). At the time of excavation, portions of the Gravel Room roof consisted of

2.0 m of frozen gravel lying below the overlying silt unit. After the winze levels out adjacent to the Gravel Room, it continues for another 10 m into what is known as the CRREL Room. The tunnel is chilled by natural ventilation in winter and by artificial refrigeration in summer, supporting permafrost stability.

Many papers have been published on the geology, paleoecology, and cryostratigraphy of the sediments exposed in the tunnel (Sellmann 1967, 1972, Watanabe 1969, Hamilton et al. 1988, Long and Péwé 1996, Shur et al. 2004, Pikuta et al. 2005, Bray et al. 2006, Katayama et al. 2007, Wooler et al. 2007, Fortier et al. 2008, Kanevskiy et al. 2008) as well as their engineering properties (Chester & Frank 1969, Pettibone & Waddell 1971, 1973, Thompson & Sayles 1972, Johansen et al. 1981, Johansen & Ryer 1982, Garbeil 1983, Weerdenburg & Morgenstern 1983, Arcane & Delaney 1984, Delaney & Arcane 1984, Huang et al. 1986, Delaney 1987, Bray 2008). The problems of tunnel construction have also been described (Chester & Frank 1969, Dick 1970, Swinzow 1970, Linnell & Lobacz 1978).

Sediments exposed within the tunnel consist mainly of frozen silts that range in age from Wisconsin to Recent (fig. 2). They are eolian (i.e. wind-blown) in nature and are largely derived from the outwash gravels and braided stream deposits of the Tanana lowlands and surrounding hills. Ice-rich silts of eolian origin were also partly reworked and re-transported by slope and fluvial processes (Péwé 1975, Hamilton et al. 1988). The silts overlie fluvial gravels of Nebraskan age (Fox Gravel) that are derived from the surrounding hills of the Yukon–Tanana Uplands. These gravels overlie Pre-Cambrian schist bedrock.

The silt overburden at the thickest point is approximately 14 m over the adit and 18 m over the Gravel Room.

Figure 1. Isometric view of the tunnel.

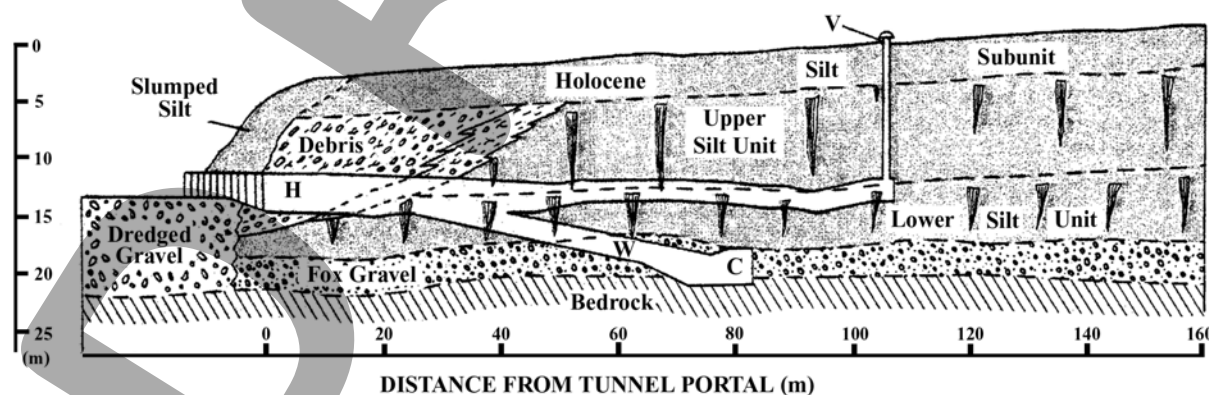
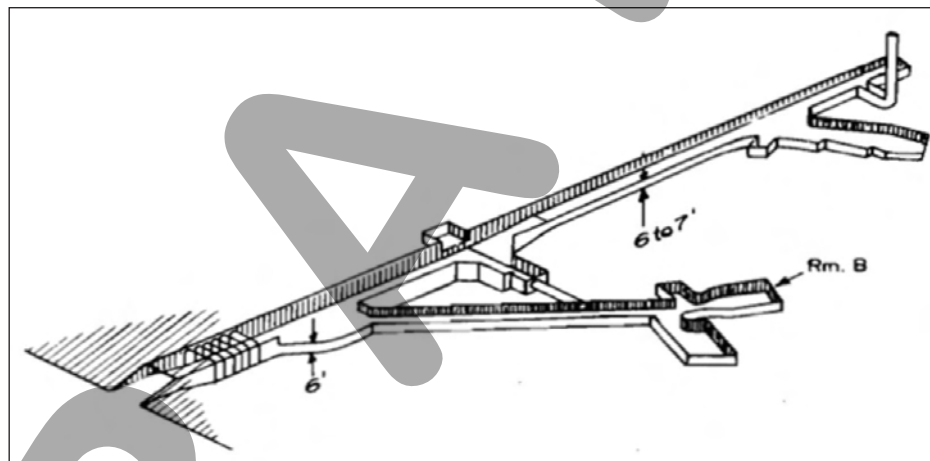


Figure 2. Cross section of the geology and permafrost features exposed in the CRREL tunnel near Fairbanks, Alaska. Two units of ice-rich Pleistocene-age silt are shown to be separated from two sets of ice wedges by an unconformity (dashed line). H—horizontal tunnel (adit); V—ventilation shaft (does not exist today); W—winze; C—chamber. (From Hamilton et al. 1988).

Near the tunnel portal, the fanlike deposits of poorly-sorted debris overlie the silts in an unconformable fashion; they formed between 12,500 and 11,000 years BP during deep erosion of the Goldstream Creek Valley slopes (Hamilton et al. 1988).

PREVIOUS OBSERVATIONS ON THE TUNNEL PERMAFROST

Sellmann (1967, 1972) was the first to provide information on the tunnel geology and permafrost. He described segregation ice, foliated wedge ice, and large clear masses of ice (buried ‘aufeis’). He also identified two ‘unconformities’. The upper was marked by the tops of small wedges and a change in soil color. The lower unconformity was identified by (i) a change in size and shape of wedges, (ii) a gap in radiocarbon ages obtained from organic material contained within the silty sediments in the tunnel walls of between 14,000 and 30,000 years BP, and (iii) a 20-fold increase in chemical concentration with depth. Sellmann suggested ‘...this unconformity was probably caused by some regional warming or local depositional or erosional event’.

Subsequently, Hamilton et al. (1988) obtained samples from the tunnel walls and reported upon 33 radiocarbon dates. The dates for silts are within the range 30,000 – 43,000 years BP. In addition, a diverse assemblage of animals’ bones (bison, horse, mammoth (?), caribou (?) and arctic ground squirrel) and plant macrofossils (grasses and sedges) indicated a tundra or shrub-tundra environment. Hamilton et al. (1988) concluded that the tunnel ‘... provides continuous and undisturbed exposures of ice-rich silt that overlies gravel and bedrock’ and that ‘...most of the pore and segregated ice formed during freezing of silt’. They identified pore ice, segregated ice, foliated wedge ice and buried surface ice, as previously documented by Péwé (1975) and concluded that ‘most of the pore ice and segregated ice formed during freezing of silt and has been preserved since that time’. They also identified two independent systems of ice wedges and inferred a thaw unconformity between them (fig. 2). Other bodies of ice, described as ‘...horizontal, saucer-shaped bodies, 2–6 m wide and 0.5–2 m deep’ (Hamilton et al. 1988) were interpreted as buried frozen thaw ponds formed in ice-wedge troughs. According to these authors, these ice bodies ‘...generally consist of 3 successive depth zones: (1) clear ice with vertical bubble trains, transitional downward into (2) ice containing reddish brown, suspended organic matter that overlies (3) a lenticular body of unusually ice-rich silt’.

CRYOSTRATIGRAPHY AND CRYOLITHOLOGY

Cryostratigraphy refers to the study of frozen layers in the Earth’s crust. It is a branch of geocryology. It was developed first in Russia where the study of ground ice gained early attention (Shumskii 1959, Katasonov 1962, 1969) and subsequently led to highly detailed studies (e.g. Vtyurin 1964, Popov 1967, 1973, Gasanov 1969, Gravis 1969, Zhestkova 1982, Shur 1988, Romanovskii 1993, Dubikov 2002) that are unparalleled in North America. A summary of cryostratigraphic principles can be found in French (2007, 153–185).

Cryostratigraphy differs from traditional stratigraphy by specifically recognizing that perennially-frozen sediment and rock contain structures that are different to those found in unfrozen sediment and rock. Cryolithology is a related branch of geocryology and refers to the relationship between the lithological characteristics of rocks and their ground ice amounts and distribution. The structures, largely determined by the amount and distribution of ice within sediments are termed ‘cryostructures’. Cryostructures are useful in determining the nature of the freezing process and the conditions under which frozen sediment accumulates.

A distinction must be made between epigenetic and syngenetic permafrost (fig. 3). Epigenetic permafrost refers to permafrost that forms subsequent to deposition of the host sediment and rock. By contrast, syngenetic permafrost refers to permafrost that forms at the same time as the host sediment is being laid down. These types of permafrost can be distinguished by analysis of cryostructures. The epigenetic-syngenetic distinction is extremely useful in the context of Quaternary paleo-environmental reconstruction.

Cryostratigraphy adopts many of the principles of modern sedimentology. For example, ‘cryofacies’ are defined according to volumetric ice content and ice-crystal size, and then subdivided according to cryostructure. Finally where a number of cryofacies form a distinctive cryostratigraphic unit, these are termed a ‘cryofacies assemblage’ (French 2007).

(i) Cryostructures

Russian permafrost scientists were the first to systematically identify cryotextures and cryostructures (Gasanov 1963, Katasonov 1969, Zhestkova 1982, Popov et al. 1985, Melnikov & Spesivtsev 2000). Unfortunately, these classifications are complex and unwieldy. For example, Katasonov’s (1969) classification lists 18 different cryostructures and Popov et al.’s (1985) classification lists 14 categories.

A simplified North American cryostructural classification by Murton & French (1994) encompasses the range of cryostructures found in permafrost (fig. 4). Several Russian terms are transliterated. All cryostructures can be recognized by the naked eye.

The common cryostructures are:

- (1) ‘structureless’ (Sl) - refers to frozen sediment in which ice is not visible and consequently lacks a cryo-structure. (This category is termed ‘massive’ in the Russian transliterated literature).
- (2) ‘lenticular’ (Le) - lens-like ice bodies that are described by inclination, thickness, length, shape and relationship to adjacent cryostructures.
- (3) ‘layered’ (La) – continuous bands of ice , sediment or a combination of both.
- (4) ‘regular reticulate’ (R) - a regular three-dimensional net-like structure of ice veins surrounding a mud-rich block
- (5) ‘irregular reticulate’ (Ri) – an irregular three-dimensional net-like structure of ice veins surrounding a mud-rich block.
- (6) ‘crustal’ (Cr) - refers to the ice crust or rim around a rock clast.
- (7) ‘suspended’ (Su) - refers to grains, aggregates and rock clasts suspended in ice. (This category is termed ‘ataxicitic’ in the Russian transliterated literature).

Figure 5 shows examples of cryostructures typical for the tunnel.

The micro-morphology of cryostructures can be observed using an environmental scanning electron microscope (ESEM). For example, Bray et al (2006) provide examples of structureless (i.e. ‘massive’) and lenticular cryostructures viewed conventionally and under ESEM (fig. 6).

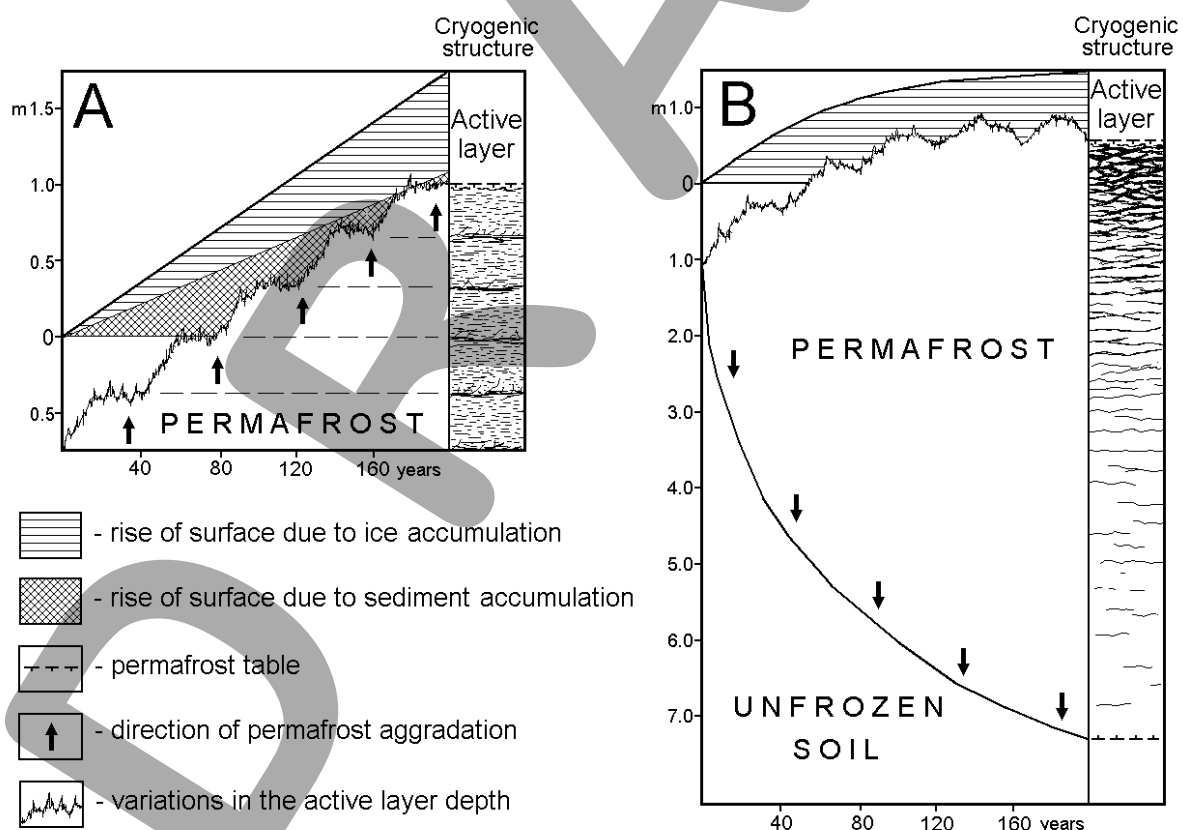


Figure 3. Mechanisms of (A) syngenetic (based upon Popov, 1967) and (B) epigenetic permafrost formation.

(ii) Thaw unconformities

Discontinuities in the nature and distribution of ground ice bodies related to permafrost thawing are termed ‘thaw unconformities’ (French 2007). They are the result of either thawing of frozen materials (primary thaw unconformity) or subsequent refreezing of previously-thawed material (secondary thaw unconformity). A primary thaw unconformity forms at depth below a residual thaw layer. In doing so, it truncates the top of an ice wedge. When permafrost subsequently aggrades, the original thaw unconformity at depth becomes a secondary (i.e. palaeo-) thaw unconformity and the new active layer-permafrost boundary becomes the primary thaw unconformity. The secondary thaw unconformity can be recognized by both the truncated ice wedge and by different cryostructures in the sediment above and below. Thaw unconformities can be further recognized by differences in stable isotope values, by heavy mineral assemblages above and below the unconformity, and by horizons of enhanced micro-organisms.

The manner in which permafrost degrades and subsequently forms again, and the cryostratigraphic evidence that it leaves, is illustrated in figure 7.

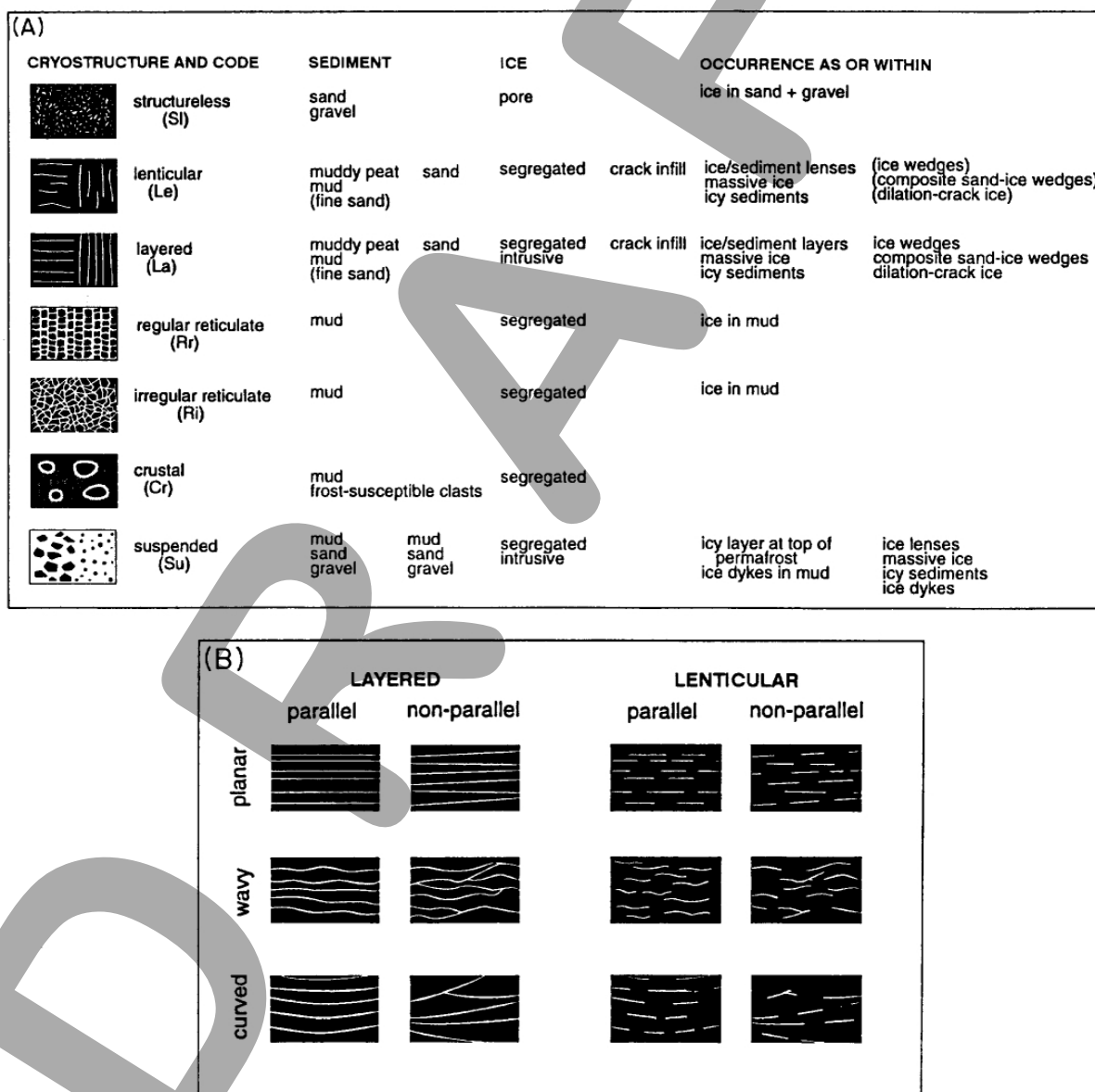


Figure 4. A North American classification of cryostructures. (A) Scheme proposed by Murton & French (1994). Ice is shown in white and sediment in black. (B) Terms and illustrations used to describe layered and lenticular cryostructures. (From Murton & French, 1994).



Figure 5. Photos showing (A) micro-lenticular cryostructure, location marker is 1.25 X 1.25 cm in size (photo by M. Kanevskiy), and (B) reticulate chaotic cryostructure, the handle of the knife is about 6 cm long (From Fortier et al. 2008).

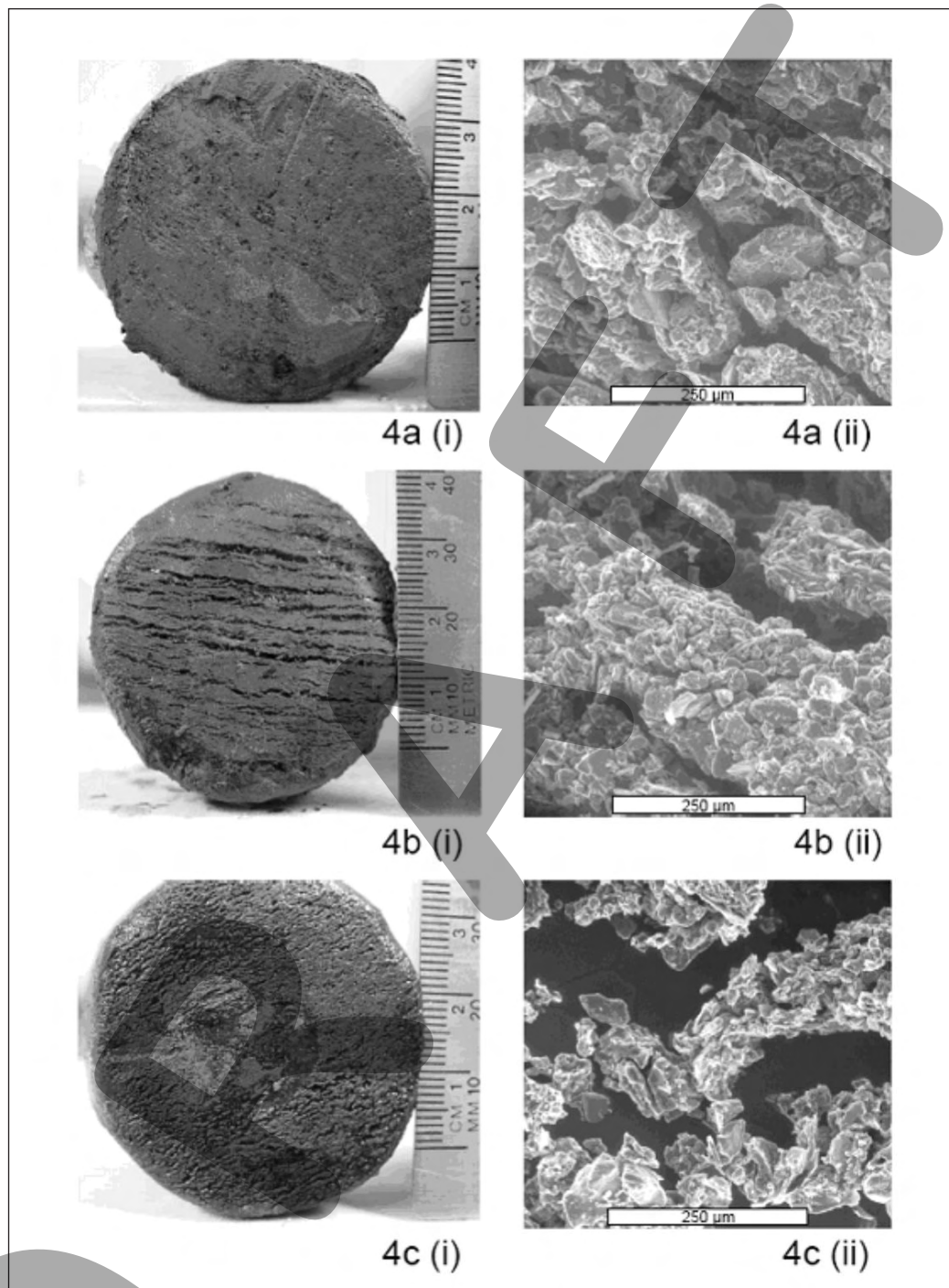


Figure 6. Example of cryostructures from the CRREL tunnel viewed conventionally and under ESEM.

(a) Massive cryostructure. Image (i) is a macro-scale image typical of silt pseudomorphs. Note centimeter scale. Image (ii) is a micro-scale image using an ESEM. Bar scale indicates 250 mm. (b) Lenticular-layered cryostructure. Image (i) is a conventional macro-scale image. Note centimeter scale. Image (ii) is a micro-scale image using an ESEM that shows the soil and micro ice-lens morphology. Bar scale indicates 250 mm. (c) Micro-lenticular cryostructure. Image (i) is a macro-scale image. Note centimeter scale. Image (ii) is a micro-scale images under ESEM in which soil particles are generally suspended in an ice matrix. Bar scale indicates 250 mm. (From Bray et al 2006).

SYNGENETIC PERMAFROST

The permafrost exposed in the CRREL tunnel is typical of the Pleistocene-age permafrost referred to in the Russian literature as “Yedoma” or “Ice Complex” (e.g. Soloviev 1959, Katasonov 1978, Popov et al. 1985, Romanovskii 1993). Ice Complex sediments have been studied mainly in Central and Northern Yakutia; similar sediments were observed also in Chukotka, West Siberia, Taimyr, Alaska, and Canada (Vtyurin 1964, Péwé 1966, 1975, Popov 1967, Gasanov 1969, Katasonov 1978, Lawson 1983, Carter 1988, Hamilton et al. 1988, Shur et al. 2004, French 2007). This permafrost developed when long periods of uninterrupted cold-climate sedimentation allowed permafrost to form syngenetically.

Syngenetic permafrost forms in response to sedimentation (alluvial, slope, aeolian, lacustrine, etc.) that causes the base of the active layer to aggrade upwards. By definition, the permafrost is syngenetic because it is of the same

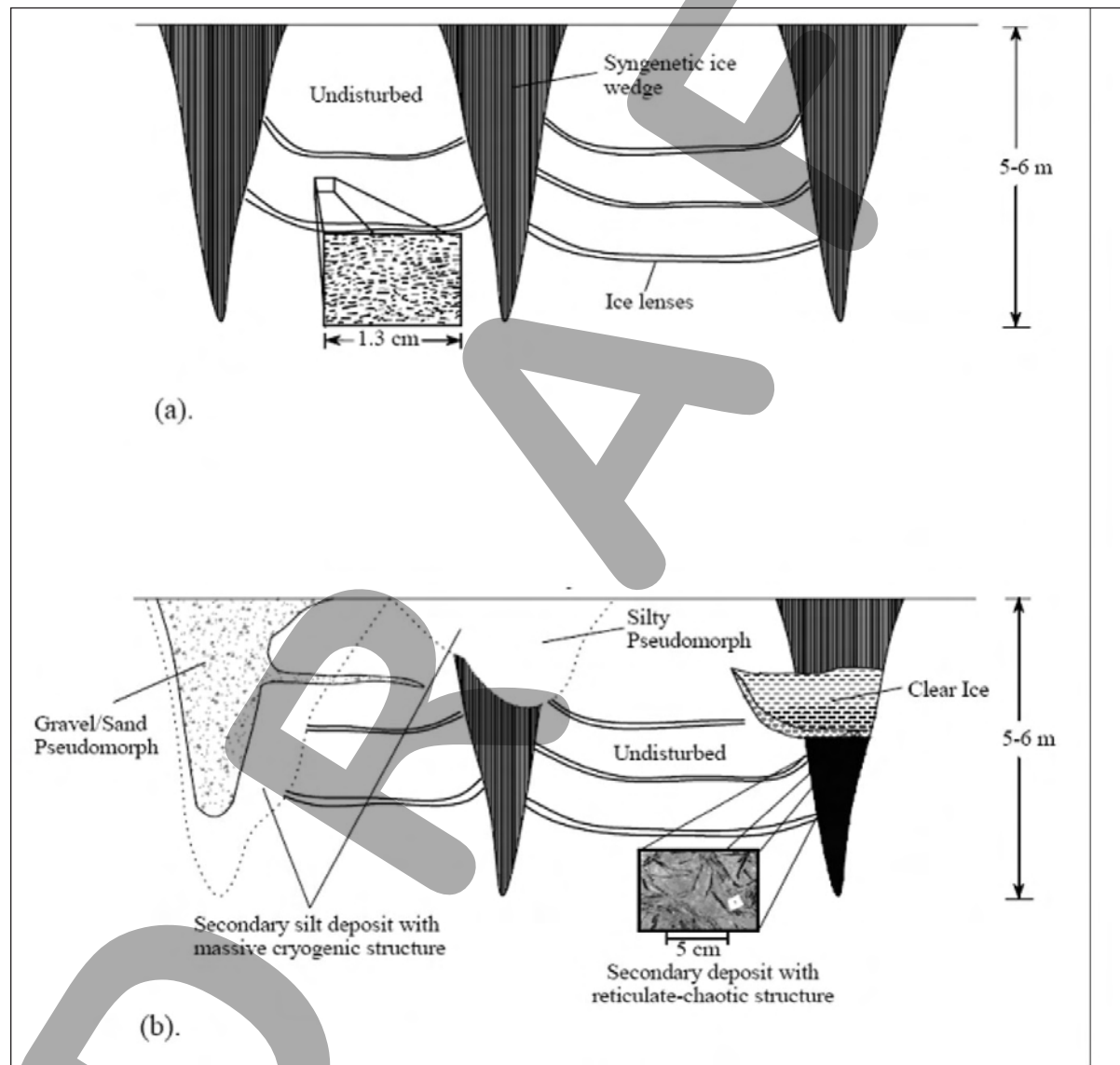


Figure 7. Schematic diagram of (a) undisturbed syngenetic permafrost and (b) typical modified permafrost exposure within the CRREL tunnel. In (a) the expanded image represents a micro-lenticular cryostructure, a reliable indicator of syngenetic permafrost. In (b) an idealized schematic shows typical secondary modification of original syngenetic permafrost. Expanded image represents reticulate-chaotic cryostructures. The reticulate-chaotic cryostructure is associated with ‘clear ice’, interpreted as thermokarst-cave (‘pool’) ice. (From Bray et al. 2006).

age (approximately) as the host sediment. It means that transformation of active-layer sediments into a perennially-frozen state occurs virtually simultaneously with sedimentation. Typically, syngenetically-frozen sediments are silty, or loess-like (up to 70-80% silt fraction), and ice-rich (the soil gravimetric moisture content may exceed 100-200%). They also contain rootlets, buried organic-rich horizons, and exhibit rhythmically-organized (i.e. layered) cryogenic structures.

The main locations where contemporary syngenetic permafrost is forming today are in the alluvial and deltaic environments (Shur & Jorgenson 1999) of Arctic North America (e.g. Colville River, Alaska; Mackenzie River, Canada), and in northern Siberia (e.g. Lena, Ob, Yenisey, Yana, Indigirka, Kolyma river valleys and deltas). Thickness of contemporary syngenetic permafrost usually does not exceed a few meters.

Pleistocene-age syngenetic permafrost occurs mainly in the continuous permafrost zone of Siberia, and its occurrence in the discontinuous permafrost zone of Alaska is a rare phenomenon. It is also found in the valleys and lowlands of adjacent unglaciated Yukon Territory, Canada. It should be mentioned that, under the current climatic conditions of the Fairbanks area, modern ice-wedge formation occurs very rarely and only in peat (Hamilton et al. 1983).

Syngenetic permafrost is often characterized by numerous ice veins and ice wedges. In contrast to epigenetic permafrost, in which ice wedges rarely exceed 4 m in depth, ice wedges in syngenetic permafrost may extend through the entire strata, either as huge wedges reaching 10-40 m in depth and 2-6 m in width or as small ice veins throughout the profile. Their varying width and depth reflect the varying rates of sedimentation and climate conditions. In syngenetic permafrost bodies, wedge ice can occupy 30-50%, and even more in some cases, of the total volume. In color, the wedges are grey because of the numerous inclusions of fine sediment. As such, they can easily be distinguished from smaller Holocene and modern ice wedges located in the top part of Yedoma sections, because the latter are usually white and opaque due to fewer soil inclusions and an abundance of air bubbles.

Radiocarbon dating and oxygen-isotope variations indicate that much of the syngenetic Pleistocene permafrost in northern Siberia formed between 40,000 and 12,000 years ago (Vasil'chuk & Vasil'chuk 1997, 2000). It was the dominant type of permafrost that formed in unglaciated lowlands during the Late Pleistocene. It is the main source of well-preserved Late-Pleistocene faunal remains (woolly mammoths etc).

CRYOSTRATIGRAPHIC MAPPING IN THE TUNNEL

Cryostratigraphic mapping uses the cryofacial method first proposed by Katasonov (1962, 1978). It is based upon two concepts, namely, that (1) the shape, size and spatial pattern of ice inclusions (i.e. cryostructures) depend on the conditions under which the sediment was deposited and then frozen, and (2) every cryofacies has its own specific cryostructure.

The results of cryostratigraphic mapping of the main adit of the tunnel (Bray et al. 2006) are shown in figures 8 and 9. Four categories of information are shown:

- (a) Mineral sediment is grouped into the general categories of silt, sand and gravel.
- (b) Cryostructures are identified as being either lenticular or micro-lenticular (i.e. syngenetic), massive (i.e. epigenetic) or reticulate-chaotic (i.e. epigenetic).
- (c) Ice bodies are mapped as being either lenses (usually a layered cryogenic structure), wedge ice (formed in thermal-contraction cracks), or clear ice (occurring in association with wedge ice).
- (d) Pseudomorphs are mapped where the sediment or ice is interpreted to be the result of ice-wedge modification.

Descriptions of the cryo-lithostratigraphic units, ice bodies and other features are shown in table 1.

In 2006, the 38 m long winze section was studied (Kanevskiy et al. 2008). Cryostratigraphic mapping of one wall and the ceiling of the winze was performed in the scale 1:20; several small sections were studied in detail (scale 1:4). Figure 10 shows the general view of the left wall and the ceiling of the winze. More detailed fragments are shown in figures 11 to 13.

CRYOSTRUCTURES

Recent publications (Shur et al. 2004, Bray et al. 2006, Fortier et al. 2008, Kanevskiy et al. 2008) show the variety of cryostructures that are present in the tunnel and describe typical features related to syngenetic permafrost formation.

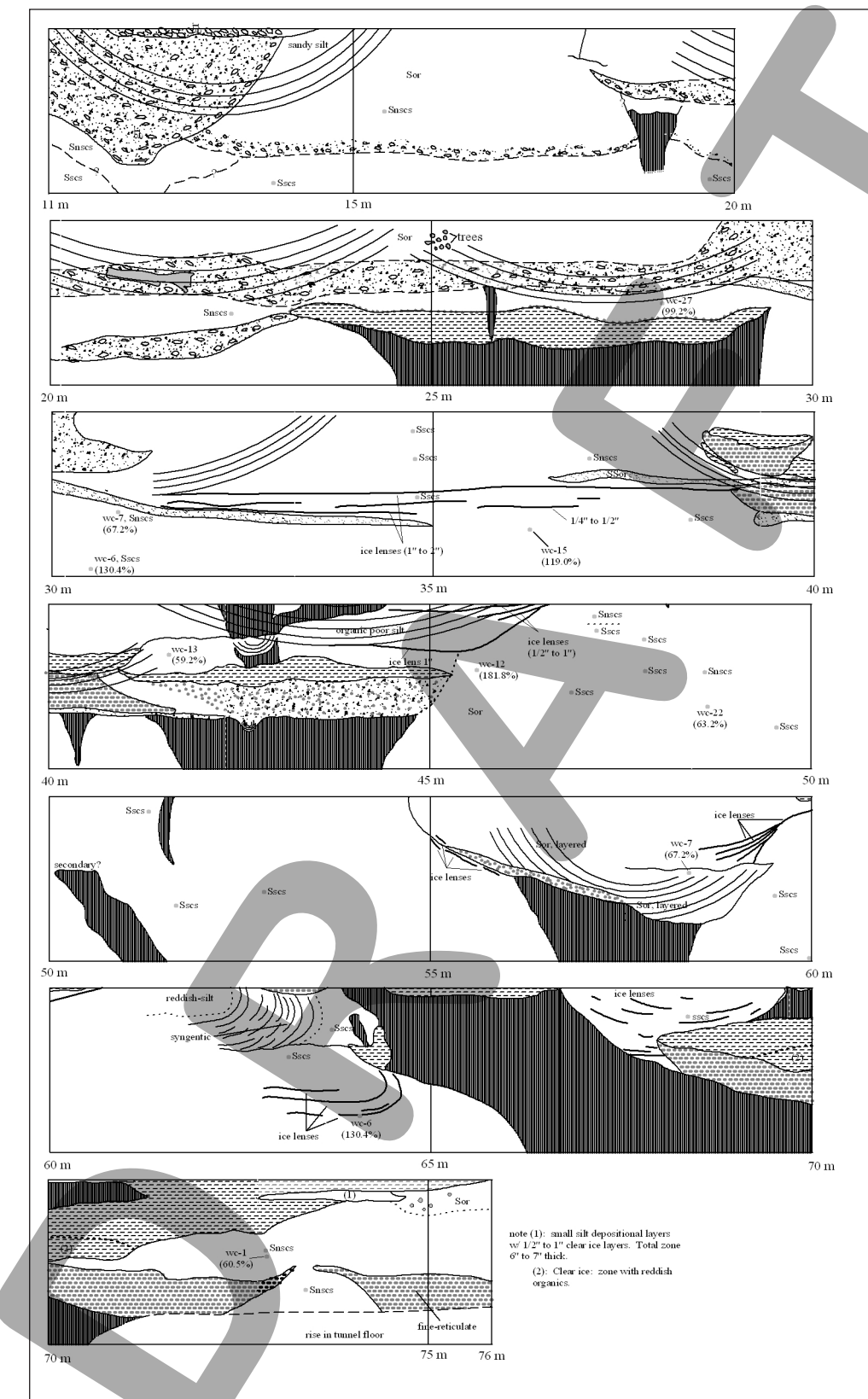


Figure 8. Cryostratigraphic map of part of the main shaft of the CRREL Permafrost Tunnel, left side (viewed from entrance) of the tunnel. For the legend, see Figure 9. (From Bray et al. 2006).

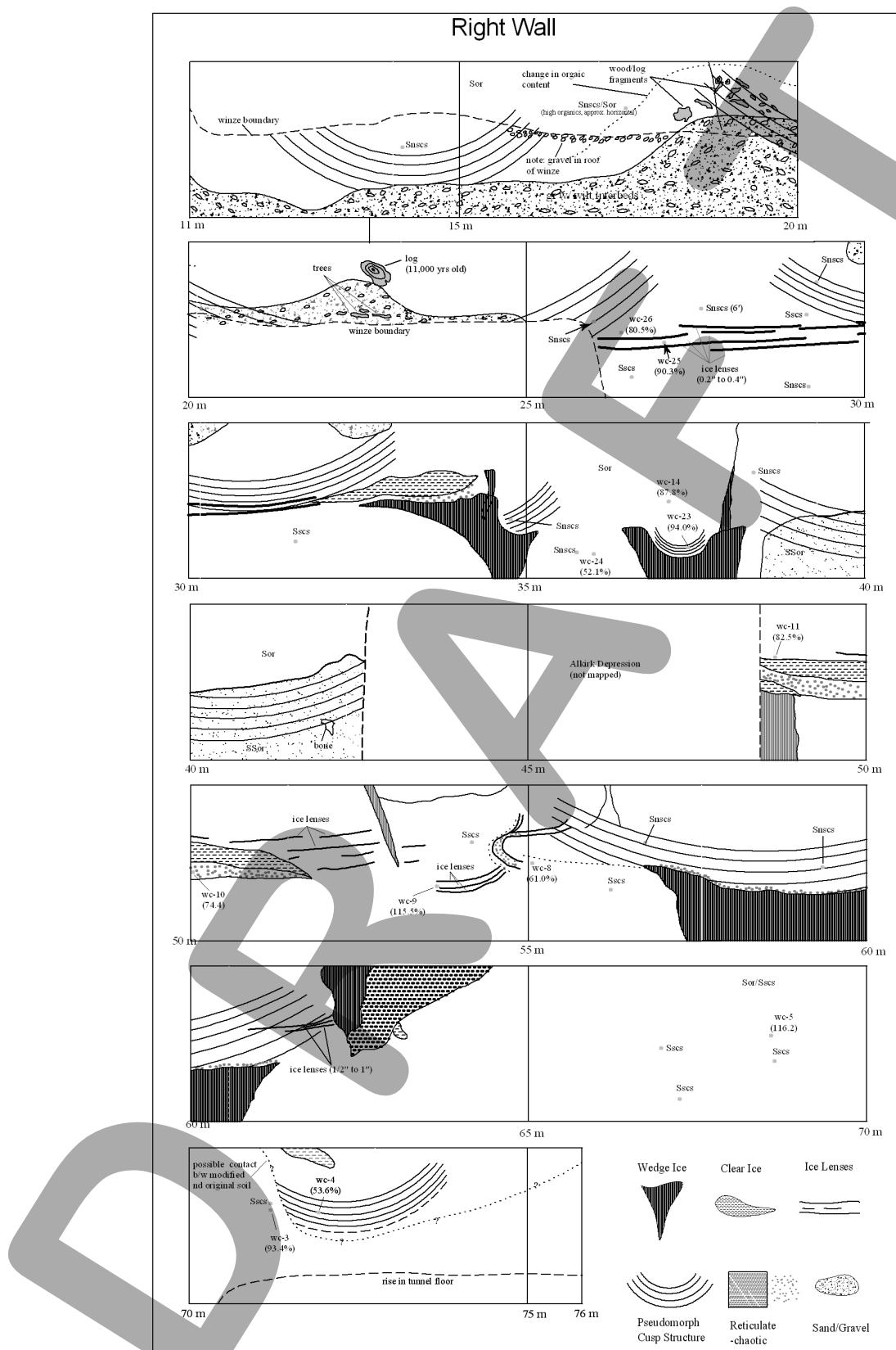


Figure 9. Cryostratigraphic map of part of the main shaft of the CRREL Permafrost Tunnel, right side (viewed from entrance) of the tunnel. (From Bray et al. 2006).

Table 1. Cryo-lithostratigraphic units, ice bodies and other features that were mapped in the CRREL tunnel (see figs. 8, 9).

1. CRYO-LITHOSTRATIGRAPHIC UNITS

- | | |
|--------|--|
| Scs: | Fairbanks silt, representative of the original syngenetic permafrost, characterized by micro-lenticular and layered cryostructures. Average gravimetric water content 130% |
| Snses: | Fairbanks silt, characterized by a massive cryostructure that is indicative of secondary modification. It contains no cryostructures typical of syngenetic permafrost. The average gravimetric water content is 69% |
| Sor: | Fairbanks silt with a massive cryostructure and possessing organics (rootlets, wood, animal bones, etc) |
| Ssor: | Sandy organic silt with a massive cryostructure and containing rootlets, wood and animal bones |
| Gr: | Gravel deposits; sandy, silt, imbricated. Where near the tunnel entrance, they may represent slope deposits. Deeper within the tunnel, the gravel deposits are directly related to the fluvial erosion and thaw-modification of ice wedges |

2. ICE BODIES

- | | |
|-------------|---|
| Ice lenses: | Lenses of ice that range in length from 10 cm to several meters and with thickness of between 0.5 to 10 cm. They form part of the micro-lenticular and layered cryostructures |
| Clear ice: | Lenticular-shaped ice bodies, often with aligned bubbles towards outer edges, and usually associated with reticulate-chaotic cryostructures in adjacent sediments. The ice is interpreted as thermokarst-cave ice |
| Wedge ice: | Foliated ice with vertical soil laminations, often grey to brownish in color |

3. OTHER FEATURES

- | | |
|---------------|---|
| Pseudomorphs: | Bodies of mineral soil ranging in composition from gravel to silt, commonly possessing high organic contents and often possessing reticulate-chaotic cryostructures. Interpreted as replacement deposits within previously thaw-eroded and truncated ice-wedge structures |
|---------------|---|

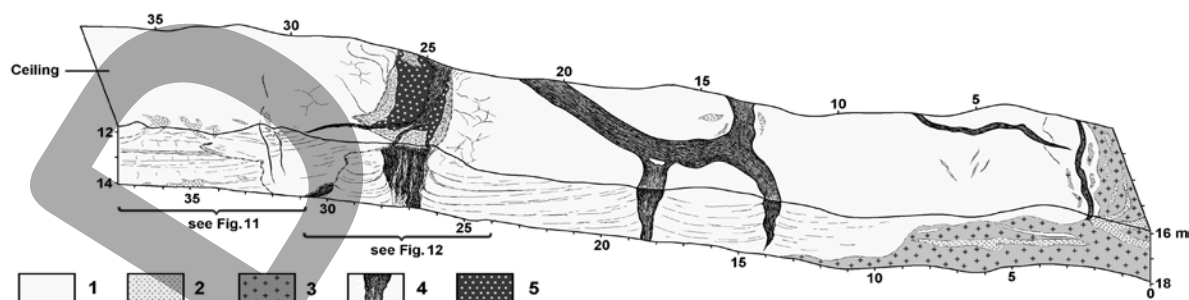


Figure 10. General view of the left wall and the ceiling of the winze. 1 – silt; 2 – sand; 3 – Fox Gravel; 4 – ice wedge; 5 – thermokarst-cave ice. See figures 11 to 13 for details. (From Kanevskiy et al. 2008).

Four types of cryogenic structure can be identified in the tunnel (Shur et al. 2004):

- (1) A micro-lenticular cryostructure is the most common; it is formed by thin and short lenses of ice practically saturating the soil (fig. 5 A). The thickness of straight and wavy ice inclusions is generally less than 0.5 mm.
- (2) A layered cryostructure is represented by repeated layers of ice with thickness of between 0.2 and 1 cm. The layers form series with the spacing between layers of between 2 and 5 cm.
- (3) A lenticular-layered cryostructure is formed by ice lenses with a thickness from 0.5 to 1.5 mm and a length from a few millimeters to 1 cm. These lenses form continuous ice layers with soil inclusions.
- (4) A reticulate-chaotic cryostructure is recognized by relatively thick multi-directional ice lenses (veins), often randomly oriented (fig. 5 B). This structure is interpreted as having formed following the closed-system freezing of a talik or thaw layer.

The dominant cryostructure that can be observed in the CRREL tunnel is micro-lenticular (Shur et al. 2004). This is typical of syngenetic permafrost formation. The micro-lenticular term refers to the occurrence of very small, sub-horizontal (sometimes wavy), relatively short ice lenses. Usually, the thickness of uniformly-distributed ice lenses (and the spacing between them) does not exceed 0.5 mm (see fig. 5 A). In the winze (section 1, see fig. 13 A), several varieties of micro-lenticular cryostructure can be distinguished (e.g. latent micro-lenticular, micro-braided). Micro-lenticular cryostructures typically form more than 50-60% of the entire thickness of the syngenetic permafrost (Kanevskiy 2003). Usually the micro-lenticular cryostructure is combined with a layered cryostructure. In the tunnel, gravimetric moisture content of the sediments with micro-lenticular cryostructure varies from 80% to 240%. The great variability of gravimetric moisture content of silts can be associated with existence of the several varieties of micro-lenticular cryostructure mentioned above (see fig. 13 A). It is typical for syngenetic permafrost, and mostly linked to different rates of sedimentation.

Certain sections of the tunnel show bodies of clear ice. These are usually underlain by silt that exhibits a reticulate-chaotic cryostructure. This cryostructure is the most obvious type that is visible in the tunnel (Shur et al. 2004). However, it is not the most common cryostructure and is restricted to a few localities where it can be easily recognized by relatively thick ice veins, randomly oriented (see fig. 5 B). These multi-directional reticulate ice veins are thought to have formed by inward freezing of saturated sediments trapped in underground channels incised within the permafrost by thermal erosion. They form following cessation of flow as freezing occurs in sediments either laid down in the channel floor or which have slumped into the channel from the sides of the gully. Formation of the reticulate-chaotic cryostructure has been reproduced in laboratory experiments (Fortier et al. 2008).

AGGRADATION OF THE PERMAFROST TABLE

Seven thin organic-rich horizons can be observed in the upper part of the winze (see fig. 11). They occur at a depth of approximately 12-14 m below the ground surface. The AMS radiocarbon dates for organic-rich layers vary from 31,000 to 35,000 yr BP (fig. 11). Below each peat horizon, at a depth of approximately 0.4 to 0.6 m, are distinct icy layers (so-called ‘belts’ in the Russian literature). These are interpreted to be the temporary positions of the former permafrost table (i.e. base of the active layer) during the time of peat accumulation. In all probability, the peat reflects an environment of slower sediment accumulation. The approximate positions of the active layer during these periods are indicated by arrows in figure 11.

Numerous small cracks partially filled with ice (ice veins) extend downwards from the peat horizons to depths of up to 0.5 m. These cracks form polygons up to 0.5 m across. It is tempting to speculate that these were seasonal-frost cracks and that the seasonal-ice veins were subsequently incorporated into the syngenetic permafrost.

MASSIVE ICE BODIES

Bodies of massive ice are exposed in the wall and ceiling of the CRREL tunnel and impress the first-time visitor. These are the most visible expression of the ice-rich nature of Pleistocene-age syngenetic permafrost. Three types of massive ice can be identified: wedge ice, clear ice, and clear ice with wedge-ice inclusions.

Many of the ice wedges in the CRREL tunnel have been thaw-modified by fluvio-thermal erosion which promotes the formation of soil and ice pseudomorphs (see below). Figure 6 is a schematic diagram showing how thermal erosional processes may modify syngenetic permafrost.

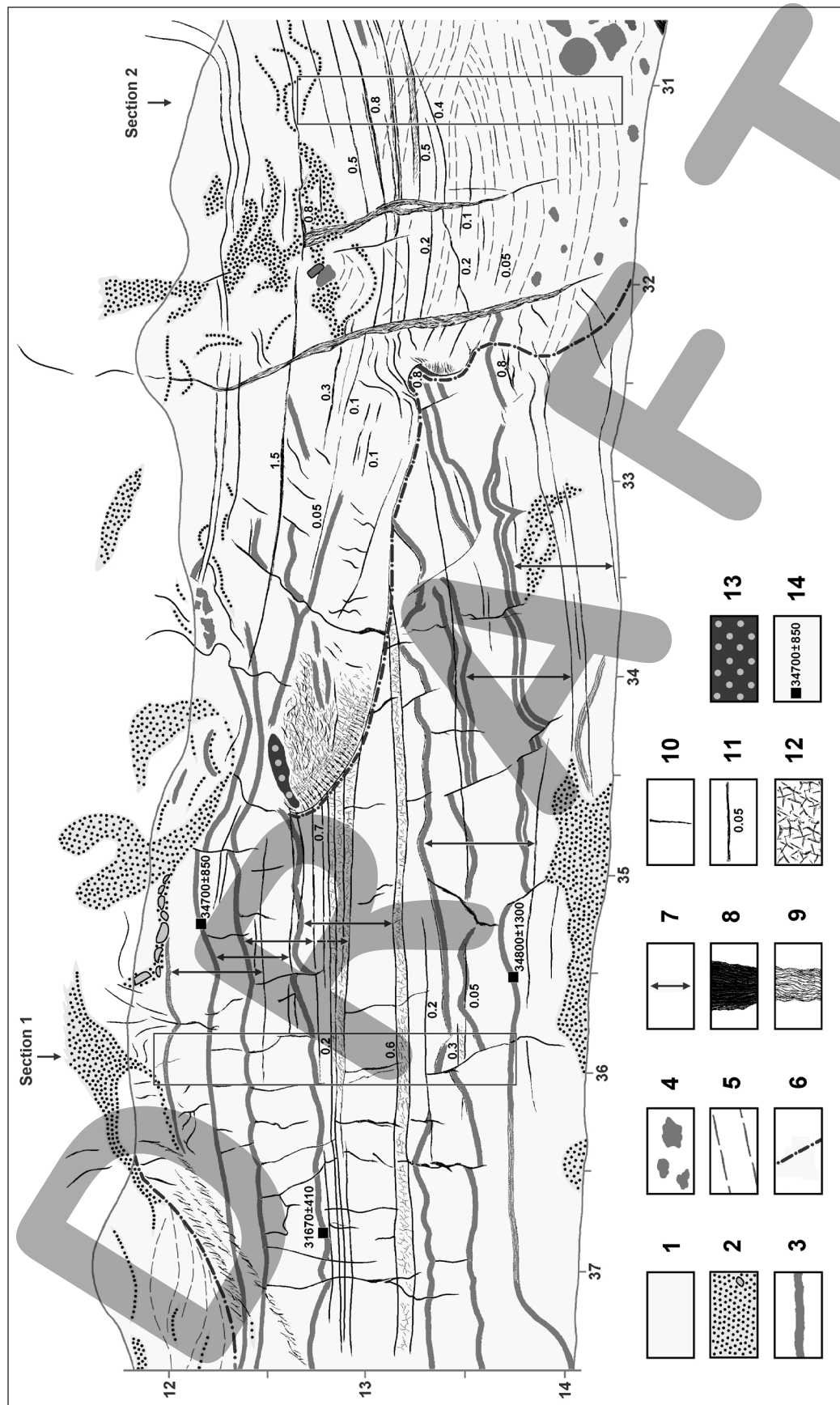


Figure 11. Cryostratigraphic map of the left wall of the winze, interval 31-37 m. 1 – sand, gravel inclusion; 2 – silt; 2 – erosion boundary; 3 – in situ peat layers; 4 – transported organic matter; 5 – lamination in silt; 7 – approximate position of active layer at the periods of slower sedimentation; 8 – ice wedge; 9 – composite wedge (ice/silt); 10 – isolated ice vein; 11 – reticulate-chaotic cryostructure; 12 – ice layer ('belt'); thickness in cm; 13 – thermokarst-cave ice; 14 – radiocarbon date, yr BP. (From Kanevskiy et al. 2008).

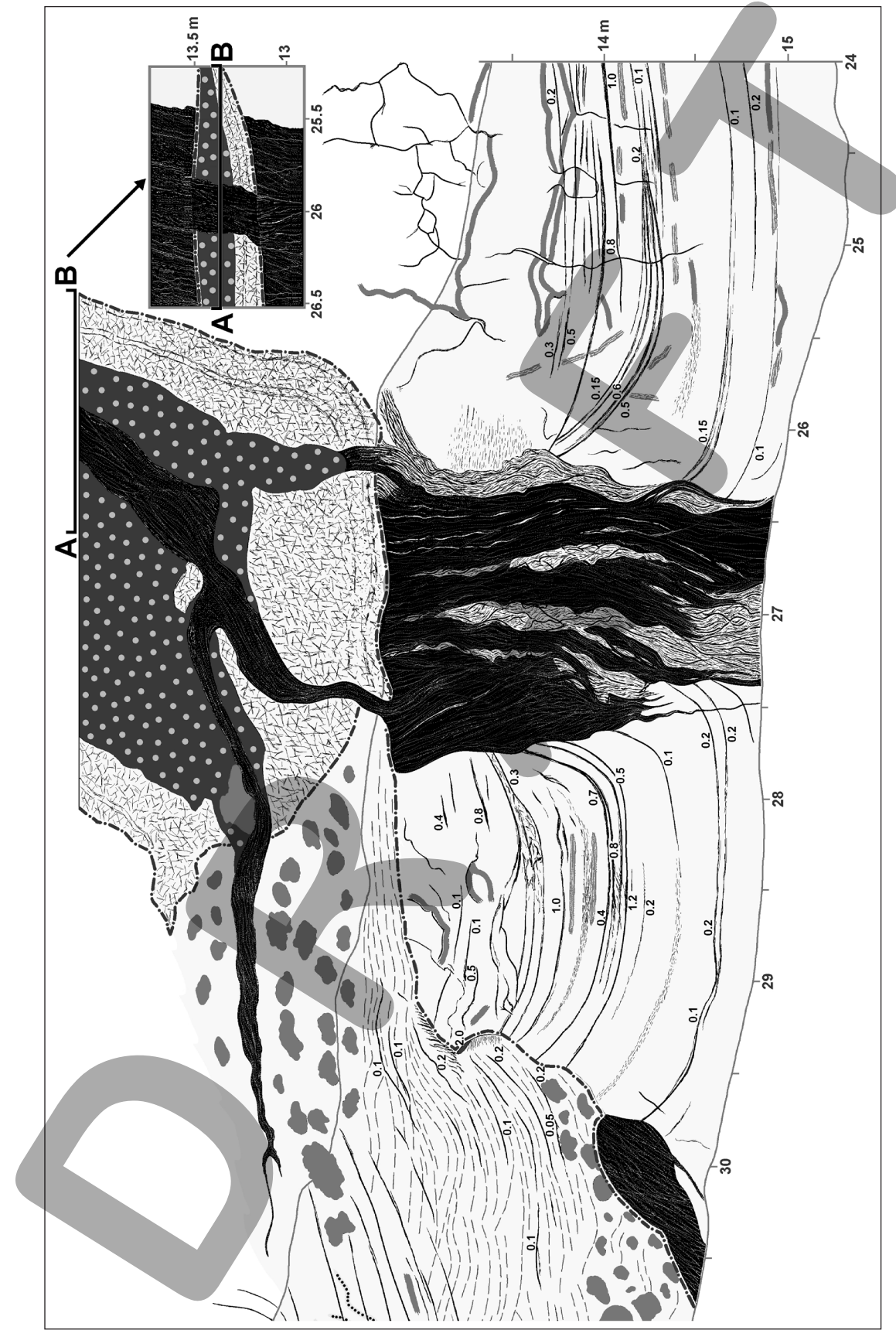


Figure 12. Cryostratigraphic map of the left wall of the winze, interval 24-31 m. For the legend, see Figure 11. A-B – schematic reconstruction of vertical section through the ice pseudomorph, located at the ceiling of the winze. (From Kanevskiy et al. 2008).

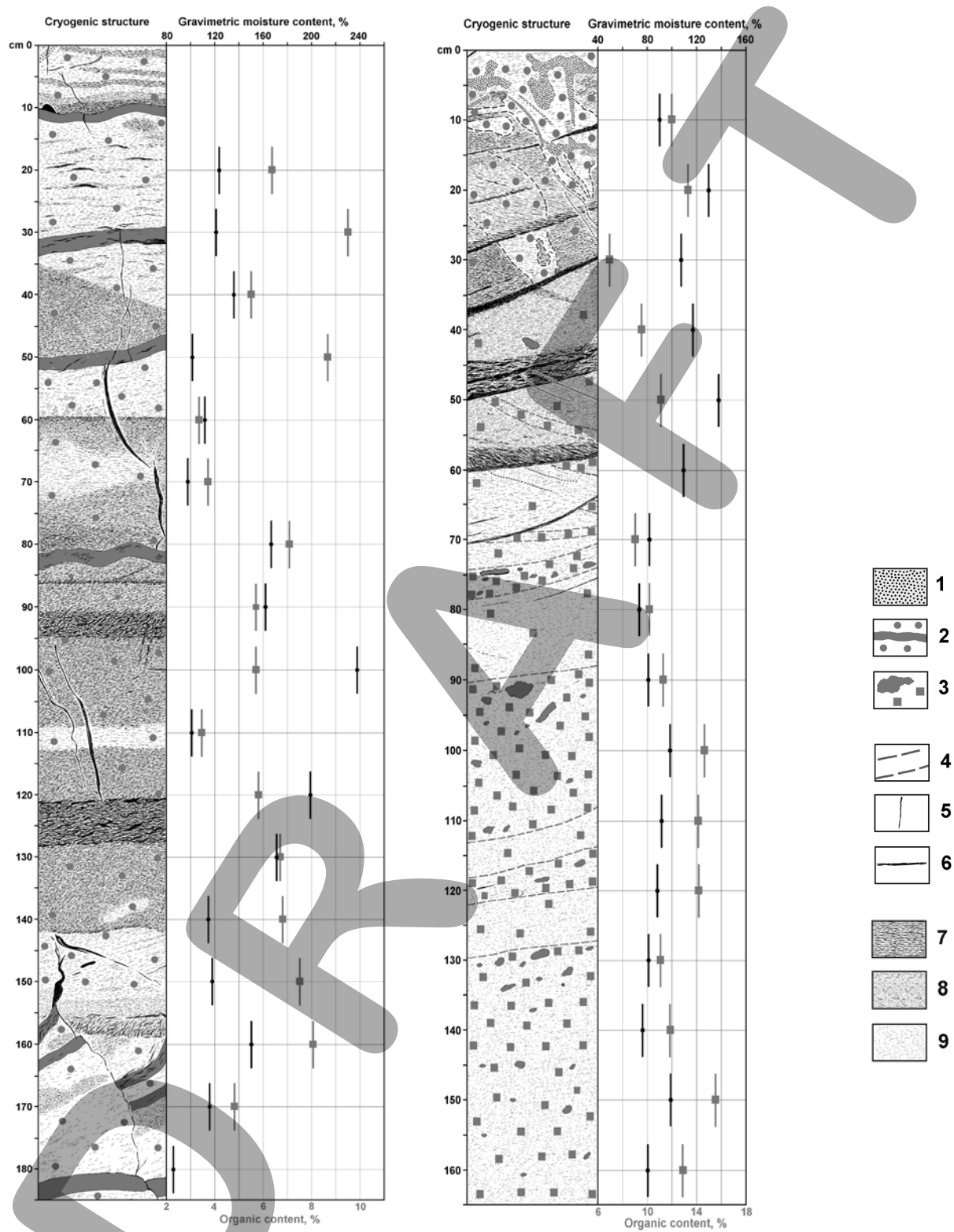


Figure 13. Details of cryogenic structure and properties of sections #1 (a) and #2 (b); location of sections is shown at Figure 11. 1 – sand; 2 – in situ peat layer and inclusions of organic matter; 3 – inclusions of retransported organic matter; 4 – lamination in silt; 5 – isolated ice vein; 6 – distinct ice layer ('belt'); 7 – micro-braided cryostructure; 8 – micro-lenticular cryostructure; 9 – latent micro-lenticular / porous cryostructure. (From Kanevskiy et al. 2008).

(a) Wedge ice

Wedge ice is the main type of massive ice that is present within the CRREL tunnel (fig. 14). It is easy to recognize by its wedge, or vertical, shape and by its foliated structure. Wedge ice is grey to dark brown in color; this reflects the presence of silt particles and organic staining within the ice. The size of the wedges is difficult to quantify. Although the wedges range in apparent width from 1 to 7 m, their true width probably varies between 0.5 and 3.0 m. It is also important to stress that only the middle and lower portions of the wedges are seen. Wedge ice is also present in the winze section where the wedges have an apparent width of up to 1.8 m. Here, the apex (nipple) of the wedge terminates at the stratigraphic contact between the overlying silts and the underlying alluvial gravels (fig. 10). The tunnel presents a great opportunity to see crossings of several ice wedges from inside: exposures of the wedge ice in the ceiling of the winze allow one to estimate the dimension of the ice-wedge polygons to reach 8-12 m (fig. 10).

When compared to the epigenetic ice wedges commonly described from northern and Central Alaska (e.g. Leffingwell 1919, Péwé, 1966), the wedges in the CRREL tunnel are average to large in size. However, when compared to some of the Late-Pleistocene syngenetic ice wedges described from Siberia along the Yana or Kolyma Rivers in northern Siberia (see Dostovalov & Popov 1966, Popov, 1973, Vasil'chuk & Vasil'chuk 1997), or the anti-syngenetic wedges inferred from the Pleistocene Mackenzie River Delta, Canada (see Mackay, 1995; French, 2007, 181), they appear to be average to small in size.

(b) Clear ice

We interpret the clear ice bodies in the CRREL tunnel to be thermokarst-cave ice (Shur et al. 2004, Bray et al. 2006). In North America, this is known colloquially as ‘pool’ ice (Mackay 1997). This is because ice-rich syngenetic permafrost is highly susceptible to thermal erosion that promotes the formation of subterra-nean channels. When these channels are finally closed by sediment, water that is ponded behind the blockage begins to freeze. This process results in formation of thermokarst-cave (‘pool’) ice. The clear ice bodies are lenticular shaped. Their visible thickness in the tunnel ranges from a few centimeters to about 2 m and their extent beyond the ceiling is not known. The largest apparent horizontal extent of this type of ice that can be viewed in the tunnel is approximately 7 m. The alternative interpretation, that these clear ice bodies are buried surface, or pond, ice (Sellmann 1967, Hamilton et al. 1988), is not supported by the cryostructures present in the tunnel.

In the winze, a horizontal body of thermokarst-cave ice crosscutting the ice wedge is exposed on the ceiling (figs. 12, 14). Its thickness varies from 0.2 to 0.35 m and it is underlain by a silt layer (0.1-0.4 m thick) having a reticulate-chaotic cryostructure (Shur et al. 2004, Fortier et al. 2008). This massive ice body is aligned with the width of the ice wedge; however, it is wider than the wedge indicating that the initial subterra-nean channel eroded laterally across the ice wedge into the enclosing sediments (see fig. 11, section A-B).

(c) Clear ice crossed by ice veins

There are many places in the tunnel where veins of wedge ice penetrate horizontal bodies of clear thermokarst-cave ice (fig. 15). This relationship demonstrates that the formation of wedge ice did not terminate when the cavity was filled with water and the water subsequently froze. Instead, it indicates that thermal-contraction cracking, ice-wedge formation, and permafrost growth continued after emplacement of the thermokarst-cave ice. The other example of where a horizontal body of thermokarst-cave ice is penetrated (i.e. crossed) by an ice wedge can be seen in the ceiling of the winze (see fig. 12, section A-B).

THERMAL EROSION, SOIL AND ICE PSEUDOMORPHS

Numerous sites of former gullies and underground channels can be observed in the silty sediments at various depths. They appear to have been cut by running water and afterwards filled with thermokarst-cave ice and soil whose structure and properties differ from the original syngenetic permafrost (Shur et al. 2004, Bray et al. 2006, Fortier et al. 2008).

The formation of thermokarst-cave ice is related to the gully erosion that must have occurred, especially during the spring snowmelt, during growth of the syngenetic permafrost on the relatively gently-sloping terrain of Goldstream Valley where the CRREL tunnel is located (Shur et al. 2004). It is necessary to stress that syngenetic permafrost, composed predominantly of ice-rich silty sediments, is especially susceptible to fluvio-thermal erosion (Shur et al. 2004, Bray et al. 2006, Fortier et al. 2007). Fluvio-thermal erosion occurs when surface runoff, from snowmelt, summer precipitation or thawing permafrost, becomes concentrated mainly along ice wedges causing preferential thaw. The gullies that result frequently assume an inverted ‘T’ cross-profile because water first erodes



Figure 14. Photo showing ice wedge dissecting a horizontal lens of white thermokarst-cave ice (ice pseudomorph), right wall of the winze. The width of the wedge is 1.0 m. The thermokarst-cave ice body is underlain by several silt layers with reticulate-chaotic cryostructure. The same wedge exposed on the opposite wall of the winze is shown in Figure 12. (Photo by M. Kanevskiy).



Figure 15. Photo showing veins of wedge ice penetrating a near-horizontal layer of thermokarst-cave ice. The location marker is 2.5 X 2.5 cm in size. (From Shur et al. 2004).

vertically and then, as the bed becomes armored with transported sediment from up-gully, laterally. This often leaves an organic-mat overhang. Slumping, piping and the creation of small tunnels above and adjacent to the partially-eroded ice wedge are also common. Fluvio-thermal erosion and the thaw-modification of ice wedges is a well known process in Arctic regions today (see French 2007, 191-2; Fortier et al. 2007). What is less well known is that, sometimes, standing water bodies accumulate in the channel floor behind slumped masses to form the ice bodies that Shumskii (1959) termed ‘thermokarst-cave ice’.

The formation of pseudomorphs is related to the thaw-modification of ice wedges that would have occurred also during fluvio-thermal or underground-erosion episodes. Soil pseudomorphs are formed by silt or gravel filling the void left by the eroded ice wedge; ice pseudomorphs are formed by thermokarst-cave ice filling the void (fig. 6). These structures represent secondary infilling. Ice, sediment or an ice-sediment mix constitutes the infill. It is not surprising that the cryogenic properties of this infill material differ from the enclosing syngenetic permafrost. Formation of these structures is regarded as typical of syngenetic permafrost growth.

Both types of pseudomorphs (soil and ice) exist in the CRREL tunnel. However, they are difficult to recognize, especially ice pseudomorphs, because some have been subsequently modified by the penetration of ice veins. The incorporation of ice veins into ice pseudomorphs demonstrates that the formation of wedge ice is not terminated by the formation of thermokarst-cave ice (Shur et al. 2004). An ice pseudomorph modified by the penetration of ice veins is shown in figure 15.

Recent examination of the main adit showed that, of 20 ice wedges identified, 19 had been subject to thermal erosion. Approximately 60% of the channels cutting through the ice wedges and the enclosing syngenetic permafrost were partially or entirely filled by thermokarst-cave ice (Fortier et al. 2008).

In the winze, a gully filled with sediments can be observed at interval 29-35 m (see figs. 10 to 13). A truncated ice wedge affected by thermal erosion is located under this gully. The sediments filling the gully are mostly ice-poor stratified silts with lenses of sands. They contain numerous inclusions of organic material, which are interpreted as having been reworked by water. The organic content of the sediments in the gully varies from 7.0% to 22.8% by weight and is much higher in comparison with the original permafrost (Section 2, fig. 13 B).

Cryostructures in the lower part of section 2 (fig. 13 B, 60-165 cm) vary from latent micro-lenticular to porous (structureless). The gravimetric moisture content of this part of section 2 varies from 70% to 100% which is smaller than the water content of the original syngenetic permafrost. Such water content is unusual for sediments with very small amount of visible ice. It can be attributed to the higher organic content (fig. 13 B). Sediments with an organic content of 9-12% have a gravimetric moisture content of 70-80%, whereas sediments with organic content of 14-16% have a moisture content of 90-100%. The cryostructures and ice contents of the upper part of the section 2 (fig. 13 B, 0-60 cm) are similar to those of the original permafrost; here, the gravimetric moisture contents vary from 110% to 140%. This indicates change of sedimentation mode and decrease of sedimentation rate at the last stages of gully infilling.

ICE CONTENT

The ice content of sediments exposed in the tunnel varies widely. Although the weathered schist exposed in the lowest part of the Gravel Room contains a very small amount of visible ice, its gravimetric moisture content varies from 6.5% to 19.9%, averaging 11.7% (Hamilton et al. 1988). Gravimetric moisture content of alluvial gravel exposed in the lowest part of the winze generally is 8.9% to 10.3% (Hamilton et al. 1988). Typically, the gravel contains crustal cryostructures with thin ice crusts enclosing the gravel clasts. Close to the contact with overlying silt the thickness of ice crusts increases: sometimes it can reach 0.5-2.0 cm. Silt is generally ice-rich: gravimetric moisture content varies from 39% to 139% (Hamilton et al. 1988).

Recent studies show that the ice content of silt strongly depends on its cryostructure. For sediments with micro-lenticular cryostructure, gravimetric moisture content in the main adit varies from 80% to 180%, averaging 130% (Bray et al. 2006). A similar range (100-240%) is found in the winze (Section 1, fig. 13 A). For modified sediments with structureless (or massive) cryostructure, which fill gullies and soil pseudomorphs, gravimetric moisture content in the main adit varies from 50% to 95%, averaging 69% (Bray et al. 2006). For similar sediments in the winze, gravimetric moisture content is 70-100% (section 2, fig. 13 B, 60-165 cm). We associate the unusually high moisture content of ice-poor silt with the high content of reworked organic material in these sediments. The average gravimetric moisture content of the cross-stratified sands with structureless (or massive) cryostructure, filling underground channels, is 44.6%, whereas it is 107.7% in the surrounding permafrost with micro-lenticular cryostructure (Fortier et al. 2008). For sediments with reticulate-chaotic cryostructure, gravimetric moisture content in the main adit varies from 60% to 115%, averaging 85% (Bray et al. 2006).

TWO SILT UNITS?

The early studies in the tunnel (Sellmann 1967, 1972, Hamilton et al. 1988) did not adequately recognize the syngenetic nature of the permafrost. Two independent systems of ice wedges and an inferred thaw unconformity that separated the silts into an upper and a lower unit were recognized (see fig. 2). Some ice bodies, described as ‘...horizontal, saucer-shaped bodies’ were interpreted as buried frozen thaw ponds formed in ice-wedge troughs, are better explained as bodies of thermokarst-cave (‘pool’) ice formed in underground channels.

There is now evidence that thermal-erosion processes were simultaneous with permafrost formation. First, the clear ice bodies are best explained as thermokarst-cave ice. Second, the occurrence of ice veins that penetrate thermokarst-cave ice means that ice wedges continued to grow after their partial thaw-modification and destruction by fluvio-thermal erosion and the subsequent pooling of water within the erosional void. Third, the dominant cryogenic structure is similar throughout the whole silt section. Fourth, the radiocarbon ages obtained from sediments within the tunnel do not reveal any sufficient break in sedimentation. In fact, no clear evidence of regional or widespread thermokarst can be found in the tunnel; instead, the thaw unconformities appear localized and connected with previous gullies and underground channels.

In summary, the cryostratigraphic data do not confirm the existence of two silt units divided by a continuous thaw unconformity, as described previously. Cryostructures, truncated ice bodies, and soil and ice pseudomorphs suggest a single sequence of continuous sedimentation and syngenetic permafrost aggradation in Late-Pleistocene time. This permafrost has been reworked by local thermal-erosional events.

REFERENCES

- Arcone, S.A. & Delaney, A.J., 1984. Field dielectric measurements of frozen silt using VHF pulses. *Cold Regions Science and Technology* 9: 29-37.
- Bray, M.T., 2008. Effects of soils cryostructure on the long term strength of ice-rich permafrost near melting temperatures. *Proceedings of the Ninth International Conference on Permafrost* (in press).
- Bray, M.T., French, H.M. & Shur, Y., 2006. Further cryostratigraphic observations in the CRREL permafrost tunnel, Fox, Alaska. *Permafrost and Periglacial Processes* 17 (3): 233-243.
- Carter, L.D., 1988. Loess and deep thermokarst basins in Arctic Alaska. *Proceedings of the Fifth International Conference on Permafrost*. Tapir publishers, Trondheim, Norway: 706-711.
- Chester, J.W., and Frank, J.N., 1969. Fairbanks Placers Fragmentation Research, Final Report. U.S. Department of Interior, Bureau of Mines, Metals Program, Auth. no. L1115-33: 52 pp.
- Delaney, A.J., 1987. Preparation and description of a research geophysical borehole site containing massive ground ice near Fairbanks, Alaska. Hanover, New Hampshire, U.S. Army CRREL Special Report 87-7, 22 pp.
- Delaney, A.J., & Arcone, S.A., 1984. Dielectric measurements of frozen silt using time domain reflectometry. *Cold Regions Science and Technology*, 9: 37-49.
- Dick, R.A., 1970. Effects of type of cut, delay and explosive on underground blasting in frozen gravel. U.S. Bureau of Mines Report of Investigations 7356, 17 pp.
- Dostovalov, B.N., and Popov, A.I., 1966. Polygon systems of ice wedges and conditions of their development. *Permafrost: International Conference Proceedings*, National Academy of Sciences – National Research Council, Washington, DC, Publication 1287: 102-105.
- Dubikov, G.I., 2002. Composition and cryogenic structure of permafrost in West Siberia. Moscow: GEOS, 246 pp (in Russian).
- Fortier, D., Allard, M., & Shur, Y., 2007. Observation of rapid drainage system development by thermal erosion of ice wedges on Bylot Island, Canadian Arctic Archipelago. *Permafrost and Periglacial Processes* 18 (3): 229-243.
- Fortier, D., Kanevskiy, M., & Shur, Y., 2008. Genesis of Reticulate-Chaotic Cryostructure in Permafrost. *Proceedings of the Ninth International Conference on Permafrost* (in press).
- French, H.M., 2007. *The Periglacial Environment*, Third Edition. John Wiley and Sons Ltd, Chichester, UK, 458 pp.
- Garbeil, H.M., 1983. Temperature effects upon the closure of a gravel room in permafrost. MS thesis, University of Alaska Fairbanks.
- Gasanov, S.S., 1963. Morphogenetic classification of cryostructures of frozen sediments. *Trudy SVKNII*, Vol. 3, Magadan (in Russian).

- Gasanov, S.S., 1969. Structure and history of formation of permafrost in Eastern Chukotka. Moscow: Nauka, 168 pp. (in Russian).
- Gravis, G.F., 1969. Slope sediments of Yakutia. Moscow: Nauka, 128 pp. (in Russian).
- Hamilton, T.D., Ager, T.A., & Robinson, S.W., 1983. Late Holocene ice wedges near Fairbanks, Alaska, USA: environmental setting and history of growth. *Arctic and Alpine Research* 15 (2): 157-168.
- Hamilton, T.D., Craig, J.L., & Sellmann P.V., 1988. The Fox permafrost tunnel: a late Quaternary geologic record in central Alaska. *Geological Society of America Bulletin* 100: 948-969.
- Huang, S.L., Aughenbaugh, N.B., and Wu, M.C., 1986. Stability study of CRREL permafrost tunnel. *Journal of Geotechnical Engineering* 112: 777-790.
- Johansen, N.I., Chalich, P.C., and Wellen, E.W., 1981. Sublimation and its control in the CRREL permafrost tunnel. Hanover, New Hampshire, U.S. Army CRREL Special Report 81-8, 12 pp.
- Johansen, N.I., and Ryer, J.W., 1982. Permafrost creep measurements in the CRREL tunnel. Proceedings of the Third International Symposium on Ground Freezing, Hanover, New Hampshire, 1982. Hanover, New Hampshire, U.S. Army CRREL, 61-63.
- Kanevskiy, M., 2003. Cryogenic structure of mountain slope deposits, northeast Russia. Proceedings of the Eighth International Conference on Permafrost, Zurich, Switzerland, July 21-25, 2003 1: 513-518.
- Kanevskiy, M., Fortier, D., Shur, Y., Bray, M., and Jorgenson, T., 2008. Detailed Cryostratigraphic Studies of Syngenetic Permafrost in the Winze of the CRREL Permafrost Tunnel, Fox, Alaska. Proceedings of the Ninth International Conference on Permafrost (in press).
- Katasonov, E.M., 1962. Cryogenic textures, ice and earth wedges as genetic indicators of perennially frozen Quaternary deposits. Issues of Cryology in Studies of Quaternary Deposits. Moscow: Izd-vo AN SSSR, 86-98 (in Russian).
- Katasonov, E.M., 1969. Composition and cryogenic structure of permafrost. National Research Council of Canada, Ottawa, Technical Translation 1358, 25-36.
- Katasonov, E.M., 1978. Permafrost-facies analysis as the main method of cryolithology. Proceedings of the Second International Conference on Permafrost, July 13-28, 1973. USSR Contribution. Washington: National Academy of Sciences, 171-176.
- Katayama, T., Tanaka, M., Moriizumi, J., Nakamura, T., Brouchkov, A., Douglas, T. A., Fukuda, M., Tomita, F., and Asano, K., 2007. Phylogenetic analysis of bacteria preserved in a permafrost ice wedge for 25,000 years. *Appl. Environ. Microbiol.* 2007 April, 73(7): 2360-2363.
- Kudryavtsev, V.A., (ed.). 1978. General Permafrost Science (Geocryology). 2nd edn. Moscow: Moscow University Press, 463 pp. (in Russian).
- Lawson, D.E., 1983. Ground ice in perennially frozen sediments, northern Alaska. In: Proceedings of the Fourth International Conference on Permafrost. National Academy Press, Washington, D.C.: 695-700.
- Linell, K.A., and Lobacz, E.F., 1978. Some experiences with tunnel entrances in permafrost. Proceedings of the Third International Conference on Permafrost, Edmonton, July 10-13, 1978. Ottawa: National Research Council of Canada, 814-819.
- Long, A., and Péwé, T.L., 1996. Radiocarbon dating by high-sensitivity liquid scintillation counting of wood from the Fox permafrost tunnel near Fairbanks, Alaska. *Permafrost and Periglacial Processes* 7: 281-285.
- Mackay, J.R., 1972. The world of underground ice. *Annals, Association of American Geographers* 62: 1-22.
- Mackay, J.R., 1995. Ice wedges on hillslopes and landscape evolution in the late Quaternary, western Arctic coast. *Canadian Journal of Earth Sciences*, 32: 1093-1105.
- Mackay, J.R., 1997. A full-scale experiment (1978-1995) on the growth of permafrost by means of lake drainage, western Arctic coast: a discussion of the method and some results. *Canadian Journal of Earth Sciences*, 34: 17-33.
- Melnikov, V.P., and Spesivtsev, V.I., 2000. Cryogenic Formations in the Earth's Lithosphere. Novosibirsk: Siberian Publishing Center UIGGM, Siberian Branch, Russian Academy of Sciences, 343 pp.
- Murton, J.B., and French, H.M., 1994. Cryostructures in permafrost, Tuktoyaktuk coastlands, western arctic Canada. *Canadian Journal of Earth Sciences* 31: 737-747.
- Pettibone, H.C., and Waddell, G.G., 1971. Stability of an underground room in frozen gravel. In Proceedings of the 9th Annual Engineering Geology and Soils Engineering Symposium, Boise, Idaho. Boise, Idaho Department of Highways: 3-30.

- Pettibone, H.C., and Waddell, G.G., 1973. Stability of an underground room in frozen gravel. Proceedings, American contribution, Second International Conference on Permafrost: Yakutsk, U.S.S.R. Publication 2115. National Academy of Science, Washington, DC: 699-706.
- Péwé, T.L., 1966. Ice wedges in Alaska – classification, distribution and climatic significance. Permafrost: International Conference Proceedings, National Research Council of Canada - National Academy of Sciences, Washington, DC, Publication 1287, 76-81.
- Péwé, T.L., 1975. Quaternary geology of Alaska. United States Geological Survey, Professional Paper 835, 145 pp.
- Pikuta, E.V., Marsik, D., Dej, A., Tang, J., Krader, P. & Hoover, R. B. 2005. *Carnobacterium pleistocenium* sp. nov., a novel psychrotolerant, facultative anaerobe isolated from permafrost of the Fox Tunnel in Alaska. *Int. J. Syst. Evol. Microbiol.*, 55, 473-478.
- Popov, A.I., 1967. Cryogenic phenomena in the Earth crust (Cryolithology). Moscow: Moscow University Press, 304 pp. (in Russian).
- Popov, A.I., 1973. Album of cryogenic formations in the Earth's crust and relief. Moscow: Moscow State University, 56 pp. (in Russian).
- Popov, A.I., Rozenbaum, G.E., and Tumel, N.V., 1985. Cryolithology. Moscow: Moscow University Press, 239 pp. (in Russian).
- Romanovskii, N.N., 1993. Fundamentals of cryogenesis of lithosphere. Moscow: Moscow University Press, 336 pp. (in Russian).
- Sellmann, P.V., 1967. Geology of the USA CRREL permafrost tunnel, Fairbanks, Alaska. Hanover, New Hampshire, US Army CRREL, Technical Report 199, 22 pp.
- Sellmann, P.V., 1972. Geology and properties of materials exposed in the USA CRREL permafrost tunnel. Hanover, New Hampshire, US Army CRREL, Special Report 177, 16 pp.
- Shumskii, P.A., 1959. Ground (subsurface) ice. In: principles of geocryology, Part I. General geocryology. Academy of Sciences of the USSR, Moscow, Chapter IX, 274-327 (in Russian) (English translation: C. de Leuchtenberg, 1964. National research Council of Canada, Ottawa, Technical Translation 1130, 118 pp).
- Shur Y.L., 1988. Upper horizon of the permafrost soils and thermokarst. Novosibirsk: Nauka, Siberian Branch, 210 pp. (in Russian).
- Shur, Y., French, H.M., Bray, M.T., and Anderson, D.A., 2004. Syngenetic permafrost growth: cryostratigraphic observations from the CRREL Tunnel near Fairbanks, Alaska. *Permafrost and Periglacial Processes* 15 (4): 339-347.
- Shur, Y., and Jorgenson, M.T., 1998. Cryostructure development on the floodplain of the Colville River Delta, Northern Alaska. Proceedings of the Seventh International Conference on Permafrost, June 23-27, 1998, Yellowknife, Canada. Université Laval, Québec: 993-999.
- Soloviev, P.A., 1959. Permafrost of northern part of Lena-Amga plain. Moscow: Academy of Sciences of the USSR Publishing House, 144 pp (in Russian).
- Swinzow, G.K. 1970. Permafrost tunnelling by a continuous mechanical method. Hanover, New Hampshire, US Army CRREL, Technical Report 221, 37 pp.
- Thompson, E. G. & Sayles, F. H. 1972. In-situ creep analysis of room in frozen soil. *Journal of Soil Mechanics and Foundation Division, ASCE*, 98: 899-915.
- Vasil'chuk, Y.K., and Vasil'chuk, A.C., 1997. Radiocarbon dating and oxygen isotope variations in Late Pleistocene syngenetic ice wedges, Northern Siberia. *Permafrost and Periglacial Processes*, 8: 335-345.
- Vasil'chuk, Y.K., and Vasil'chuk, A.C., 2000. AMS-dating of Late Pleistocene and Holocene syngenetic ice wedges. *Nuclear Instruments and Methods in Physics Research B* 172: 637-641.
- Vtyurin, B.I. 1964. Cryogenic structure of Quaternary deposits. Moscow: Nauka, 151 pp. (in Russian).
- Watanabe, O., 1969. On permafrost ice. *Journal of Japanese Society of Snow and Ice* 31 (3): 53-62 (in Japanese, translated by CRREL).
- Weerdenburg, P.C., and Morgenstern, N.R., 1983. Underground cavities in ice-rich frozen ground. Proceedings of the Fourth International Conference on Permafrost, Fairbanks, Alaska, July 17-22, 1983. Washington, D.C.: National Academy Press, 1384-1389.
- Wooler, M.J., Zazula, G.D., Edwards, M., Froese, D.G., Boone, R.D., Parker, C., and Bennett, B., 2007. Stable carbon isotope compositions of eastern Beringian grasses and sedges: investigating their potential as paleoenvironmental indicators. *Arctic, Antarctic and Alpine Research* 39 (2): 318-331.
- Zhestkova T.N., 1982. Formation of the cryogenic structure of ground. Moscow: Nauka, 209 pp. (in Russian).

SITE #14

SHEEP CREEK THAW POND: THERMOKARST LAKES AND METHANE EMISSIONS

Katey Walter

In some permafrost-dominated regions of the North, thermokarst (thaw) lakes occupy as much as 22-48% of the land surface and are major sources of methane, a potent greenhouse gas, to the atmosphere. Thermokarst lakes form when permafrost thaws, ice melts and the ground surface subsides. Thermokarst ponds can initiate naturally, in response to climate warming and wetting or in response to both natural (i.e. wildfire) or human-caused disturbance (i.e. road construction). Once initiated, small thermokarst ponds can grow into large lakes rapidly, on time scales of decades to centuries due to thermal and mechanical erosion processes. This thermokarst expansion leads to the release of organic matter previously sequestered in permafrost in anaerobic lake bottoms, providing a substrate for organic decomposition by microbes and production and emission of methane. Methane is a potent greenhouse gas, 25 times stronger than CO₂ on a per molecule basis. Radiocarbon ages of methane bubbles released from thermokarst lakes in the retranslocated loess valleys of the Fairbanks area range from 14,000-26,000 years old, demonstrating the important contribution of this ancient permafrost-contained organic matter source. Modern terrestrial and aquatic ecosystems also contribute organic matter sources to methanogens. The balance of 14C-depleted permafrost organic matter versus that from modern ecosystems in fueling methane production from thermokarst lakes is the subject of ongoing research. Methane bubbling rates are measured with bubble traps and gas collected for geochemical and isotopic analyses to help constrain processes controlling methane production and emission from thermokarst lakes. In winter, methane bubbles trapped in lake ice are mapped in order to estimate whole-lake emissions and relate emissions to rates of permafrost thaw.



"Drunken forest" along thermokarst margin of lake.



Hotspots of methane bubbling.



Early winter survey transects on lake ice for methane bubbles.

This area is perennially frozen, late Pleistocene-aged retransported organic-rich loess.

DRAFT

PART II

**PERMAFROST FEATURES IN CARIBOU-POKER
CREEKS RESEARCH WATERSHED (CPCRW)
AND ENVIRONS OF FAIRBANKS ALASKA**

DRAFT

PERMAFROST FEATURES IN CARIBOU-POKER CREEKS RESEARCH WATERSHED (CPCRW) AND ENVIRONS OF FAIRBANKS ALASKA

Kenji Yoshikawa, Vladimir Romanovsky, Les Viereck, and Larry Hinzman
University of Alaska, Fairbanks

SUMMARY OF ITINERARY

Stop	Time		Page
1	12:30pm	Pearl Creek Elementary School Permafrost/Active Layer Monitoring Site (active layer, permafrost temperature)	71
2	1:00pm	Goldstream Creek tussock tundra (permafrost condition and Holocene ice wedge)	72
3	1:30pm	O'Connor Creek pingo site open system pingo.....	72
4	2:00pm	Fox gold mining site permafrost outcrop (Pleistocene ice wedge).....	73
5	2:30pm	Chatanika (gold mine and convection heat transfer).....	73
6	3:00pm	Caribou Poker Creeks Research Watershed oil spill experiments: Oil Spill and Frost Fire Experiments.....	74
7	3:15pm	Aufveis (Icing) and permafrost hydrology	78
8	3:30pm	Caribou Poker Creeks Research Watershed fire impact/ thermokarst developments	81
9	4:00pm	Isabella Creek bog lake.....	82
10	4:40pm	Grenac Creek (Farmer's loop) pingo	82

DRAFT

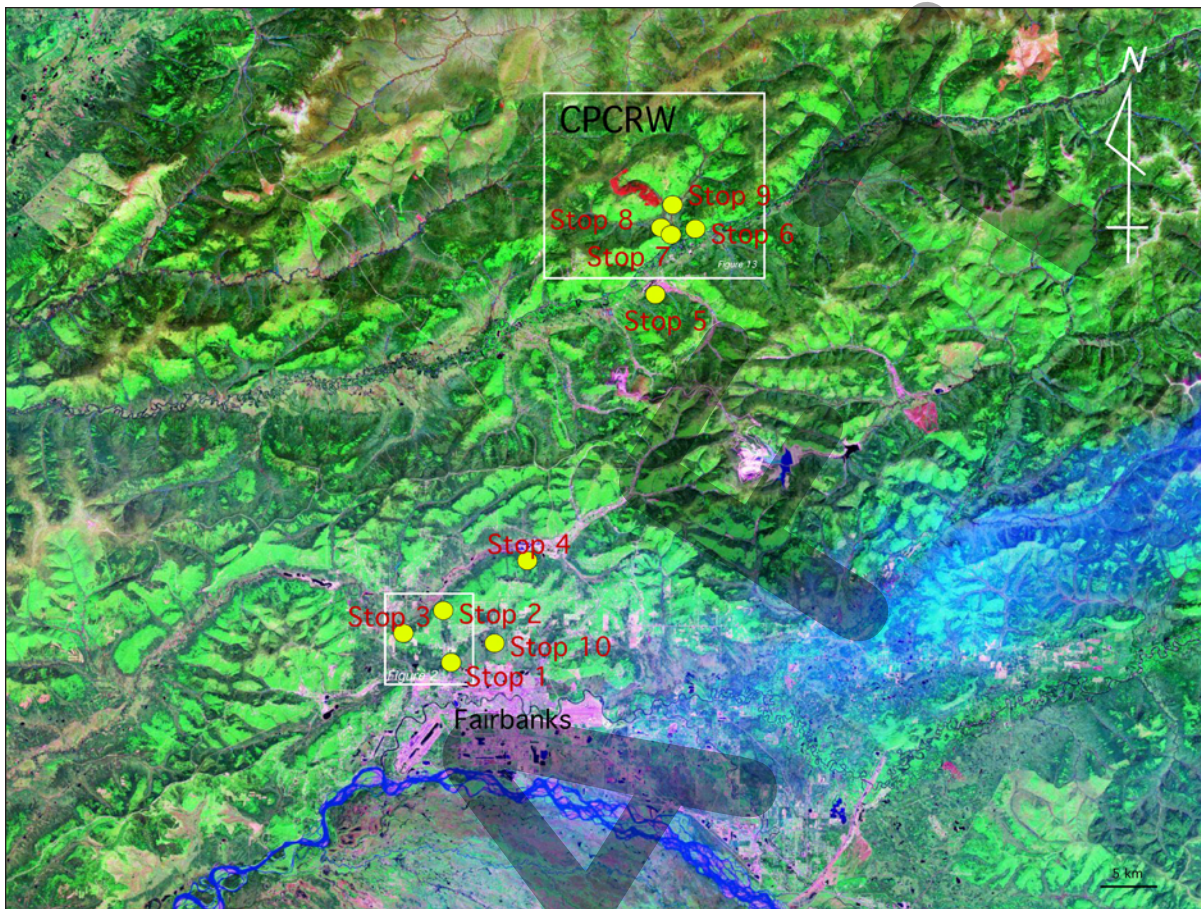


Figure 1. Index map (Landsat image) showing route of CPCRW trip.

SOIL AND PERMAFROST

Most of the interior Alaskan boreal forests are underlain by discontinuous permafrost. The discontinuous character of permafrost distribution creates a complex interrelationship between permafrost and vegetation in the Alaskan boreal forest. Permafrost thickness varies in this area from 0 to 150 – 200 meters (Ferrians, 1965; Brown et al., 1997) with the most typical values of 20 to 120 meters. Lateral continuity of the perennially frozen layer changes from practically continuous (90-95%) in the southern foothills of the Brooks Range to discontinuous (50-90%) in interior Alaska and in most of the Alaska Range, to sporadic (10-50%) and isolated patches (0-10%) south of the Alaska Range, Talkeetna, and Wrangell Mountains (Brown et al., 1997). Permafrost temperature is the most important indicator of permafrost stability. The closer the temperature is to 0°C, the more susceptible permafrost is to surface disturbances. In interior Alaska, permafrost temperature varies seasonally within the upper 3 to 15 meters, explaining why the temperature at the depth of zero seasonal amplitude (typically 3 to 15 m) is usually used to describe the permafrost thermal state. Permafrost temperatures in the Alaskan boreal forest are 0 to -4°C and typically warmer than -2°C (Osterkamp and Romanovsky, 1999). Other natural factors that influence permafrost temperature regime include the thickness, thermal properties and duration of the snow cover (Brown and Pewe, 1973; Romanovsky and Osterkamp, 1995). The mean annual ground surface temperatures are usually 3 to 6°C warmer than the mean annual air temperatures. As a result of relatively warm air temperatures and the effect of snow cover in reducing winter heat loss from soil, the mean annual ground surface temperatures in the Alaskan boreal forest often exceed 0°C and can be as high as 4°C.



Figure 2 Aerial photograph of first three field stops just north of Fairbanks, Pearl Creek, Goldstream Creek, and O'Connor Creek

STOP 1: PEARL CREEK ELEMENTARY SCHOOL PERMFROST/ACTIVE LAYER MONITORING SITE

Permafrost monitoring K12 outreach program

This purpose of this project is to establish long-term permafrost monitoring sites adjacent to schools within the circum-polar permafrost region. Permafrost is one of the important indicators useful for monitoring climatic change. Change in permafrost conditions also affects local ecosystems, hydrological regimes and may trigger certain natural disasters such as landslides. This long-term permafrost observatory is valuable for contemporary and future scientific objectives, but it can also benefit students and teachers in urban and remote village schools. Most remote villages depend on a subsistence lifestyle and will be directly affected by changing climate and permafrost degradation. Monitoring the permafrost temperature in the Arctic to develop a better understanding of the spatial distribution and thermal condition of permafrost and having students participate in collecting the data is an ideal IPY (International Polar Year) project. Our outreach project involves drilling boreholes at local schools throughout Alaska and western Canada and installing a micro data logger with temperature sensors to measure hourly air and permafrost temperatures. Trained teachers help students download data several times a year and discuss the results in class. The data gathered from these stations are shared and can be viewed by anyone through the internet (<http://www.uaf.edu/permafrost>). Using the internet teachers can also compare their data with data from other monitoring stations.

This project is becoming a useful science project for these remote villages, which tends to have limited exposure to science, despite their changing surroundings. NSF (EPSCoR) funded the preliminary seed outreach program. Currently NSF, NASA and the International Polar Year (IPY) program support this project. The broader impacts

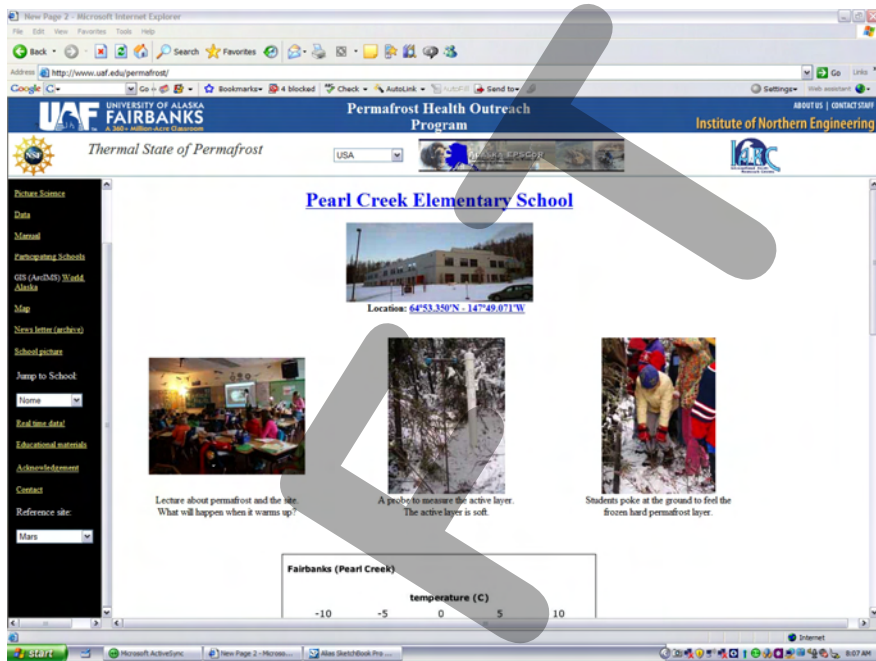


Figure 3. The permafrost data collected at each participating school are available via an internet based data server. Most of the schools have 6m boreholes and temperature recording on a 1hour interval. Over 40 village schools now participate and over 100 villages will be partners by the end of IPY.

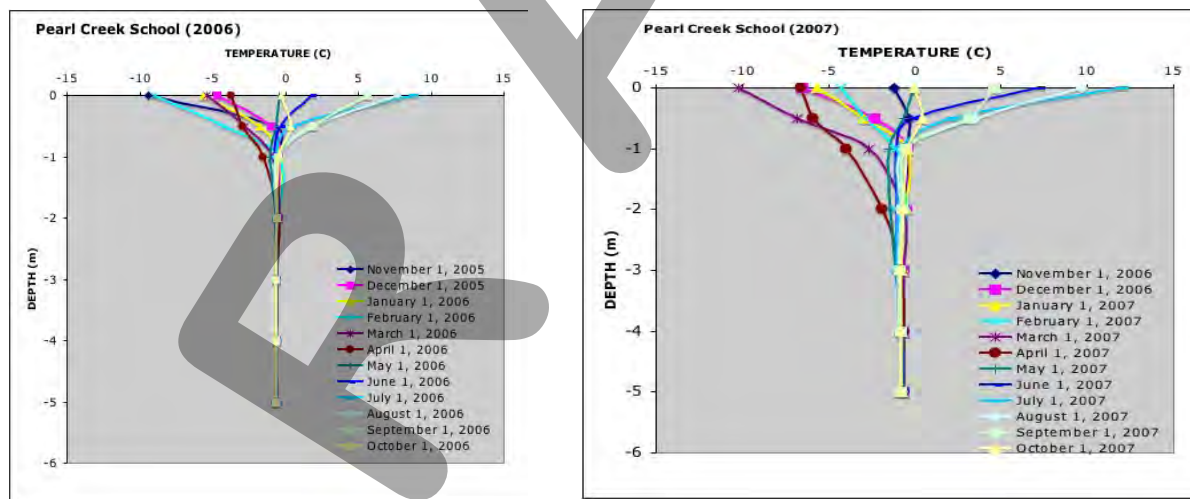


Figure 4. Monthly ground temperatures from the Pearl Creek school site. The spring of 2007 was extremely cold (-40°C) affecting April's ground temperature.

of this project are 1). To provide opportunities for field experience and educational participation at levels ranging from elementary school to high school. 2). To provide a high-resolution characterization of the spatial distribution of the thermal state of permafrost, especially in Alaska. 3). To assist in improving the general knowledge of the Earth's climatic patterns and provide the opportunity for younger generations to take part in understanding the climatic systems. These data and on-line Q&A systems help students improve their understanding of the relationship between permafrost condition and the arctic climate system. As well as being a strong outreach program to support village science education, the date sets from this project will establish a baseline for future permafrost monitoring investigations.

Ground temperature transects

Permafrost temperatures are strongly affected by the slope and aspect in this region. South facing slopes, in general, are absent of permafrost while permafrost is usually present on north facing slopes and in the valley bottoms. A series of shallow boreholes were installed from UAF to Goldstream Creek. Permafrost temperature is between -1°C and -0.17°C, depend on the site. We estimated freezing (thawing) point of the local Fairbanks silt to be -0.17°C. The freezing point depression between the observed thawing soil and the thawing temperature of free water is due to both solutes in the soil water and the matric potential of the fine grained soils.

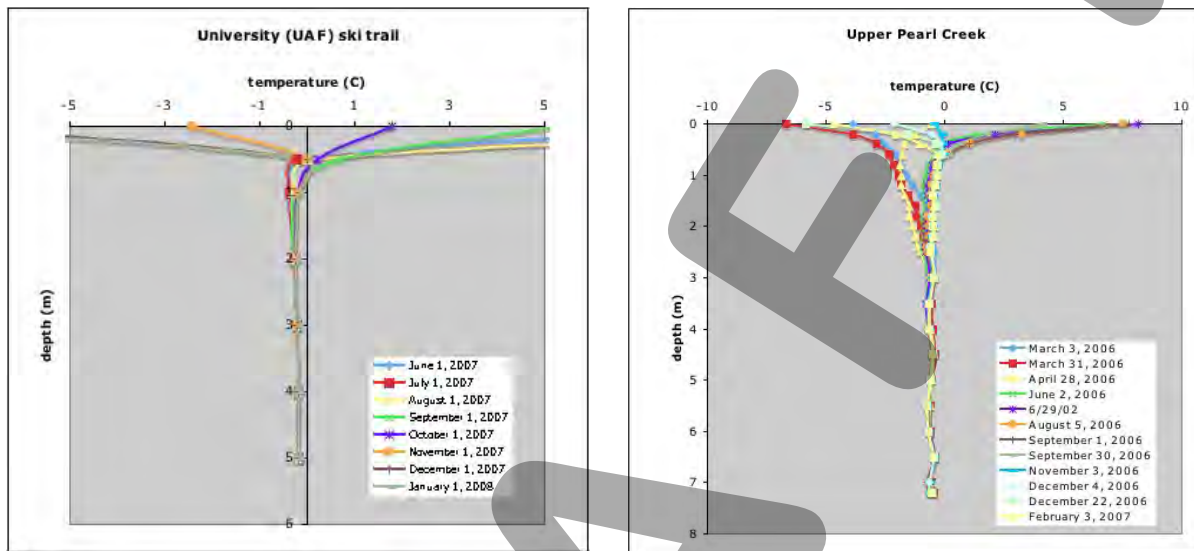


Figure 5. Monthly ground temperatures from selected sites. The permafrost temperature at University (UAF) ski trail site meet thawing point (-0.17°C).

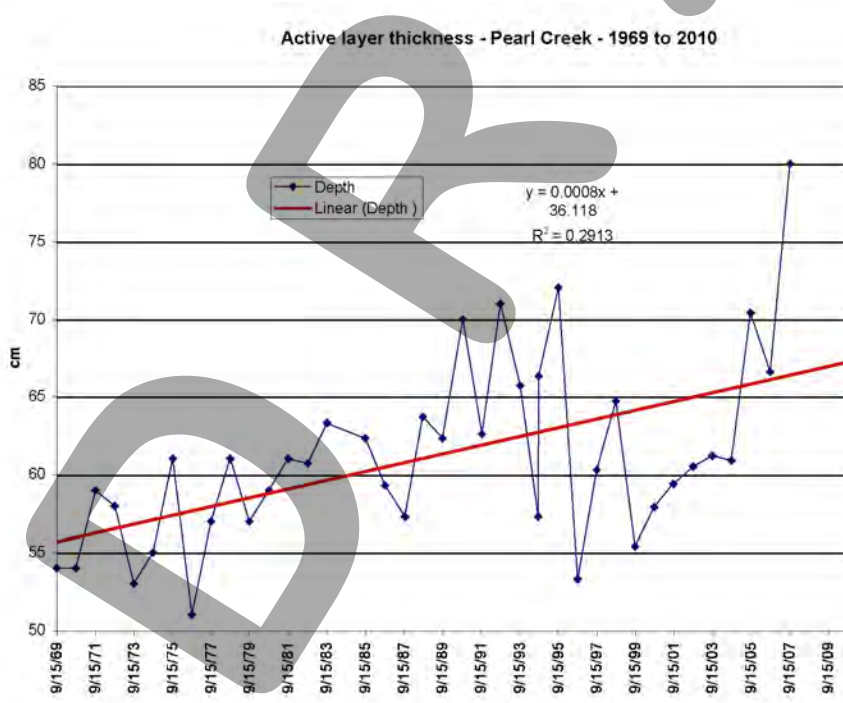


Figure 6. Active layer thickness including last 30 years at Upper Pearl Creek site. The thaw depths of the Year 1996, 1999-2002 were similar to the 1970s, otherwise we can see a clear increasing trend. These permafrost temperatures are very close to the thawing point and have significant unfrozen liquid water in soil.

STOP 2: GOLDSTREM CREEK



Figure 7. Ice wedge polygons are observed at the bottom of Goldstream Creek valley. These ice wedges remain active feature and still experience contraction cracking during low snow winters.

HOLOCENE ICE WEDGE AND GROUND TEMPERATURE TRANSECTS

Active ice wedge polygons may be observed in the Goldstream Creek valley. In general, the frost contraction process is inactive at Fairbanks area under the contemporary climate. Many of these ice wedges developed 32,000 -39,000 yBP (MIS-3). However, Holocene (current) ice wedges are present in this area. Frost contraction cracking still occurs approximately every 10 years or longer, particularly, during low-snow winters in areas that have substantial micro-topography (such as well developed tussocks).

Non-conductive heat transfer in tussock tundra

The permafrost stability of discontinuous permafrost regions is strongly controlled by soil type and the physical and thermal properties of the surface of active layer. In general, the organic rich (peat or moss) layer increases the stability of permafrost, perhaps to the extent where the mean annual ground surface temperature may reach a positive temperature, due to the effect of the thermal offset (Gold et al., 1972). The thermal offset describes the process where more heat may escape from the active layer in the winter than enters the soil in the summer. This results because of the difference between frozen and unfrozen thermal conductivity of the surface soil. Non-conductive heat transfer is also a very important process influencing the stability of the permafrost. Most areas



Figure 8. Four permafrost temperature monitoring sites are within 500m of the University of Alaska Fairbanks. The tussock tundra site is more than 3°C colder than an open black spruce forest.

in the lower (southern) boundary of mountain permafrost are occupied by rock glaciers or frozen block slopes. Rock glaciers or block slopes have the maximum pore space available for convective heat transfer during winter periods, also protect from sun ray during summer months. Sawada and Ishikawa (2002) found permafrost under block slopes as a result of convective heat flow in Hokkaido Island, Japan. Woodcock (1974) reported 14 m of thickness of the permafrost at Mauna-Kea, Hawaii, despite a mean annual ground surface temperature at the summit of Mauna-Kea of +1.2°C. Permafrost or massive ice body has been observed in many warm (positive ground surface temperature) locations due simply to the site specific heat transfer process that is enhanced by convection during the winter by but diminished during the warmer period. Goering and Kumar (1996) designed a road-bed that promotes winter-time convection in open graded embankments for cooling of the unstable permafrost. The road embankments are cooler than the surround ground during winter periods, driven by convective heat transfer as the cold, dense air circulates in the pore space. During the summer, the surface is warmer and convective heat transfer is minimal as the warmer, less-dense air mass in the pore space does not sink. This structure is commonly seen in the cold region engineering designs today such as Tibet- Qinghai railway.

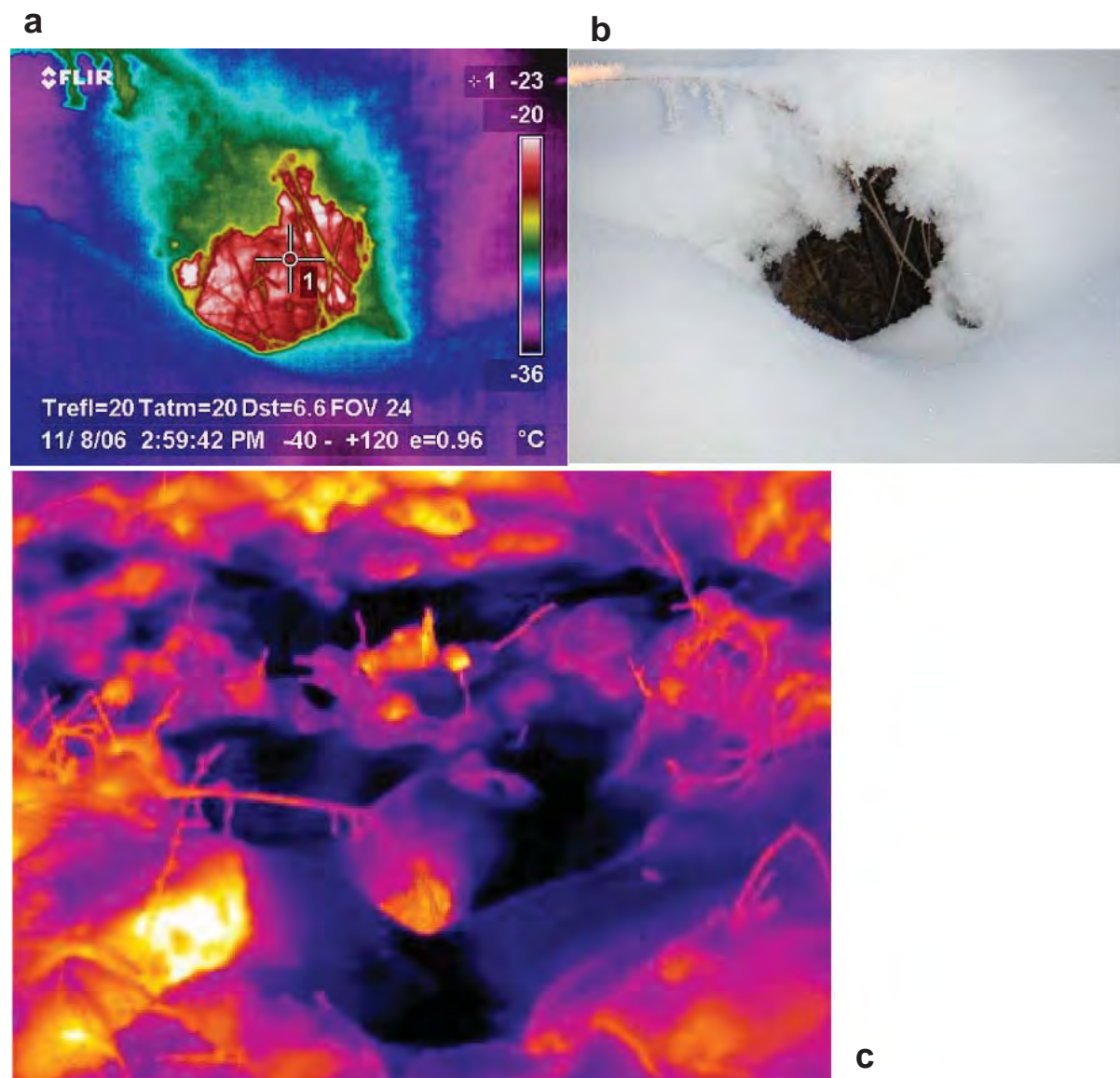


Figure 9. A thermal infrared camera captured an image of the warm sub-snow terrain in early winter (a) and (c) (November 8, 2006). Condensation was observed at the warm air output (b). This process only occurred during low-snow winters, which partially exposed the tussocks and enhanced thermal gradients.

Tussock tundra is a common vegetation observed in interior, western and northern Alaska. Tussocks develop as earth hummock type mounds (ca. 50cm diameter) with relatively deep (20-50cm) gaps sometimes filling with standing water. This micro topography produces conditions that are very difficult for people to walk or work. Tussock tundra also experiences colder thermal conditions by non-conductive heat transfer. Cooling is enhanced by the convective heat transfer during winter months, evapotranspiration during the summer and blocking of direct solar radiation by the rough surface tussock vegetation.

Table 1. Surface roughness and physical conditions of four study sites

	Depth (m) of the Temperature	Average Temperature	Minimum Temperature	Maximum Temperature	Surface roughness (rms)
mixed forest	3.00m	-0.75	-1.59	-0.44	ND
closed spruce	2.96m	-1.74	-3.89	-0.79	3.78
open spruce	3.00m	-0.39	-0.47	-0.35	4.59
tussock	2.80m	-4.11	-9.22	-1.26	8.95

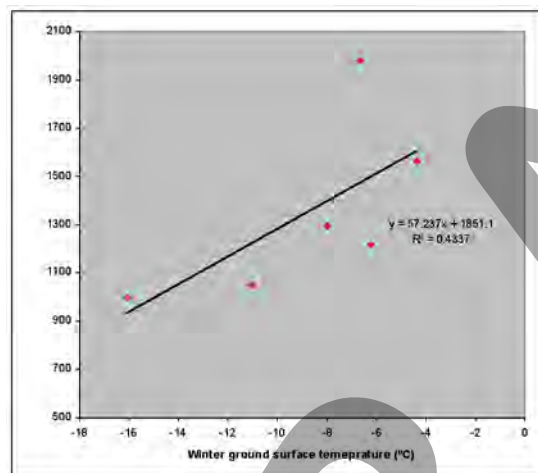


Figure 10. Greater snow depths provide more insulation and yields warmer ground temperatures, particularly if snow falls early in the winter.

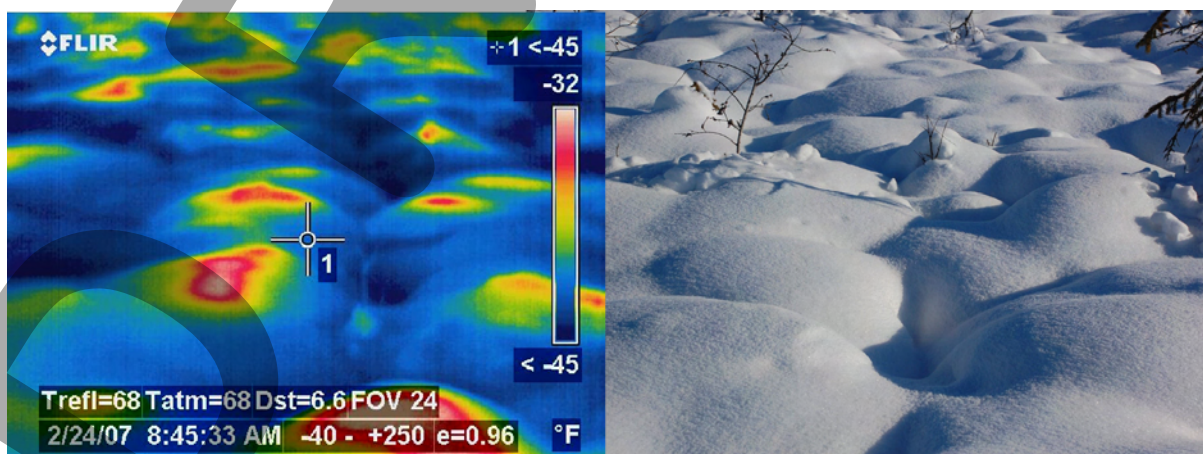


Figure 11. Thermal infrared image captures the cold sub-snow terrain between tussocks in late winter (left) (February 24, 2007).

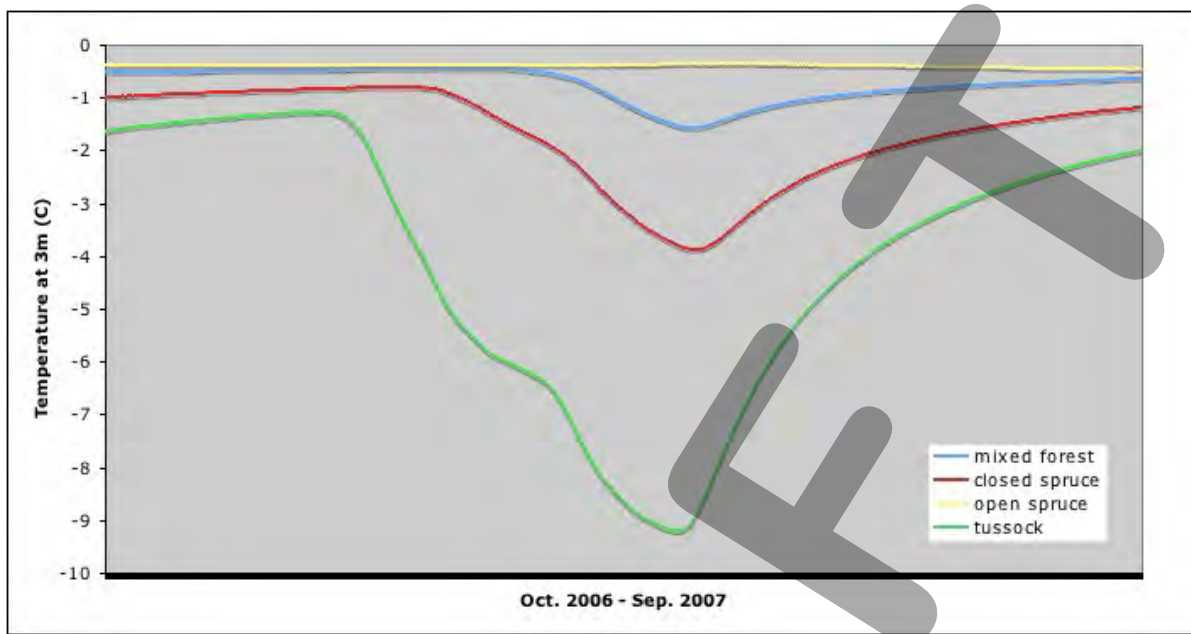


Figure 12. Ground temperature regime at a depth of 2.9m ±10cm within a 500m apart all of the sites. Tussocks are much colder than other sites. This Interior Alaska tussock site displays a temperature regime that is similar to North Slope.

STOP 3: O'CONNER CREEK PINGO SITE

Five small open system pingos are located near O'Conner Creek. They occur near the toe of an alluvial fan. These pingos are among the oldest research pingos in Alaska In the 1950s, T. Pewe named these pingos, biggest to smallest, as alpha, beta, and gamma. Alpha pingo is an elliptical mound about 100m long, 60m wide, and 10.4m high. The pingo has a breached crater ~6m deep in the center. Most of the pingo's overburden is composed of dry silt. The active layer thickness is 1-3m. Pingo ice was found from 6m to 10 m below surface, including organic layers. The area surrounding the pingos was originally black spruce, muskeg, and bog that had been cleared for farming.

Beta pingo lies about 120m to the northeast of Alpha pingo and is about one-half the size. It has no depression in the center. On the south side, which is steep and slumping, growing trees are deformed and several have split trunks. It seems the mounds have been relatively stable over 40 years. Some of the old bench marks, which Pewe and his student installed in September 1964, still exist without deformation.

In a nearby drill hole, the silt is 27m thick and overlies 15m of creek gravel. The permafrost is 43m thick. The hydraulic potential of the pingos and the nearby alluvium deposits are high (>68kPa), creating artesian conditions. Most of the homeowners have installed groundwater wells for domestic usage. Heating the well to prevent freezing by the permafrost is critically important and risky work. The permafrost temperature is very warm (>-1°C) and sub-permafrost groundwater is close to the freezing point. Groundwater leaking around the outside of the well casing is a typical problem in artesian wells. In some cases the ensuing discharge from the wells continued to flow through the winter that creating large masses of aufeis (icings), some of which have destroyed houses and covered roads. In November 2005, serious well leakage occurred near the pingo site. Liquid nitrogen was injected to freeze the seepage around the well on February 24, 2006. The well was completely frozen stopping the groundwater discharge. We had the opportunity to monitor sub-permafrost groundwater potentials during and after this event. After the well leakage was stopped, the groundwater hydraulic potential immediately began rising and within a few weeks, har returned to the original pressure.

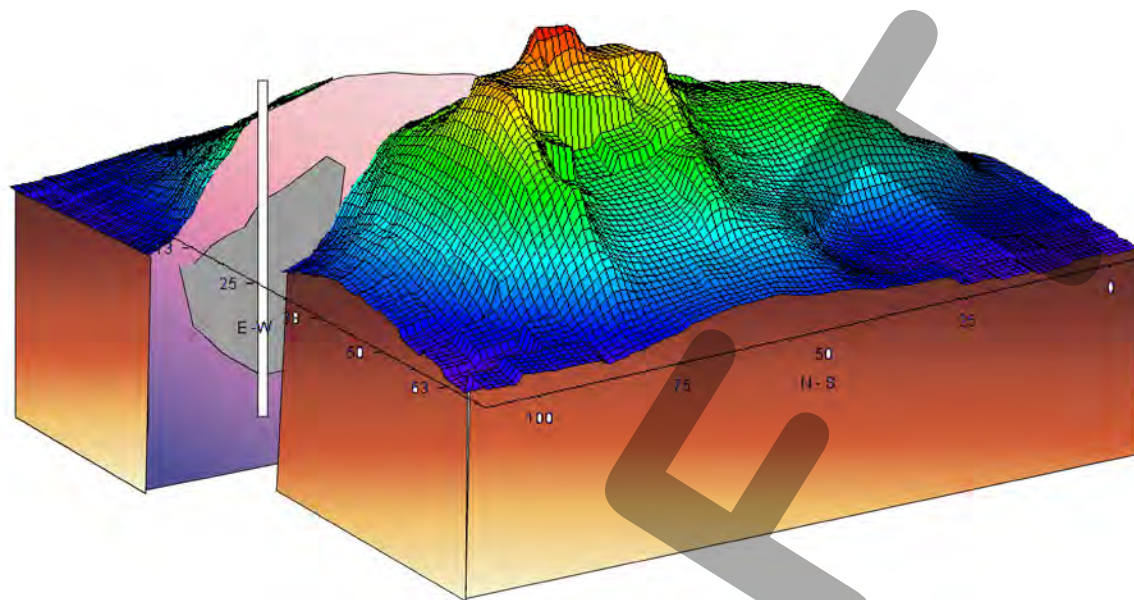


Figure 13. The alpha pingo sketch viewed from north west side. A massive ice core was found 6-10m deep at the north side of the shoulder of pingo (drilled by Yoshikawa 2005).

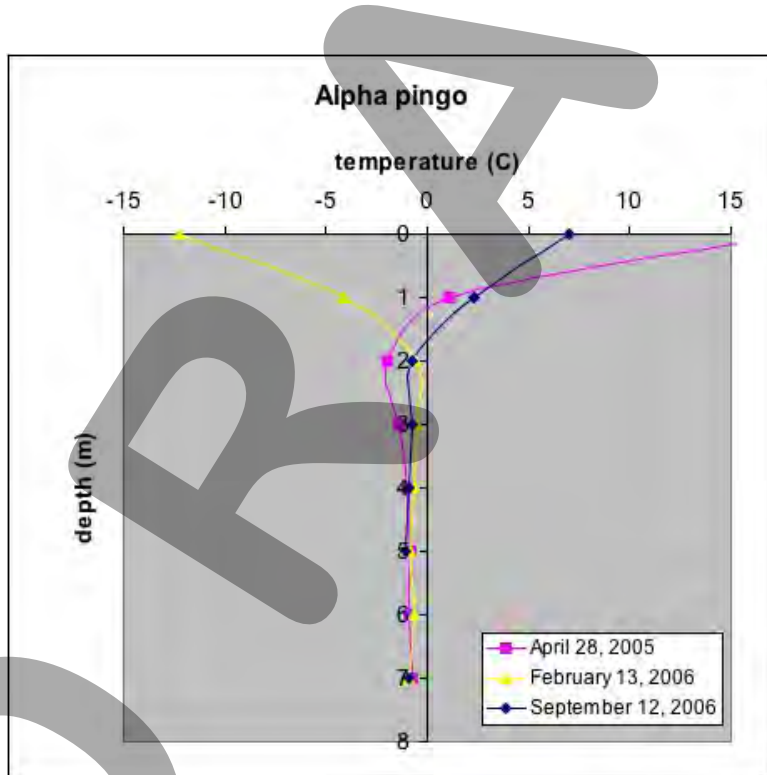


Figure 14. The temperature profile at Alpha Pingo displays stable cold temperatures below 2 m. A massive ice core was found between 6-10m.



Figure 15. South facing slope of beta pingo (palsa) photo taken in 1965 (top) by D. Hopkins and 1998 (bottom) by K. Yoshikawa.

	Caribou Cr. A	Caribou Cr. B	O'Conner Cr. α & β	Alder Cr.	Cripple Cr.	Grenac Cr.
Max. active layer	5.60m	2.8m	2.55m	ND	ND	2.2m
Permafrost temp.	-0.70°C @10m	-0.63°C @13m	-0.63°C @6m	ND	ND	-0.72°C @4.5m
groundwater level	+>4 m	ND	+12.3m	ND	ND	+1m
depth to the ice	<5.35m	7.35m	4m	ND	10m	6.5m
activity	No (but icing blister) since 1987 survey	No since 1987 survey	No since Sep. 1963 by T. Pewe	No since 1949 aerial photo	No since 1949 aerial photo	No since 1965 by T. Pewe
method						
permafrost thickness (m)	60m est.	60m est.	48.8m	ND	ND	33m
discharge water	1.25 L/sec	No flow	0.06 L/sec	1.25 L/sec	ca. 3 L/sec	0.13 L/sec
water temp.	-0.02 °C	ND	0.02 °C	0.03 °C	ND	ND

Figure 16. Characteristics of the pingos around Fairbanks area.

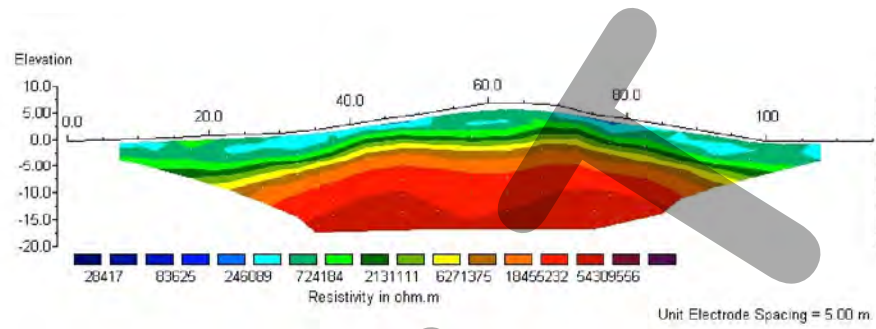


Figure 17. Resistivity tomography result at the Alpha pingo

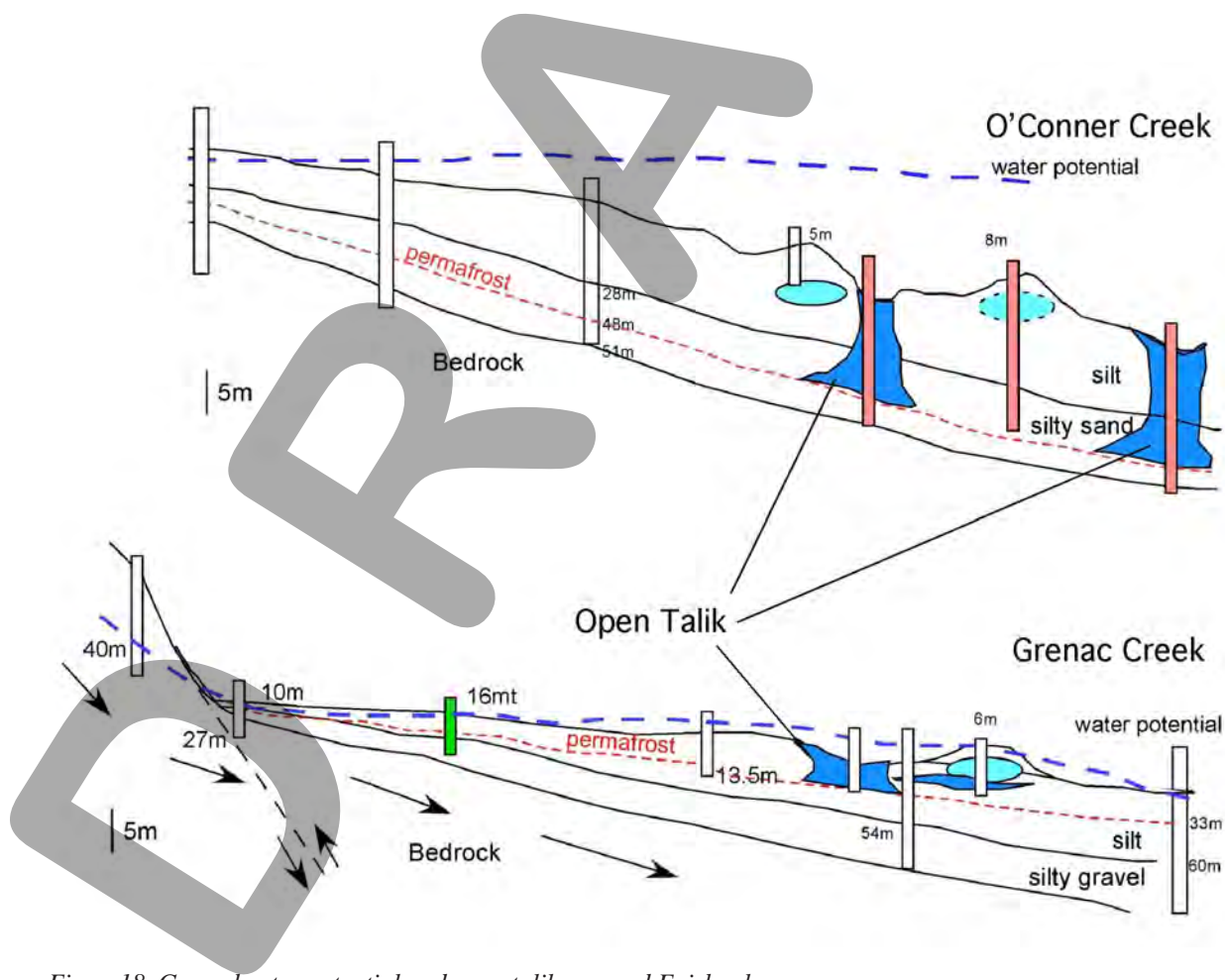


Figure 18. Groundwater potential and open taliks around Fairbanks.

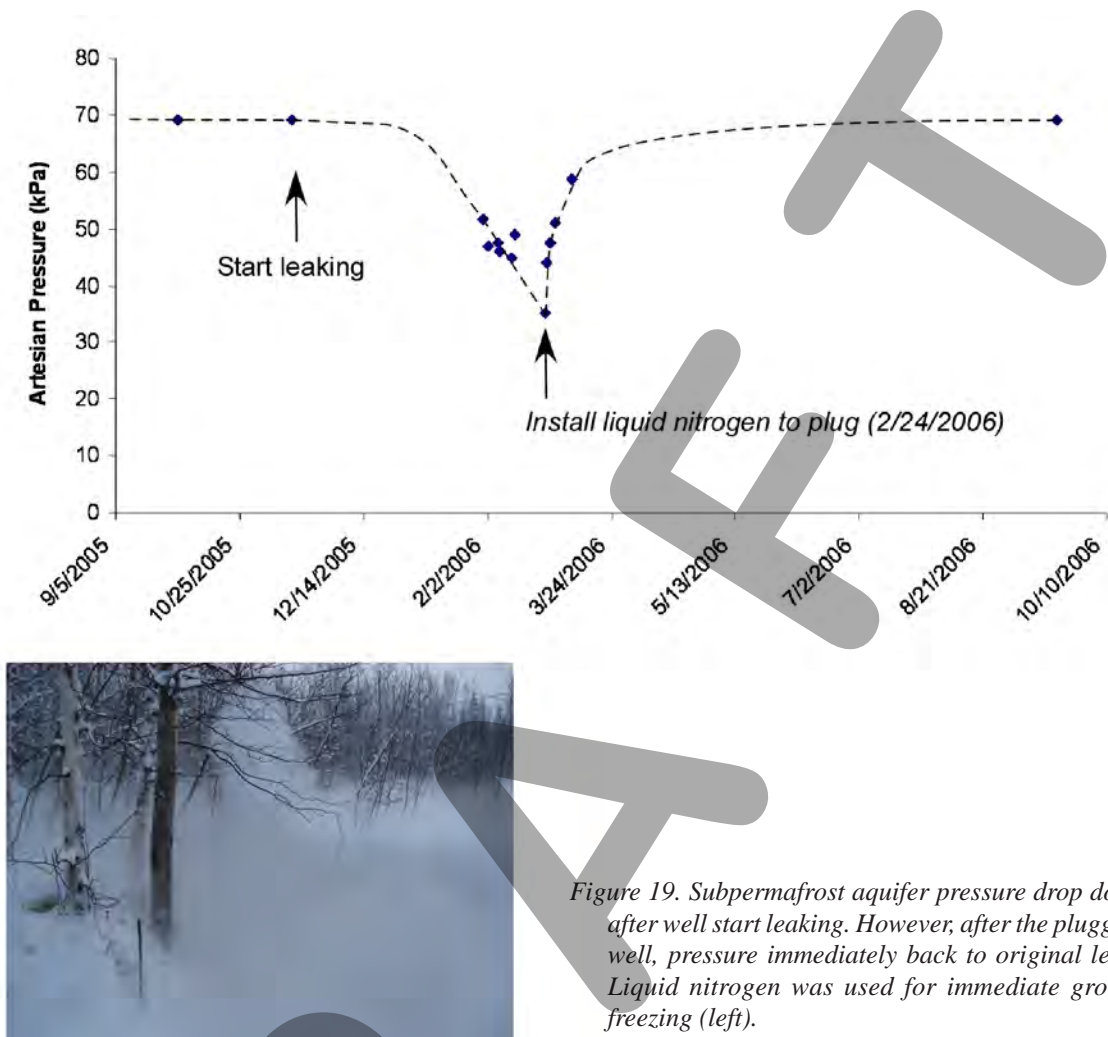


Figure 19. Subpermafrost aquifer pressure drop down after well start leaking. However, after the plugging well, pressure immediately back to original level. Liquid nitrogen was used for immediate ground freezing (left).

STOP 4: FOX GOLD MINING SITE PERMAFROST OUTCROP

A variety of ages of ice wedges have been observed in the Fairbanks area especially due to the gold mining activities. The majority of the ice wedge bodies developed around 30k-40kyBP (MIS-3). Stable isotopes variations in the ice wedges vary with the chronological sequences. Most of the stable isotope distributions (deuterium vs. oxygen 18) fit the present local meteorological water line very well. This indicates that the snowmelt water was the most consistent source of water filling the frost cracks after the cold winter. The oldest ice wedge group in the Fairbanks region was found about 21m below the ground surface. A tephra layer from these sediments indicate the possible age of around MIS 9-11. The stable isotopes of this group ($\delta^{18}\text{O}$: -24 ‰, $\delta^2\text{H}$: -170 ‰) were heavier than the late Wisconsinan ice wedges complex (MIS-3), most of which were observed to be formed 39,000–32,000 y.B.P. The stable isotopes of this major Wisconsinan group ($\delta^{18}\text{O}$: -28 ‰, $\delta^2\text{H}$: -210 ‰) were the lightest numbers than any other ice wedge group. Not many ice wedges were observed to have formed during Last Glacial Maximum (MIS 2). Large amounts of loess were deposited in this period, but the ice wedges are relatively slender, caused by less winter precipitation.

The stable isotopes of the Holocene (MIS 1) ice wedges ($\delta^{18}\text{O}$: -18 ‰, $\delta^2\text{H}$: -150 ‰) were heavier values than any other ice wedges group. They are also found at stop 2 (Goldstream Creek valley). The total snow accumulation in Fairbanks had a nearly constant $\delta^{18}\text{O}$ value between -22 and -23 ‰ in 2003. The average stable isotopes of snow are little lighter than the Holocene ice wedge group. The heavier infilling water might be coming from some soil moisture and/or a condensation process may be involved.

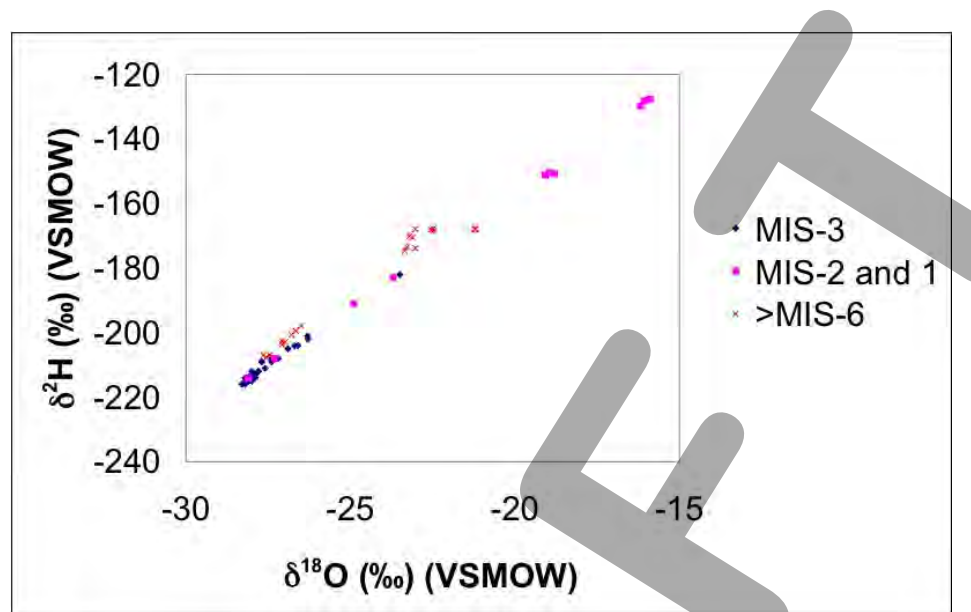


Figure 20. isotope variations from the numerous ages of ice wedge ice around the Fairbanks area.

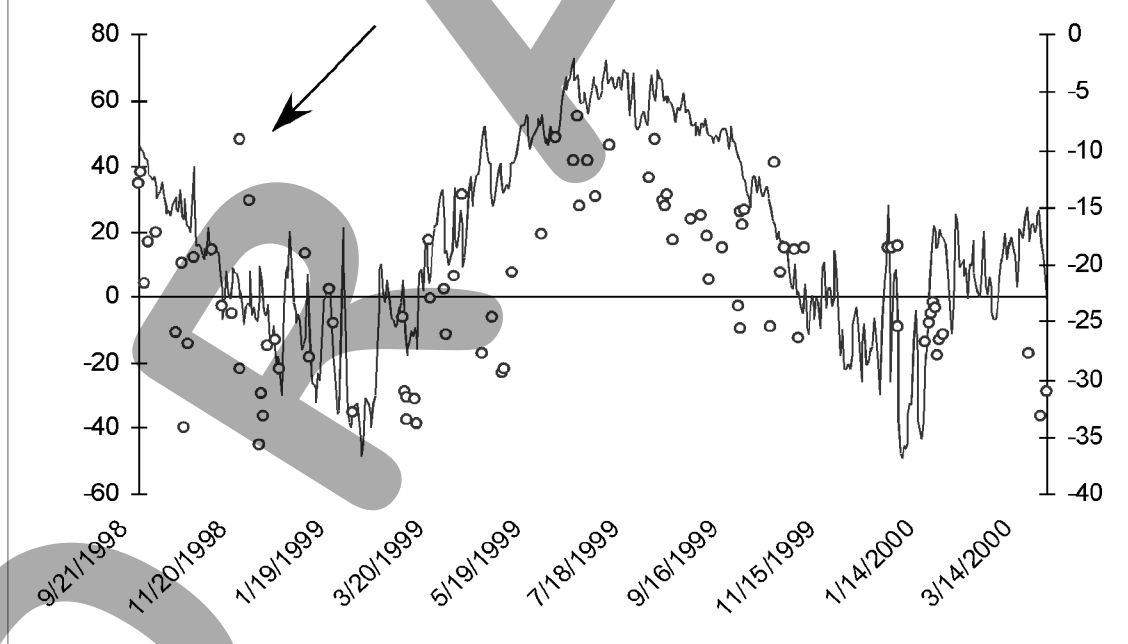


Figure 21. $\delta^{18}\text{O}_{\text{VSMOW}}$ value of precipitation (right axis) and air temperature ($^{\circ}\text{F}$) (left axis) at Fairbanks Alaska. In general, the isotope value and air temperature have positive trend except during Chinook storms that occur occasionally in winter (see arrow).

The present $\delta^{18}\text{O}$ value of the precipitation has a strong seasonal signal in Fairbanks area. Most of the snow precipitation was lighter than -20 ‰ , and rain was heavier than snow. However, there were several strong southern wind events (the jet stream brought large air masses from the Pacific Ocean), which carried heavier $\delta^{18}\text{O}$ water from Gulf of Alaska during the middle of winter (see fig. 21 arrow).

The spatial distribution of the stable isotopes in Interior Alaska varies between -40 ‰ and -20 ‰ . The lightest snow values are observed at the summit of Denali (south peak) 6194 m above sea level. And the heaviest snow values (-15 ‰ or more) were in Fairbanks during the jet stream's irregular cycles (fig. 22). The jet stream is located far south of Alaska almost all winter. However, 2-3 times of the each winter, the circulation patterns of the jet stream break through to Alaska, carrying warm humid air from the Pacific Ocean. These humid snowstorms from the south (Gulf of Alaska) usually have a steeper trend than the other local meteorological line.

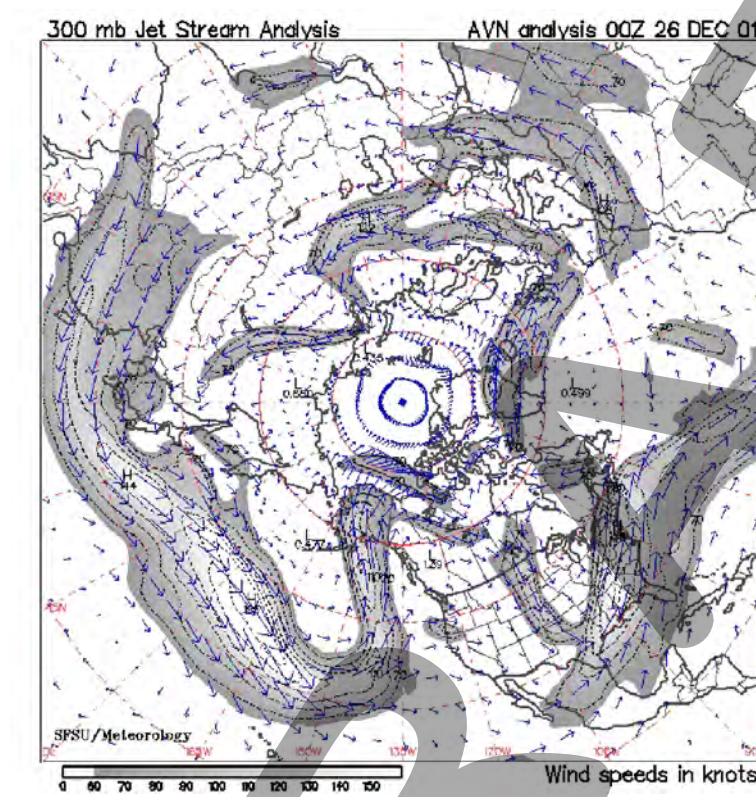


Figure 22. Jet stream distribution during a “Chinook” storm in the Northern Hemisphere on December 26, 2001 from San Francisco State University (<http://squall.sfsu.edu/crws/jetstream.html>). During this circulation pattern, heavy isotopic snow was observed in Interior Alaska.



Figure 23. one of the oldest ice wedges in the mining tunnel (left). And MIS-3 ice wedges exposed mining activity (right).

STOP 5: CHATANIKA

Gold Mining History

In 1902 a miner named Felice Pedroni located good gold prospects in the Tanana River valley. Felix Pedro, as he was known, lacked the supplies for wide-scale exploration. Then, in 1901, a grandiose scheme to build a railroad led to a grubstake for the miner. The result was another gold rush. John J. Healy, who had founded the North American Trading and Transportation Company, proposed a railroad from Southcentral Alaska to the Tanana River valley. News of Pedro's gold discovery spread. By September 1902, dozens of prospectors had arrived in the area. A settlement grew around a trading post opened by Elbridge Truman "E.T." Barnette. At the urging of Judge Wickersham, Barnette suggested to the new residents that they name the new community Fairbanks. The name honored Indiana Senator Charles Fairbanks who was chairman of the Joint High Commission charged with settling the Alaska-Canada boundary dispute. Within a year, Fairbanks had attracted 1,200 people. Near the new community was a better location for sternwheelers to dock. A second town, Chena, grew at this site. Fairbanks promoters, however, successfully waged war with the competing town. The deciding factor was Judge Wickersham's transfer of the seat of the third judicial district from Eagle to Fairbanks. The first project was the Tanana Mines Railroad. Narrow-gauge rails were laid from Chena to Gilmore 21 miles to the northeast. From there, spur tracks provided freight and passenger service to camps as far north as Chatanika, some 10 miles away. The Fairbanks merchants built on this service. They pooled their resources and built wagon roads to the outlying districts.

Driving north from Fairbanks on the Steese Highway, it is possible to see two pipelines. One is bright and shiny and carries oil; the other is old and rusted and carried water years ago. They are both remarkable examples of engineering for their day. The rusty pipe, almost exactly the same diameter (46 to 56 inches) as the Trans-Alaska Pipeline (48 inches), represents the remnants of a project undertaken during the years 1924 to 1929 to bring water to the Fairbanks area gold mining operations. The operation was carried out under the auspices of the Fairbanks Exploration Company (known locally as F.E.), a subsidiary of United States Smelting, Refining and Mining Company (U.S.S.R. & M.). This project, known as the Davidson Ditch, was a 90-mile-long conduit designed to divert water from the Chatanika River at a point below the junction of Faith and McManus Creeks to hydraulic sluicing (stripping) operations at Cleary and Goldstream, just north of Fairbanks. The term "ditch" does not do the project justice because, although the open earthwork section comprised most of its length, the course included a 0.7 mile long tunnel near Fox, and 6.13 miles of inverted siphons along the way. (Anyone who has tried to suck gas from a gasoline tank and drain it into a bucket through a hose knows what a siphon is. It carries fluid over a high point into a lower one. An inverted siphon carries fluid across a low point--in this case, a stream bed, back to a higher one.). The inverted siphons, which are the pipes visible today, were masterpieces of engineering at the time. There were fifteen in all, crossing ridges and the creek beyond. The longest was a 7,961 foot section which crossed the Chatanika River with a head of 544 feet (the reason that Chatanika water crossed above its source river downstream from the inlet is that the Davidson Ditch had a gradient of only 2.112 feet per mile, whereas the river's gradient is significantly higher). (*History of Alaskan Operations of U.S.S.R. & M.* written by John C. Boswell and published by the Mineral Industries Research Laboratory of the University of Alaska.)

Poker Flat Research Range

Poker Flat Research Range (PFRR) is the only non-federal, university owned and operated rocket range in the world and the only high-latitude, auroral-zone rocket launching facility in the United States of America. The name *Poker Flat* was taken from an old Bret Harte rags-to-riches short story, *The Outcasts of Poker Flat*; the name may have been suggested by the nearby Poker Creek, or perhaps by the way in which the original launch site was constructed from begged and borrowed materials. Owned and operated by the University of Alaska's Geophysical Institute since 1968, the range has been primarily dedicated to the launch of sounding rockets for the purpose of auroral and middle to upper atmospheric research. Range operations are funded through contracts with the National Aeronautics and Space Administration (NASA) and the range has been operating under a cooperative agreement between NASA and the Geophysical Institute since 1979.

A small band of university employees work year-round at the facility to maintain the physical plant, to provide launch support, and to obtain the various waivers, approvals and agreements necessary to the operation. Past funding sources include the Defense Nuclear Agency, the U.S. Air Force Geophysics Laboratory, the National Science Foundation, and the National Oceanic and Atmospheric Administration.

The 5,132-acre site located about 30 miles northeast of Fairbanks, Alaska, is the world's largest, land-based rocket range and has an established chain of downrange flight and observing facilities from inland Alaska to Spitzbergen in the Arctic Ocean for monitoring and recovery purposes. Data from various scientific instruments are collected by

Poker Flat's Geospace Environment Data Display System (GEDDS) (<http://www.pfrr.alaska.edu/tour/pfrr/gedds.htm>) and at the Data Analysis Center (<http://www.pfrr.alaska.edu/tour/uaf/dac.htm>) in the Geophysical Institute. Summary plots of the data sets are provided to allow users to quickly look through the data and identify periods of interest. Numerical data sets may be used to generate additional plots or in other types of analysis.



Figure 24. Chatanika gold rush town in the early 1900s (upper above) and today (lower above). These pictures were taken towards the north (e.g. showing the south-facing slope). The vegetation on the south facing slope was already shrubs with spruce at the bottom of valley and the top of the hill.

STOP 6: CARIBOU-POKER CREEKS RESEARCH WATERSHED (CPCRW)

The Caribou-Poker Creeks Research Watershed (CPCRW) is a 104 km² basin near Chatanika, Alaska reserved for ecological, hydrological, and climatic research. It is owned jointly by the State of Alaska and the University of Alaska Fairbanks. The entrance to the Research Watershed is located on the Steese Highway about 31 miles from Fairbanks (<http://www.lter.alaska.edu/>).

Following the 1967 Fairbanks flood, it was realized that very little was known about the precipitation and hydrology of upland headwater streams in interior Alaska, and that all the USGS gages were on major rivers and did not predict the 1967 flood. The Inter-Agency Technical Committee for Alaska (IATCA), which had been set up under the President's Water Research Council, had a mandate to "develop a comprehensive plan for use as a general guide by all agencies in establishing hydrologic stations required in connection with developing the water resources of Alaska" (Slaughter and Lotspeich 1977). A research coordination committee was created to, among other things, identify an upland taiga watershed for designation as a research watershed for "long term studies of complete catchments in permafrost-dominated uplands" (Slaughter and Lotspeich 1977). The Caribou and Poker Creek watersheds were identified as the most likely, because they would provide ease of access, were of manageable size, had a lack of human influence, and were owned by state and federal agencies. In 1969, a Cooperative Agreement between the IATCA and the Alaska Department of Natural Resources (DNR) was written and signed, designating the basin as the CARIBOU-POKER CREEKS WATERSHED for a period of 50 years, and outlining the responsibilities of the signing parties. This document says that DNR will "recognize research into water and land/water related resources... ...as being the presently known highest and best use of these lands, and to permit only compatible uses." The agreement was amended to delegate to the Institute of Northern Forestry (INF), USDA Forest Service, "authority and responsibilities" set forth in the original agreement. INF managed the site from the early 1970s until 1993.

In December of 1993, the leadership of the Bonanza Creek Long Term Ecological Research (BNZ-LTER) program requested of the National Science Foundation that CPCRW be added to the Bonanza Creek Experimental Forest (the main site for BNZ), and that the name and acronym be changed to BNZ-CPW to reflect the additional

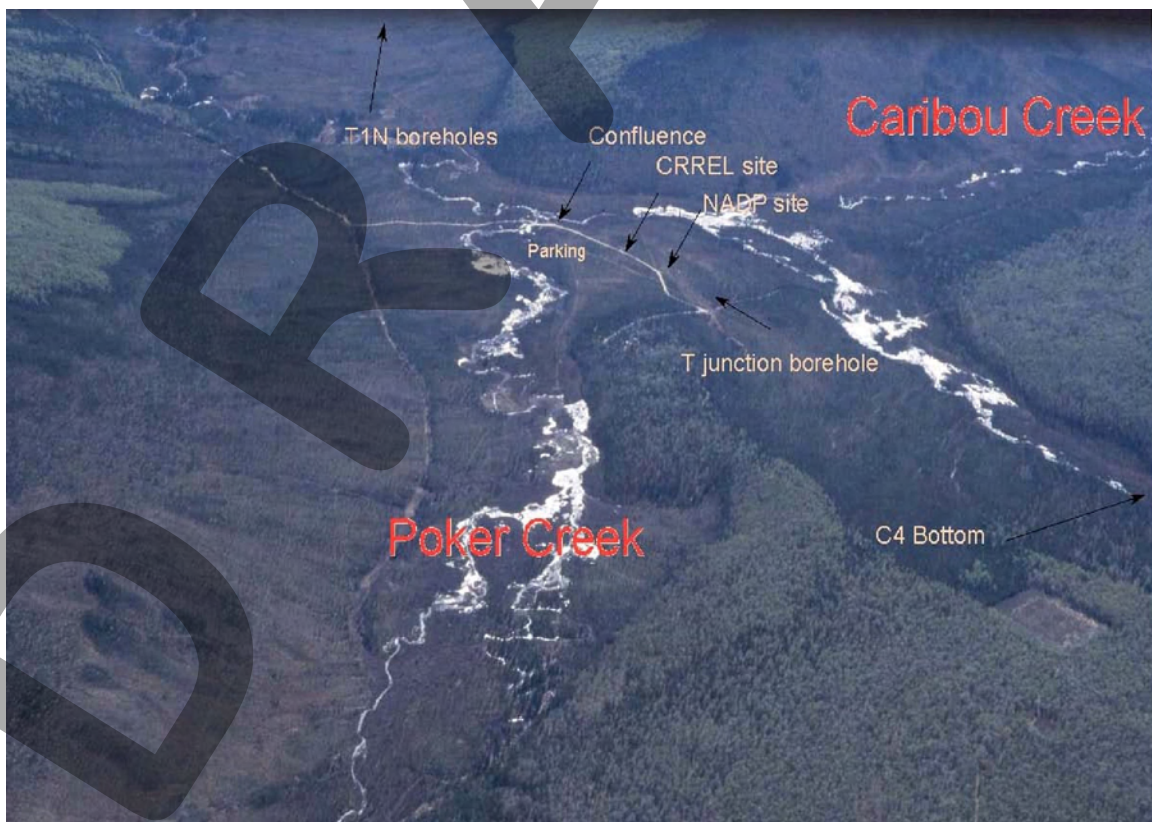


Figure 25. Bird view for Caribou-Poker Creeks Research watershed confluence area.

site. The addition was approved, but the name change was not, so now the BNZ LTER actually includes both the original site at the Bonanza Creek Experimental Forest (BCEF) and the CPCRW site even though the name does not reflect that. Prior to 1993, most of the LTER-related research in CPCRW was aquatic, but since then, terrestrial research on the effects of large-scale disturbance such as climate warming, wildfire and timber harvest have been greatly expanded.

Much effort has gone into improving the infrastructure of CPCRW over the years. In the initial years of the early 1970s, access was by foot or by helicopter. Various structures and instruments were donated by cooperating agencies, including a laboratory trailer that was airlifted onto site by a Chinook helicopter and another laboratory trailer donated by the Geophysical Institute and airlifted in with a Sikorsky skycrane helicopter. Trails were cut during the early 1970s for snow machine and off-road vehicles, and the primary access was over Haystack Mountain from the Elliott Highway. Several miles (perhaps 10) of gravel roads, including four bridges, passable by four-wheel drive pickup truck were constructed in the late 1970s. These roads and one bridge are in need of repair. Since the construction of the road “system,” the main access to CPCRW has been by fording the Chathanika River at about mile 31 Steese Highway. As one might imagine, access was limited or impossible during spring breakup and summer storm events. A steel cable and a basket on pulleys provided limited access in times of high water. In 1995, with cooperation from the US Army and the Cold Regions Research and Engineering Laboratory (CRREL) and funding support from the US Forest Service, a Bailey Bridge was constructed across the Chathanika River, immensely improving access to CPCRW.

Since its inception, research at CPCRW has focused on hydrology and climate. Initially, streams were gauged by manual methods on a circum-weekly schedule by personnel that hiked into the watershed. In the mid-to late 1970s, fiberglass Partial flumes with water level recorders were installed at five sites, and water level recorders were installed at several other sites with streams too large for flumes. Many of the large capacity rain gauges were installed by helicopter. Hydrology and climate data have been collected continuously since 1970, although individual sites may not have a complete record. Also, due to logistical difficulties, discharge data for snowmelt runoff are often missing.

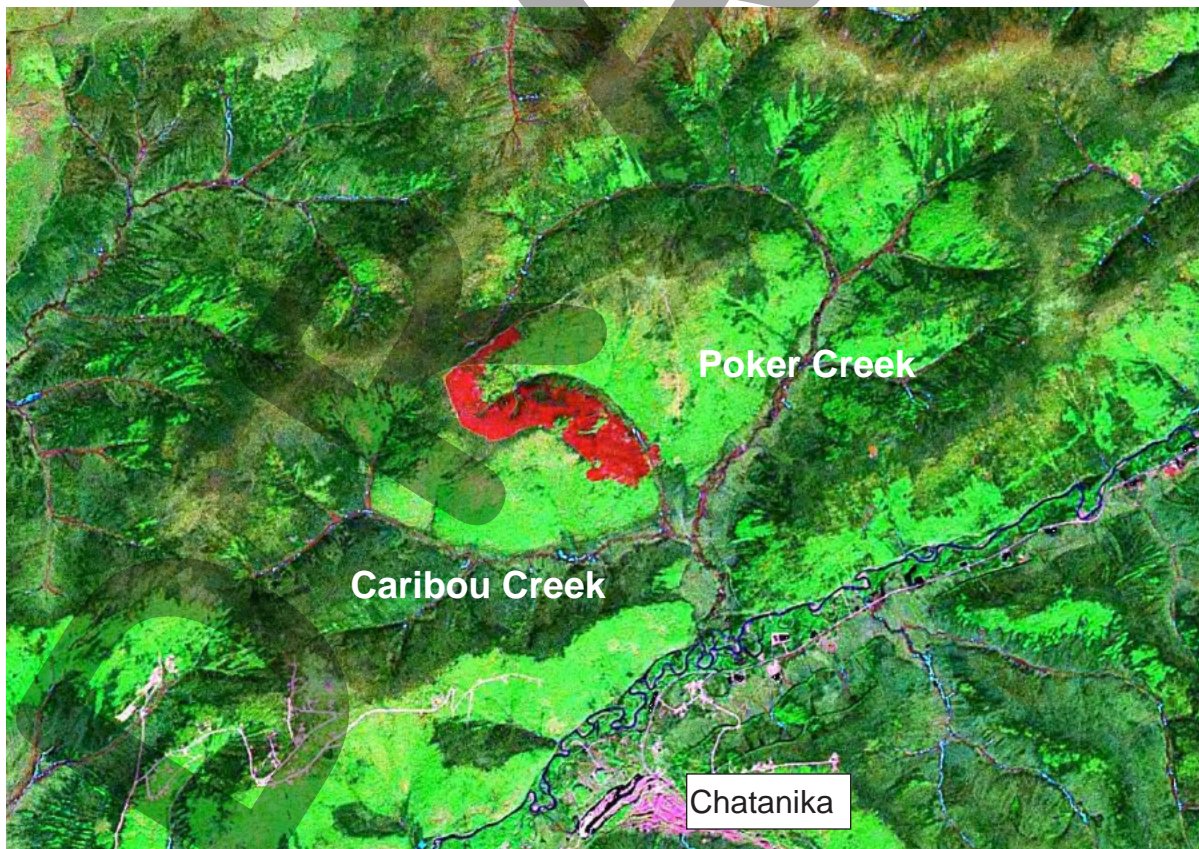


Figure 26. Caribou-Poker Creeks Research watershed image from Landsat. 1999 “Frost fire” experiment burn site (C4 watershed) was indicated by red color.

Permafrost

The presence of permafrost strongly influences many above- and below-ground processes, including site ecology and hydrology as well as the thermal conductivity of active layer material (thermal offset). Interior Alaska has very warm discontinuous permafrost, with temperatures often above -1°C. Since 1969, there have been many research studies conducted in the Caribou-Poker Creeks Research Watershed (CPCRW). In CPCRW, permafrost dominates shaded ground or north-facing slopes, but is largely absent on south-facing slopes that receive appreciable warmth from sunlight. Since permafrost-dominated and permafrost-free slopes support significantly different vegetation types (Haugen, et al. 1993). Rieger et al. (1972) mapped the soil distribution at CPCRW based upon extensive field surveys and aerial photography. They concluded that a strong relationship exists between permafrost distribution and the type of soil, because the factors that control permafrost formation also affect soil genesis. Saulich silt loam, Ester silt loam, Karshner silt loam, and Bradway silt loam all have permafrost. There are several sharp permafrost boundaries along the Caribou Creek and Little Poker Creek. These boundaries are caused by a geological boundary formed by eolian origin deposits and weathering bedrock. However, it is not possible to use soil type alone to completely explain the permafrost distribution because many other factors influence it.

Morrissey and Strong (1986) mapped permafrost using TM (Thematic Mapper) satellite imagery and a geographic database (vegetation distribution and equivalent latitude). Vegetation is a helpful indicator of ground condition and possible to classify from satellite imagery or aerial photography. Their mapping had 78% accuracy and compared well with the Rieger et al. (1972) classification of permafrost distribution. The analysis of Morrissey and Strong (1986) indicated that, in general, permafrost was located under the spruce forest at CPCRW, but recent field studies have shown there are many areas free of permafrost under the spruce forest. Koutz and Slaughter (1973), Digman and Koutz (1974), Jorgenson and Kreig (1988), and Haugen et al. (1993) noted a strong correspondence between the presence or absence of permafrost and the equivalent latitude. Equivalent latitude is an index of the long-term potential of direct-beam solar radiation incident on a surface and is calculated from the slope and aspect (Frank and Lee, 1966). The equation used to calculate equivalent latitude is:

$$\phi' = \sin^{-1}(\sin k \cos h \cos \phi + \cos k \sin \phi)$$

Eq. 1

where

k: slope of the surface [°]

h: aspect of the surface [°]

φ: actual latitude of the area [°]

φ': equivalent latitude of the area [°]

Approximately 200 probes were installed along a transect from the north-facing slope to the south-facing slope in 1998. Probes were installed from the ground surface to a depth of 1.5 m below the surface (30, 90, 150 cm). Deep ground temperature profiles were obtained from boreholes installed by Collins et al. (1988), Yoshikawa (1997). Their analysis of the ground thermal regime examined the relationship between mean annual ground surface temperature (T_{mas}) and equivalent latitude. The coefficient of determination (r^2) for this relationship is 0.68 ($T_{mas} = -0.155\phi' + 9.751$). The permafrost boundary occurs at approximately 63° equivalent latitude. Measurement of soil temperature below the depth of significant annual variation is the best indication of permafrost at a single point, while an indirect or modeling method is the better approach to map permafrost distribution over broad areas. However, validation of any new approach and verification of predictive models require intensive measurements of permafrost distribution and condition.

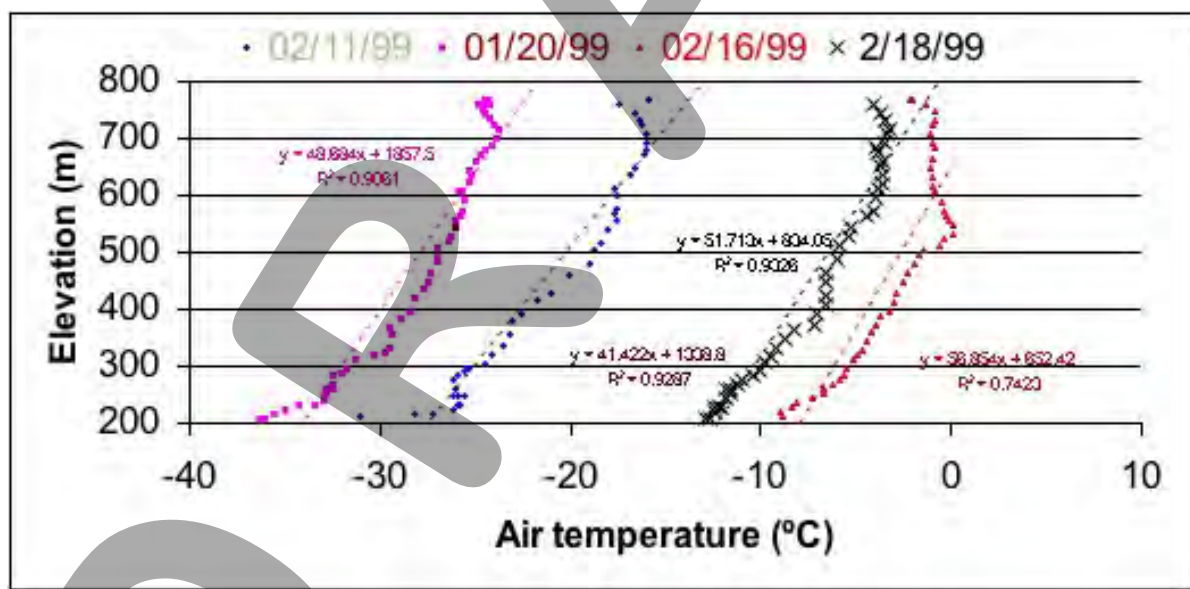
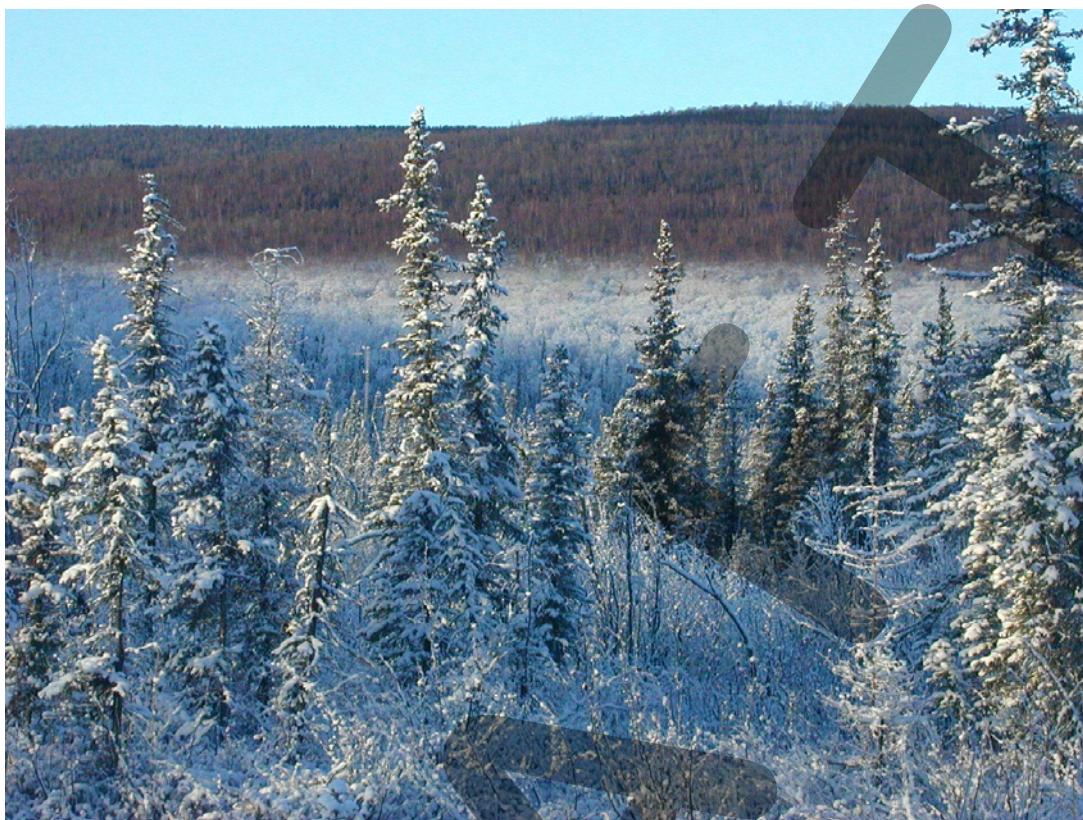


Figure 27. Temperature inversions are very common during winter/spring periods in interior Alaska. The upper picture above displays frost forming on the trees at lower elevation with no frost forming in the higher elevations. Stable temperature inversions occur with a similar slope even under different air temperature profiles (lower image). In CPCRW, the difference in the air temperature inversion is about 10°C between hilltop and valley bottom. Two major climatic agents control the natural formation and degradation of permafrost: (1) solar radiation determines energy input to a site and (2) temperature inversions control the Freezing Degree-Days (FDD) during wintertime. As a result, the distribution of the permafrost is strongly influenced by topography, being located mostly on north-facing slopes and valley bottoms.

OIL SPILL AND FROST FIRE EXPERIMENTS

Two large experimental crude oil spills were conducted in the winter and summer of 1976 at CPCRW. The impact to the permafrost and thaw depth were measured for more than 20 years (fig. 29) (Collins et al. 1994, White et al. 2004). Even though the volume of oil applied was the same, the effects on the permafrost were far more pronounced on the winter spill site due to a larger surface oiled area. Since the active layer was completely frozen, the oil did not infiltrate, but flowed along the surface for a much greater distance yielding a much greater impact. The winter spill also had a more drastic effect on the vegetation. Where the asphalt-like surface oil was present, black spruce mortality was 100% and there was very little live plant cover except for cotton grass tussocks that recovered in the nearly 30 years following the spill. These sites were burned in a wildfire in 2004. Changes in oil chemistry varied with depth; surface samples had signs of microbiological degradation, whereas some subsurface samples taken just above the permafrost had no evidence of degradation in 1991 and still contained volatile fractions (Collins et al. 1994).

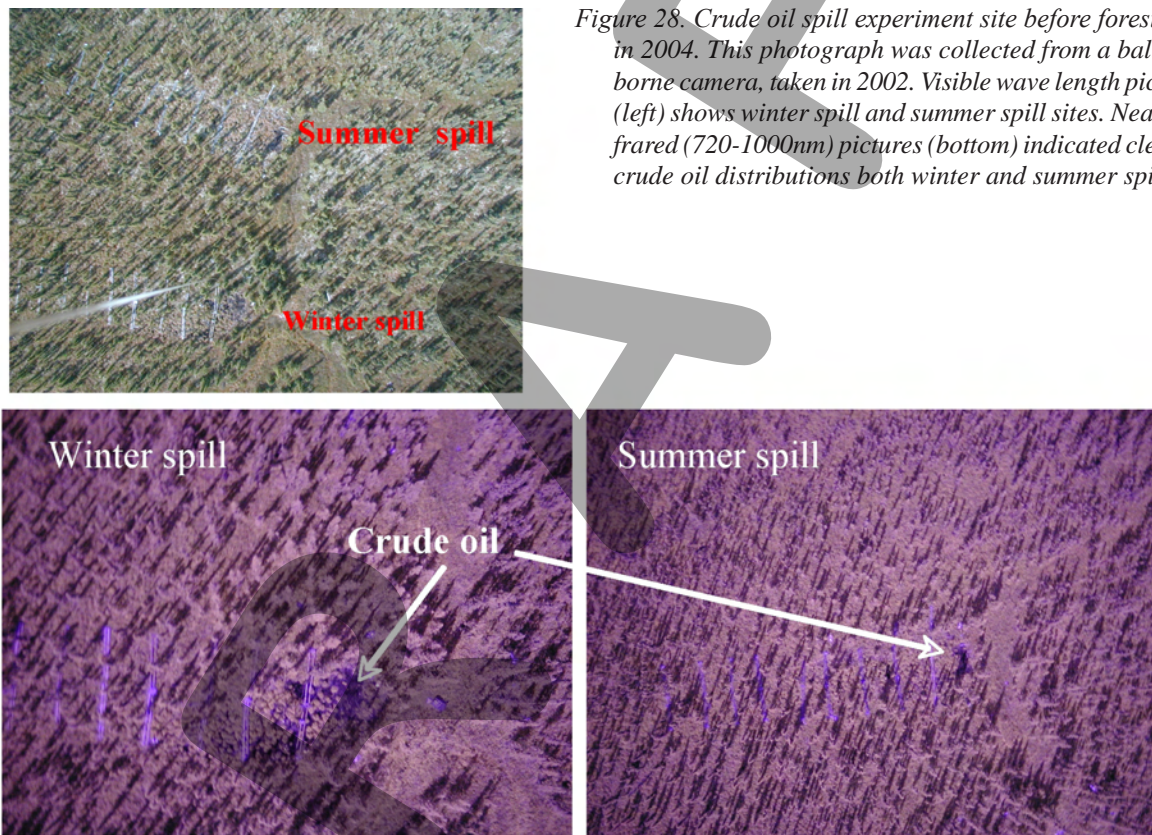


Figure 28. Crude oil spill experiment site before forest fire in 2004. This photograph was collected from a balloon borne camera, taken in 2002. Visible wave length picture (left) shows winter spill and summer spill sites. Near infrared (720-1000nm) pictures (bottom) indicated clearly crude oil distributions both winter and summer spill.

Alaska Science Forum (June 23, 2005)
Oil Spill Persists for Nearly 30 Years (#1756)
by Ned Rozell

On a cold day in February 1976, about 2,000 gallons of steaming Prudhoe Bay crude oil spilled over the snow and percolated into the frozen floor of a black spruce forest. Much of that oil spill remains today, even after a wildfire burned through the area last summer.

The 1976 oil spill that killed more than 40 black spruce trees and almost all the vegetation around them was no accident. Scientists with the Cold Regions Research and Engineering Laboratory dumped the oil on the muskeg in both summer and winter that year to simulate what might happen if the soon-to-be-built trans-Alaska oil pipeline sprung a leak in a black spruce forest underlain by frozen soil, a common environment in Interior Alaska.

That site, in the Caribou-Poker Creeks watershed north of Fairbanks, still has not recovered from the manmade oil spill, according to Jessica Garron, of the UAF Forest Soils Lab. Garron is completing a master's degree project about the site under the guidance of her advisor, UAF microbiologist and Dean of the College of Natural Science and Mathematics Joan Braddock.

"Nearly 25 years after the oil spill, only 10 percent of the oil in mineral soil has been degraded. In the organic layer, 40 percent has degraded," said Garron at a recent chemistry conference in Fairbanks. "If Alaska were in the tropics, a month after the spill there'd be serious changes."

Bacteria in the soil can consume crude oil, but they work better in places where plenty of soil nutrients, water, and warmth exist. Both Garron and Braddock think the Caribou-Poker creeks oil spill area is short of nitrogen and probably limited in oxygen.

While Garron was studying the site in the summer of 2004, a wildfire swept through. Still, the circa-1976 crude survived.

"The hydrocarbon chemistry hasn't changed much after the burn," Braddock said. "There's tons of oil out there still."

Garron said the wildfire that burned through her study site stimulated microbes that might help clean the hydrocarbons from the soil in time. On the site, horsetails have now joined sedge tussocks, one of the few plants to survive the oil spill.

The intentional oil spill has persisted for decades at Poker Creek. By contrast, an area that absorbed the most famous accidental spill in Alaska's history has recovered to a large degree. In a paper published in *Environmental Science and Technology*, Braddock and others estimated that in 1992, about 20 percent of the oil spilled in 1989 from the Exxon Valdez had evaporated. Clean-up crews recovered about 14 percent, about 13 percent was still in Prince William Sound beach sediments, less than one percent remained in the water, and 50 percent underwent biodegradation, a process in which microorganisms fed on the crude oil and convert it to carbon dioxide and water vapor.

The cleansing ability of microscopic creatures also was apparent in a fuel spill in Barrow in the mid-1990s that was treated with nitrogen Braddock and others stirred into the gravelly soil.

"Within a summer, it was clean," Braddock said.

The persistence of the 1976 spill near Poker Creek seems to indicate that black spruce growing above permafrost, one of the widest spread ecosystems in Alaska, is also one of its most fragile.

"The black spruce environment is probably one of the trickiest to clean up after a spill," Braddock said.

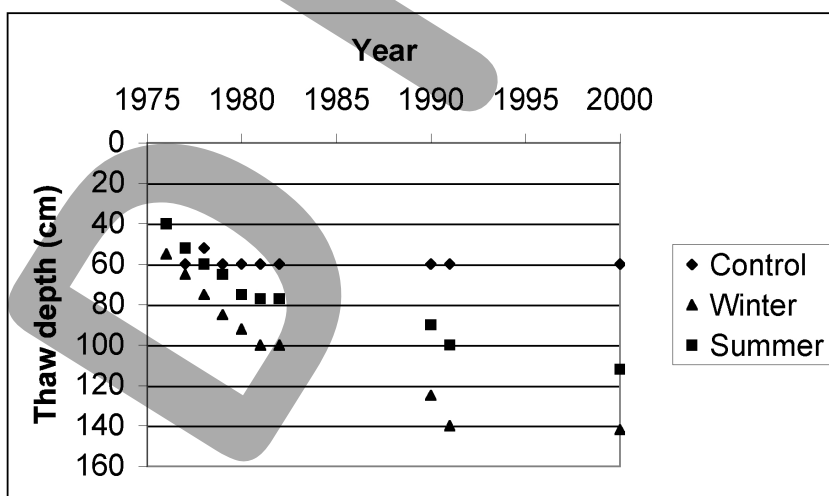


Figure 29. Average thaw depths for each of the plots as function of elapsed time (after White et al. 2004).

Fire impact

Wild fires occur commonly throughout most of the boreal forest in Alaska including CPCRW. The fire history of CPCRW was studied using fire scars on tree rings (Fastie, 2000). Most of the black spruce were burned and replaced in 1920s. A particularly severe fire occurred in 1924, killing most of the trees in the watershed, except some wet areas and valley bottoms. The age of the spruce trees in CPCRW today is about 70-80 years. In addition, we conducted an experimental, controlled fire to burn most of the black spruce forest in the C4 watershed (Hinzman et al., 2003a). In 2004, the Boundary wildfire burned most of the Poker Creek watershed.

The impact to the permafrost during and after wildfire was studied at CPCRW during the “Frost Fire” experiment. Heat transfer by conduction to the permafrost was not significant during fire. Immediately following fire, the ground thermal conductivity may increase 10-fold, and the surface albedo can decrease by 50% depending upon the severity, which is defined as the extent of burning of the surficial organic soil. The thickness of the remaining organic layer strongly affects permafrost degradation. If the organic layer thickness was not reduced during the burn, then the active layer did not change after the burn, in spite of the decrease in surface albedo. Any significant disturbance to the surface organic layer will increase heat flow through the active layer into the permafrost. Approximately three to five years after severe disturbance, depending upon site conditions, the active layer will increase to a thickness that does not completely refreeze the following winter. This results in formation of a talik, or unfrozen mass of soil surrounded by permafrost below and seasonally frozen ground above. The thickness (depth) of the talik under the severe burn was around 4m (4.15m at Rosie Creek Fire in 1983, 3.6m at Wickersham Fire in 1971). Model studies suggest that if an organic layer of more than 7-12 cm remains following a wildfire, then the thermal impact to the permafrost will be minimal in the boreal forests of interior Alaska. The thermal models used for these studies were described in Osterkamp and Romanovsky (1996), Romanovsky et al. (1997) and Yoshikawa et al. (2003).

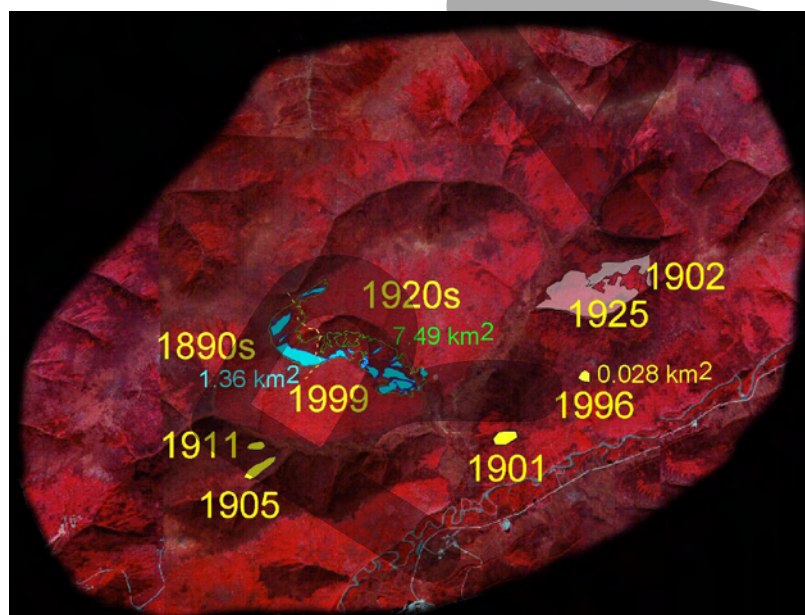


Figure 30. Fire history of CPCRW.
This distribution excludes the 2004 Boundary fire (Fastie, 2000).

The radiation budget before and after the CPCRW controlled burn was measured using shortwave, longwave and net radiometers. Sensors measuring short wave and long wave incoming and reflected (emitted) were installed on a 3m tower (unburned site) and a 1.5 m tower (burned site), both were higher than the black spruce canopy. The radiation balance (Q) is expressed in terms of incoming solar radiation K_{\downarrow} , surface albedo α , incoming long-wave radiation L_{\downarrow} and emitted long wave radiation L_{\uparrow} in the form:

$$Q = K_{\downarrow} (1-\alpha) + L_{\downarrow} - L_{\uparrow}$$

Table 2 Radiation balance of burned and control areas at site 1 (net radiation Q , incoming solar radiation $K\downarrow$, reflected short wave radiation $K\uparrow$, surface albedo (%) α , incoming longwave radiation $L\downarrow$ and emitted longwave radiation $L\uparrow$, Radiation efficiency Re , Total net radiation ΣQ) (after Yoshikawa et al. 2002).

Radiation	$K\downarrow$	$K\uparrow$	α (%)	$L\downarrow$	$L\uparrow$	Re	Q	ΣQ (MJ/m ²)	Max. (W/m ²)	Min. (W/m ²)
Burn(site 1)	100	4.6	0.05	105	122	0.47	47.43	97.7	458	-37.6
Unburn(site 1)	100	13.5	0.14	105	118	0.74	73.59	160.2	537	-48.7

From 23 July 1999 to 10 August 1999 (sensor height 1m at burn, 1.5m unburn)

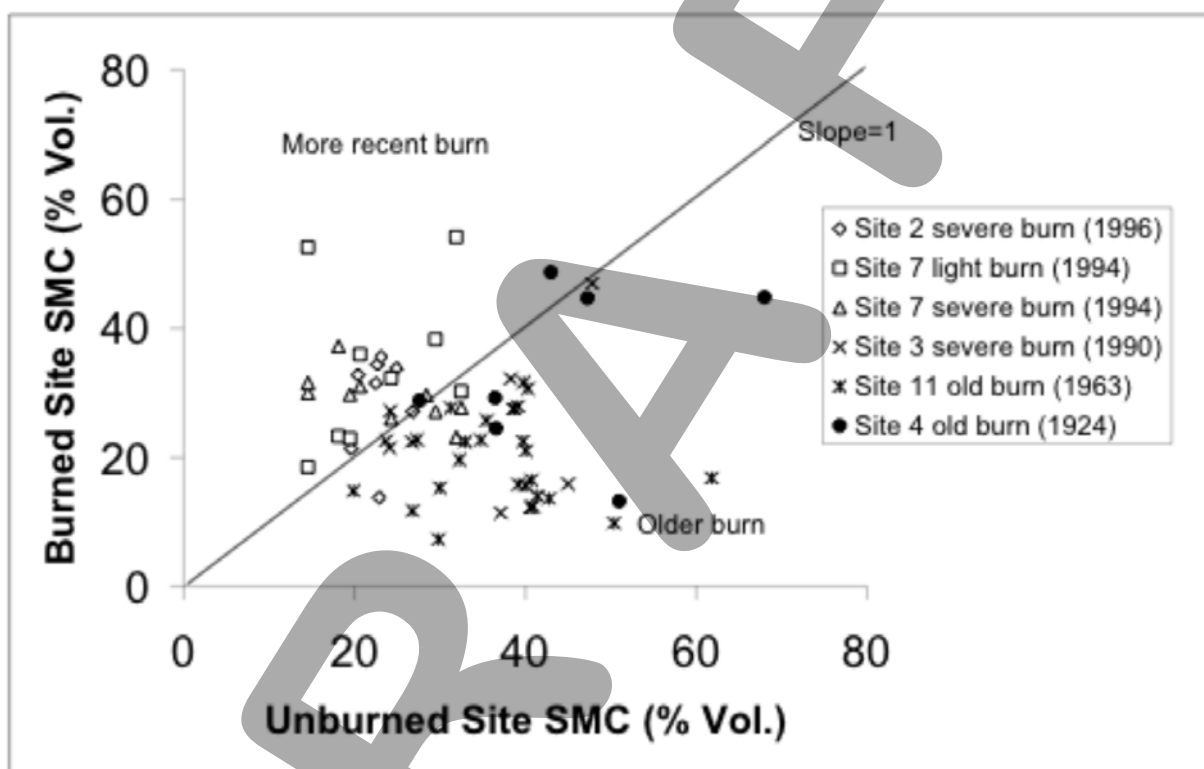


Figure 31. Comparison of the soil moisture contents (SMC) between burned areas and adjacent unburned control areas at fires of various ages show that in general, more recent fires have higher mineral soil moisture contents in burned areas while older fires have higher mineral soil moisture contents in unburned areas (after Yoshikawa et al. 2003).

Succession change in active layer

Long term observations such as those made on the active layer and vegetation changes over the last 36 years at the Wickersham Fire (in 1971) site are extremely valuable for developing an understanding of the effects of fire and fireline construction in the taiga of Alaska. At the Wickersham Fire site, a layer of seasonal frost formed that eventually remained frozen throughout the entire year and continued to remain frozen for the next ten years.

Permafrost is recovering at the Wickersham fire site on the burned stand but not on the fireline. The increased maximum thaw depth pattern for the two sites is similar, with a maximum thaw of 266 cm for the fireline and 302 cm for the burn (fig. 32). Also, the development of an upper frozen zone in 1986 and 1996 was similar. The difference is that the upper zone has become intermittent on the fireline but may be rejuvenated by another cold snowless year.

A temperature profile from the borehole during the period of maximum thaw in September of 2003 (fig. 33) shows an active layer of 1.4 m. The new frozen layer was approximately 50 cm thick and extended from 1.4 - 1.9 m below the current active layer. This new permafrost layer divided the active layer and the talik formation. The talik temperatures were very close to 0 °C. Below 3.4 m the temperatures of the permafrost layer decreased to - 0.09 °C at the bottom of the borehole (6.5 m). The lower permafrost depth stabilized at 3.5 - 4.0 m and an unfrozen soil zone (talik) remained between the two frozen layers. However, in September of 2006, the temperature profile (fig. 33) shows the disappearing talik layer. The permafrost temperature at 6 m depth is more than 0.3 °C colder after 3 years. The new permafrost development, since 1996, accelerated the refreezing of the talik layer. As a result of the three years of permafrost aggradations, the ground temperature profile is approaching a “normal” gradient (0.1 °C/m).

Figure 34 illustrates what actually happened at the burned site after the Wickersham Fire. The active layer did increase for the first 25 years following the fire. However, an upper layer of seasonal frost remained frozen 17 years after the fire and then became discontinuous for the next ten years. Since 1996 the seasonal frost layer has remained frozen. This created a new permafrost layer with an active layer of 90 cm and an unfrozen talik between the upper layer and the lower frozen layer. This new permafrost layer has accelerated the refreezing of the talik layer, and by 2006 the talik layer disappeared and the permafrost has returned to the pre-fire thermal conditions.

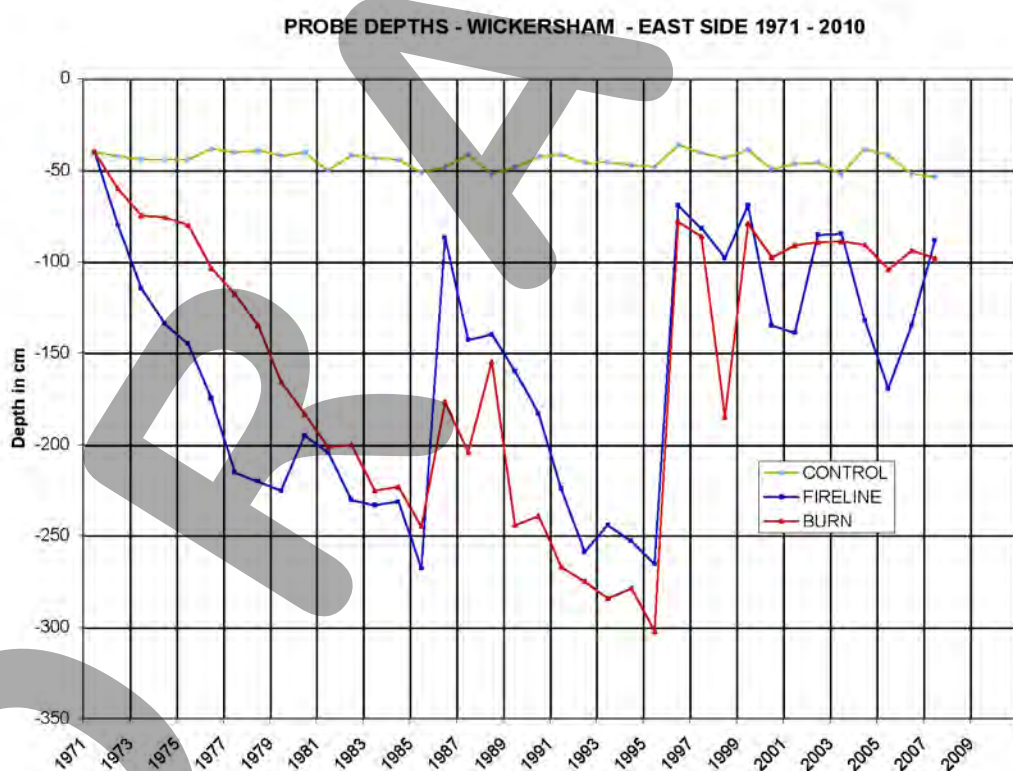


Figure 32. Maximum thaw depth of an unburned black spruce stand, a burned black spruce stand, and a fireline from 1971 to 2006 (after Viereck et al. 2008).

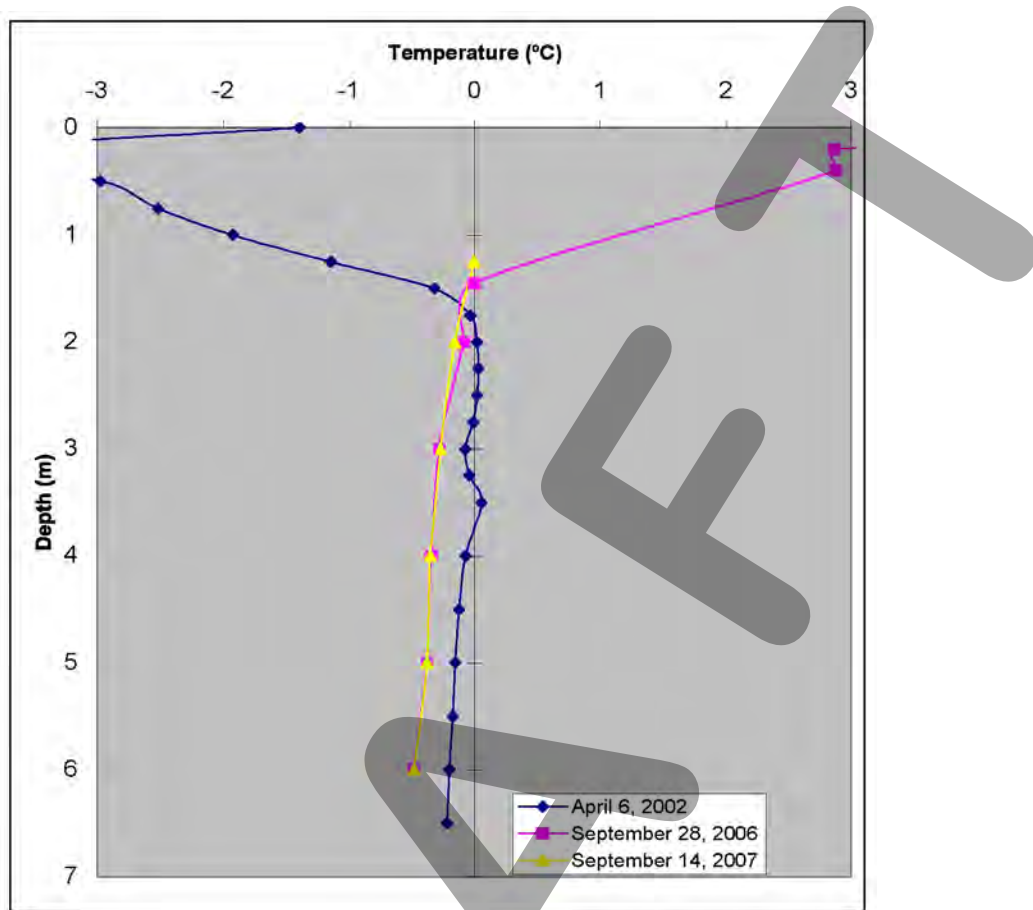


Figure 33. 6.5 m deep ground temperature profiles from Wickersham Fire burned site. In 2002 the profile showed a new frozen layer approximately 50 cm thick extending from 1.4 to 1.9 m below the active layer. In 2006 and 2007 profiles show complete freezing of the talik.

STOP 7: AUFEIS (ICING) AND PERMAFROST HYDROLOGY

There have been many research studies conducted in CPCRW including the groundwater source, pathway, residence time, and relationship with aufeis and open (hydraulic) system pingos. Figure 35 displays the aufeis distribution, springs, and major fault system at CPCRW. The annual mean ground temperature of CPCRW varies between -3 to 0.5°C in permafrost areas and up to 2.5°C for south facing slopes. The thermal and hydraulic properties of the soil are strongly affected by the absence or presence of permafrost. These hydrologic and thermal regimes directly control the aufeis or pingo formation. There are 463 open system pingos reported in interior Alaska, including the Brooks Range (Holms et al. 1968, Hamilton and Obi, 1982, Slaughter and Hartzmann, 1993). Many of the open system pingos in other areas have a different type of groundwater system and genesis, such as glacier fed type and near shore type (Yoshikawa and Harada, 1995).

The type of the aufeis (icing) and the source of water were classified using the dissolved organic carbon (DOC) and the inorganic carbon (IC) concentrations in the ice and water during wintertime. The three types of aufeis: spring aufeis, stream aufeis and ground aufeis were distinguished by DOC and IC ratios from the aufeis and water samples. The ground aufeis had the highest DOC content (8-9mg/l in ice, 35-40mg/l in water). The source of this water is believed to be of shallow origin. Permafrost was distributed throughout most of the valley bottom and on the north-facing slopes in the research watershed. The active layer was usually completely frozen between January and early February. After February, almost all of the stream baseflow came from natural groundwater springs, which had high concentrations of IC and low concentrations of DOC. The ground aufeis volume was less than 1% of total aufeis ice volume. The source of the water for ground aufeis came from within the seasonal frozen layer

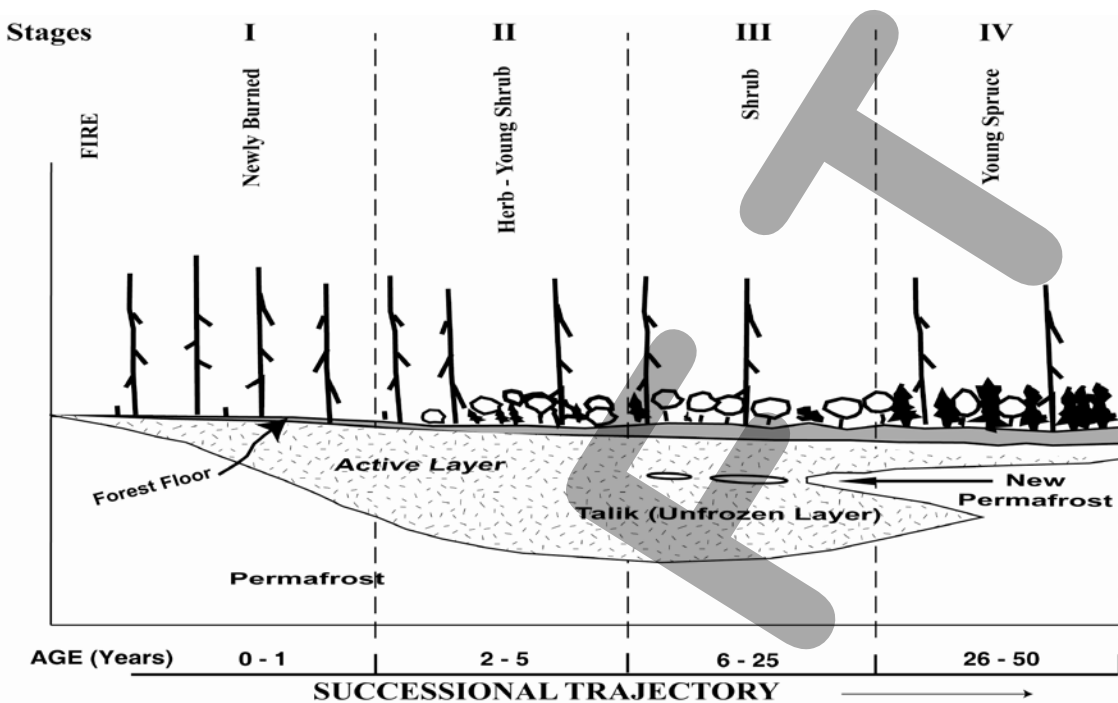
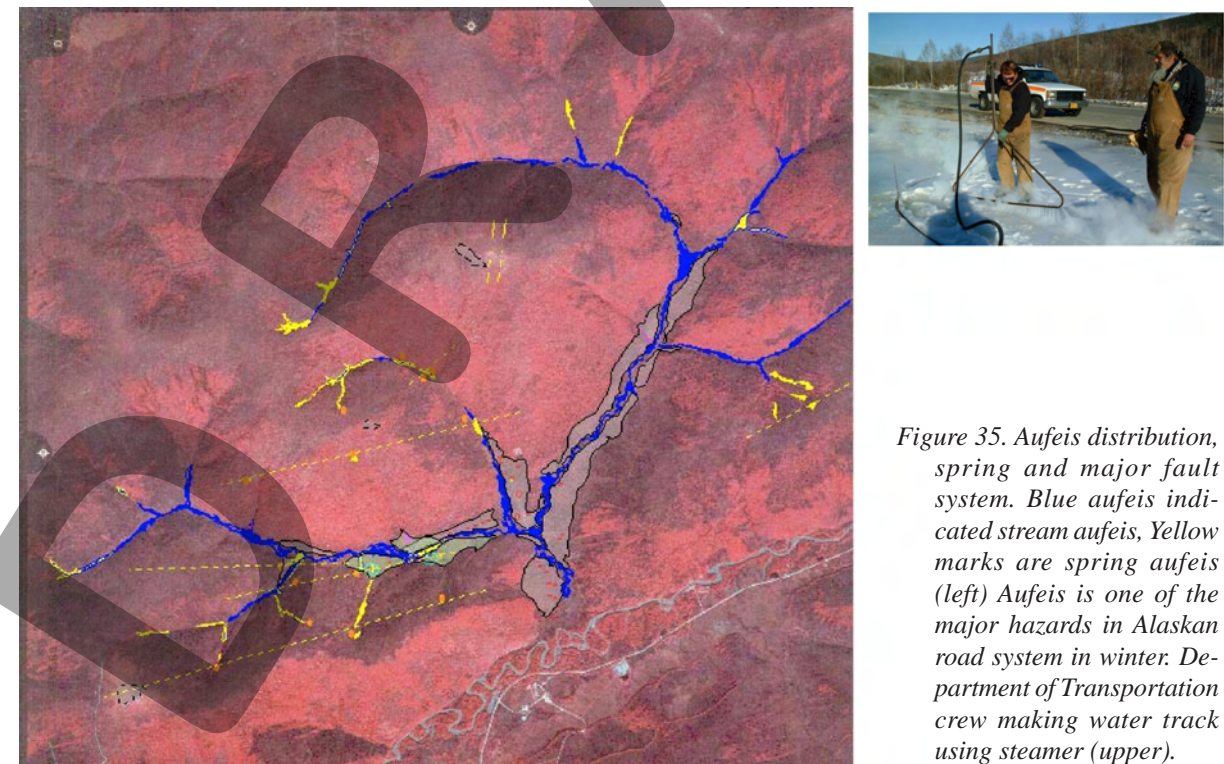


Figure 34. Successional changes observed in vegetation and the active layer at the burned site following the Wickersham Fire (after Viereck et al. 2008).



(ca. 2.2-3m thickness) on the permafrost free south facing slopes. Most of the south-facing slopes have thin surface sediments. Ground aufeis developed at the interface of the permafrost boundary near the base of the south-facing slope, usually beginning in late February. On the other hand, spring aufeis began forming in late October or November and melted in May, yielding the longest lasting and thickest ice formation in the watershed. Spring aufeis is characterized by the high IC content (30 mg/l). The water from springs on north and south facing slopes had similar DOC/IC ratios, demonstrating that permafrost is not a controlling factor of the spring water DOC/IC ratio. Most of the spring water came from a deep geologic feature such as a fault. Spring locations were generally linear and found along the major fault formations. The DOC/IC ratio of the stream aufeis fell between spring aufeis and ground aufeis, because it is a mixture of water from both sources. The stream aufeis starts developing late December to January and the DOC content decreases until mid winter and increases from early March until spring melt. Over the last 30 years, the aufeis records at the watershed demonstrate that up to 40% of stream baseflow may be stored in aufeis. However, during heavy snow years such as 1971, 1972 and 1995, aufeis will not develop or minimum.

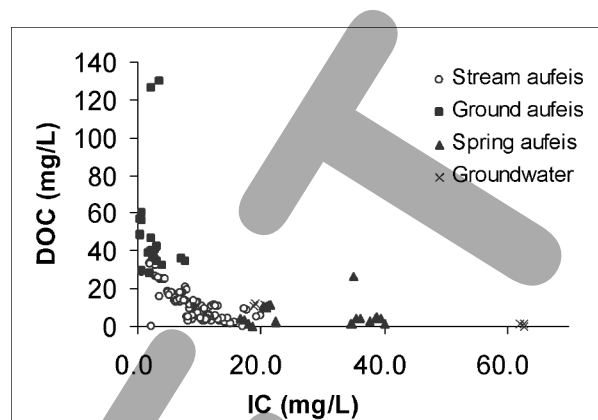


Figure 36. The relationship between DIC and IC from different source of aufeis water (after Yoshikawa et al. 2003).

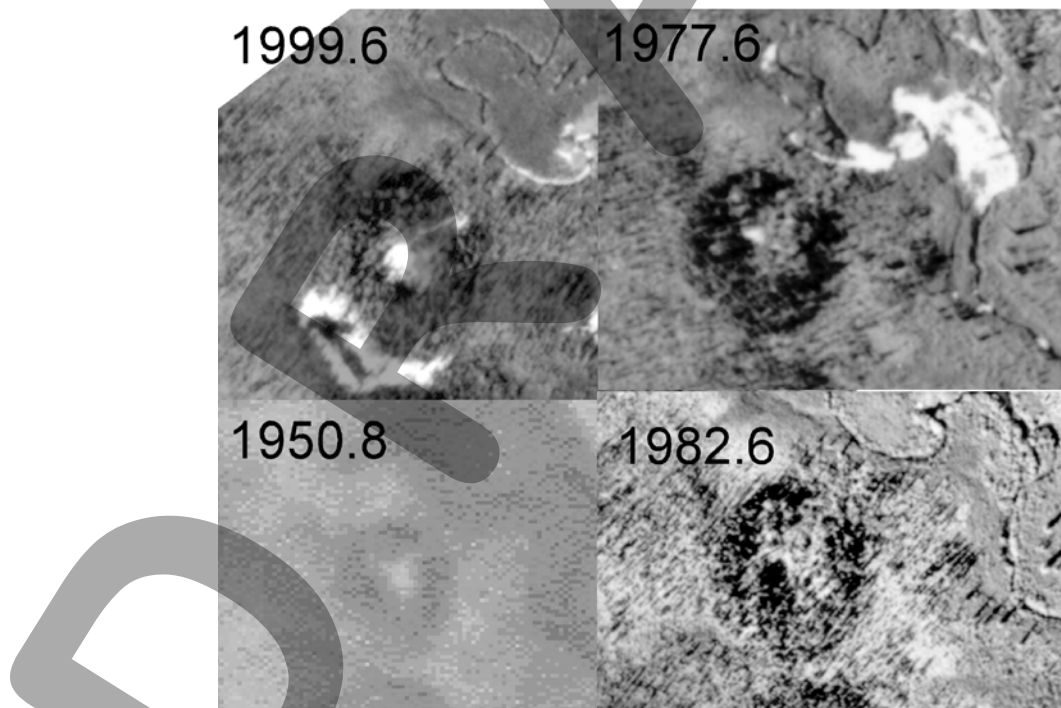


Figure 37. Four different stages of the collapse pingo along the Caribou Creek.

There is already a crater forming in 1950. The spring discharging point shifted out of the rim in 1999 (aufeis suggests the presence of an active spring) (after Yoshikawa et al. 2003).

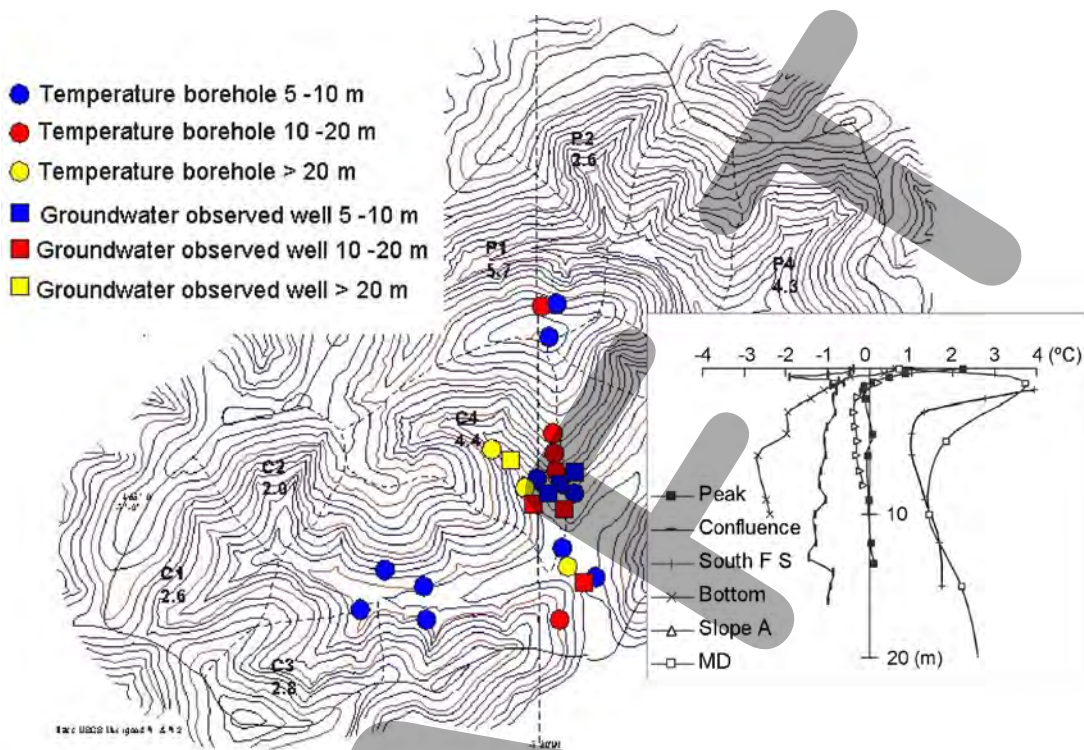


Figure 38. Ground temperature profiles at the different geographical locations. Autumn data (September, 2001) shows absence or presence of the permafrost and collapsing around pingo. A new pingo (or frost blister) developed on the upper slope of the pingo (after Yoshikawa et al. 2003).

Infiltration processes

Evapotranspiration creates relatively dry soil conditions within the root zone during the summer. Minor summer precipitation events are offset by evapotranspiration (Kane, 1980). The snowmelt and summer heavy storm events were the most reliable sources of groundwater recharge. The $\delta^{18}\text{O}$ value of the precipitation has strong seasonal signals in Fairbanks area. The groundwater mixing ratio from the snowmelt and summer storm water was distinguished using a two member mixing model (Rantz, et al. 1982).

$$Q = \frac{Q_s(I_s - I_{gw})}{(I_{gw} - I_r)} \quad \text{eq. 3}$$

where Q = discharge of spring; Q_s = infiltration volume of snowmelt water; I_s = $\delta^{18}\text{O}$ value of the snowmelt water; I_{gw} = $\delta^{18}\text{O}$ value of the groundwater; and I_r = $\delta^{18}\text{O}$ value of the summer storm water.

The springs and base flow at CPCRW had a nearly constant value of $\delta^{18}\text{O}$ value between -17 and -18.5 ‰ (Caribou Creek; $\sigma = 0.12$, pingo spring; $\sigma = 0.89$), which indicates 33-40% of the groundwater will be derived from snowmelt infiltration. The infiltration process during snowmelt through the seasonally frozen dry materials mainly occurs near the upper part of the hill. The infiltration rate is reduced to about one-half that for the unfrozen condition (Kane, 1980). The area of recharge is estimated by NOM based on different types of forest floors using py-GC/MS. Table 3 shows the statistical correlation of major components between the NOM in each spring's water and leachates from different forest floor materials. A shaded value indicates a significant relationship.

The pingo spring water and TR1 water have the only significant relationship with a birch floor, suggesting a possible recharge area. TR1 is located in a south facing birch forest community; however, the pingo spring and other springs (C3, CB and DB) are located at the bottom of the north-facing slope in an open black spruce community. This result suggests that water in the pingo spring came from infiltration through soils underlying a birch forest, perhaps some distance from the pingo and separate from the spruce stand immediately upslope from the pingo.

Table 3. Correlation coefficients between spring water and forest floor leachates.

	Birch	feathermoss	Spruce	organic silt
			fiberic NOM	
Haystack	0.142	0.483	0.775	0.782
C3	0.139	0.453	0.687	0.702
CB	0.391	0.644	0.793	0.800
SB	0.200	0.334	0.405	0.434
SF	0.238	0.367	0.426	0.426
DG	0.206	0.449	0.611	0.618
MD	0.279	0.422	0.445	0.453
Pingo	0.777	0.672	0.399	0.427
TR-1	0.944	0.805	0.536	0.528

Water- Rock (permafrost) interactions

There were no isotope exchange processes observed in the water from spring sites such as exchange with CO₂ or hydration of silicates. The ratio between δ¹⁸O and δ²H of the groundwater is aligned with the local meteoric waterline (δ²H = 6.7469 δ¹⁸O - 21.589). The strontium concentration of water from pingo springs and south-facing slope wells was relatively high (table 4), as was uranium. Pingo spring and Cabin well water (schist bedrock aquifer 18m below surface), at the base of the south-facing slope, also had higher Ca concentrations. The source of the Ca, such as limestone bedrock materials, is possibly located in these areas.

The strontium isotope ⁸⁷Sr/⁸⁶Sr data also indicate pingo spring water had passed through highly weathered, fractured Birch Creek Schist formation (0.74071±1 ppb) (Farmer et al, 1998). The current seasonal variation of the tritium value was 4.96 (summer) and 10.96 (winter) TU. The residence time (*t*) is calculated following an equation using the Anchorage, Alaska, tritium database (IAEA/WMO, 2001).

$$t = -17.93 \ln \frac{a_t {}^3H}{a_0 {}^3H} \quad \text{eq.4}$$

where *a_t*³H is the tritium value of sample water (TU); *a₀*³H is the tritium value of infiltration water. Preliminary data from chlorofluorocarbons (CFCs) analysis was also used for dating. Preliminary results seem to indicate that the pingo water (30 years old) is of different origin than the other springs in the watershed; however, additional results are needed to verify the actual dates of the water.

Table 4. Characteristics of major spring flow (sampled March 2000)

	Sr ug/L	Na mg/L	Mg mg/L	SO ₄ mg/L	K mg/L	Ca mg/L	U ug/L	Conductivit μS/cm	δ ¹⁸ O	δ ² H	temperature
C3	105	1.55	3.48	37	0.98	34	0.96	113	-18.68	-149.0	0.00
Pingo	345	2.43	11.7	52	2.1	54.4	3.71	380	-19.80	-147.0	-0.01
TR6	ND	ND	ND	ND	ND	ND	ND	113	ND	-125.9	0.10
MD	87.6	0.96	2.66	8	0.78	13.3	0.05	97	-18.25	-154.0	0.96
SS	41.5	1.62	1.8	<2	1.2	15	.009	74	-18.56	ND	2.40
SB	ND	ND	ND	ND	ND	ND	ND	155	-18.34	-125.4	0.43
DG	65.6	1.53	2.9	4	0.7	12	0.01	75	-20.60	-154.0	1.10
CB	68.9	1.91	3.06	12	0.81	17.2	0.01	118	-20.30	-152.0	0.12
Cabin Well	524	3.33	14.1	56	7	94.2	3.65	524	-16.52	ND	ND
MD Well	53.7	9.63	4.55	11	1.2	16.7	0.17	201	-17.93	ND	2.60
Haystack	119.8	1.63	2.96	ND	0.35	15.2	0	120	-18.40	-141.9	ND

Discharge process

The three different types of aufeis are classified by the discharge process: spring aufeis, ground aufeis, and stream aufeis. Many of the springs are associated with a local fault system (ENE-WSW). Most of the springs develop aufeis starting in October. The shape of the aufeis varied (e.g. dome: pingo spring; shield: MD, CB) depending upon the water temperature and discharge volume as well as freezing conditions of each year. Aufeis never developed at SB spring, where the water temperature was 0.43°C and discharge was 0.8L/sec. During relatively cold winters (such as 1999, 2002), impressive ground aufeis, caused by subsurface seeping water was observed. Ground aufeis frequently occurs as freezing of intra-permafrost water. Intra-permafrost water flow is observed near the silt and bedrock interface. The source of this interface water is from the upper part of permafrost-free slopes and is also connected with bedrock fractured groundwater system. This groundwater level has annually fluctuated about 2m (max.: September- October, min.: just before snowmelt). The bedrock groundwater level also displays similar trends at the valley bottom (MD well: 18m below the bedrock aquifer) (fig. 38).

The genesis of the pingo is also related to the thermal processes of groundwater system. There has been no remarkable uplift or subsidence in both pingos since observations began in 1987. Figure 39 displays topographic change at the collapse pingo site detected over 15 years. The inner wall of the pingo crater rim is the only place of major changes due to mass wasting. Since 1999, icing blisters have developed on the upper hillslope of the pingo, where the spring emerged. The artesian pressure was measured and calculated based on 2001-02 winter period (50kPa). The pingo ice still existed 5.6m below the pond in 2002. The melting rate of pingo ice was 2.1cm/year since it was first drilled in 1995.

CPCRW contains two pingos along the Caribou Creek at the base of the north facing slopes. The thickness of the permafrost is about 120 m and the annual mean upper permafrost temperature is -0.7° C. The Caribou Creek corn pingo has a 60 – 80 m base diameter, and is more than 10 m tall. The massive ice core starts 7.35 m below the ground surface and extends down to 23.5 m. Several segregation and inclusive ice layers (a few cm to 30 cm thick) occur in the overburden silty permafrost. This pingo survived wildfire several times. A charcoal layer was observed 15 cm below the surface where the radiocarbon age is 820 ± 40 y.B.P. (GX-28572). The active layer fluctuated between 1 m (present) to 2 m (post fire disturbance) during the Holocene. The increase in active layer depth during climatic optimum and/or post wild fire disturbance decreases the ice content of the upper part of permafrost. The bedrock (schist) appeared just below the lower horizontal contact of the massive ice.

The Ground Penetrating Radar (GPR) responses at the top of the pingo are shown in Figure 43e. A linear gain is applied to accentuate some of the deeper anomalies. Several reflections are present within these waveforms, and there seems to be a general trend of a decrease in center frequency and bandwidth from the deeper reflections. This is not unusual, as one would expect increased attenuation at higher frequencies. From the reflection profile, the ice body's possible locations can be estimated.

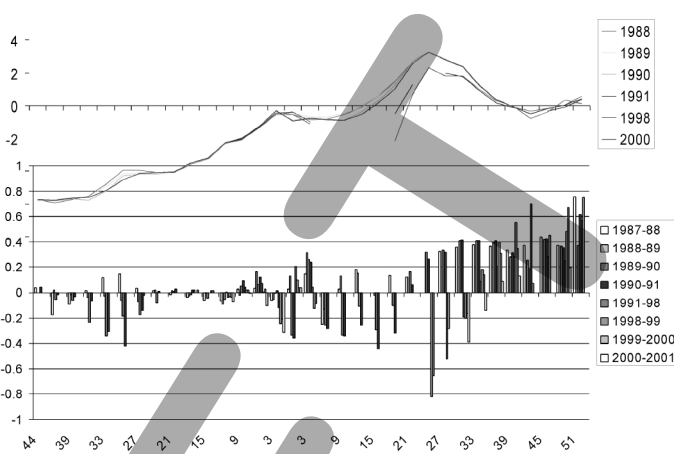


Figure 39. Ground shifting (heaving and collapsing) around pingo. A new pingo (or frost blister) developed on the upper slope fo the pingo.

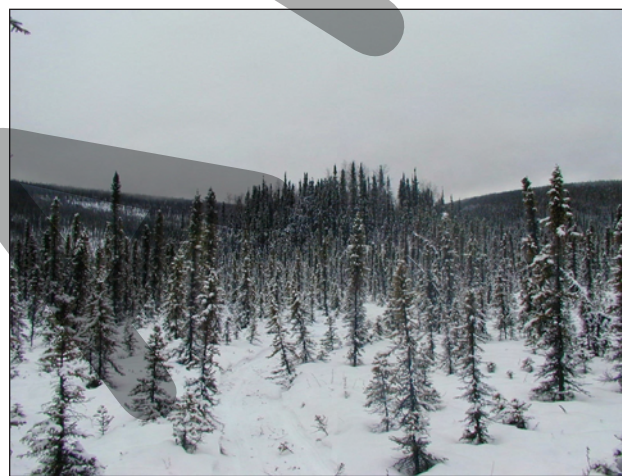


Figure 40. Winter view of corn pingo, which contained 16m thickness of massive ice core.

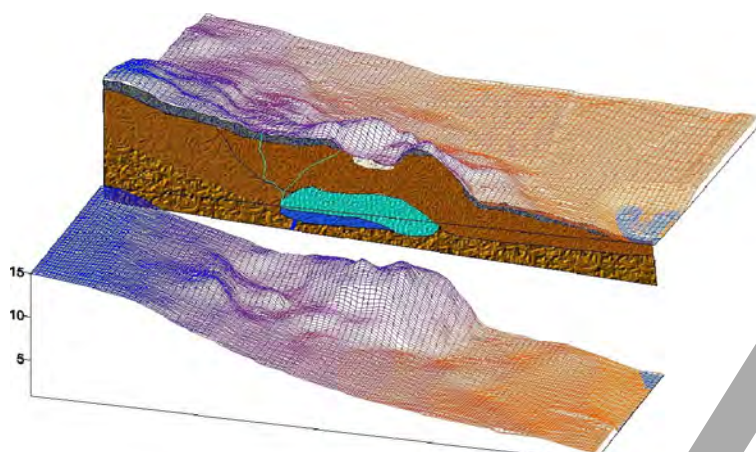


Figure 41. (left) Open system pingo and massive ice 7.35-23.5 m below surface at the top of the pingo.

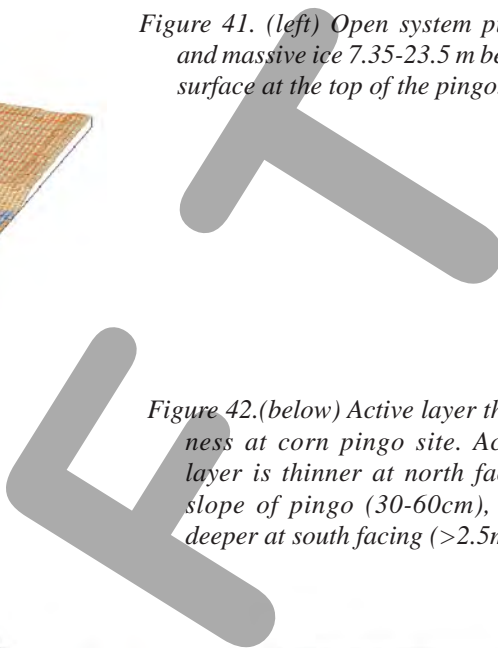
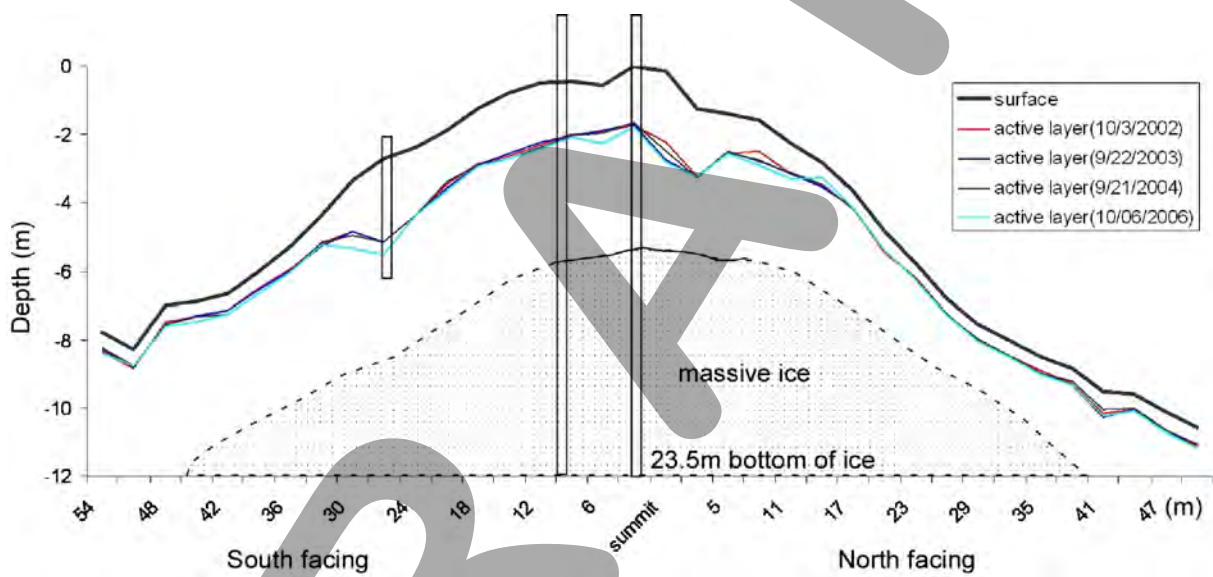


Figure 42.(below) Active layer thickness at corn pingo site. Active layer is thinner at north facing slope of pingo (30-60cm), and deeper at south facing (>2.5m).



Two of the reflections indicate the top and bottom of the pingo ice core (fig. 43e). The first is around 150 to 160 ns and has amplitude of about 5% of the surface response. The second is around 360 to 390 ns and has amplitude of about 4% of the surface response. Figure 43d shows impulse radar profile from the 80 MHZ systems. Ice was observed as free of reflection around 155 and 370 ns.

Seismic refraction measurements are employed between the south-facing slope and the top of the pingo. The direct observation with a thaw probe indicated that the active layer was thicker at the south facing slope (>3 m) and 2 m at the top of pingo. P-wave velocity was configured with a two-layer structure at 360 m/sec and 2800 m/sec. The first layer (360 m/sec) is 3 m thick on the south-facing flank of the pingo and 4 m thick at the top. The first layer represents the active layer, although the thickness is different from the direct observation. The thick organic layer on the top of the pingo may weaken the signals, which results in the contradiction. No signal from the massive ice body was observed because the survey line was slightly short (30 m) to enable investigation of the deeper structure. The weak signals through the thick organic layer prevented us from extending the survey line more than 30 m on this site.

DC resistivity profiling results were useful for (fig. 43b) identifying the massive ice core, except at the bedrock interface. An ice resistivity of 8600 ohm-m was obtained, which is a reasonable value. Resistivity studies permit better investigation of the detailed sub surface structure, especially distinguishing the frozen silt layer and the upper boundary of the ice core but not bedrock contact. Results from drilling a borehole indicate the pingo's ice core contacts bedrock at 23.5 m.

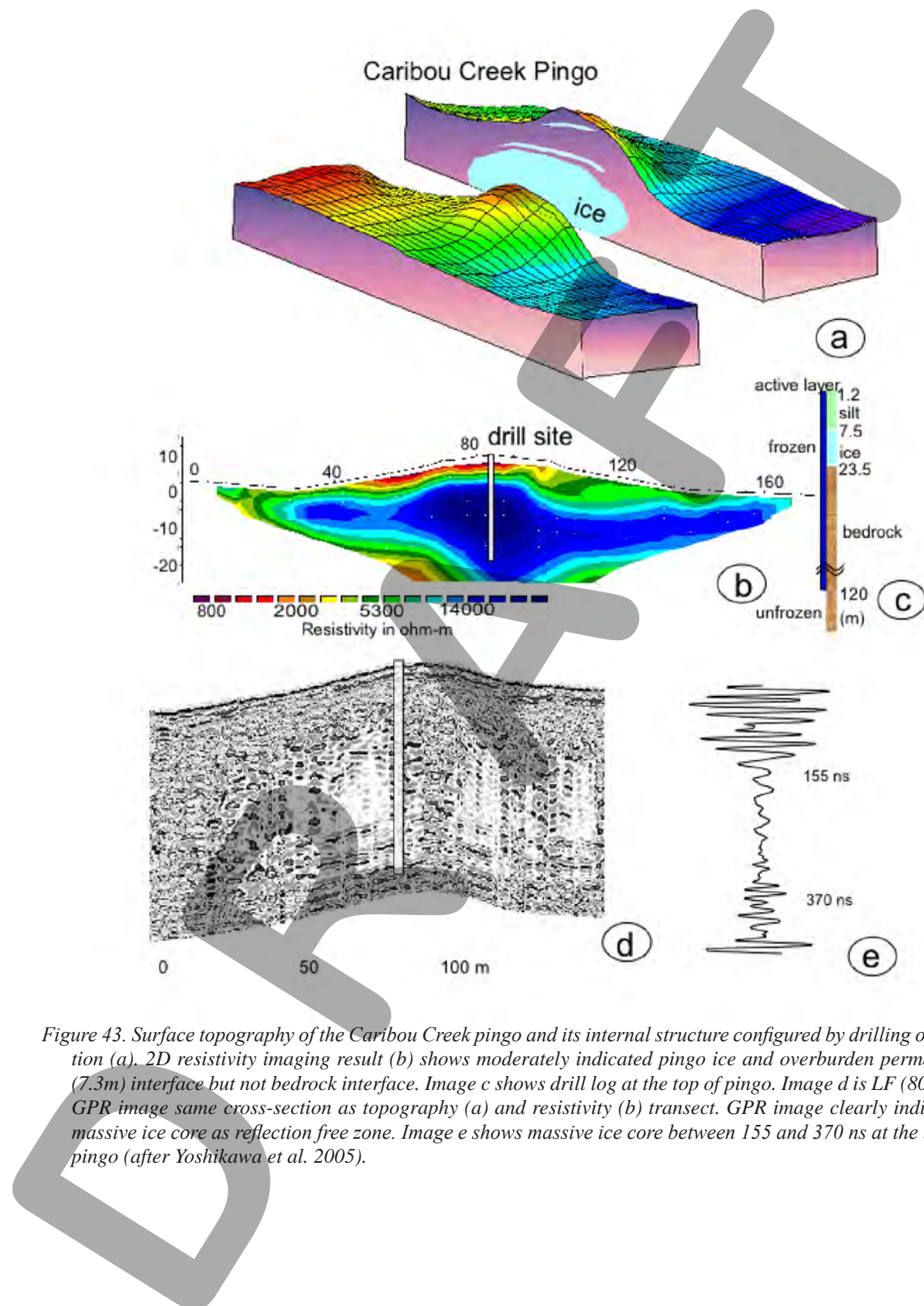


Figure 43. Surface topography of the Caribou Creek pingo and its internal structure configured by drilling operation (a). 2D resistivity imaging result (b) shows moderately indicated pingo ice and overburden permafrost (7.3m) interface but not bedrock interface. Image c shows drill log at the top of pingo. Image d is LF (80Mhz) GPR image same cross-section as topography (a) and resistivity (b) transect. GPR image clearly indicated massive ice core as reflection free zone. Image e shows massive ice core between 155 and 370 ns at the top of pingo (after Yoshikawa et al. 2005).

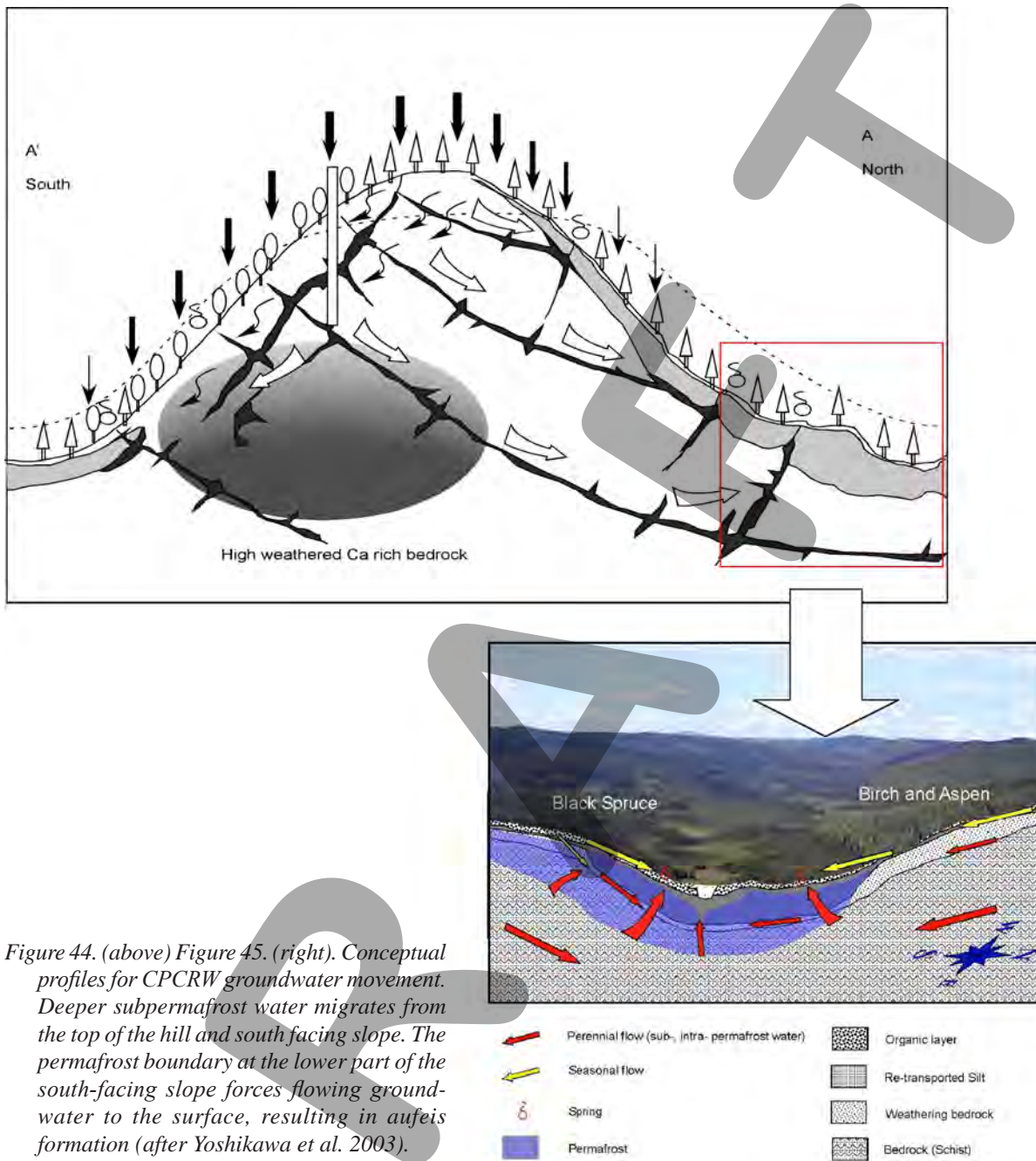


Figure 44. (above) Figure 45. (right). Conceptual profiles for CPCRW groundwater movement. Deeper subpermafrost water migrates from the top of the hill and south facing slope. The permafrost boundary at the lower part of the south-facing slope forces flowing groundwater to the surface, resulting in aufeis formation (after Yoshikawa et al. 2003).

STOP 8: THERMOKARST

Thermokarst depressions and related mass wasting and erosions occur in the valley bottoms of the Caribou Poker Creeks Research Watershed (CPCRW). While it is clear that their occurrence is limited to areas of loess and/or retransported silt accumulation, there is little known about the factors contributing to the initiation of thermokarst development, or the rate at which they have progressed. Before the Frostfire experiment (Hinzman et al., 2002), trees from the proposed burn area were used tree ring data to reconstruct the ground surface morphology of thermokarsts over time, and eventually determine the climatological and site-specific events that may have contributed to the initiation and growth of these thermokarsts. The growth rings of 279 live trees (plus 8 dead trees from within the thermokarst pond) were examined for the years between 1930-1998. Old aerial photography (from the year 1951) supports the ground surface reconstruction. It appears that the development of thermokarst site 3 began in the late 1800s, while the other two appear to have begun between 1940 and 1950. There has been extremely active thermokarst progression during the last 20 years. It also appears that wild fires trigger the development of thermokarsts due to the change in the thermal balance of the permafrost.

Site 1 consists of a thermokarst developing primarily through permafrost thaw. The thermokarst center presents standing water supporting a sedge-herb wet meadow. All of the sampled spruce trees ($n=178$) in this site started growth after the 1924 fire (Fastie, 2000). The thermokarst started developing between 1945-49. As the area of the thermokarst increases, it encroaches into the surrounding closed spruce forest. The number of the trees leaning toward the thermokarst is presented in different zones (fig. 46 site 1). The definition of each zone are as follows: Zone 1 is wet meadow area, Zone 2 is less than 10m from the wet meadow, Zone 3 is more than 10m from the thermokarst wet meadow (fig. 47). The thermokarst extended into zone 3 mainly after 1970s. Figure 47 indicates progress and spatial development of the thermokarst.

Compared to the benchmark survey before and after experimental fire in 1999, ground subsidence was quite large (5-14cm). Zone 3 had a particularly large amount of subsidence. There was not much subsidence near the center of the thermokarst (zone 1) as a result of the fire. This may be due to the wet environment, thicker active layer and talik.

Site 2 consists of a thermokarst developing via a combination of progressive thawing and mass wasting towards the center of the depression. On this site, fresh ground slumps were observed and the thermokarst center consists of a pond approximately 1.2 meters in depth (fig. 48). The year of death of the dead trees standing in the pond ranged between 1988 – 92 (Dead tree #2: 1989, #3:1988, #4:1992, #5:1990). Several submerged trees were found under the center of the pond; however, we could not date these trees.

Examination of the archival aerial photography revealed that the pond was formed before 1951. The ground depression would have started in the late 1930s. The acceleration of the thermokarst development occurred after 1980s. The pond rapidly expanded during the last two decades.

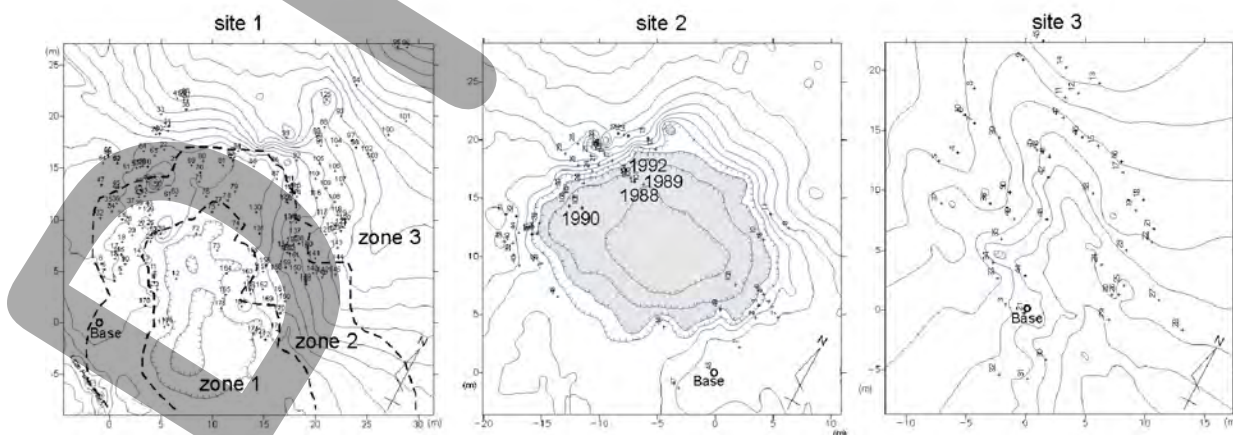


Figure 46. Thermokarst monitoring sites.

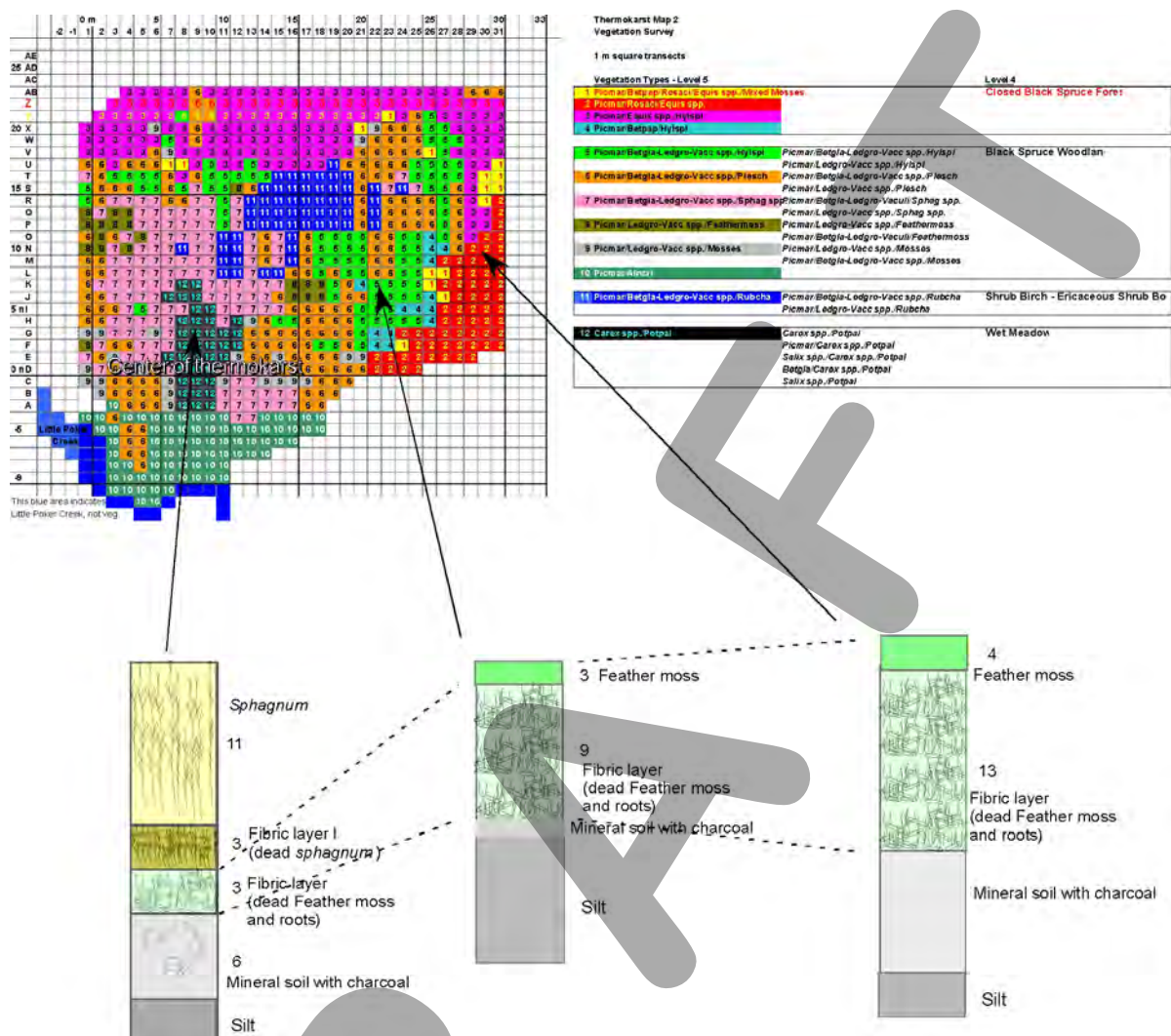


Figure 47. Vegetation map from site 1 thermokarst investigated by J. Knudson.

Site 3 presents a series of thermokarsts, developing primarily by the rain erosion. Over time, the thermokarsts on this site have networked with each other. Eight trees were established in the early 1800's. The tree leaning record indicates that the thermokarst was continuously developing since the 19th century. The organic sediment is thin (9cm) compared with other sites. Erosion is currently one of the major driving forces of this site.

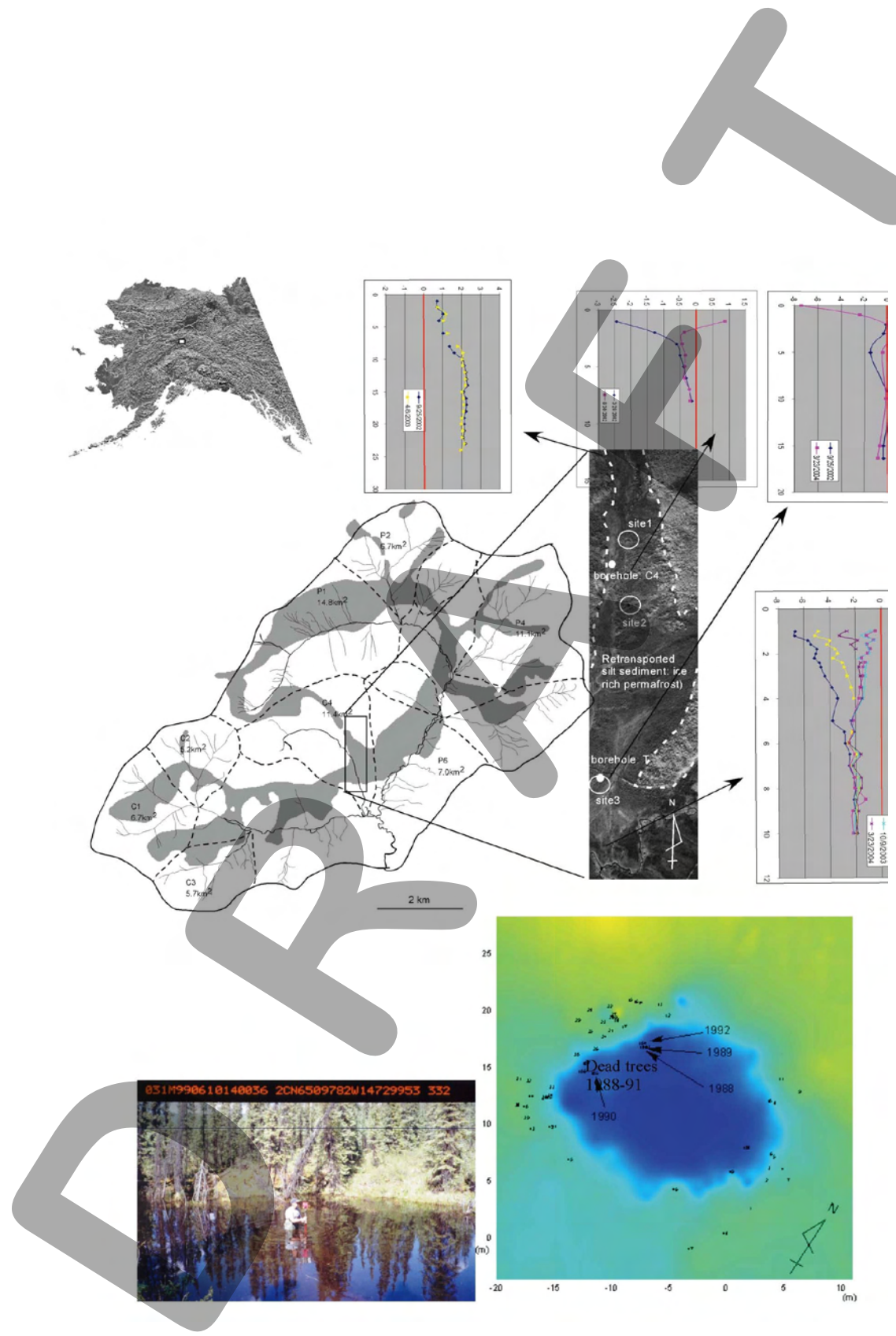


Figure 48. Thermokarst monitoring sites. All three sites are located on the ice rich silt.

Ground surface morphology was determined by the characterization of compression wood in the growth rings of *Picea mariana* (black spruce) growing within the boundary of the thermokarst on each site. By measuring the direction of compression wood occurrence within the trees for each year, it was possible to create three-dimensional maps (contour resolution: 10 cm) of the development of the thermokarsts over time.

Thermokarst ponds are important groundwater regulated features. In interior Alaska, permafrost is generally absent beneath these ponds. Sub- (intra-) permafrost water is discharged into the pond during maximum water ground water potential periods. However, most of the time, pond water drains vertically (recharge) to the intra-permafrost aquifer.

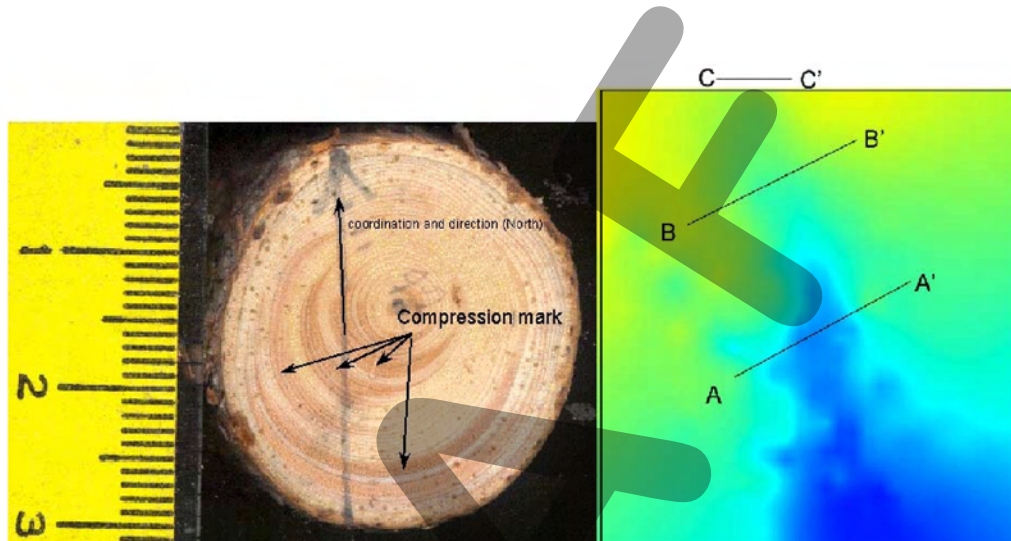


Figure 49. Compression mark (left) and profiles location for Figure 51.

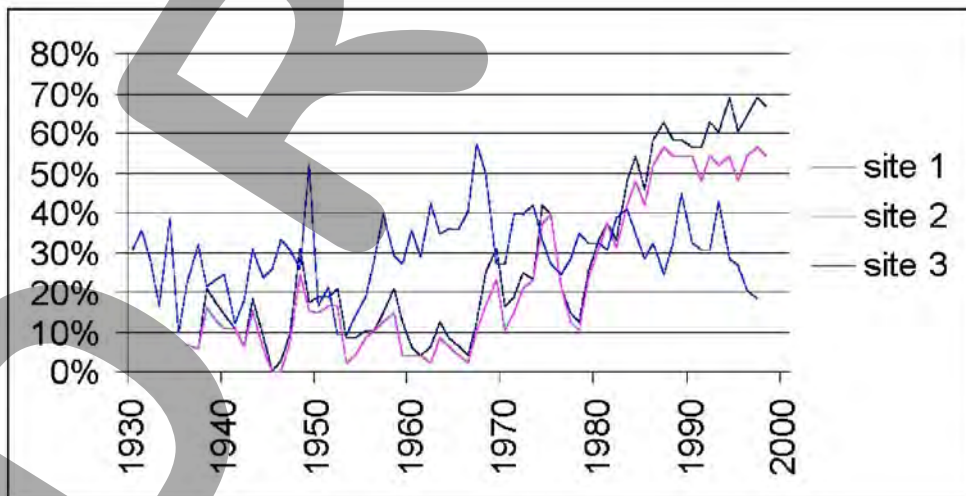


Figure 50. Tree leaning trends last 70 years.

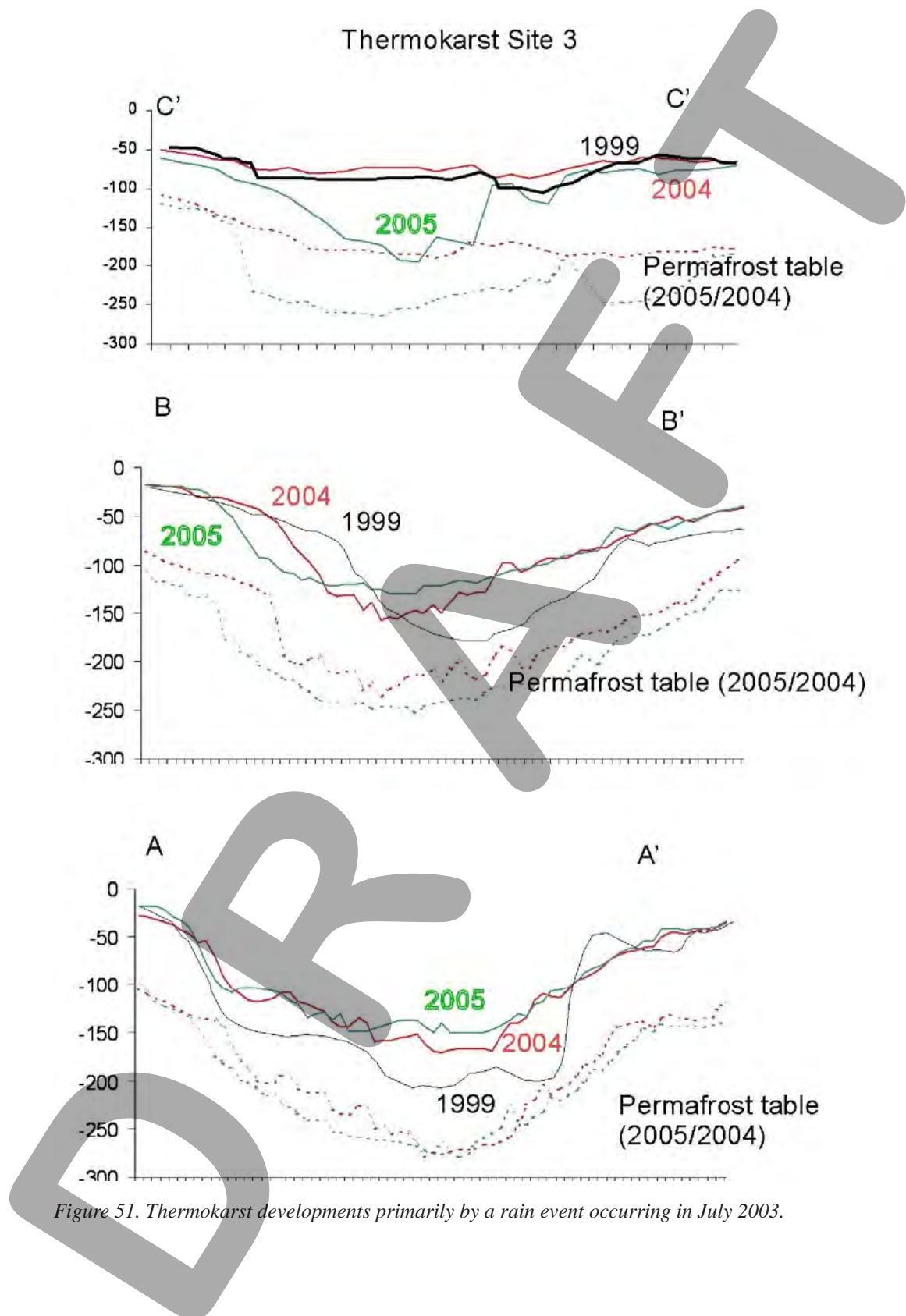


Figure 51. Thermokarst developments primarily by a rain event occurring in July 2003.

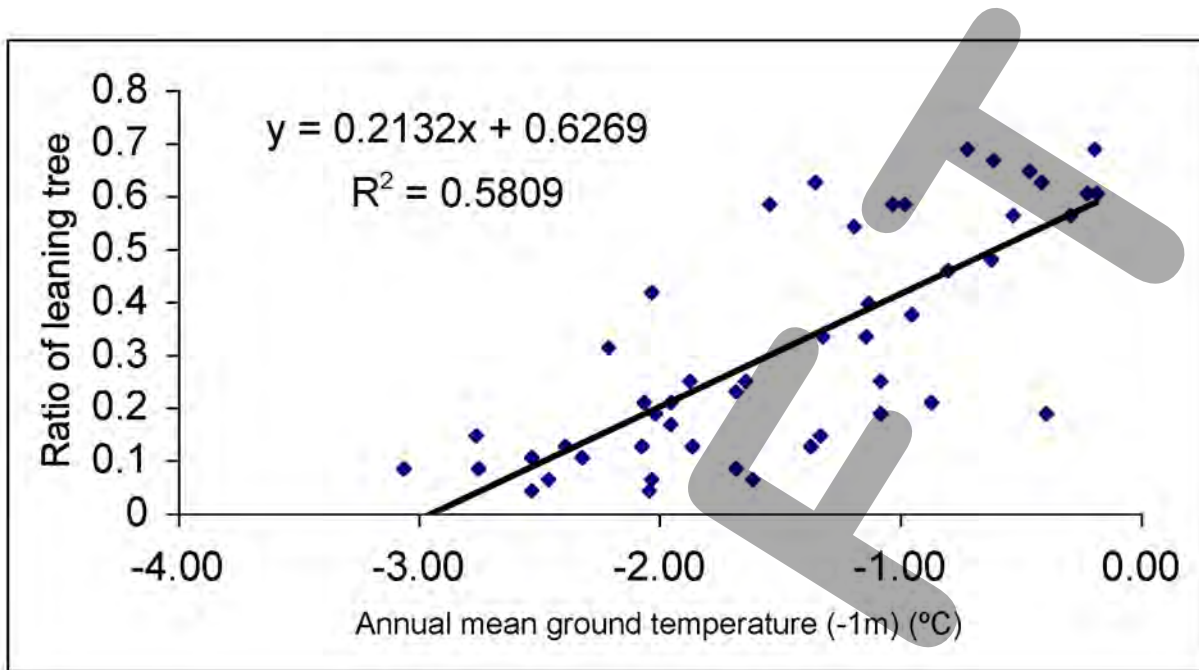


Figure 52. Modeled ground temperature at 1m deep versus leaning trees trend. This positive trend indicated that the warmer temperature has a more chance to developed “drunken trees”.

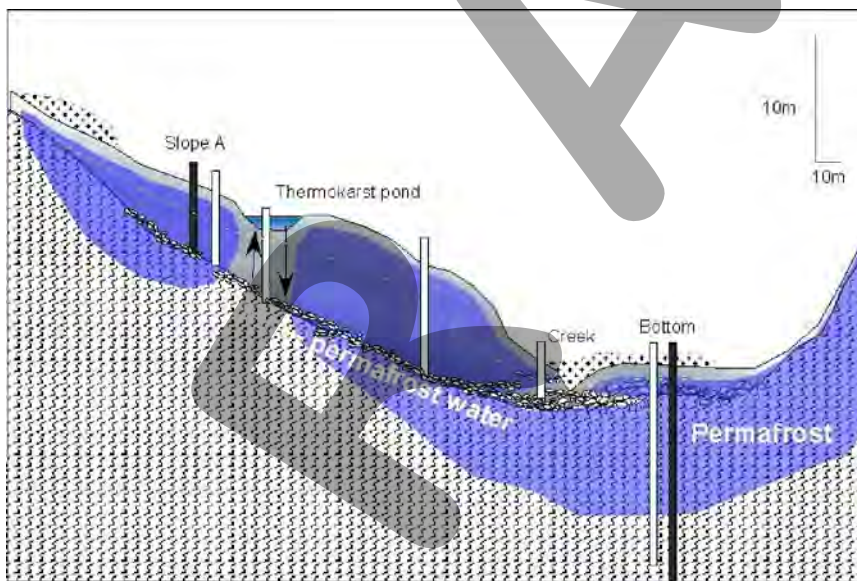


Figure 53. Cross section profiles of bedrock and silt deposits, interface based on geophysical surveys and borehole data. Silt and bedrock interface is typical in the aquifer system in CPCRW at the base of south facing slope. Scales are indicated in the figures, borehole locations are indicated solid line (temperature) and white (well). Shaded blue patterns indicate permafrost (after Yoshikawa et al. 2003).

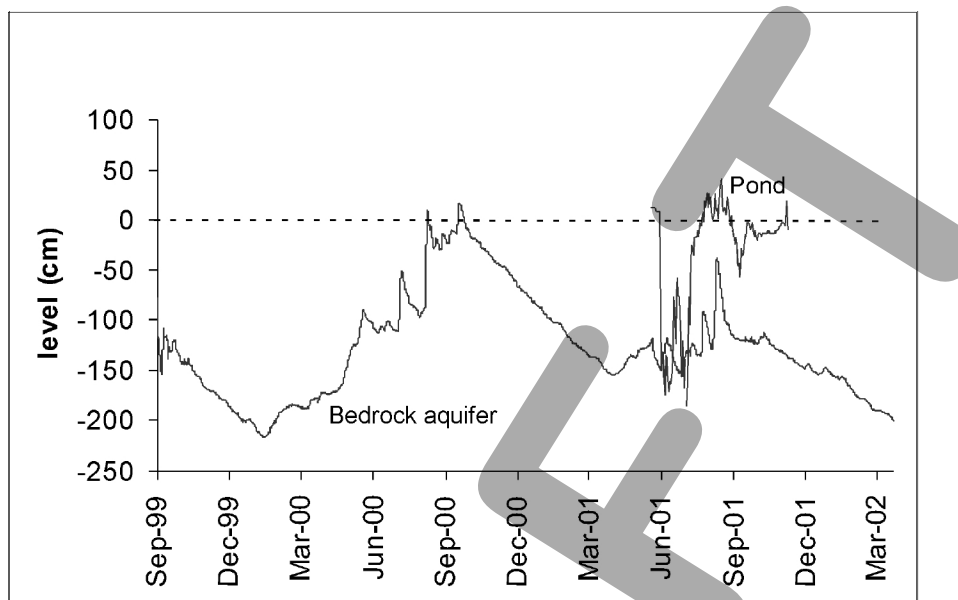


Figure 54. Seasonal variation of the groundwater level at the bottom of valley; MD well (bedrock aquifer 18m below surface) and thermokarst pond (5.7m below surface) (after Yoshikawa et al. 2003).

STOP 9: ISABELLA CREEK

One of the mature thaw lake features is a floating mat covering. More than 1m of the floating mat can be comfortably walked over the lake all year round. This Isabella Creek bog lake is a 7m deep water body with an open talik underneath. Five L/sec. of discharge from the lake was measured in 2003. This area has permafrost with artesian conditions, which means the groundwater recharges the lake water all year round. Kane and Carlson (1972) studied this lake to estimate discharge and hydrological conductivity using piezometric measurement at different depths at the middle of lake. They determined the silt permeability and discharge using Darcy's Equation. The hydraulic gradients are 0.2 – 0.5 m/m. The rate of discharge (Q) is calculated based on the talik area (A), hydraulic conductivity (k) and groundwater gradient (dx/dz). The piezometric pressure was obtained 4 different depths of piezometric pressure monitoring wells. A positive vertical gradient was measured all year round (1969-1970) allowing these ponds to recharge via the taliks throughout the year. The recharge rate was calculated by Darcy's flow:

$$Q = k A \frac{dx}{dz} \quad \text{eq.5}$$

where Q : discharge; k : hydraulic conductivity; A : cross-sectional area of thaw, and dx/dz : hydraulic gradient. Hydraulic conductivities of the materials beneath the lakes were estimated based on unfrozen silt. Field observations in 2003 support discharge rate of earlier work.

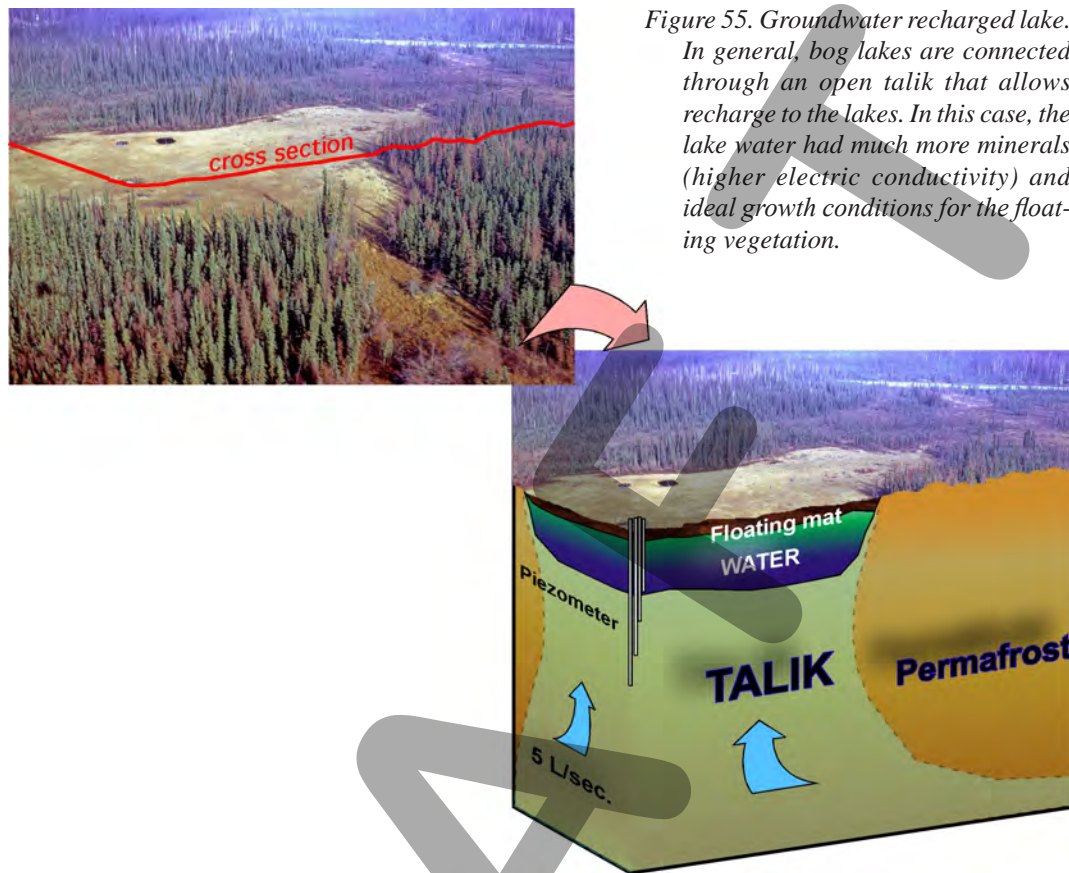


Figure 55. Groundwater recharged lake.

In general, bog lakes are connected through an open talik that allows recharge to the lakes. In this case, the lake water had much more minerals (higher electric conductivity) and ideal growth conditions for the floating vegetation.

STOP 10: GRENAC CREEK (FARMER'S LOOP) PINGO

Grenac Creek is located about 3 km north of Fairbanks along the Farmer's Loop Road. One pingo is located at the toe of a fluvial fan. The thickness of the permafrost is 38 m, and the annual mean temperature of the upper permafrost is -0.7 °C.

This pingo is 50 m wide, 6 m high, and has a massive ice core extending from 6.5 m to 12.5 m depth from the top of the pingo. Water lenses existed between 13.5 m and 18 m at the bottom of the pingo ice. Permafrost was found between 18 m and 38 m depth. The sub permafrost groundwater is under active artesian conditions. The bedrock was located at a depth of about 48 m, which is 36m below the pingo's ice body. Figure 56 shows 1D, 2D resistivity soundings, the drill log, 60-MHz GPR signals, and swept-frequency radar results at Grenac Creek pingo.

There are two easily detectable reflections occurring at about 100 ns and 150 ns extending from the top of the hill to about 25 m using the swept-frequency system (fig. 56c). Shifting time zero to the surface response, assuming an average dielectric constant of about 8, and converting to range places these reflections occur at about 4-5 m for the top and 7-8 meters for the bottom. GSSI impulse system GPR measurements are employed using the 40-MHz bistatic antenna as well as velocity analysis by CMT. Radar signals have strong reflection at the top (200 ns) and the bottom (450 ns) of the ice core (fig. 56d).

A seismic refraction measurement was employed at the top of the pingo. Two layers were identified from the travel time curves. The upper layer has a P-wave velocity of 390 m/sec and the lower layer of 2300 m/sec. The calculated depth of the boundary is about 6 m, which is close to the top of the massive ice core (6.5 m) and much deeper than the frost table (about 2 m). The result is problematic because the upper part of permafrost only showed P-wave velocity lower than 1000 m/sec, even if a theoretically undetectable layer from the travel time curve was considered. One of the travel time curves shows a large lateral gap at the northern part of the survey line, which possibly results from considerable melting of the permafrost, except for the northern part of the pingo.

Resistivity investigations have been conducted at this pingo. We employed classic one-dimensional resistivity sounding (fig. 56e) and two-dimensional resistivity profiling (fig. 56a) for these investigations with the Wenner electrode configuration. Inversion results indicate a reasonable ice body (>6000 ohm-m) with sub pingo ice talik (<100 ohm-m).

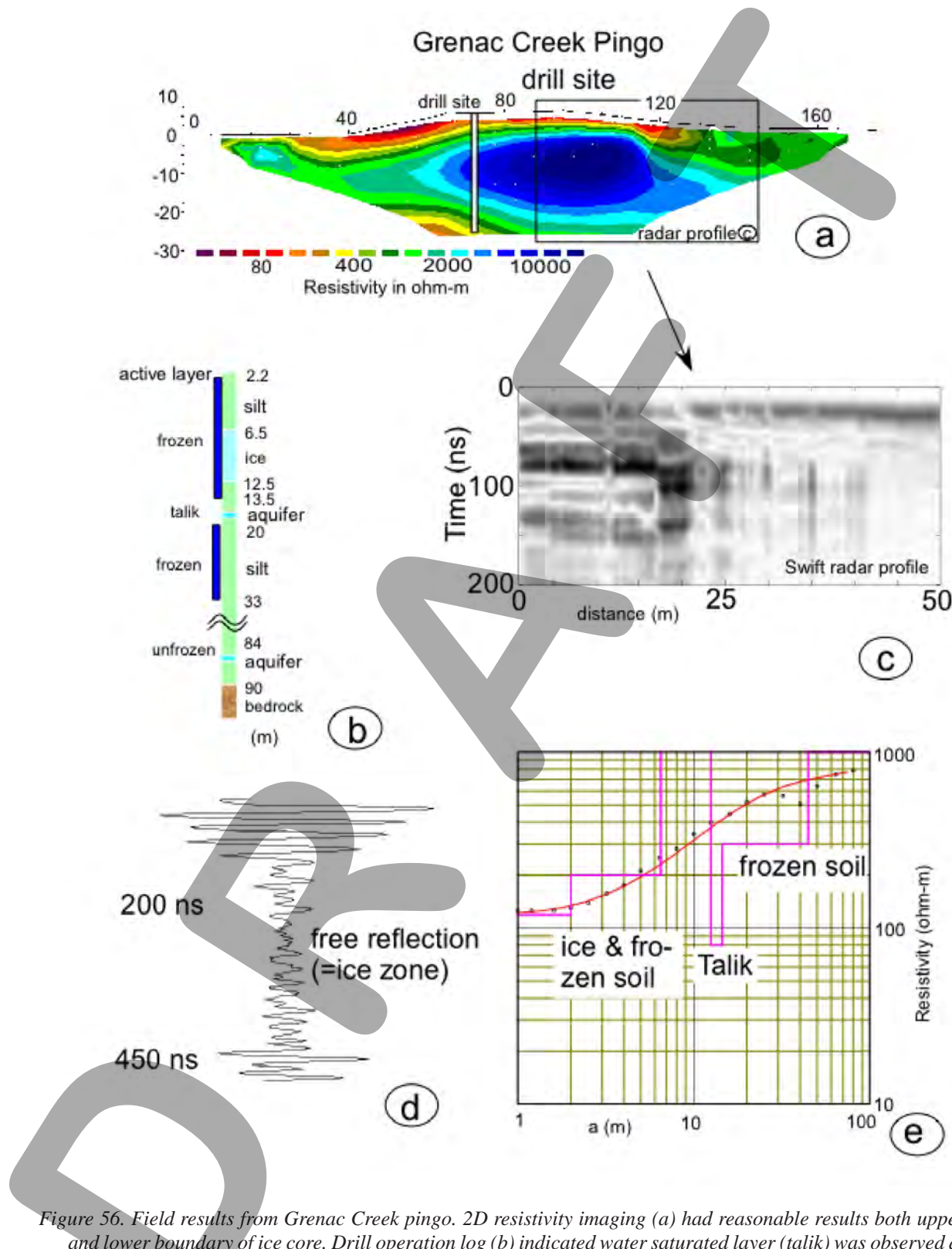


Figure 56. Field results from Grenac Creek pingo. 2D resistivity imaging (a) had reasonable results both upper and lower boundary of ice core. Drill operation log (b) indicated water saturated layer (talik) was observed at the bottom of ice core (13.5-18m depth). GPR wiggle curve at LF (60MHz) indicated massive ice core between 200 and 450 ns (c and d). 1D DC resistivity at Wenner array results had some problems for fitting curve as the heterogeneously of the horizontal structure of pingo massive ice core (after Yoshikawa et al. 2005).

REFERENCES

- Boike, J., and Yoshikawa, K., 2003, Mapping of Periglacial Geomorphology using Kite/Balloon Aerial Photography. *Permafrost Periglac. Process.* 14: 81–85.
- Farmer, G.L., Goldfarb, R.J., Lilly, M.R., Bolton, W., Meier, A.L., and Sanzolone, R.F. 1998, The chemical characteristics of ground water near Fairbanks, Alaska. U.S. Geological Survey Professional Paper 1615. 167-178.
- Fastie, C.L., Fire history of the C4 and P6 basins of the Caribou-Poker Creeks Research Watershed, Alaska. FROSTFIRE Synthesis Workshop 21-23 March 2000, The Role of Fire in the Boreal Forest and its Impacts on Climatic Processes. Fairbanks, Alaska, The University of Alaska Fairbanks: 45 p.
- Gold, L.W., Johnston, G.H., Slusarchuk, W.A., and Goodrich, L.E. 1972, Thermal effects in permafrost. Proceedings of the Canadian Northern Pipeline Conference, National Research Council Associate Committee for Geotechnical Research Technical Memorandum 104. 25-45.
- Hamilton, T.D., and Obi, C.M., 1982, Pingos in Brooks Range, northern Alaska, USA. *Arctic and Alpine Research*, 14.13-20.
- Haugen, R.K., Slaughter, C.W., Howe, K.E., and Dingman, S.L. 1982, Hydrology and climatology of the Caribou-Poker Creeks Research Watershed, Alaska. CRREL Report 82-26.
- Hinzman, L., Fukuda, M., Sandberg, D.V., Chapin, F.S., III, and Dash, D., FROSTFIRE: An experimental approach to predicting the climate feedbacks from the changing boreal fire regime, *J. Geophys. Res.*, 108(D1), 8153, doi:10.1029/2001JD000415, 2003a.
- Hinzman, L.D., Ishikawa, N., Yoshikawa, K., Bolton W.R., and Petrone K.C., 2003b, Hydrologic studies in Caribou-Poker Creeks Research Watershed in support of long term ecological research. *Eurasian J. For. Res.* 5-2: 67-71.
- Hinzman, L.D., Kane, D.L., and Yoshikawa, K., 2003c, Soil Moisture Response to a changing climate in arctic regions. *Tôhoku Geophysical Journal*. 36(4):369-373.
- Hinzman, L.D., Kane, D.L., Yoshikawa, K., Carr, A., Bolton, W.R., Fraver M., 2003d, Hydrological Variations Among Watersheds with Varying Degrees of Permafrost. 2003, Proceedings of 8th International Conference on Permafrost, Zurich, Switzerland, 21-25 July 2003. p 407-411.
- Hinzman L.D., K. Yoshikawa, M. Fukuda, V.I. Romanovsky, K. Petrone and W. Bolton. 2001. Wildfire in the Subarctic Boreal Forests, Ecosystem Impacts and Response to a Warming Climate. *Tôhoku Geophysical Journal*. 36(2):230-232.
- Holmes, G.W., Hopkins, D.M., and Foster, H.L., 1968, Pingos in central Alaska, U.S. Geological Survey Bulletin 1241-H, 40 p.
- Leuschen, C., Kanagaratnam, P., Yoshikawa, K., Arcone S., and Gogineni, S., 2003, Design and Field Experiments of a Surface-Penetrating Radar for Mars Exploration, *The Journal of Geophysical Research.*, 108(E4), 8034, doi: 10.1029/2002JE001876, 2003.
- IAEA/WMO 2001. Global Network for Isotopes in Precipitation. The GNIP Database. Accessible at: <http://isohis.iaea.org>.
- Kane, D.L., 1980, Snowmelt infiltration into seasonally frozen soils. *Cold Regions Science and Technology*. 3. 153-161.
- Neary, M.P., 1997,. Tritium enrichment: To enrich or not to enrich? *Radioactivity and Radiochemistry* 8:4. 23-35.
- Rantz, S.E., et al., 1982, Measurement and computation of streamflow: measurement of stage and discharge. USGS Water Sup. Paper 2175. 284pp.
- Rohsenow, W.M., J.P. Hartnett, and E.N. Ganic, 1985, *Handbook of Heat Transfer Fundamentals*, McGraw-Hill, New York, p. 4-163.
- Romanovsky, V.E., Burgess, M., Smith, S., Yoshikawa, K., and Brown, J., 2002, Permafrost Temperature Records: Indicators of Climate Change, *Eos*, 83, 50, 586-594.
- Ping, C.L., Michaelson, G.J., Packee, E.C., Stiles, C.A., Swanson, D.K., and Yoshikawa, K., 2005, Soil catena sequences and fire ecology in the boreal forest of Alaska. *Soil Sci.Soc. Am. J.* 69. 1761-1772. doi:10.2136/sssaj2004.0139.
- Slaughter, C.W., and Hartzmann, R.J., 1993, Hydrologic and water quality characteristics of a degrading open-system pingo. IN Permafrost Sixth International Conference Proceedings, vol. 1. pp. 574-579.

- Stow, D.A., Hope, A., McGuire, D., Verbyla, D., Gamon, J., Huemmrich, F., Houston, S., Racine, C., Sturm, M., Tape, K., Hinzman, L., Yoshikawa, K., Tweedle, C., Noyle, B., Silapaswan, C., Douglas, D., Griffith, B., Gensu, J., Epstein, H., Walker, D., Daeschner, S., Petersen, A., Zhou, L., and Myneni, R., 2004, Remote Sensing of Vegetation and Landcover Change in Arctic Tundra Ecosystems, *Remote Sensing of Environment*, 89 (2004) 281-308, doi:10.1016/j.rse.2003.10.018.
- Viereck, L.A., Werdin-Pfisterer, N.R., Adams P.C., and Yoshikawa, K., 2008, Effect of Wildfire and Fireline Construction on the Annual Depth of Thaw in a Black Spruce Permafrost Forest in Interior Alaska: a 36-Year Record of Recovery. 9th International Conference on Permafrost. Fairbanks Alaska, USA 28, June- 2 July 2008.
- White, D.M., Garland S.D., Beyer L., and Yoshikawa K., 2004, Pyrolysis-GC/MS fingerprinting of environmental samples. *Journal of Analytical and Applied Pyrolysis*. vol. 71, Issue1, 107-118. doi:10.1016/S0165-2370(03)00101-3.
- White, D.M., Collins, C., Barnes, D., and Byard, H., 2004, Effects of a Crude Oil Spill on Permafrost after 24 Years in Interior Alaska, Proceedings of the 2004 Cold Regions Engineering and Construction Conference.
- White, D., Yoshikawa, K., and Garland, D.S., 2002, Use of dissolved organic matter to support hydrologic investigations in a permafrost-dominated watershed. *Cold Regions Science and Technology*. 35, 27-33.
- Yoshikawa, K., Bolton, W.R., Romanovsky, V.E., Fukuda, M., and Hinzman, L.D., 2002, Impacts of wildfire on the permafrost in the boreal forests of Interior Alaska, *J. Geophys. Res.*, 107, 8148, doi:10.1029/2001JD000438, 2002. [printed 108(D1), 2003]
- Yoshikawa, K., and Harada, K., 1995, Observations on Nearshore Pingo Growth, Adventdalen, Spitsbergen. *Permafrost and Periglacial Processes*, 6:361-372.
- Yoshikawa K., Hinzman, L.D., and, D.L., 2007, Spring and aufeis (icing) hydrology in Brooks Range, Alaska, *J. Geophys. Res.*, 112, G04S43, doi:10.1029/2006JG000294.
- Yoshikawa, K., Leuschen, C., Ikeda, A., Harada, K., Gogineni, P., Hoekstra, P., Hinzman, L., Sawada, Y., and Matsuoka, N., 2006, Comparison of geophysical investigations for detection of massive ground ice (pingo ice), *J. Geophys. Res.*, 111, E06S19, doi:10.1029/2005JE002573.
- Yoshikawa, K., Hinzman, L.D., and Gogineni, P., 2002, Ground temperature and permafrost mapping using an equivalent latitude/elevation model. *Jour. Glaciology and Geocryology*. 24. 5. 526-531.
- Yoshikawa, K., and Harada, K., 1995, Observations on Nearshore Pingo Growth, Adventdalen, Spitsbergen. *Permafrost and Periglacial Processes*, 6:361-372.
- Yoshikawa, K., D. White, L. Hinzman, D. Goering, K. Petrone, W. Bolton, and N. Ishikawa. Water in permafrost; case study of aufeis and pingo hydrology in discontinuous permafrost. 8th International Conference on Permafrost. Zurich, Switzerland 21- 25 July 2003.
- Yoshikawa, K., Romanovsky, V., Duxbury, N., Brown, J., and Tsapin, A. 2004, The use of geophysical methods to discriminate between brine layers and freshwater taliks in permafrost regions. *Jour. Glaciology and Geocryology*, vol. 26. 301-309.
- Yoshikawa , K., and Hinzman, L.D., 2003, Shrinking thermokarst ponds and groundwater dynamics in discontinuous permafrost near Council, Alaska. *Permafrost Periglac. Process* 14: 151-160. DOI:10.1002/ppp.451
- Yoshikawa, K., White, D., Hinzman, L., Goering, D., Petrone, K., Bolton, W., and Ishikawa, N., 2003, Water in permafrost; case study of aufeis and pingo hydrology in discontinuous permafrost. In *Permafrost*, 8th International Conference on Permafrost. Phillips, Springman & Arenson (Eds). vol. 2. 1259-1264.

DRAFT

DRAFT



STATE OF ALASKA

Sarah Palin, *Governor*
Tom Irwin, *Commissioner, Department of Natural Resources*
Robert F. Swenson, *State Geologist and Acting Director*